Supporting Information

Widespread False Negatives in DNA-Encoded Library Data: How Linker Effects Impair Machine Learning-Based Lead Prediction

Alba L. Montoya,[a,†] Adam Hogendorf,[a,†] Steven Tingey,[b] Aadarsh Kuberan,[c] Lik Hang Yuen,[a] Herwig Schüler,[d] Raphael M. Franzini[a,e]*

[a] Department of Medicinal Chemistry, College of Pharmacy, University of Utah, 30 S 2000 E, Salt Lake City, UT 84112, USA
[b] Waterford School, 1480 E 9400 S, Sandy, UT 84093, USA
[c] West High School, 241 N 300 W, Salt Lake City, UT 84103, USA
[d] Center for Molecular Protein Science, Department of Chemistry, Lund University, 22100 Lund, Sweden
[e] Huntsman Cancer Institute, University of Utah, 2000 Circle of Hope, Salt Lake City, UT 84112, USA

† These authors contributed equally

Table of Contents:

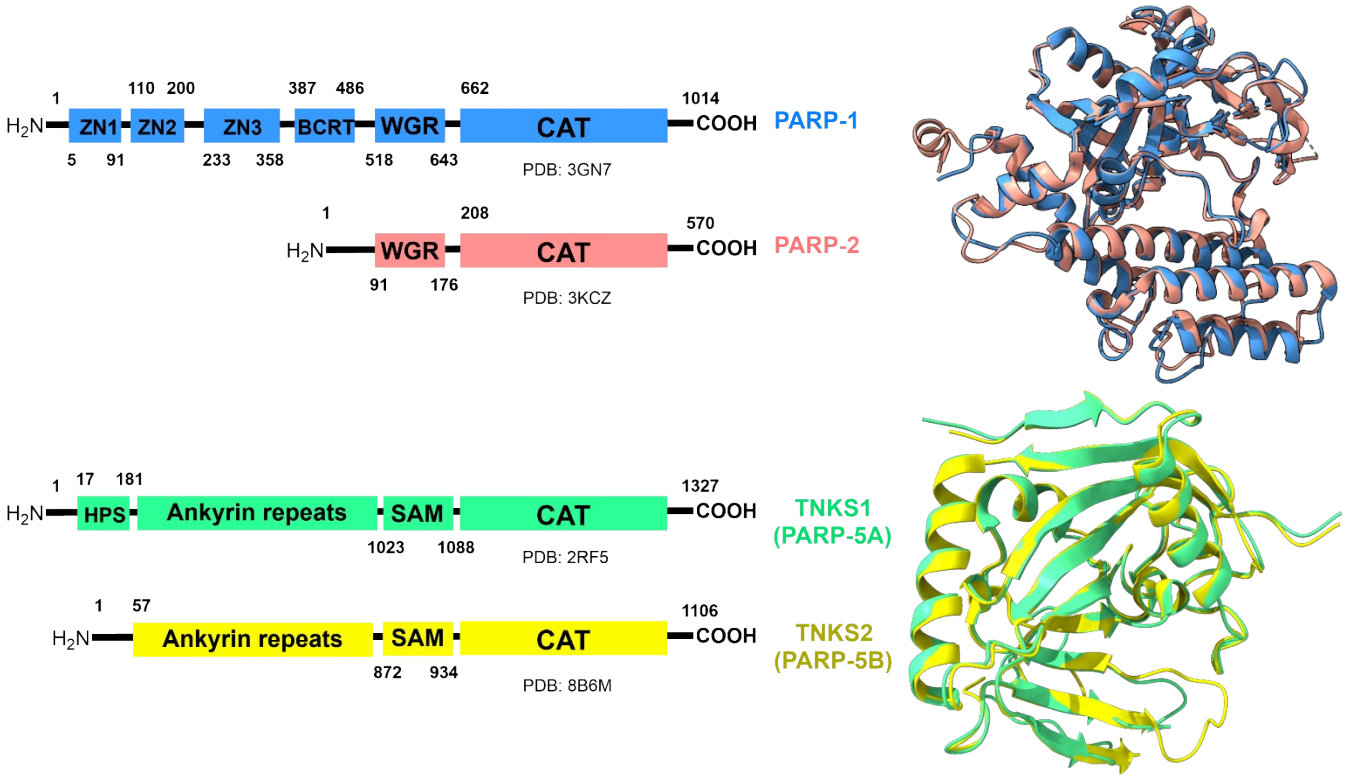

Supporting Figure 1. Poly-ADP Ribose Polymerase (PARP) Family.

Experimental

General Information:

Standard reagents and ACS-grade solvents were purchased from commercial sources and used without further purification. Carboxylic acid building blocks, linkers, and amines were obtained from suppliers including Ambeed (Arlington Hts, IL), Enamine (Kiev, Ukraine), Combi-Blocks (San Diego, CA), ChemBridge (San Diego, CA), Sigma-Aldrich (St. Louis, MO), Oakwood Chemical (Columbia, SC), Alfa Aesar (Ward Hill, MA), Matrix Scientific (Columbia, SC), and Acros Organics (Geel, Belgium). Reactions were conducted under a normal atmosphere and monitored by thin-layer chromatography (TLC) using J.T. Baker Si250F silica gel plates, with spots detected under UV light (254 nm). Compound purification was performed via flash column chromatography (FCC) on silica gel (40-60 µm) from Tyger Scientific Inc. using a Biotage Isolera One system (version 3.3.0).

High-performance liquid chromatography (HPLC) analysis and purification were carried out on an UltiMate 3000 HPLC system (Thermo Fisher Scientific, Waltham, MA) using C18 reversed-phase solid support and elution with gradient mixtures with 0.1% trifluoroacetic acid in acetonitrile. All compounds were >95% pure by HPLC.

^{1}H nuclear magnetic resonance (NMR) spectra were recorded on a Varian Inova 400 MHz spectrometer. Chemical shifts (δ, ppm) were determined relative to tetramethylsilane (0.00 ppm) as internal standard in $CDCl_3$ and CD_3OD, or relative to the DMSO solvent residue signal. The following abbreviations were used: s = singlet, d = doublet, dd = doublet of doublets, t = triplet, q = quartet, m = multiplet, br. s = broad singlet. NMR data were processed using MestReNova software.

Mass spectrometry (MS) data were recorded on standalone Waters Acquity QDa Detector in ESI+ ionization mode, scanning the 100–1200 m/z range at a 10 Hz sampling rate with a cone voltage of 15V. Samples were prepared in 0.1% TFA in acetonitrile and injected at 0.3 mL/min.

Synthesis and characterization of PARP2 inhibitor compounds:

General procedures for sequential amide couplings:

A. Synthesis of carboxylic acids A/B with -tert-butyl (2-aminoethyl) carbamate (A/B-En-Boc):

The corresponding carboxylic acid **A/B** (1.0 mmol), *N*-hydroxysuccinimide (NHS, 1.5 mmol) and 1-ethyl-3-(-3-dimethylaminopropyl) carbodiimide hydrochloride (EDC·HCl salt, 1.5 mmol) were dissolved in dimethylformamide (DMF, 2.0 mL) and stirred for 15 min at room temperature (rt). *N*-Boc-ethylenediamine (1.5 mmol) in DMF (2.0 mL) was added to the solution, and the mixture was stirred for 12 h at rt. The product was precipitated from hot water and collected by filtration. Some compounds required further purification by recrystallization in MeOH or by flash column chromatography (FCC) on silica gel with mixtures of DCM/MeOH. Yields ranged between 60-90%.

B. Synthesis of carboxylic acids A/B with ethylenediamine as TFA salts (A/B-En-NH_2·TFA):

Carboxylic acid **A/B** with Boc-protected diamine was dissolved in a trifluoroacetic acid (TFA, 2.0 mL) solution containing 4% *m*-cresol, 4% thioanisole, and 2% water as additives. The mixtures were monitored by TLC until Boc protecting group was removed, which generally required between 15-30 min. The mixture was added to cold diethyl ether (Et_2O, 25 mL), let it stand at 4 C overnight, centrifugate, and the precipitate collected by filtration. The products were used without further purification. Yields were between 75-95%.

C. Synthesis of ethylenediamine coupled to carboxylic acid building blocks A and B (A-En-B):

Carboxylic acid **B/A** (1.0 mmol), NHS (1.5 mmol) and EDC (HCl·salt, 1.5 mmol) were dissolved in DMF (2.0 mL). After 15 min incubation, N,N-Diisopropylethylamine (DIEA, 1.5 mmol) and **A/B-En-NH_2** as TFA salts (1.2 mmol) were added consecutively and the mixture was stirred for 12 h at rt. Possible precipitate was dissolved by heating and the solution was added to hot water (20 mL) to precipitate the product or co-evaporated with xylenes. Final compounds were purified by recrystallization in MeOH, by FCC on silica gel, or by C18 reverse phase HPLC to furnish the desired compounds. The yields of the final compounds ranged between 45-85%.

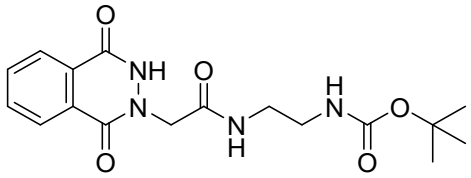

A96-En-Boc

2-(1,4-dioxo-3,4-dihydrophthalazin-2(1H)-yl)acetic acid-*tert*-butyl (2-(2-(1,4-dioxo-3,4-dihydrophthalazin-2(1H)-yl)acetamido)ethyl)carbamate-*tert*-butyl (2-aminoethyl)carbamate **(A96-En-Boc)**: **^{1}H NMR (400 MHz, DMSO-d_6, 300K) δ**: 11.91 (s, 1H), 8.25 – 8.09 (m, 3H), 7.98 – 7.85 (m, 2H), 6.85 (t, *J* = 5.7 Hz, 1H), 4.68 (s, 2H), 3.14 (q, *J* = 6.4 Hz, 2H), 3.00 (q, *J* = 6.4 Hz, 2H), 1.33 (s, 9H) ppm.

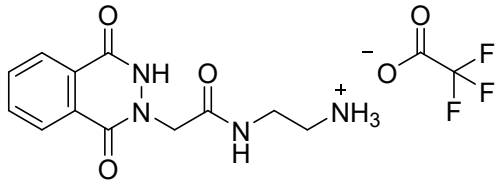

A96-En-NH_2·TFA

2-(2-(1,4-dioxo-3,4-dihydrophthalazin-2(1H)-yl)acetamido)ethan-1-aminium **(A96-En-NH_2·TFA)**: **^{1}H NMR (400 MHz, Methanol-d_4, 300K) δ**: 8.31 (d, *J* = 7.9 Hz, 1H), 8.24 (d, *J* = 7.9 Hz, 1H), 7.99 - 7.86 (m, 2H), 4.88 (s, 2H), 3.58 (t, *J* = 6.0 Hz, 2H), 3.11 (t, *J* = 6.0 Hz, 2H) ppm.

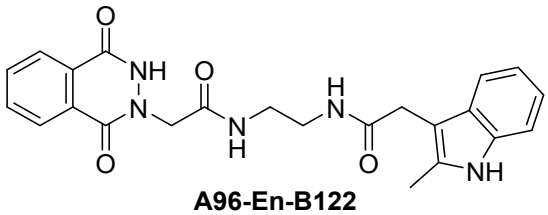

A96-En-B122

2-(1,4-dioxo-3,4-dihydrophthalazin-2(1H)-yl)-N-(2-(2-(2-methyl-1H-indol-3-yl)acetamido)ethyl)acetamide **(A96-En-B122)**: **^{1}H NMR (400 MHz, Methanol-d_4, 300K) δ**: 8.27 (m, 1H), 8.12 (m, 1H), 7.89 - 7.80 (m, 2H), 7.31 (d, *J* = 7.8 Hz, 1H), 7.10 (d, *J* = 7.8 Hz, 1H), 6.95 - 6.81 (m, 2H), 4.54 (s, 2H), 3.54 (s, 2H), 3.36 (br. s, 4H), 2.31 (s, 3H) ppm.

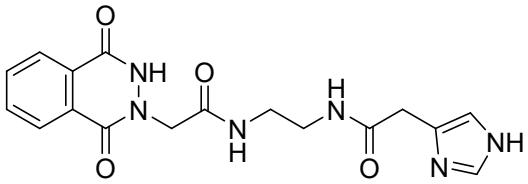

A96-En-B101

N-(2-(2-(1H-imidazol-4-yl)acetamido)ethyl)-2-(1,4-dioxo-3,4-dihydrophthalazin-2(1H)-yl)acetamide **(A96-En-B101)**: **^{1}H NMR (400 MHz, Methanol-d_4, 300K) δ**: 8.79 (s, 1H), 8.31 (d, *J* = 8.6 Hz, 1H), 8.25 (d, *J* = 7.4 Hz, 1H), 8.00 – 7.86 (m, 2H), 7.37 (s, 1H), 4.83 (s, 2H), 3.68 (s, 2H), 3.45 – 3.40 (m, 2H), 3.40 – 3.33 (m, 2H) ppm.

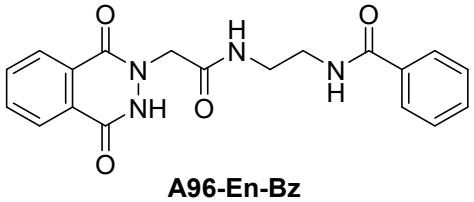

A96-En-Bz

N-(2-(2-(1,4-dioxo-3,4-dihydrophthalazin-2(1H)-yl)acetamido)ethyl)benzamide **(A96-En-Bz)**: **^{1}H NMR (400 MHz, DMSO-d_6, 300K) δ**: 11.93 (s, 1H), 8.55 (t, *J* = 5.3 Hz, 1H), 8.28 (t, *J* = 5.5 Hz, 1H), 8.20 (t, *J* = 6.6 Hz, 2H), 7.92 (dq, *J* = 15.3, 7.1 Hz, 2H), 7.78 (d, *J* = 7.5 Hz, 2H), 7.49 (t, *J* = 7.1 Hz, 1H), 7.42 (t, *J* = 7.4 Hz, 2H), 4.70 (s, 2H) ppm.

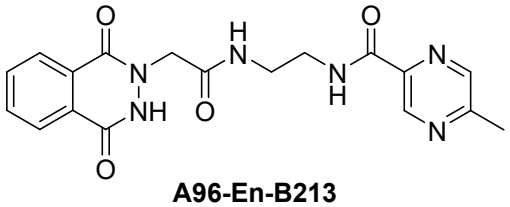

A96-En-B213

N-(2-(2-(1,4-dioxo-3,4-dihydrophthalazin-2(1H)-yl)acetamido)ethyl)-5-methylpyrazine-2-carboxamide **(A96-En-B213)**: The NMR characterization of this compound was previously reported.[1]

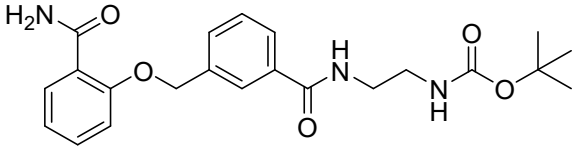

A45-En-Boc

tert-butyl (2-(3-((2-carbamoylphenoxy)methyl)benzamido)ethyl)carbamate **(A45-En-Boc)**: **^{1}H NMR (400 MHz, DMSO-d_6, 300K) δ**: 8.47 (t, *J* = 5.7 Hz, 1H), 7.95 (s, 1H), 7.78 (t, *J* = 7.7 Hz, 2H), 7.64 (d, *J* = 7.6 Hz, 1H), 7.58 (s, 1H), 7.54 – 7.39 (m, 3H), 7.18 (d, *J* = 8.4 Hz, 1H), 7.02 (t, *J* = 7.5 Hz, 1H), 6.89 (t, *J* = 5.8 Hz, 1H), 5.28 (s, 2H), 3.28 (q, *J* = 6.2 Hz, 2H), 3.10 (q, *J* = 6.4 Hz, 2H), 1.34 (s, 9H) ppm.

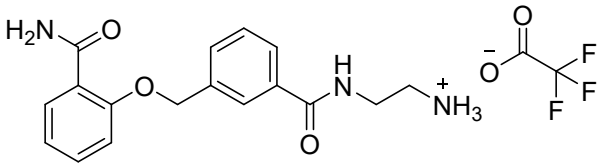

A45-En-NH_2·TFA

2-(3-((2-carbamoylphenoxy)methyl)benzamido)ethan-1-aminium **(A96-En-NH_2·TFA)**: **^{1}H NMR (400 MHz, Methanol-d_4, 300K) δ**: 7.97 (s, 1H), 7.87 (d, *J* = 7.6 Hz, 1H), 7.81 (d, *J* = 7.6 Hz, 1H), 7.65 (d, *J* = 7.6 Hz, 1H), 7.51 - 7.39 (m, 2H), 7.15 (d, *J* = 8.2 Hz, 1H), 7.02 (t, *J* = 7.4 Hz, 1H), 5.28 (s, 2H), 3.64 (br. s, 2H), 3.29 (br. s, 2H) ppm.

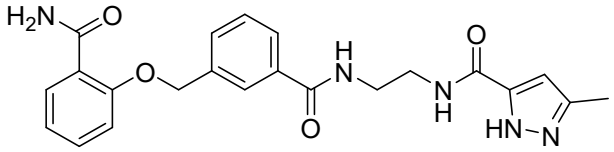

A45-En-B299

N-(2-(3-((2-carbamoylphenoxy)methyl)benzamido)ethyl)-3-methyl-1H-pyrazole-5-carboxamide **(A45-En-B299)**: **^{1}H NMR (400 MHz, DMSO-d_6, 300K) δ**: 8.59 (br. s, 1H), 8.24 (br. s, 1H), 7.95 (s, 1H), 7.83 – 7.72 (m, 2H), 7.64 (d, *J* = 7.6 Hz, 1H), 7.58 (br. s, 1H), 7.54 – 7.38 (m, 3H), 7.18 (d, *J* = 8.4 Hz, 1H), 7.02 (t, *J* = 7.5 Hz, 1H), 6.36 (s, 1H), 5.28 (s, 2H), 2.21 (s, 3H) ppm.

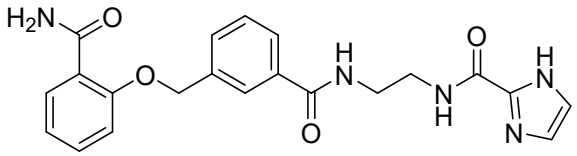

A45-En-B295

N-(2-(3-((2-carbamoylphenoxy)methyl)benzamido)ethyl)-1H-imidazole-2-carboxamide **(A45-En-B295)**: **^{1}H NMR (400 MHz, DMSO-d_6, 300K) δ**: 12.99 (s, 1H), 8.64 – 8.52 (m, 2H), 7.96 (s, 1H), 7.77 (dd, *J* = 15.4, 7.7 Hz, 2H), 7.64 (d, *J* = 7.4 Hz, 1H), 7.57 (d, *J* = 15.3 Hz, 2H), 7.45 (dt, *J* = 20.6, 8.1 Hz, 2H), 7.23 (s, 1H), 7.19 (d, *J* = 8.3 Hz, 1H), 7.06 – 6.96 (m, 2H), 5.28 (s, 2H), 3.42 (s, 4H) ppm.

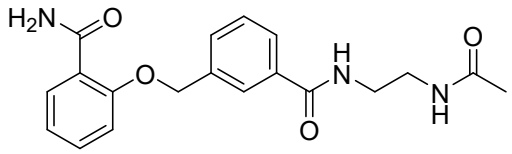

A45-En-Ac

N-(2-acetamidoethyl)-3-((2-carbamoylphenoxy)methyl)benzamide **(A45-En-Ac)**: **^{1}H NMR (400 MHz, DMSO-d_6, 300K) δ**: 8.54 (t, *J* = 5.6 Hz, 1H), 8.00 – 7.93 (m, 2H), 7.82 – 7.73 (m, 2H), 7.65 (d, *J* = 7.6 Hz, 1H), 7.59 – 7.38 (m, 4H), 7.18 (d, *J* = 8.3 Hz, 1H), 7.02 (t, *J* = 7.5 Hz, 1H), 5.28 (s, 2H), 3.30 – 3.23 (m, 2H), 3.22 – 3.11 (m, 2H), 1.78 (s, 3H) ppm.

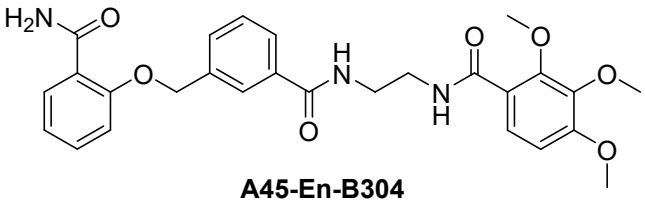

A45-En-B304

N-(2-(3-((2-carbamoylphenoxy)methyl)benzamido)ethyl)-2,3,4-trimethoxybenzamide **(A45-En-B304)**: **^{1}H NMR (400 MHz, DMSO-d_6, 300K) δ**: 8.58 (br. s, 1H), 8.25 (br. s, 1H), 7.96 (s, 1H), 7.80 (d, *J* = 7.8 Hz, 1H), 7.76 (d, *J* = 7.7 Hz, 1H), 7.65 (d, *J* = 7.6 Hz, 1H), 7.57 (br. s, 1H), 7.52 – 7.38 (m, 4H), 7.18 (d, *J* = 8.3 Hz, 1H), 7.02 (t, *J* = 7.5 Hz, 1H), 6.86 (d, *J* = 8.8 Hz, 1H), 5.28 (s, 2H), 3.80 (s, 3H), 3.76 (s, 3H), 3.72 (s, 3H), 3.45 (s, 4H) ppm.

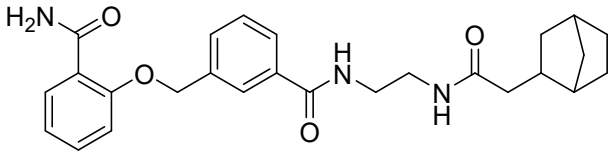

A45-En-B21

N-(2-(2-(bicyclo[2.2.1]heptan-2-yl)acetamido)ethyl)-3-((2-carbamoylphenoxy)methyl)benzamide **(A45-En-B21)**: **^{1}H NMR (400 MHz, Methanol-d_4, 300K) δ:** 7.97 – 7.91 (m, 2H), 7.80 (d, *J* = 7.8 Hz, 1H), 7.67 (d, *J* = 7.7 Hz, 1H), 7.54 – 7.44 (m, 2H), 7.21 (d, *J* = 8.3 Hz, 1H), 7.07 (t, *J* = 7.5 Hz, 1H), 5.32 (s, 2H), 3.56 – 3.35 (m, 4H), 2.17 – 2.08 (m, 2H), 1.99 (dd, *J* = 13.7, 7.6 Hz, 1H), 1.91 (br. s, 1H), 1.82 (m, 1H), 1.47 – 1.26 (m, 4H), 1.18 – 0.96 (m, 4H) ppm.

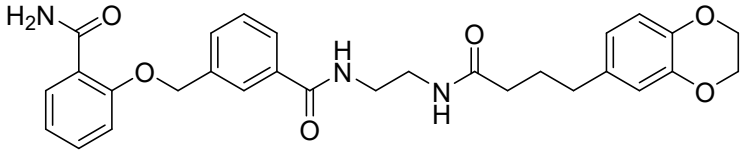

A45-En-B111

3-((2-carbamoylphenoxy)methyl)-N-(2-(4-(2,3-dihydrobenzo[b][1,4]dioxin-6-yl)butanamido)ethyl)benzamide **(A45-En-B111)**: **^{1}H NMR (400 MHz, DMSO-d_6, 300K) δ**: 8.49 (t, *J* = 5.6 Hz, 1H), 7.94 (s, 1H), 7.89 (t, *J* = 5.6 Hz, 1H), 7.80 – 7.73 (m, 2H), 7.64 (d, *J* = 7.6 Hz, 1H), 7.59 – 7.36 (m, 4H), 7.17 (d, *J* = 8.3 Hz, 1H), 7.02 (t, *J* = 7.4 Hz, 1H), 6.70 (d, *J* = 8.2 Hz, 1H), 6.62 (d, *J* = 2.0 Hz, 1H), 6.57 (dd, *J* = 8.2, 2.1 Hz, 1H), 5.26 (s, 2H), 4.16 (s, 4H), 3.25 – 3.12 (m, 2H), 2.39 (t, *J* = 7.6 Hz, 2H), 2.03 (t, *J* = 7.6 Hz, 2H), 1.70 (p, *J* = 7.6 Hz, 2H) ppm.

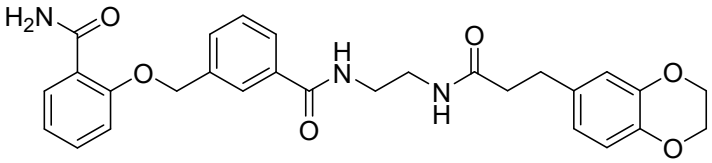

A45-En-B111-A

3-((2-carbamoylphenoxy)methyl)-N-(2-(3-(2,3-dihydrobenzo[b][1,4]dioxin-6-yl)propanamido)ethyl)benzamide **(A45-En-B111-A)**: **^{1}H NMR (400 MHz, Methanol-d_4, 300K) δ:** 7.94 (br. s, 2H), 7.79 (d, *J* = 7.7 Hz, 1H), 7.69 (d, *J* =

7.6 Hz, 1H), 7.56 – 7.44 (m, 2H), 7.22 (d, *J* = 8.4 Hz, 1H), 7.08 (t, *J* = 7.5 Hz, 1H), 6.69 – 6.56 (m, 3H), 5.33 (s, 2H), 4.13 (s, 4H), 3.44 (d, *J* = 5.1 Hz, 2H), 3.39 (d, *J* = 5.1 Hz, 2H), 2.77 (t, *J* = 7.5 Hz, 2H), 2.43 (t, *J* = 7.5 Hz, 2H) ppm.

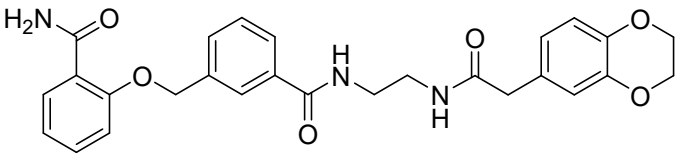

A45-En-B111-B

3-((2-carbamoylphenoxy)methyl)-N-(2-(2-(2,3-dihydrobenzo[b][1,4]dioxin-6-yl)acetamido)ethyl)benzamide **(A45-En-B111-B)**: **^{1}H NMR (400 MHz, DMSO-d_6, 300K) δ**: 8.83 (br. s, 1H), 8.40 (br. s, 1H), 8.28 (br. s, 1H), 8.10 (d, *J* = 7.1 Hz, 2H), 7.99 (d, *J* = 7.5 Hz, 1H), 7.94 – 7.72 (m, 4H), 7.53 (d, *J* = 8.2 Hz, 1H), 7.36 (t, *J* = 7.3 Hz, 1H), 7.10 – 6.95 (m, 3H), 5.62 (s, 2H), 4.50 (s, 4H), 3.61 – 3.47 (m, 6H) ppm.

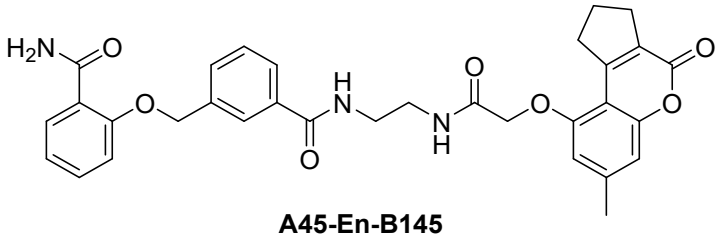

A45-En-B145

3-((2-carbamoylphenoxy)methyl)-N-(2-(2-((7-methyl-4-oxo-1,2,3,4-tetrahydrocyclopenta[c]chromen-9-yl)oxy)acetamido)ethyl)benzamide **(A45-En-B145)**: The NMR characterization of this compound was previously reported.[1]

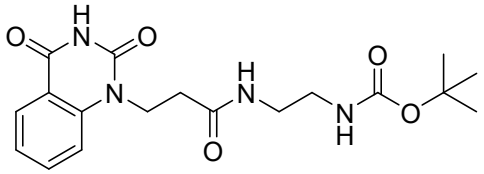

A11/A108-En-Boc

tert-butyl (2-(3-(2,4-dioxo-3,4-dihydroquinazolin-1(2H)-yl)propanamido)ethyl)carbamate **(A11/A108-En-Boc)**: **^{1}H NMR (400 MHz, DMSO-d_6, 300K) δ**: 11.56 (s, 1H), 8.04 (t, *J* = 5.8 Hz, 1H), 7.98 (d, *J* = 7.7 Hz, 1H), 7.73 (t, *J* = 8.0 Hz, 1H), 7.44 (d, *J* = 8.5 Hz, 1H), 7.25 (t, *J* = 7.5 Hz, 1H), 6.77 (t, *J* = 5.8 Hz, 1H), 4.21 (t, *J* = 7.5 Hz, 2H), 3.05 – 2.97 (m, 2H), 2.96 – 2.83 (m, 2H), 2.40 (t, *J* = 7.5 Hz, 2H), 1.35 (s, 9H) ppm.

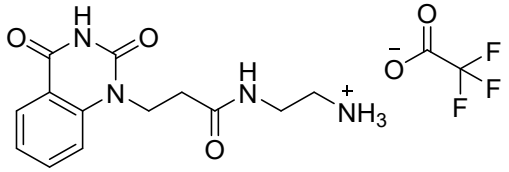

A11/A108-En-NH_2·TFA

2-(3-(2,4-dioxo-3,4-dihydroquinazolin-1(2H)-yl)propanamido)ethan-1-aminium **(A11/A108-En-NH_2·TFA)**: **^{1}H NMR (400 MHz, Methanol-d_4, 300K) δ**: 8.14 (d, *J* = 7.8 Hz, 1H), 7.79 (t, *J* = 7.9 Hz, 1H), 7.50 (d, *J* = 8.5 Hz, 1H), 7.32 (t, *J* = 7.6 Hz, 1H), 4.45 (t, *J* = 6.8 Hz, 2H), 3.43 (t, *J* = 5.7 Hz, 2H), 3.04 (t, *J* = 5.7 Hz, 2H), 2.61 (t, *J* = 6.8 Hz, 2H) ppm.

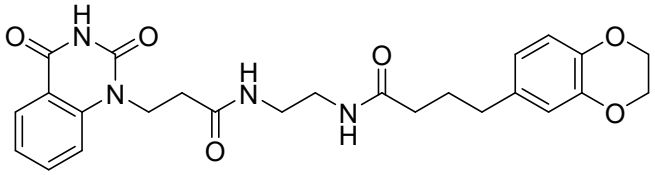

A11/A108-En-B111

4-(2,3-dihydrobenzo[b][1,4]dioxin-6-yl)-N-(2-(3-(2,4-dioxo-3,4-dihydroquinazolin-1(2H)-yl)propanamido)ethyl)butanamide **(A11/A108-En-B111)**: **^{1}H NMR (400 MHz, DMSO-d_6, 300K) δ**: 11.57 (s, 1H), 8.04 (br. s, 1H), 7.98 (d, *J* = 7.8 Hz, 1H), 7.77 (br. s, 1H), 7.71 (t, *J* = 7.2 Hz, 1H), 7.43 (d, *J* = 8.5 Hz, 1H), 7.24 (t, *J* = 7.5 Hz, 1H), 6.78 – 6.51 (m, 3H), 4.25 – 4.09 (m, 6H), 3.02 (s, 4H), 2.39 (t, *J* = 7.4 Hz, 4H), 2.01 (t, *J* = 7.5 Hz, 2H), 1.70 (p, *J* = 7.6 Hz, 2H) ppm.

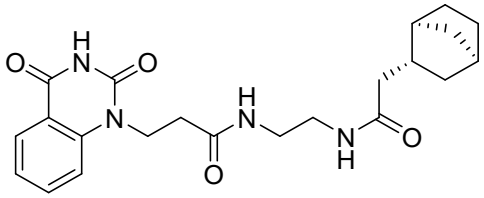

A11/A108-En-B21

N-(2-(2-((1S,2R,4R)-bicyclo[2.2.1]heptan-2-yl)acetamido)ethyl)-3-(2,4-dioxo-3,4-dihydroquinazolin-1(2H)-yl)propanamide **(A11/A108-En-B21)**: **^{1}H NMR (400 MHz, DMSO-d_6, 300K) δ**: 11.57 (s, 1H), 8.03 (br. s, 1H), 7.98 (d, *J* = 6.7 Hz, 1H), 7.81 – 7.66 (m, 2H), 7.44 (d, *J* = 8.5 Hz, 1H), 7.25 (t, *J* = 7.5 Hz, 1H), 4.21 (t, *J* = 7.5 Hz, 2H), 3.01 (s, 4H), 2.40 (t, *J* = 7.5 Hz, 2H), 2.12 (s, 1H), 1.98 (dd, *J* = 13.6, 7.9 Hz, 1H), 1.89 – 1.80 (m, 2H), 1.74 (dt, J = 12.6, 7.8 Hz, 1H), 1.47 – 1.21 (m, 4H), 1.18 – 0.87 (m, 4H) ppm.

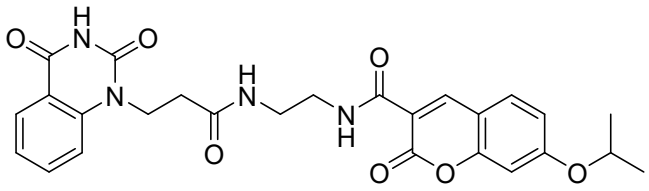

A11/A108-En-B227

N-(2-(3-(2,4-dioxo-3,4-dihydroquinazolin-1(2H)-yl)propanamido)ethyl)-7-isopropoxy-2-oxo-2H-chromene-3-carboxamide **(A11/A108-En-B227)**: **^{1}H NMR (400 MHz, DMSO-d_6, 300K) δ**: 11.56 (s, 1H), 8.82 (s, 1H), 8.72 (t, *J* = 5.4 Hz, 1H), 8.19 (m, 1H), 7.97 (d, *J* = 7.9 Hz, 1H), 7.88 (d, *J* = 8.7 Hz, 1H), 7.72 (t, *J* = 7.8 Hz, 1H), 7.46 (d, *J* = 8.5 Hz, 1H), 7.23 (t, *J* = 7.6 Hz, 1H), 7.09 (br. s, 1H), 7.00 (d, *J* = 8.5 Hz, 1H), 4.82 (m, 1H), 4.23 (t, *J* = 7.6 Hz, 2H), 3.22 – 3.16 (m, 2H), 2.43 (t, *J* = 7.5 Hz, 2H), 1.31 (s, 3H), 1.30 (s, 3H) ppm.

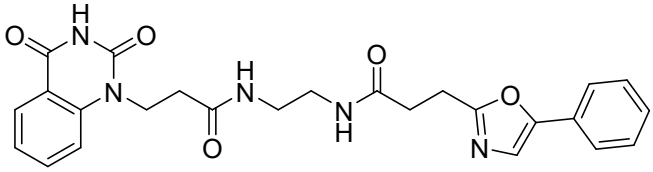

A11/A108-En-B139

3-(2,4-dioxo-3,4-dihydroquinazolin-1(2H)-yl)-N-(2-(3-(5-phenyloxazol-2-yl)propanamido)ethyl)propanamide **(A11/A108-En-B139)**: **^{1}H NMR (400 MHz, DMSO-d_6, 300K) δ**: 11.57 (s, 1H), 8.05 (br. s, 1H), 7.98 (d, *J* = 7.4 Hz, 2H), 7.73 (t, *J* = 7.8 Hz, 1H), 7.63 (d, *J* = 7.6 Hz, 2H), 7.51 (s, 1H), 7.47 – 7.39 (m, 3H), 7.31 (t, *J* = 7.4 Hz, 1H), 7.24 (t, *J* = 7.5 Hz, 1H), 4.22 (t, *J* = 7.6 Hz, 2H), 3.12 – 2.95 (m, 6H), 2.56 (t, *J* = 7.4 Hz, 2H), 2.40 (t, *J* = 7.4 Hz, 2H) ppm.

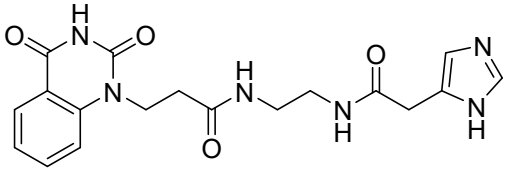

A11/A108-En-B101

N-(2-(2-(1H-imidazol-5-yl)acetamido)ethyl)-3-(2,4-dioxo-3,4-dihydroquinazolin-1(2H)-yl)propanamide **(A11/A108-En-B101)**: **^{1}H NMR (400 MHz, DMSO-d_6, 300K) δ**: 11.57 (s, 1H), 8.92 (d, *J* = 1.4 Hz, 1H), 8.16 (s, 1H),

8.10 (s, 1H), 7.99 (d, *J* = 6.4 Hz, 1H), 7.72 (t, *J* = 7.1 Hz, 1H), 7.43 (d, *J* = 5.9 Hz, 2H), 7.25 (t, *J* = 7.5 Hz, 1H), 4.21 (t, *J* = 7.5 Hz, 2H), 3.10 – 3.03 (m, 4H), 2.40 (t, *J* = 7.4 Hz, 2H) ppm.

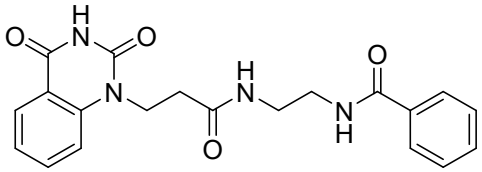

A11/A108-En-Bz

N-(2-(3-(2,4-dioxo-3,4-dihydroquinazolin-1(2H)-yl)propanamido)ethyl)benzamide **(A11/A108-En-Bz)**: **^{1}H NMR (400 MHz, DMSO-d_6, 300K) δ**: 11.57 (s, 1H), 8.48 (t, *J* = 5.7 Hz, 1H), 8.17 (t, *J* = 5.8 Hz, 1H), 7.98 (d, *J* = 7.8 Hz, 1H), 7.82 (d, *J* = 7.5 Hz, 2H), 7.71 (t, *J* = 7.8 Hz, 1H), 7.50 (t, *J* = 7.2 Hz, 1H), 7.44 (d, *J* = 7.1 Hz, 3H), 7.24 (t, *J* = 7.5 Hz, 1H), 4.23 (t, *J* = 7.5 Hz, 2H), 3.27 (q, *J* = 6.2 Hz, 2H), 3.17 (q, *J* = 6.2 Hz, 2H), 2.42 (t, *J* = 7.5 Hz, 2H) ppm.

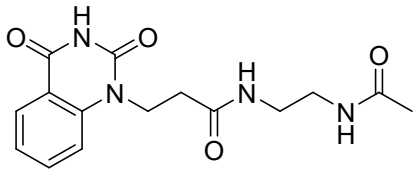

A11/A108-En-Ac

N-(2-acetamidoethyl)-3-(2,4-dioxo-3,4-dihydroquinazolin-1(2H)-yl)propanamide **(A11/A108-En-Ac)**: **^{1}H NMR (400 MHz, DMSO-d_6, 300K) δ**: 11.54 (s, 1H), 8.06 (s, 1H), 7.99 (d, *J* = 7.7 Hz, 1H), 7.83 (s, 1H), 7.73 (t, *J* = 7.7 Hz, 1H), 7.45 (d, *J* = 8.5 Hz, 1H), 7.25 (t, *J* = 7.5 Hz, 1H), 4.22 (t, *J* = 7.4 Hz, 2H), 3.01 (s, 4H), 2.40 (t, *J* = 7.5 Hz, 2H), 1.76 (s, 3H) ppm.

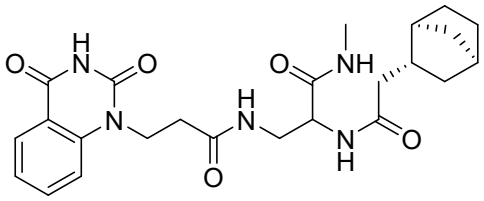

A11/A108-CONHMe-B21

2-(2-((1S,2R,4R)-bicyclo[2.2.1]heptan-2-yl)acetamido)-3-(3-(2,4-dioxo-3,4-dihydroquinazolin-1(2H)-yl)propanamido)-N-methylpropanamide **(A11/A108-CONHMe-B21)**: **^{1}H NMR (400 MHz, Methanol-d_4, 300K) δ:** 8.13 (d, *J* = 7.7 Hz, 1H), 7.78 (t, *J* = 7.9 Hz, 1H), 7.50 (d, *J* = 8.6 Hz, 1H), 7.31 (t, *J* = 7.4 Hz, 1H), 4.58 (s, 1H), 4.47 – 4.35 (m, 2H), 3.52 – 3.33 (m, 3H), 2.77 – 2.51 (m, 6H), 2.26 – 1.81 (m, 4H), 1.55 – 1.05 (m, 7H) ppm.

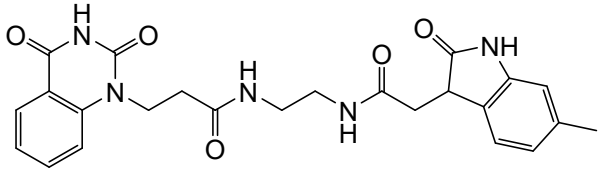

A11/A108-En-B182

3-(2,4-dioxo-3,4-dihydroquinazolin-1(2H)-yl)-N-(2-(2-(6-methyl-2-oxoindolin-3-yl)acetamido)ethyl)propenamide **(A11/A108-En-B182)**: The NMR characterization of this compound was previously reported.[1]

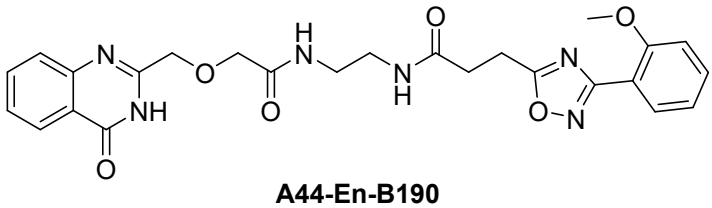

A44-En-B190

3-(3-(2-methoxyphenyl)-1,2,4-oxadiazol-5-yl)-N-(2-(2-((4-oxo-3,4-dihydroquinazolin-2-yl)methoxy)acetamido)ethyl)propenamide **(A44-En-B190)**: **^{1}H NMR (400 MHz, DMSO-d_6, 300K) δ**: 12.25 (s, 1H), 8.30 (s, 1H), 8.13 (s, 1H), 8.09 (d, *J* = 7.9 Hz, 1H), 7.82 – 7.72 (m, 2H), 7.61 (d, *J* = 8.1 Hz, 1H), 7.56 – 7.43 (m, 2H), 7.18 (d, *J* = 8.4 Hz, 1H), 7.06 (t, *J* = 7.5 Hz, 1H), 4.49 (s, 2H), 4.03 (s, 2H), 3.83 (s, 3H), 3.23 – 3.06 (m, 6H), 2.63 (t, *J* = 7.3 Hz, 2H) ppm.

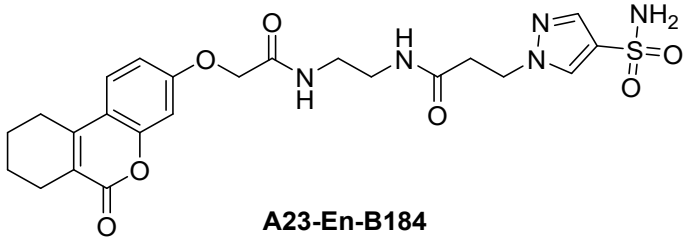

A23-En-B184

N-(2-(2-((6-oxo-7,8,9,10-tetrahydro-6H-benzo[c]chromen-3-yl)oxy)acetamido)ethyl)-3-(4-sulfamoyl-1H-pyrazol-1-yl)propenamide **(A23-En-B184)**: The NMR characterization of this compound was previously reported.[2]

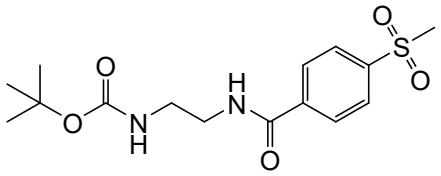

B316-En-Boc

tert-butyl (2-(4-(methylsulfonyl)benzamido)ethyl)carbamate **(B316-En-Boc)**: **^{1}H NMR (400 MHz, Methanol-d_4, 300K) δ**: 8.73 (t, *J* = 5.7 Hz, 1H), 8.09 – 7.98 (m, 4H), 6.95 (t, *J* = 5.9 Hz, 1H), 3.35 – 3.26 (m, 2H), 3.26 (s, 3H), 3.16 – 3.07 (m, 2H), 1.37 (s, 9H) ppm.

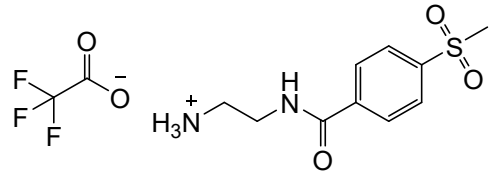

B316-En-NH_2·TFA

2-(4-(methylsulfonyl)benzamido)ethan-1-aminium **(B316-En-NH_2·TFA)**: **^{1}H NMR (400 MHz, Methanol-d_4, 300K) δ**: 8.12 – 8.02 (m, 4H), 3.69 (t, *J* = 5.9 Hz, 2H), 3.19 (t, *J* = 5.9 Hz, 2H), 3.16 (s, 3H) ppm.

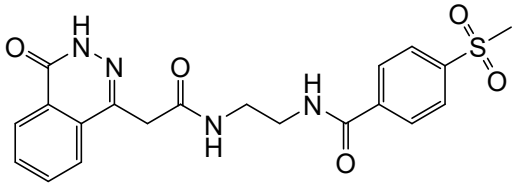

A153-En-B316

4-(methylsulfonyl)-*N*-(2-(2-(4-oxo-3,4-dihydrophthalazin-1-yl)acetamido)ethyl)benzamide **(A153-En-B316)**: **^{1}H NMR (400 MHz, DMSO-d_6, 300K) δ**: 12.54 (s, 1H), 8.70 (m, 1H), 8.31 (m, 1H), 8.20 (d, *J* = 7.4 Hz, 1H), 7.98 (br. s, 4H), 7.87 – 7.73 (m, 3H), 3.78 (br. s, 2H), 3.25 (br. s, 5H), 2.57 (br. s, 2H) ppm.

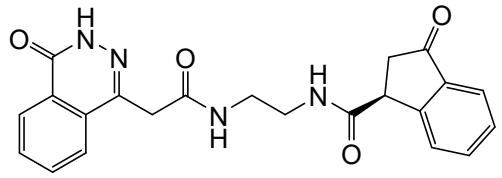

A153-En-B356

(*S*)-3-oxo-N-(2-(2-(4-oxo-3,4-dihydrophthalazin-1-yl)acetamido)ethyl)-2,3-dihydro-1H-indene-1-carboxamide **(A153-En-B356)**: **^{1}H NMR (400 MHz, DMSO-d_6, 300K) δ**: 12.56 (s, 1H), 8.55 (s, 1H), 8.31 – 8.18 (m, 2H), 7.91 – 7.77 (m, 3H), 7.70 – 7.57 (m, 3H), 7.45 (m, 1H), 4.15 (t, *J* = 5.2 Hz, 1H), 3.79 (s, 2H), 3.25 – 3.06 (m, 4H), 2.75 (d, *J* = 5.3 Hz, 2H) ppm.

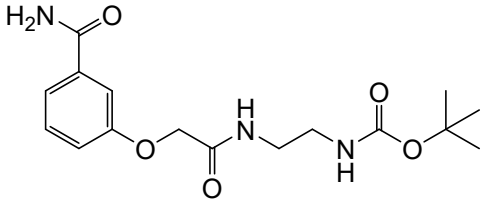

A131-En-Boc

tert-butyl (2-(2-(3-carbamoylphenoxy)acetamido)ethyl)carbamate **(A131-En-Boc)**: **^{1}H NMR (400 MHz, DMSO-d_6, 300K) δ**: 8.12 (t, *J* = 5.8 Hz, 1H), 7.94 (s, 1H), 7.50 – 7.42 (m, 2H), 7.39 – 7.30 (m, 2H), 7.09 (m, 1H), 6.85 (t, *J* = 5.8 Hz, 1H), 4.48 (s, 2H), 3.15 (q, *J* = 6.3 Hz, 2H), 3.00 (q, *J* = 6.3 Hz, 2H), 1.35 (s, 9H) ppm.

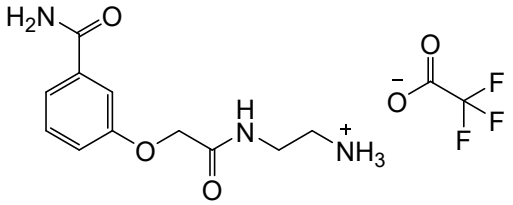

A131-En-NH_2·TFA

2-(2-(3-carbamoylphenoxy)acetamido)ethan-1-aminium **(A131-En-NH_2·TFA)**: **^{1}H NMR (400 MHz, DMSO-d_6, 300K) δ**: 8.30 (t, *J* = 5.9 Hz, 1H), 7.96 (br. s, 1H), 7.80 (br. s, 2H), 7.50 – 7.45 (m, 2H), 7.40 – 7.34 (m, 2H), 7.11 (dd, *J* = 8.2, 2.5 Hz, 1H), 4.53 (s, 2H), 2.90 (s, 2H) ppm.

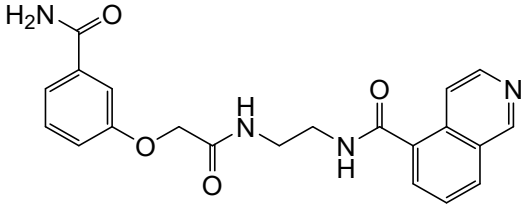

A131-En-B199

N-(2-(2-(3-carbamoylphenoxy)acetamido)ethyl)isoquinoline-5-carboxamide **(A131-En-B199)**: **^{1}H NMR (400 MHz, DMSO-d_6, 300K) δ**: 9.35 (s, 1H), 8.72 – 8.62 (m, 1H), 8.47 (d, *J* = 6.0 Hz, 1H), 8.30 (t, *J* = 5.6 Hz, 1H), 8.21 (d, *J* = 8.2 Hz, 1H), 8.10 (d, *J* = 5.9 Hz, 1H), 7.95 (s, 1H), 7.87 (d, *J* = 7.0 Hz, 1H), 7.69 (t, *J* = 7.7 Hz, 1H), 7.49 – 7.44 (m, 2H), 7.39 – 7.30 (m, 2H), 7.11 (dd, *J* = 8.2, 2.5 Hz, 1H), 4.53 (s, 2H), 3.46 – 3.37 (m, 4H) ppm.

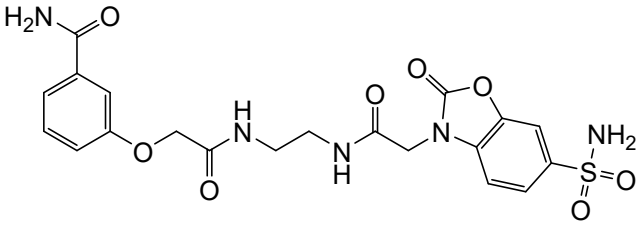

A131-En-B355

3-(2-oxo-2-((2-(2-(2-oxo-6-sulfamoylbenzo[d]oxazol-3(2H)-yl)acetamido)ethyl)amino)ethoxy)benzamide **(A131-En-B355)**: **^{1}H NMR (400 MHz, Methanol-d_4, 300K) δ**: 7.77 – 7.72 (m, 2H), 7.49 (d, *J* = 7.7 Hz, 1H), 7.44 (s, 1H), 7.39 (t, *J* = 8.0 Hz, 1H), 7.22 (d, *J* = 8.2 Hz, 1H), 7.16 (d, *J* = 7.8 Hz, 1H), 4.56 (s, 2H), 4.53 (s, 2H), 3.42 (s, 4H) ppm.

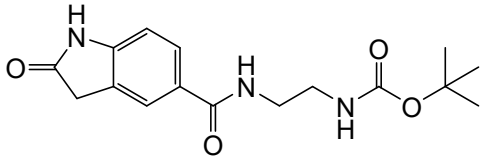

A88-En-Boc

tert-butyl (2-(2-oxoindoline-5-carboxamido)ethyl)carbamate **(A88-En-Boc)**: **^{1}H NMR (400 MHz, DMSO-d_6, 300K) δ**: 10.58 (s, 1H), 8.25 (t, *J* = 5.7 Hz, 1H), 7.72 – 7.66 (m, 2H), 6.90 – 6.80 (m, 2H), 3.50 (s, 2H), 3.24 (q, *J* = 6.4 Hz, 2H), 3.06 (q, *J* = 6.4 Hz, 2H), 1.35 (s, 9H) ppm.

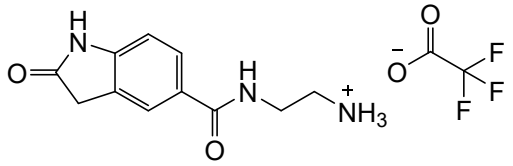

A88-En-NH$_2$·TFA

2-(2-oxoindoline-5-carboxamido)ethan-1-aminium **(A88-En-NH$_2$·TFA)**: **^{1}H NMR (400 MHz, Methanol-d_4, 300K) δ**: 7.81 – 7.73 (m, 2H), 6.95 (d, *J* = 8.1 Hz, 1H), 3.64 (t, *J* = 6.0 Hz, 2H), 3.57 (s, 2H), 3.16 (t, *J* = 6.0 Hz, 2H) ppm.

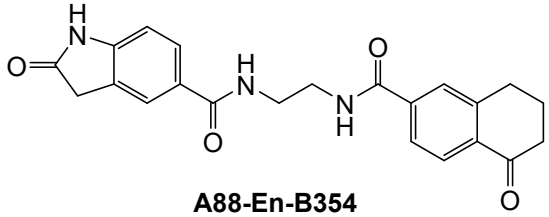

A88-En-B354

2-oxo-*N*-(2-(5-oxo-5,6,7,8-tetrahydronaphthalene-2-carboxamido)ethyl)indoline-5-carboxamide **(A88-En-B354)**: **^{1}H NMR (400 MHz, DMSO-d_6, 300K) δ**: 10.59 (s, 1H), 8.74 – 8.66 (m, 1H), 8.45 – 8.38 (m, 1H), 7.89 (d, *J* = 8.1 Hz, 1H), 7.80 – 7.67 (m, 4H), 6.83 (d, *J* = 8.0 Hz, 1H), 3.51 (s, 2H), 2.97 (t, *J* = 6.0 Hz, 2H), 2.61 (t, *J* = 6.4 Hz, 2H), 2.48 (br. s, 4H), 2.04 (p, *J* = 6.3 Hz, 2H) ppm.

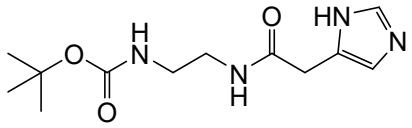

B101-En-Boc

tert-butyl (2-(2-(1H-imidazol-5-yl)acetamido)ethyl)carbamate **(B101-En-Boc)**: **^{1}H NMR (400 MHz, Methanol-d_4, 300K) δ**: 7.62 (s, 1H), 6.95 (s, 1H), 3.49 (s, 2H), 3.25 (t, *J* = 6.0 Hz, 2H), 3.14 (t, *J* = 6.0 Hz, 2H), 1.42 (s, 9H) ppm.

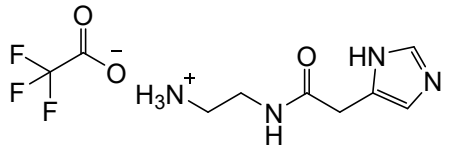

B101-En-NH_2·TFA

2-(2-(1H-imidazol-5-yl)acetamido)ethan-1-aminium **(B101-En-NH_2·TFA)**: **^{1}H NMR (400 MHz, Methanol-d_4, 300K) δ**: 8.83 (d, *J* = 1.5 Hz, 1H), 7.42 (s, 1H), 3.77 (s, 2H), 3.50 (t, *J* = 5.9 Hz, 2H), 3.08 (t, *J* = 5.9 Hz, 2H) ppm.

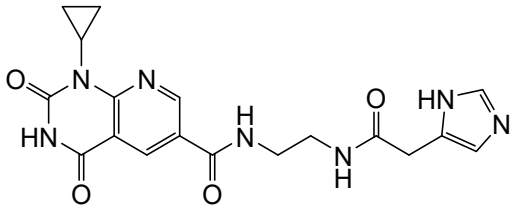

A61-En-B101

N-(2-(2-(1H-imidazol-5-yl)acetamido)ethyl)-1-cyclopropyl-2,4-dioxo-1,2,3,4-tetrahydropyrido[2,3-d]pyrimidine-6-carboxamide **(A61-En-B101)**: **^{1}H NMR (400 MHz, Methanol-d_4, 300K) δ**: 9.10 (d, *J* = 2.4 Hz, 1H), 8.81 (s, 1H), 8.74 (d, *J* = 2.4 Hz, 1H), 7.40 (s, 1H), 3.72 (s, 2H), 3.55 (t, *J* = 5.7 Hz, 2H), 3.46 (t, *J* = 5.8 Hz, 2H), 2.91 (tt, *J* = 7.2, 3.9 Hz, 1H), 1.26 – 1.19 (m, 2H), 0.92 – 0.85 (m, 2H) ppm.

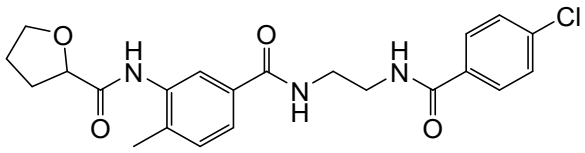

A12-En-B286

N-(5-((2-(4-chlorobenzamido)ethyl)carbamoyl)-2-methylphenyl)tetrahydrofuran-2-carboxamide **(A12-En-B286)**: **^{1}H NMR (400 MHz, DMSO-d_6, 300K) δ**: 9.29 (s, 1H), 8.68 (s, 1H), 8.55 (s, 1H), 7.89 – 7.78 (m, 3H), 7.58 (d, *J* = 7.9 Hz, 1H), 7.52 (d, *J* = 8.5 Hz, 2H), 7.29 (d, *J* = 7.9 Hz, 1H), 4.41 (dd, *J* = 8.3, 5.3 Hz, 1H), 4.01 (m, 1H), 3.83 (m, 1H), 3.47 – 3.36 (m, 4H), 2.19 (s, 4H), 1.99 (dq, *J* = 12.3, 6.3 Hz, 1H), 1.87 (p, *J* = 6.9 Hz, 2H) ppm.

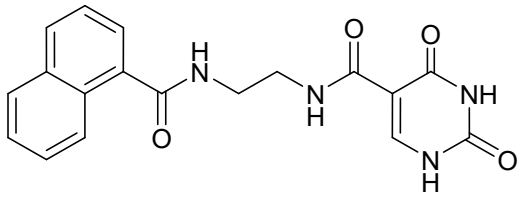

A7-En-B277

N-(2-(1-naphthamido)ethyl)-2,4-dioxo-1,2,3,4-tetrahydropyrimidine-5-carboxamide **(A7-En-B277)**: **^{1}H NMR (400 MHz, DMSO-d_6, 300K) δ**: 11.66 (s, 2H), 8.92 (t, *J* = 5.6 Hz, 1H), 8.60 (t, *J* = 5.2 Hz, 1H), 8.21 – 8.15 (m, 1H), 8.14 (s, 1H), 8.03 – 7.92 (m, 2H), 7.63 – 7.46 (m, 4H), 3.58 – 3.42 (m, 4H) ppm.

Synthesis of representative compounds (A45/B299 and A45/B145) attached to hexa-thymidine TTTTTT-C12-NH_2

The conjugates were synthesized following a reported procedure.[2]

1. TTTTTT-C12-NH-Mtt protecting group removal and linker installation

TTTTTT-C12-NH-Mtt, functionalized with a terminal 5'-amino modifier C12 and immobilized on controlled pore glass (CPG 500, 10^4 nmol, ~40 mg beads), was secured to a vacuum manifold. The solid support was sequentially washed with dichloromethane (DCM), acetonitrile (MeCN), and DCM (300 µL each, repeated three times). A 3% trichloroacetic acid (TCA) solution in DCM (200 µL) was then applied, incubated for 2 minutes, and eluted dropwise, followed by a DCM wash (300 µL). These steps were repeated six times, and successful Mtt group removal was confirmed via HPLC monitoring.

The solid support was subsequently rinsed with DCM (500 µL), MeCN (500 µL), and dimethylformamide (DMF; 300 µL). It was then treated with a freshly prepared reaction solution containing Fmoc-L-Dap(Mtt)-OH (50 mM), HATU (50 mM), and DIEA (150 mM) in DMF (300 µL) and allowed to react overnight at room temperature. **Note:** Stock solutions of the reagents were prepared immediately before use, and the mixture was activated for no more than 5 minutes prior to addition. After the reaction, the solution was removed, and the solid support was rinsed sequentially with DMF (300 µL), MeCN (300 µL), and DCM (2 × 1 mL). Linker installation with Mtt and Fmoc protecting groups was confirmed by HPLC.

2. TTTTTT-C12-Linker-NH_2 conjugation of carboxylic acid building block A (BB-A)

The Mtt group was removed from the linker using the protocol described above and rinsed with DCM (500 µL), MeCN (500 µL), and DMF (300 µL). Then, the solid support was treated with a reaction solution containing the carboxylic acid building block A (50 mM), HATU (50 mM), and DIEA (150 mM) in DMF (300 µL) and allowed to react overnight. The solution was removed, and the support was rinsed with DMF (300 µL), MeCN (300 µL), and DCM (2 × 1 mL), then dried under a stream of air. A small portion of the beads was taken for HPLC analysis to monitor BB-A coupling.

3. TTTTTT-C12-Linker-BB-A-NH_2 conjugation of carboxylic acid building block B (BB-B)

Following BB-A attachment, the Fmoc group was deprotected from the linker. The solid support was treated with diethylamine (Et_2NH) in MeCN (300 µL) for 5 minutes, repeated three times, followed by treatment with 20% piperidine in DMF (300 µL) for 10 minutes, repeated three times. A final flush with 500 µL of 20% piperidine completed the deprotection.

After deprotection, the solution was removed, and the support was rinsed sequentially with DMF (300 µL), MeCN (300 µL), DCM (300 µL), and DMF (300 µL). The solid support, now with a free -NH_2 group, was treated with a solution of carboxylic acid building block B (50 mM), HATU (50 mM), and DIEA (150 mM) in DMF (300 µL) and allowed to react overnight. The solution was removed, and the support was rinsed with DMF (300 µL), MeCN (300 µL), and DCM (2 × 1 mL), then dried under a stream of air.

4. DNA cleavage and purification

The DNA was cleaved from the solid support by exposure to a concentrated solution of NH_3/$MeNH_2$ (AMA; 1 mL) at room temperature for 1 hour. After centrifugation (2 minutes), the solution was diluted with an additional 1 mL of AMA and incubated for another hour to ensure complete removal of DNA-protecting groups. The AMA solution was removed using a centrifugal evaporator, and the residue was dissolved in water (200 µL). The DNA conjugates were purified by reverse-phase HPLC (solvent A: triethylammonium acetate (TEAA); solvent B: acetonitrile) and characterized by mass spectrometry (MS).

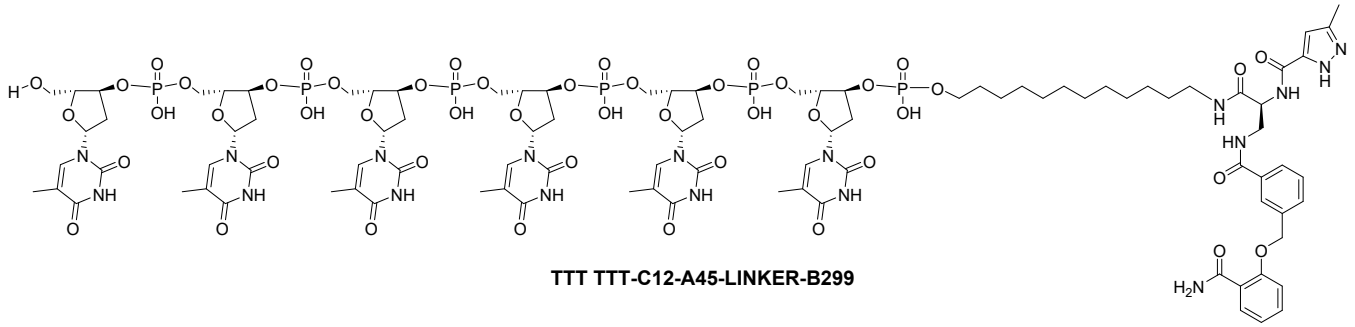

TTT TTT-C12-A45-LINKER-B299

ESI-TOF HRMS: *m*/*z* calcd for $C_{95}H_{126}N_{18}O_{48}P_6$ 2472.6398, found 2472.6398.

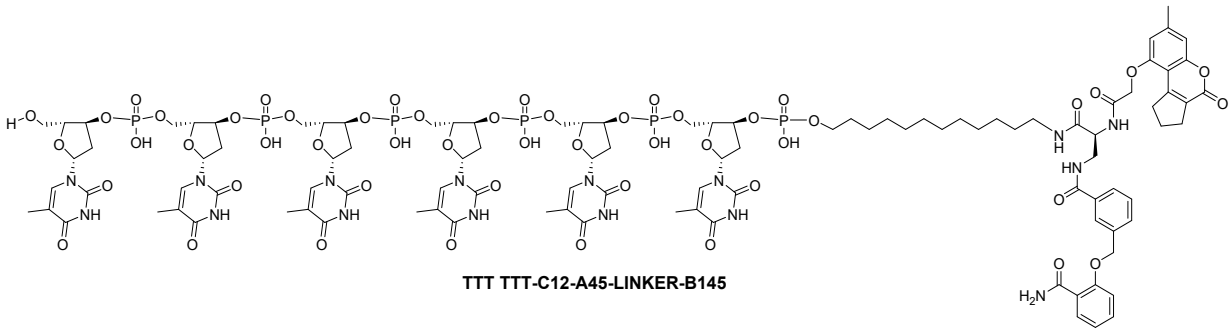

TTT TTT-C12-A45-LINKER-B145

ESI-TOF HRMS: *m*/*z* calcd for $C_{105}H_{134}N_{16}O_{51}P_6$ 2620.6810, found 2620.6819.

PROTAC-like compound intermediates

General procedures for linker synthesis:

D. Synthesis of A linkers:

Pomalidomide-chloroacetamide (203 mg, 0.58 mmol), K_2CO_3 (241 mg, 1.74 mmol, 3 eq.), KI (48 mg, 0.29 mmol, 0.5 eq.) and Boc-protected diamine (0.7 mmol, 1.2 eq.) were suspended in 20 mL acetonitrile in a screw-top vial with a septum. The vial was flushed with nitrogen and the mixture stirred at 70°C overnight. The mixture was concentrated on a rotavap, partitioned between H_2O (30 mL) and AcOEt (20 mL). The mixture was extracted 3x 20 mL AcOEt. The organic extracts were washed with brine, dried over $MgSO_4$, filtered and evaporated. The crude mixture was purified via FCC (SiO_2, DCM:MeOH). Linkers A contained a small amount of impurity that could not be removed by FCC and thus were used without further purification. The greenish color of the linkers can be removed by recrystallization from EtOH:heptane mixtures, although it does not improve purity (NMR).
The Boc-protected linker (approx. 0.25 mmol) was cooled in an ice bath in a small RB flask. There was added 1 mL of the deprotecting cocktail (TFA:thioanisole:*m*-cresol:H_2O 90:4:4:2, vol/vol). After 30 min, the mixture was poured into diethyl ether (24 mL) and the precipitated product was centrifuged. The precipitate was resuspended in Et_2O, mixed thoroughly, sonicated and centrifuged again. After brief vacuum drying, the precipitate was redissolved in hot isopropanol (2 mL) and precipitated again using 10 mL Et_2O. Precipitate was centrifuged again and vacuum dried (speed-vac). The yields of the linker TFA salts ranged between 43-85%.

E. Synthesis of B linkers:

Boc-aminoacid (0.249 mmol, 1 eq.), NHS (47 mg, 0.41 mmol, 1.5 eq.) and DMF (1 mL) were added to a screw-top vial followed by EDC·HCl (79 mg, 0.41 mmol, 1.5 eq.) and briefly stirred. After 5 min activation, a suspension of the deprotected linker B intermediate (0.273 mmol, 1.1 eq., TFA salt) and DIPEA (143 µL, 0.819 mmol, 3 eq.) in DMF was added to the mixture and stirring was continued overnight. DMF was co-evaporated with xylenes. Boc-protected linker was purified via FCC (DCM:MeOH 5%) and deprotected using 1 mL trifluoroacetic acid (TFA, 2.0 mL) solution containing 4% *m*-cresol, 4% thioanisole, and 2% water as additives. The products were precipitated with diethyl ether (24 mL) and separated via centrifugation.

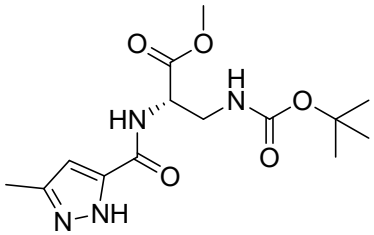

B299-DAP N-Boc Me ester

(S)-methyl 3-((tert-butoxycarbonyl)amino)-2-(3-methyl-1H-pyrazole-5-carboxamido)propanoate **(B299DAP N-Boc Me ester) ^{1}H NMR (400 MHz, CD_3OD, 300K) δ**: 6.50 (s, 1H), 4.65 (t, *J* = 5.7 Hz, 1H), 3.74 (s, 3H), 3.57 – 3.50 (m, 2H), 2.31 (s, 3H), 1.40 (s, 9H) ppm.

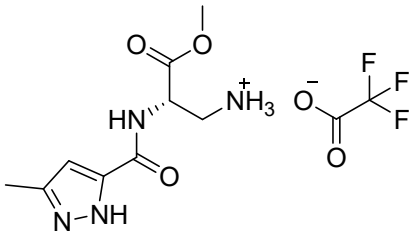

B299-DAP N-Boc Me ester TFA salt

(S)-3-methoxy-2-(3-methyl-1H-pyrazole-5-carboxamido)-3-oxopropan-1-aminium 2,2,2-trifluoroacetate **(B299 DAP Me ester TFA salt) ^{1}H NMR (400 MHz, CD_3OD, 300K) δ:** 6.52 (s, 1H), 3.79 (s, 3H), 3.57 – 3.48 (m, *J* = 13.2, 5.0 Hz, 1H), 3.39 – 3.32 (m, 1H), 2.32 (s, 3H) ppm.

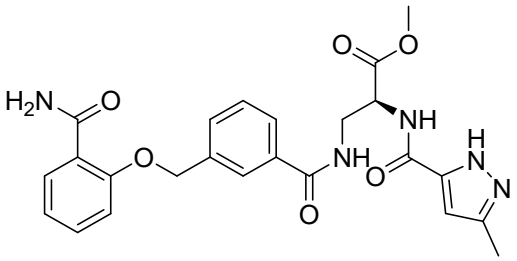

A45-DAP-B299 Me ester

(S)-methyl 3-(3-((2-carbamoylphenoxy)methyl)benzamido)-2-(3-methyl-1H-pyrazole-5-carboxamido)propanoate **(A45DAPB299 Me ester) ^{1}H NMR (400 MHz, CD_3OD, 300K) δ**: 8.15 (s, 1H), 8.04 – 7.89 (m, 3H), 7.80 – 7.70 (m, *J* = 9.8 Hz, 1H), 7.66 (d, *J* = 7.7 Hz, 1H), 7.55 – 7.42 (m, 3H), 7.20 (t, *J* = 7.6 Hz, 1H), 7.07 (t, *J* = 7.5 Hz, 1H), 6.47 (s, 1H), 5.33 (s, 1H), 5.29 (s, 2H), 3.96 – 3.80 (m, *J* = 13.9, 5.9 Hz, 2H), 3.75 (s, 3H), 3.20 (q, *J* = 7.3 Hz, 1H), 2.32 – 2.23 (m, 3H), 1.30 (t, *J* = 7.3 Hz, 1H) ppm.

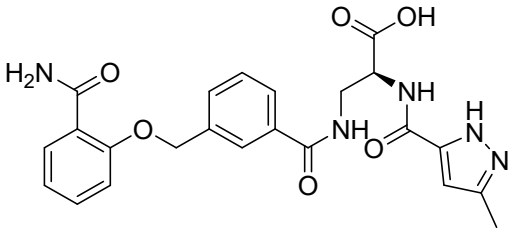

A45-DAP-B299

(S)-3-(3-((2-carbamoylphenoxy)methyl)benzamido)-2-(3-methyl-1H-pyrazole-5-carboxamido)propanoic acid **(A45-DAP-B299)**: **^{1}H NMR (400 MHz, DMSO-d_6, 300K) δ**: 8.75 (t, *J* = 5.8 Hz, 1H), 8.29 (d, *J* = 7.7 Hz, 1H), 7.94 (s, 1H), 7.77 (dd, *J* = 7.6, 1.3 Hz, 2H), 7.67 (d, *J* = 7.6 Hz, 1H), 7.58 (br. s, 1H), 7.54 – 7.40 (m, 3H), 7.20 (d, *J* = 8.3 Hz, 1H), 7.03 (t, *J* = 7.4 Hz, 1H), 6.38 (s, 1H), 5.29 (s, 2H), 4.59 (q, *J* = 6.3, 5.8 Hz, 1H), 3.73 (d, *J* = 5.8 Hz, 2H), 2.24 (s, 3H) ppm.

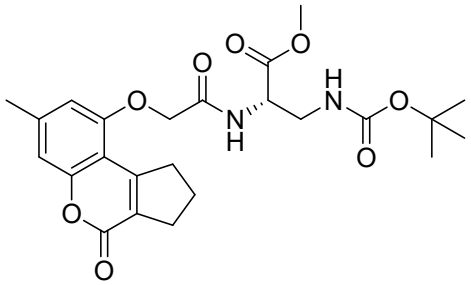

B145-DAP N-Boc Me ester

(S)-methyl 3-((tert-butoxycarbonyl)amino)-2-(2-((7-methyl-4-oxo-1,2,3,4-tetrahydrocyclopenta[c]chromen-9-yl)oxy)acetamido)propanoate **(A45DAPB145 N-Boc Me ester) ^{1}H NMR (400 MHz, CD_3OD, 300K) δ**: 6.79 (s, 1H), 6.66 (s, 1H), 4.68 (s, 1H), 4.64 – 4.57 (m, 2H), 3.76 (d, *J* = 10.3 Hz, 3H), 3.57 – 3.37 (m, 4H), 2.71 (t, *J* = 7.8 Hz, 2H), 2.38 (d, *J* = 9.5 Hz, 3H), 2.19 – 2.03 (m, 2H), 1.30 (s, 9H) ppm.

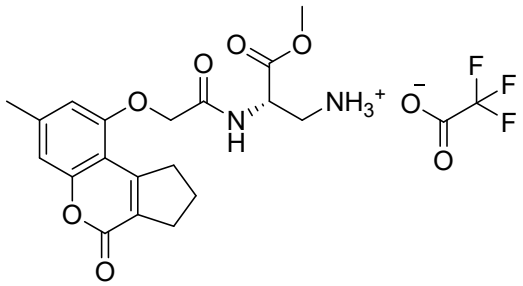

B145-DAP Me ester TFA salt

(S)-3-methoxy-2-(2-((7-methyl-4-oxo-1,2,3,4-tetrahydrocyclopenta[c]chromen-9-yl)oxy)acetamido)-3-oxopropan-1-aminium 2,2,2-trifluoroacetate **(A45DAP Me ester TFA salt) ^{1}H NMR (400 MHz, DMSO-d_6, 300K) δ**: 6.83 (s, 1H), 6.69 (s, 1H), 4.81 – 4.66 (m, 2H), 3.52 (dd, *J* = 13.3, 5.4 Hz, 1H), 3.41 (m, 2H), 2.76 – 2.66 (m, 2H), 2.41 (s, 3H), 2.24 (s, 1H), 2.12 (p, *J* = 7.8 Hz, 2H) ppm.

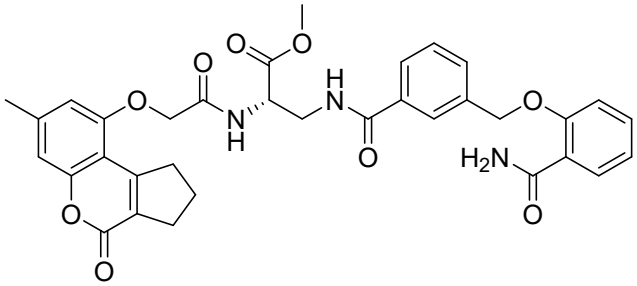

A45-DAP-B145 Me ester

(S)-methyl 3-(3-((2-carbamoylphenoxy)methyl)benzamido)-2-(2-((7-methyl-4-oxo-1,2,3,4-tetrahydrocyclopenta[c]chromen-9-yl)oxy)acetamido)propanoate **(A45-DAP-B145 Me ester) ^{1}H NMR (400 MHz, DMSO-d_6, 300K) δ**: 8.66 (t, *J* = 5.8 Hz, 1H), 8.45 (d, *J* = 7.5 Hz, 1H), 7.85 (s, 1H), 7.76 (dd, *J* = 7.7, 1.6 Hz, 1H), 7.67 (t, 2H), 7.56 (s, 1H), 7.53 – 7.37 (m, 4H), 7.17 (d, *J* = 8.3 Hz, 1H), 7.01 (t, *J* = 7.5 Hz, 1H), 6.77 (s, 1H), 6.64 (s, 1H), 5.25 (s, 2H), 4.72 – 4.52 (m, *J* = 16.3, 10.2 Hz, 4H), 3.63 (s, 3H), 3.29 (t, *J* = 7.6 Hz, 3H), 2.65 – 2.55 (m, 3H), 2.28 (s, 3H), 1.96 – 1.82 (m, *J* = 14.8, 7.1 Hz, 2H) ppm.

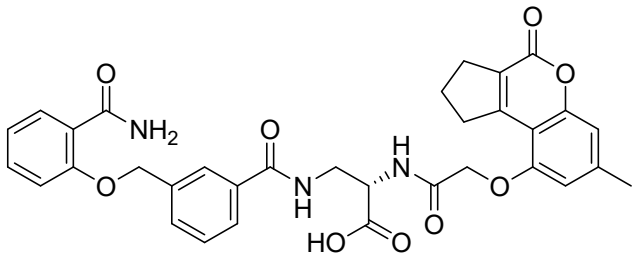

A45-DAP-B145

(*S*)-3-(3-((2-carbamoylphenoxy)methyl)benzamido)-2-(2-((7-methyl-4-oxo-1,2,3,4-tetrahydrocyclopenta[c]chromen-9-yl)oxy)acetamido)propanoic acid **(A45-DAP-B145)**: **^{1}H NMR (400 MHz, DMSO-d_6, 300K) δ**: 8.62 (t, *J* = 5.9 Hz, 1H), 8.32 (d, *J* = 7.6 Hz, 1H), 7.85 (s, 1H), 7.75 (dd, *J* = 7.7, 1.9 Hz, 1H), 7.66 (dd, *J* = 12.7, 7.6 Hz, 2H), 7.55 (br. s, 1H), 7.51 – 7.37 (m, 3H), 7.17 (d, *J* = 8.4 Hz, 1H), 7.01 (t, *J* = 7.5 Hz, 1H), 6.78 (s, 1H), 6.66 (s, 1H), 5.24 (s, 2H), 4.72 – 4.57 (m, 2H), 4.54 – 4.44 (m, 1H), 3.75 – 3.54 (m, 2H), 2.61 (t, *J* = 7.9 Hz, 2H), 2.27 (s, 3H), 2.01 – 1.83 (m, 2H) ppm.

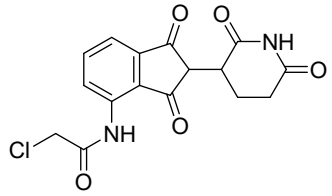

pomalidomide chloroacetamide

2-chloro-N-(2-(2,6-dioxopiperidin-3-yl)-1,3-dioxo-2,3-dihydro-1H-inden-4-yl)acetamide **(pomalidomide-chloroacetamide)** Chloroacetyl chloride was added to a suspension of pomalidomide in THF in a 50 ml RB flask. After 10 min of stirring, the mixture was heated to 50°C. Over the course of 1h, the mixture became pale, almost colorless, with off-white precipitate at the bottom. Heating and stirring continued for 6h, then THF was stripped on a rotavap. The mixture was suspended in water (20 ml) and AcOEt (20 ml) and sonicated. It was filtered and the precipitate washed with AcOEt. The precipitate thus obtained (off-white powder) weighed 1.877 g (94% yield) and was pure. **^{1}H NMR (400 MHz, DMSO-d_6, 300K) δ:** 11.14 (s, 1H), 10.29 (s, 1H), 8.52 (d, *J* = 8.4 Hz, 1H), 7.87 (t, *J* = 7.9 Hz, 1H), 7.67 (d, *J* = 7.3 Hz, 1H), 5.15 (dd, *J* = 12.7, 5.4 Hz, 1H), 4.52 (s, 1H), 2.94 – 2.80 (m, 2H), 2.65 – 2.51 (m, 2H), 2.10 – 2.00 (m, 2H) ppm.

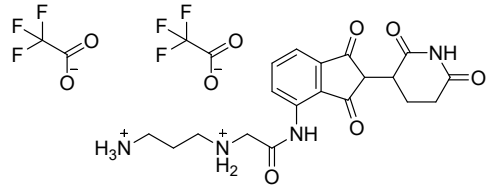

linker A3

2-((3-aminopropyl)amino)-N-(2-(2,6-dioxopiperidin-3-yl)-1,3-dioxo-2,3-dihydro-1H-inden-4-yl)acetamide **(linker A3 TFA salt)** Synthesized according to general procedure D, 0.24 g obtained (85% yield) **^{1}H NMR (400 MHz, DMSO-d_6)** δ 11.16 (s, 1H), 10.46 (s, 1H), 9.24 (s, 1H), 8.33 (s, 1H), 7.91 (t, *J* = 7.9 Hz, 1H), 7.73 (d, *J* = 7.3 Hz, 1H), 5.16 (dd, *J* = 12.8, 5.3 Hz, 1H), 4.12 (s, 2H), 3.05 (m, 2H), 2.91 (m, 3H), 2.71 – 2.53 (m, 2H), 2.15 – 2.03 (m, 1H), 2.03 – 1.75 (m, 2H) ppm.. **ESI+ MS:** *m/z* calculated 388.2, found 388.17.

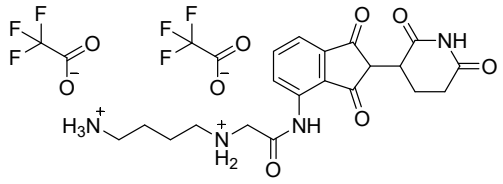

linker A4

N1-(2-((2-(2,6-dioxopiperidin-3-yl)-1,3-dioxo-2,3-dihydro-1H-inden-4-yl)amino)-2-oxoethyl)butane-1,4-diaminium 2,2,2-trifluoroacetate **(linker A4 TFA salt)** Synthesized according to general procedure D 0.142 g obtained 49% yield **^{1}H NMR (400 MHz, DMSO-d_6)** δ 11.14 (s, 1H), 10.40 (s, 1H), 9.16 (s, 2H), 8.28 (d, *J* = 8.3 Hz, 1H), 7.89 (t, 3H), 7.86 – 7.74 (m, 2H), 7.71 (d, *J* = 7.3 Hz, 1H), 5.13 (dd, *J* = 12.8, 5.4 Hz, 1H), 4.12 (s, 2H), 3.06 – 2.95 (m, 2H), 2.95 – 2.85 (m, *J* = 22.0, 9.3 Hz, 1H), 2.85 – 2.72 (m, *J* = 16.7 Hz, 3H), 2.66 – 2.50 (m, 2H), 2.11 – 1.99 (m, 1H), 1.74 – 1.50 (m, 6H) ppm. **ESI+ MS:** *m*/*z* calculated 402.2, found 402.18.

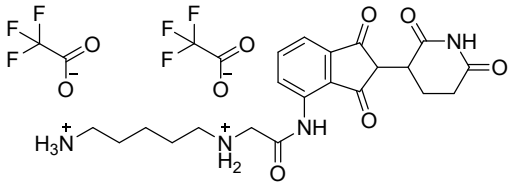

linker A5

N1-(2-((2-(2,6-dioxopiperidin-3-yl)-1,3-dioxo-2,3-dihydro-1H-inden-4-yl)amino)-2-oxoethyl)pentane-1,5-diaminium 2,2,2-trifluoroacetate **(linker A5 TFA salt)** Synthesized according to general procedure D, 0.22 g obtained (43% yield) **^{1}H NMR (400 MHz, DMSO-d_6)** δ 11.14 (s, 1H), 10.37 (s, 1H), 9.08 (s, 2H), 8.28 (d, *J* = 8.3 Hz, 1H), 7.89 (t, *J* = 7.9 Hz, 1H), 7.79 (s, 3H), 7.71 (d, *J* = 7.3 Hz, 1H), 5.13 (dd, *J* = 12.8, 5.4 Hz, 1H), 4.13 (s, 2H), 3.00 – 2.91 (m, *J* = 7.5 Hz, 2H), 2.91 – 2.82 (m, 1H), 2.82 – 2.71 (m, 2H), 2.65 – 2.50 (m, 2H), 2.10 – 2.02 (m, 1H), 1.68 – 1.58 (m, *J* = 15.4, 7.8 Hz, 2H), 1.58 – 1.48 (m, 2H), 1.38 – 1.28 (m, *J* = 14.8, 7.4 Hz, 2H) ppm. **ESI+ MS:** *m*/*z* calculated 416.2, found 416.28.

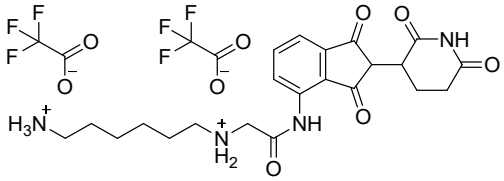

linker A6

N1-(2-((2-(2,6-dioxopiperidin-3-yl)-1,3-dioxo-2,3-dihydro-1H-inden-4-yl)amino)-2-oxoethyl)hexane-1,6-diaminium 2,2,2-trifluoroacetate (**linker A6 TFA salt**) **^{1}H NMR (400 MHz, DMSO-d_6)** δ 11.14 (s, 1H), 10.37 (s, 1H), 9.06 (s, 2H), 8.28 (d, *J* = 8.3 Hz, 1H), 7.89 (t, *J* = 7.8 Hz, 1H), 7.76 (s, 3H), 7.72 (d, *J* = 7.3 Hz, 1H), 5.13 (dd, *J* = 12.8, 5.4 Hz, 1H), 4.13 (s, 2H), 3.02 – 2.91 (m, 2H), 2.91 – 2.81 (m, 1H), 2.81 – 2.68 (m, *J* = 13.1, 6.4 Hz, 2H), 2.66 – 2.50 (m, 2H), 2.12 – 2.01 (m, 1H), 1.69 – 1.56 (m, 2H), 1.56 – 1.41 (m, 2H), 1.35 – 1.22 (m, 4H) ppm. **ESI+ MS:** *m*/*z* calculated 430.25, found 430.19.

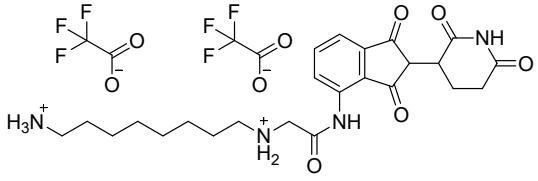

linker A8

N1-(2-((2-(2,6-dioxopiperidin-3-yl)-1,3-dioxo-2,3-dihydro-1H-inden-4-yl)amino)-2-oxoethyl)octane-1,8-diaminium 2,2,2-trifluoroacetate (**linker A8 TFA salt**) 0.244 g (44%) **^{1}H NMR (400 MHz, DMSO-d_6) δ** 11.16 (s, 1H), 10.36 (s, 1H), 8.98 (s, 2H), 8.28 (d, *J* = 8.1 Hz, 1H), 7.89 (t, *J* = 7.9 Hz, 1H), 7.72 (d, *J* = 7.3 Hz, 1H), 7.67 (s, 2H), 5.14 (dd, *J* = 12.8, 5.5 Hz, 1H), 4.12 (s, 2H), 2.99 – 2.90 (m, 2H), 2.90 – 2.82 (m, *J* = 4.8 Hz, 1H), 2.79 – 2.69 (m, *J* = 13.9,

6.5 Hz, 2H), 2.63 – 2.50 (m, *J* = 31.6, 11.3 Hz, 2H), 2.10 – 2.01 (m, 2H), 1.64 – 1.54 (m, 2H), 1.54 – 1.44 (m, 2H), 1.32 – 1.17 (m, 7H) ppm. **ESI+ MS:** *m*/*z* calculated 458.3, found 458.2.

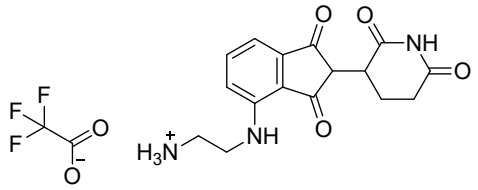

linker B2 intermediate

2-((2-(2,6-dioxopiperidin-3-yl)-1,3-dioxo-2,3-dihydro-1H-inden-4-yl)amino)ethanaminium 2,2,2-trifluoroacetate **(linker B2 intermediate)** Boc-ethylenediamine (0.7 g, 4.37 mmol, 1.1 eq.) was weighed into a 30 ml screw-top vial, followed by NMP (20 ml), DIPEA (2 ml, 1.484 g, 11.5 mmol, approx. 3 eq) and fluorothalidomide (1.1 g, 3.98 mmol, 1 eq). The vial was evacuated, filled with argon and held in an oil bath overnight at 90°C. Most of NMP was evaporated using Speed-vac. The mixture was redissolved in ethyl acetate (30 ml) on an ultrasound bath and water (10 ml) was added. The organic phase was extracted 5x15 ml H_2O to remove the remaining NMP, washed 1x15 ml brine and dried over $MgSO_4$. The solvent was stripped on a rotavap, and the product purified via FCC (DCM:MeOH 0-5%) providing yellow powder yield: (92 mg, 87%). The product was deprotected and precipitated as in general procedure D. Yellow powder (96%) **^{1}H NMR (500 MHz, DMSO-d_6)** δ 11.10 (s, 1H), 7.79 (s, 3H), 7.63 (t, *J* = 7.8 Hz, 1H), 7.18 (d, *J* = 8.6 Hz, 1H), 7.10 (d, *J* = 7.0 Hz, 1H), 6.83 (t, *J* = 5.5 Hz, 1H), 5.07 (dd, *J* = 12.7, 5.2 Hz, 1H), 3.62 – 3.52 (m, *J* = 5.9 Hz, 2H), 3.00 (s, 2H), 2.96 – 2.83 (m, 1H), 2.65 – 2.52 (m, 2H), 2.09 – 1.97 (m, 1H) ppm.

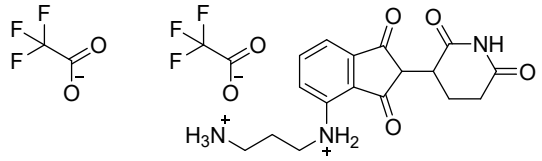

linker B3 intermediate

N1-(2-(2,6-dioxopiperidin-3-yl)-1,3-dioxo-2,3-dihydro-1H-inden-4-yl)propane-1,3-diaminium 2,2,2-trifluoroacetate **(linker B3 intermediate)** Compound was synthesized identically as (linker B2 intermediate) starting from N-Boc-diaminopropane (340 mg, 1.95 mmol)**.** Yellow powder, 43% yield. **^{1}H NMR (400 MHz, DMSO-d_6)** δ 11.08 (s, 1H), 7.70 (s, 2H), 7.64 – 7.51 (m, 1H), 7.12 (d, *J* = 8.6 Hz, 1H), 7.03 (d, *J* = 7.0 Hz, 1H), 6.74 (t, *J* = 6.2 Hz, 1H), 5.04 (dd, *J* = 12.7, 5.3 Hz, 1H), 3.42 – 3.36 (m, 2H), 2.92 – 2.79 (m, 3H), 2.62 – 2.50 (m, 1H), 2.06 – 1.95 (m, 1H), 1.81 (qnt, 2H) ppm.

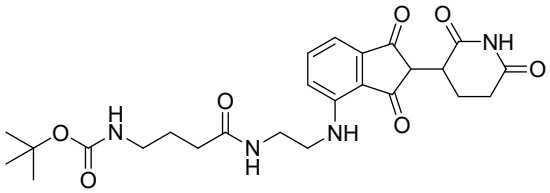

linker B2-3 N-Boc

tert-butyl (4-((2-((2-(2,6-dioxopiperidin-3-yl)-1,3-dioxo-2,3-dihydro-1H-inden-4-yl)amino)ethyl)amino)-4-oxobutyl)carbamate **(linker B2-3 N-Boc) ^{1}H NMR (400 MHz, $CDCl_3$)** δ 8.10 (s, 1H), 7.56 – 7.47 (m, 1H), 7.12 (d, *J* = 6.9 Hz, 1H), 7.01 (d, *J* = 8.5 Hz, 1H), 6.85 (d, *J* = 8.7 Hz, 1H), 6.60 (s, 1H), 6.44 (s, 1H), 4.91 (dd, *J* = 12.2, 5.2 Hz, 1H), 4.78 (s, 1H), 3.57 – 3.41 (m, 5H), 3.15 (m, 2H), 2.81 (m, 5H), 2.22 (t, *J* = 6.8 Hz, 2H), 2.13 (m, 2H), 1.79 (qnt, 2H), 1.76 (s, 1H), 1.42 (s, 9H) ppm.

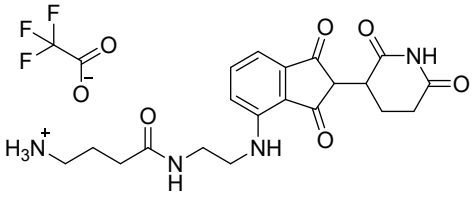

linker B2-3

4-((2-((2-(2,6-dioxopiperidin-3-yl)-1,3-dioxo-2,3-dihydro-1H-inden-4-yl)amino)ethyl)amino)-4-oxobutan-1-aminium 2,2,2-trifluoroacetate **(linker B2-3) ^{1}H NMR (400 MHz, DMSO-d_6, 300K) δ**: 11.06 (s, 1H), 8.13 (t, 1H), 7.65 (s, 1H), 7.57 (t, 1H), 7.15 (d, *J* = 8.6 Hz, 1H), 7.02 (d, *J* = 6.9 Hz, 1H), 6.71 (t, *J* = 6.0 Hz, 1H), 5.03 (dd, *J* = 12.7, 5.3 Hz, 1H), 3.41 – 3.33 (m, 2H), 3.27 – 3.20 (m, *J* = 5.7 Hz, 2H), 2.92 – 2.80 (m, 1H), 2.80 – 2.72 (m, *J* = 14.1, 6.4 Hz, 2H), 2.62 – 2.50 (m, *J* = 25.3, 13.6 Hz, 2H), 2.15 (t, *J* = 7.1 Hz, 2H), 2.04 – 1.95 (m, *J* = 10.9 Hz, 1H), 1.73 (qnt, *J* = 6.74 Hz, 2H), 1.02 (d, *J* = 6.1 Hz, 1H) ppm. **ESI+ MS:** *m*/*z* calculated 402.2, found 402.18.

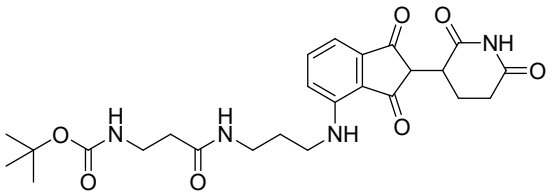

linker B3-2 N-Boc

tert-butyl (3-((3-((2-(2,6-dioxopiperidin-3-yl)-1,3-dioxo-2,3-dihydro-1H-inden-4-yl)amino)propyl)amino)-3-oxopropyl)carbamate **(linker B3-2 N-Boc) ^{1}H NMR (400 MHz, $CDCl_3$)** δ 8.22 (s, 1H), 7.50 (t, 1H), 7.10 (d, *J* = 7.1 Hz, 1H), 6.89 (d, *J* = 8.6 Hz, 1H), 6.40 (s, 1H), 6.07 (s, 1H), 5.14 (s, 1H), 4.93 (dd, *J* = 11.9, 5.3 Hz, 1H), 3.45 – 3.38 (m, 2H), 3.34 (dd, *J* = 12.1, 6.1 Hz, 2H), 2.94 – 2.67 (m, 4H), 2.45 – 2.36 (m, 2H), 2.15 – 2.08 (m, 2H), 1.90 – 1.80 (m, 2H), 1.42 (s, 9H) ppm.

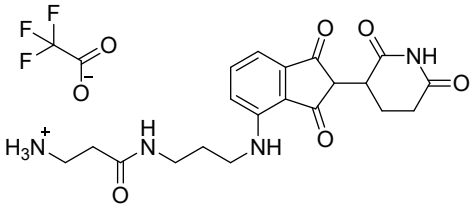

linker B3-2

3-((3-((2-(2,6-dioxopiperidin-3-yl)-1,3-dioxo-2,3-dihydro-1H-inden-4-yl)amino)propyl)amino)-3-oxopropan-1-aminium 2,2,2-trifluoroacetate **(linker B3-2)**.

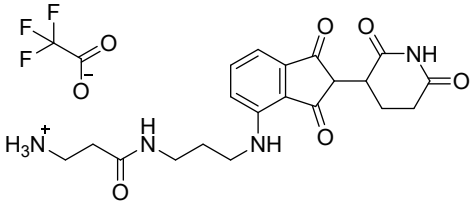

linker B3-3

3-((3-((2-(2,6-dioxopiperidin-3-yl)-1,3-dioxo-2,3-dihydro-1H-inden-4-yl)amino)propyl)amino)-3-oxopropan-1-aminium 2,2,2-trifluoroacetate **(linker B3-3)** was synthesized according to general procedure E. Yellow solid, yield (70%) **^{1}H NMR (400 MHz, DMSO-d_6)** δ 11.09 (s, 1H), 8.01 (t, *J* = 5.3 Hz, 1H), 7.76 (s, 3H), 7.57 (t, *J* = 7.8 Hz, 1H), 7.08 (d, *J* = 8.6 Hz, 1H), 7.02 (d, *J* = 6.9 Hz, 1H), 6.67 (t, *J* = 5.9 Hz, 1H), 5.04 (dd, *J* = 12.7, 5.3 Hz, 1H), 3.32 – 3.25 (m, *J* = 6.5 Hz, 2H), 3.12 (q, *J* = 12.2, 6.2 Hz, 2H), 2.93 – 2.71 (m, 3H), 2.63 – 2.51 (m, 2H), 2.18 (t, *J* = 7.1 Hz, 2H), 2.07 – 1.97 (m, 1H), 1.80 – 1.60 (m, 4H) ppm.

PROTAC-like compounds

F. Synthesis of PROTAC-like conjugates, linker A/B:

Acid **A45DAPB145** or **A45DAPB299** (approx. 8 µmol) was weighed out into a screw top vial. There was added NHS (1.4 mg, 12 µmol 1.5 eq.), followed by DMF (0.5 ml), DIEA (4.5 mg, 34 µmol, 4.25 eq., 6 µL) and EDC·HCl (2.3 mg, 12 µmol 1.5 eq.). After 5 min preactivation, the 'linker A/B' was added as a TFA salt (8 µmol, 1 eq.). The mixture was stirred overnight, and the progress of the reaction monitored by HPLC. The reaction mixture was evaporated on a rotavap (<10 mbar). The residue was dissolved in 100 µL od DMSO, diluted with 200 µL MeOH and the mixture was filtered through a spin column. The column was washed with 200 µL MeOH and the combined solution was directly used for C18 HPLC purification. Yields ranged from 8-82% and were typically higher for A45DAPB299.

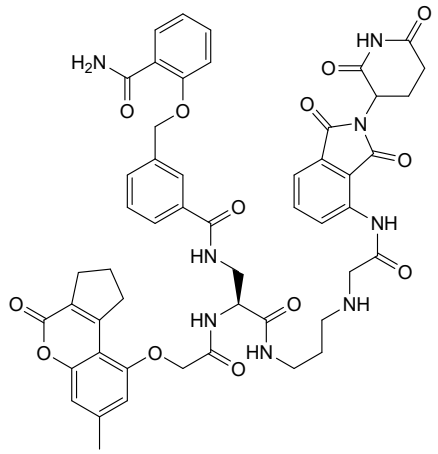

A45DAPB145 linker A3

3-((2-carbamoylphenoxy)methyl)-N-((2S)-3-((3-((2-((2-(2,6-dioxopiperidin-3-yl)-1,3-dioxoisoindolin-4-yl)amino)-2-oxoethyl)amino)propyl)amino)-2-(2-((7-methyl-4-oxo-1,2,3,4-tetrahydrocyclopenta[c]chromen-9-yl)oxy)acetamido)-3-oxopropyl)benzamide **(A45DAPB145-A3)** was synthesized according to general procedure F. **ESI+ MS:** *m/z* calculated 983.4, found 983.4.

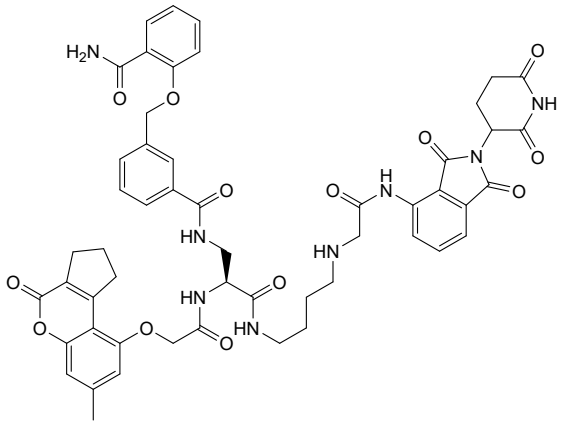

A45DAPB145 linker A4

3-((2-carbamoylphenoxy)methyl)-N-((2S)-3-((4-((2-((2-(2,6-dioxopiperidin-3-yl)-1,3-dioxoisoindolin-4-yl)amino)-2-oxoethyl)amino)butyl)amino)-2-(2-((7-methyl-4-oxo-1,2,3,4-tetrahydrocyclopenta[c]chromen-9-yl)oxy)acetamido)-3-oxopropyl)benzamide **(A45DAPB145-A4)** was synthesized according to general procedure F. Yield: 1 mg (8%) **ESI+ MS:** *m/z* calculated 997.4, found 997.4.

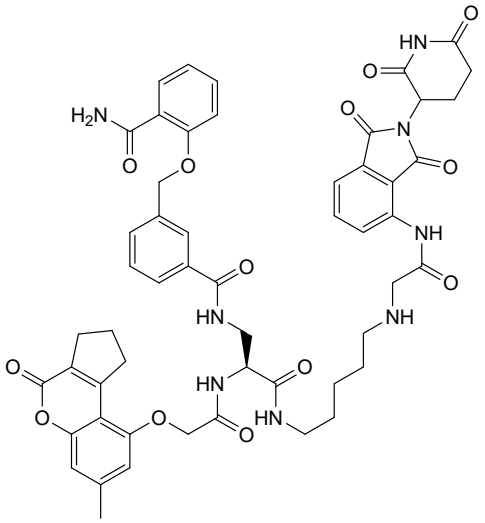

A45DAPB145 linker A5

3-((2-carbamoylphenoxy)methyl)-N-((2S)-3-((5-((2-((2-(2,6-dioxopiperidin-3-yl)-1,3-dioxoisoindolin-4-yl)amino)-2-oxoethyl)amino)pentyl)amino)-2-(2-((7-methyl-4-oxo-1,2,3,4-tetrahydrocyclopenta[c]chromen-9-yl)oxy)acetamido)-3-oxopropyl)benzamide **(A45DAPB145-A5)** was synthesized according to general procedure F, yield: 3.1 mg (26%) **ESI+ MS:** *m/z* calculated 1011.4, found 1011.5.

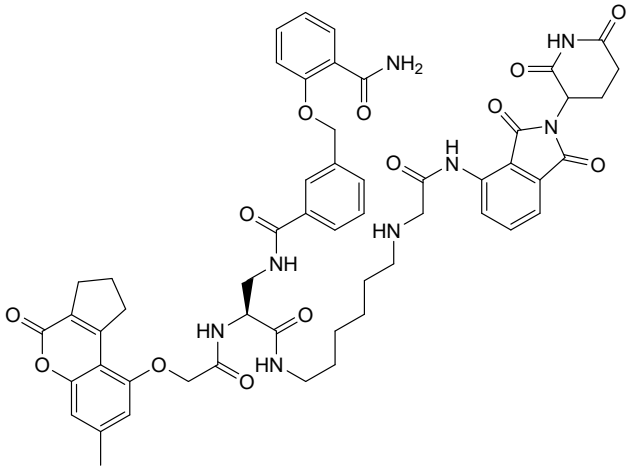

A45DAPB145 linker A6

3-((2-carbamoylphenoxy)methyl)-N-((2S)-3-((6-((2-((2-(2,6-dioxopiperidin-3-yl)-1,3-dioxoisoindolin-4-yl)amino)-2-oxoethyl)amino)hexyl)amino)-2-(2-((7-methyl-4-oxo-1,2,3,4-tetrahydrocyclopenta[c]chromen-9-yl)oxy)acetamido)-3-oxopropyl)benzamide **(A45DAPB145-A6) ESI+ MS:** *m/z* calculated 1025.4, found 1025.5.

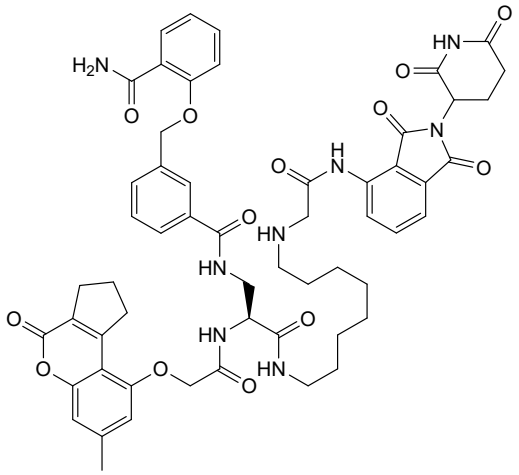

A45DAPB145 linker A8

3-((2-carbamoylphenoxy)methyl)-N-((2S)-3-((8-((2-((2-(2,6-dioxopiperidin-3-yl)-1,3-dioxoisoindolin-4-yl)amino)-2-oxoethyl)amino)octyl)amino)-2-(2-((7-methyl-4-oxo-1,2,3,4-tetrahydrocyclopenta[c]chromen-9-yl)oxy)acetamido)-3-oxopropyl)benzamide **(A45DAPB145-A8) ESI+ MS:** *m/z* calculated 1053.4, found 1053.5.

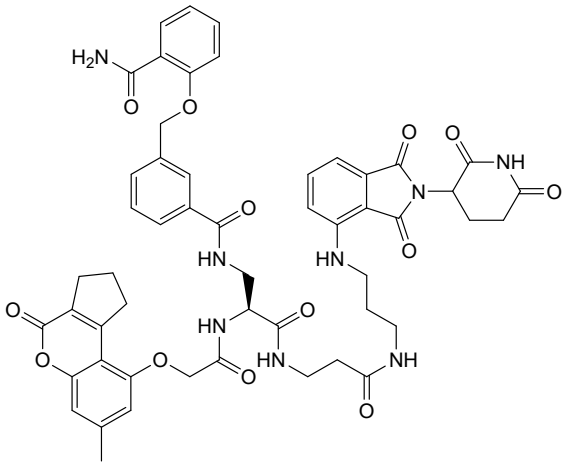

A45DAPB145 linker B3/2

3-((2-carbamoylphenoxy)methyl)-N-((2S)-3-((3-((3-((2-(2,6-dioxopiperidin-3-yl)-1,3-dioxoisoindolin-4-yl)amino)propyl)amino)-3-oxopropyl)amino)-2-(2-((7-methyl-4-oxo-1,2,3,4-tetrahydrocyclopenta[c]chromen-9-yl)oxy)acetamido)-3-oxopropyl)benzamide **(A45DAPB145-B3/2)** was synthesized according to general procedure F, yield: 6.1 mg (67%) **ESI+ MS:** *m*/*z* calculated 997.4, found 997.3.

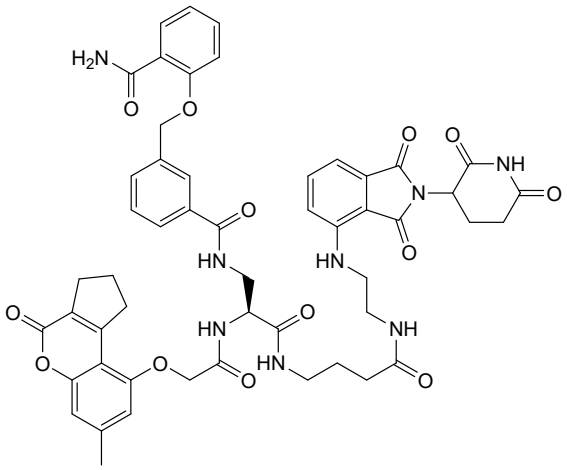

A45DAPB145 linker B2/3

3-((2-carbamoylphenoxy)methyl)-N-((2S)-3-((4-((2-((2-(2,6-dioxopiperidin-3-yl)-1,3-dioxoisoindolin-4-yl)amino)ethyl)amino)-4-oxobutyl)amino)-2-(2-((7-methyl-4-oxo-1,2,3,4-tetrahydrocyclopenta[c]chromen-9-yl)oxy)acetamido)-3-oxopropyl)benzamide **(A45DAPB145-B2/3)** was synthesized according to general procedure F, yield: 5.5 mg (53%) **ESI+ MS:** *m*/*z* calculated 997.4, found 997.3.

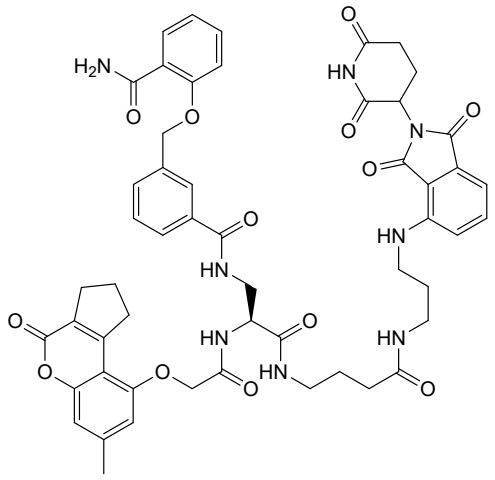

A45DAPB145 linker B3/3

3-((2-carbamoylphenoxy)methyl)-N-((2S)-3-((4-((3-((2-(2,6-dioxopiperidin-3-yl)-1,3-dioxoisoindolin-4-yl)amino)propyl)amino)-4-oxobutyl)amino)-2-(2-((7-methyl-4-oxo-1,2,3,4-tetrahydrocyclopenta[c]chromen-9-yl)oxy)acetamido)-3-oxopropyl)benzamide **(A45DAPB145-B3/3)** was synthesized according to general procedure F, yield: 4.2 mg (46%).

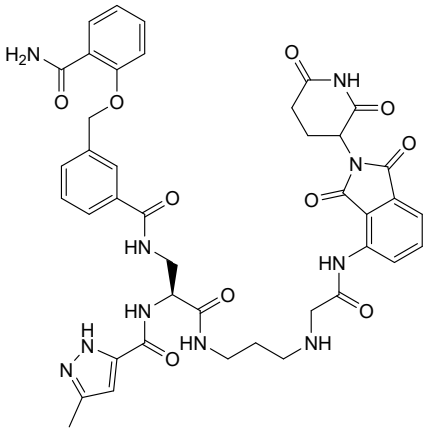

A45DAPB299 linker A3

N-((2S)-3-(3-((2-carbamoylphenoxy)methyl)benzamido)-1-((3-((2-((2-(2,6-dioxopiperidin-3-yl)-1,3-dioxoisoindolin-4-yl)amino)-2-oxoethyl)amino)propyl)amino)-1-oxopropan-2-yl)-3-methyl-1H-pyrazole-5-carboxamide **(A45DAPB299 linker A3)** was synthesized according to general procedure F, yield 5.1 mg (52%) **ESI+ MS:** *m/z* calculated 835.3, found 835.41.

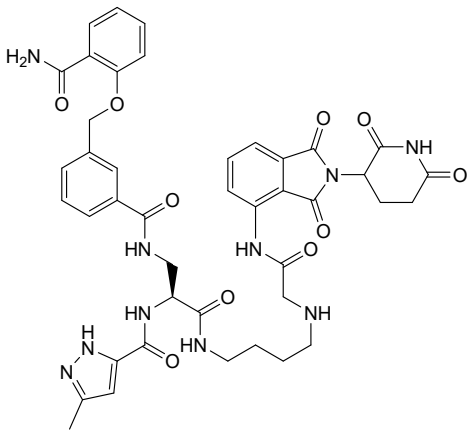

A45DAPB299 linker A4

N-((2S)-3-(3-((2-carbamoylphenoxy)methyl)benzamido)-1-((4-((2-((2-(2,6-dioxopiperidin-3-yl)-1,3-dioxoisoindolin-4-yl)amino)-2-oxoethyl)amino)butyl)amino)-1-oxopropan-2-yl)-3-methyl-1H-pyrazole-5-carboxamide **(A45DAPB299-A4)** was synthesized according to general procedure F, yield 5.4 mg (51%) **ESI+ MS:** *m/z* calculated 849.3, found 849.41.

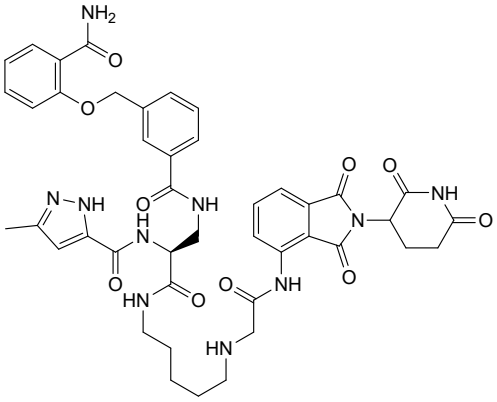

A45DAPB299 linker A5

N-((2S)-3-(3-((2-carbamoylphenoxy)methyl)benzamido)-1-((5-((2-((2-(2,6-dioxopiperidin-3-yl)-1,3-dioxoisoindolin-4-yl)amino)-2-oxoethyl)amino)pentyl)amino)-1-oxopropan-2-yl)-3-methyl-1H-pyrazole-5-carboxamide **(A45DAPB299-A5)** was synthesized according to general procedure F, yield 4.3 mg (40%) **ESI+ MS:** *m/z* calculated 863.3, found 863.41.

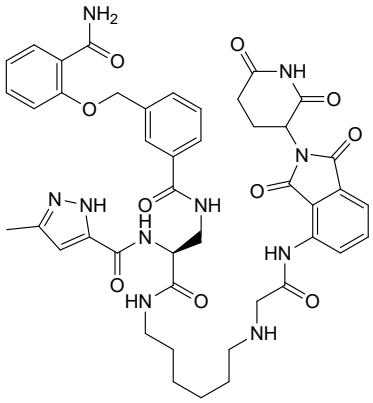

A45DAPB299 linker A6

N-((2S)-3-(3-((2-carbamoylphenoxy)methyl)benzamido)-1-((6-((2-((2-(2,6-dioxopiperidin-3-yl)-1,3-dioxoisoindolin-4-yl)amino)-2-oxoethyl)amino)hexyl)amino)-1-oxopropan-2-yl)-3-methyl-1H-pyrazole-5-carboxamide **(A45DAPB299-A6)** was synthesized according to general procedure F, yield 7.8 mg (47%) **ESI+ MS:** *m/z* calculated 877.4, found 877.41.

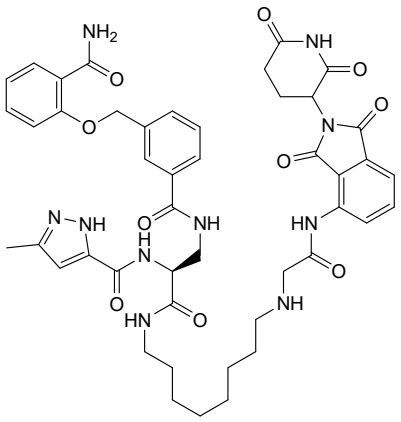

A45DAPB299 linker A8

N-((2S)-3-(3-((2-carbamoylphenoxy)methyl)benzamido)-1-((8-((2-((2-(2,6-dioxopiperidin-3-yl)-1,3-dioxoisoindolin-4-yl)amino)-2-oxoethyl)amino)octyl)amino)-1-oxopropan-2-yl)-3-methyl-1H-pyrazole-5-carboxamide **(A45DAPB299-A8)** was synthesized according to general procedure F, yield 8.6 mg (52%) **ESI+ MS:** *m*/*z* calculated 905.4, found 905.51.

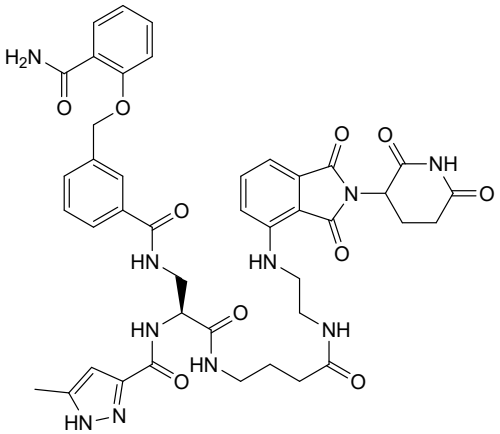

A45DAPB299 linker B2/3

N-((2S)-3-(3-((2-carbamoylphenoxy)methyl)benzamido)-1-((4-((2-((2-(2,6-dioxopiperidin-3-yl)-1,3-dioxoisoindolin-4-yl)amino)ethyl)amino)-4-oxobutyl)amino)-1-oxopropan-2-yl)-5-methyl-1H-pyrazole-3-carboxamide **(A45DAPB299-B2/3)** was synthesized according to general procedure F, yield 6 mg (65%) **ESI+ MS:** *m*/*z* calculated 849.3, found 849.11.

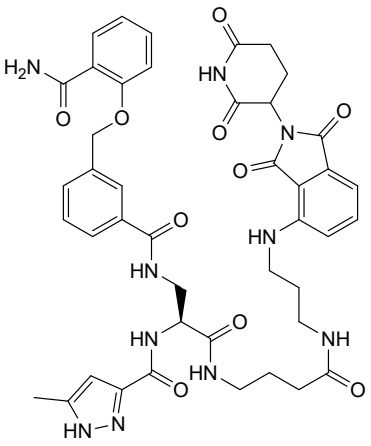

A45DAPB299 linker B3/3

N-((2S)-3-(3-((2-carbamoylphenoxy)methyl)benzamido)-1-((3-((3-((2-(2,6-dioxopiperidin-3-yl)-1,3-dioxoisoindolin-4-yl)amino)propyl)amino)-3-oxopropyl)amino)-1-oxopropan-2-yl)-5-methyl-1H-pyrazole-3-carboxamide **(A45DAPB299-B3/2)** was synthesized according to general procedure F, yield 6.8 mg (82%).

Protocol for NADEL library selections[3, 4]

Affinity selections were run in duplicates on 96-well plates using KingFisher Duo Prime magnetic particle dispenser. Dynabeads™ His-Tag Isolation and Pulldown (8.64 µL in 100 µL of the buffer per experiment) were used for the selections. Two protein concentrations were used: 1.6 µM and 3.2 µM. The solutions were prepared from a 6His-tagged PARP2 stock (MW = 43,419 Da) at 2.5 mg/mL (57 µM). The selections were run in 20 mM HEPES buffer (pH = 7.5) containing 300 mM NaCl, 10% glycerol, 0.5 mM TCEP. Library was incubated with the beads at 10 nM, 100 µL total volume.

The following program was used: Beads pick-up: 30 s; protein incubation: 30 min; wash 1: 3 min; wash 2: 3 min; wash 3: 3 min; DEL incubation 1h; wash 1': 30s; wash 2': 30s; wash 3': 30s; wash 4': 30s; wash 5': 30s; elution: 30min. The experiments were run at room temperature.

The beads were removed, washed with buffer, and incubated with elution buffer (Buffer EB; Qiagen). DNA conjugates were released by heat denaturation of the proteins (96 °C for 5 min). The coding DNAs of the oligonucleotide conjugates were amplified by PCR after selection experiments and submitted to the University of Utah-HCI, Genomics Core for high-throughput DNA sequencing on an Illumina HiSeq 2000/2500.

Protocol for enzymatic activity of recombinant PARP1/2 and TNKS1/2 enzymes by using an *in vitro* enzymatic assay.

Assay Conditions:

Single concentration measurements and inhibition assays for hit compounds were performed by BPS Biosciences (San Diego, CA) following the BPS PARP assay protocol. The enzymatic reactions were performed in duplicate at room temperature for 1 hour using a 96-well plate pre-coated with histone substrate. Each 50 µL reaction mixture, prepared in PARP assay buffer, contained the substrate, +/- activated DNA, enzyme, and test or control compound (refer to Supporting Table 1). **Note:** Test and control compounds were initially prepared as 10 mM stock solutions in DMSO and subsequently diluted with assay buffer to achieve a final DMSO concentration of 1% in all reactions. Following the 60-minute incubation at room temperature, the wells were washed five times with PBST (phosphate-buffered saline containing Tween 20). Subsequently, 50 µL of streptavidin-horseradish peroxidase (prepared in blocking buffer) was added to each well, and the plate was incubated at room temperature for an additional 30 minutes. After this incubation, the wells were washed again, and 100 µL of ELISA ECL substrate was added to each well. Luminescence was measured using a BioTek Synergy™ 2 microplate reader.

Data Analysis:

PARP and TNKS activity assays were conducted in duplicate. Luminescence data were analyzed using GraphPad Prism software. In each dataset, luminescence in the absence of the test compound (Lt) was defined as 100% activity, while luminescence in the absence of PARP or TNKS (Lb) was defined as 0% activity. The percentage activity in the presence of each compound was calculated using the equation:

$$\textbf{\% Activity} = [(L - Lb) / (Lt - Lb)] \times 100$$

where L represents the luminescence in the presence of the compound. Subsequently, the percentage inhibition was determined as:

$$\textbf{\% Inhibition} = 100 - \% \text{ Activity}$$

The percentage activity values across various compound concentrations were plotted and analyzed using nonlinear regression to fit a sigmoidal dose-response curve, described by the equation:

$$\textbf{Y} = \text{Bottom} + (\text{Top} - \text{Bottom}) / (1 + 10\text{^}((\text{LogEC50} - X) * \text{HillSlope}))$$

In this equation, Y represents the percent activity, Bottom is the minimum percent activity, Top is the maximum percent activity, X denotes the logarithm of the compound concentration, LogEC50 is the logarithm of the concentration that yields half-maximal activity, and HillSlope (or Hill coefficient) indicates the steepness of the curve. The IC50 value, representing the concentration at which there is 50% inhibition, was determined from this analysis.

Supporting Table 1. Commercial chemiluminescent assay, proteins, and reagents for hit validation.

Enzyme/Control Compound	Catalog # (Lot #)	Substrate / Activated DNA	Supplier, Assay Kit Catalog #
PARP1	80501 (220210-1-D)	13.5 µM NAD/1.5 µM Biotin-NAD / 625 ng/ml	BPS Bioscience, #80551
PARP2	80502 (230317-2)	27 µM NAD/3 µM Biotin-NAD / 625 ng/ml	BPS Bioscience, #80552
TNKS1	80504 (210316-3)	60 µM NAD/30 µM Biotin-NAD / N/A	BPS Bioscience, #80573
TNKS2	80505 (221209-G1)	15 µM NAD/7.5 µM Biotin-NAD / N/A	BPS Bioscience, #80578
Olaparib	O-9201		LC Laboratories
AZD-5305	HY-132167		MedChemExpress
XAV-939	13596		Cayman Chemical

Supporting Table 2. Determination of false-positive rates for NADEL hits of the enzymes PARP1, PARP2, TNKS1, and TNKS2. Activity is defined as >50% inhibition at c = 10 µM. Original results are presented in Yuen et al. *J. Am. Chem. Soc.* 2019, 141, 5169, Montoya et al. *Eur. J. Med. Chem.* 2023, 246, 114980, and this manuscript.

NADEL hit	Structure	Target protein	Active
A11/B101	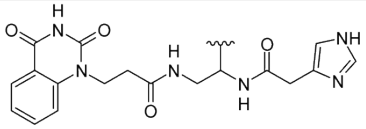	PARP1	Yes
A11/B111	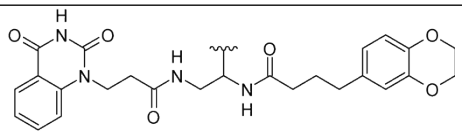	PARP2	Yes
A11/B139	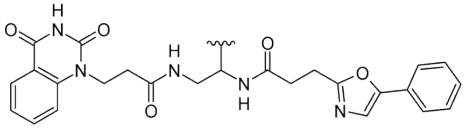	PARP2	Yes
A11/B227	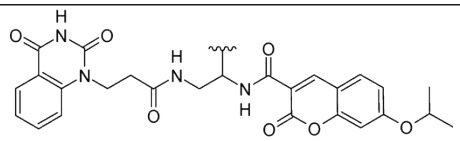	TNKS1/TNKS2/PARP2	Yes
A11/B141	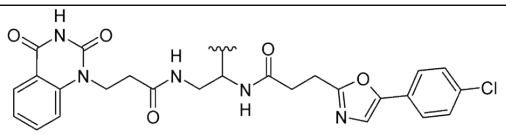	TNKS1/TNKS2/PARP2	Yes
A11/B151	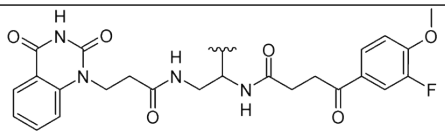	TNKS1/TNKS2/PARP2	Yes
A11/B152	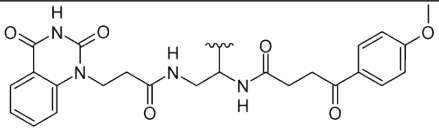	TNKS1/TNKS2/PARP2	Yes
A11/B182	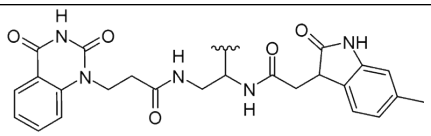	TNKS1	Yes
A11/B184	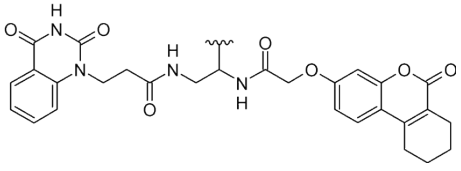	TNKS1/TNKS2	Yes
A11/B193	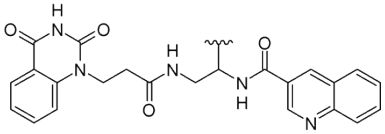	PARP2/TNKS1/TNKS2	Yes

A11/B21	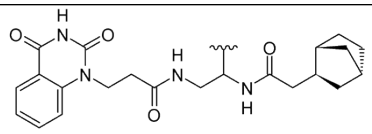	PARP2	Yes
A11/B227	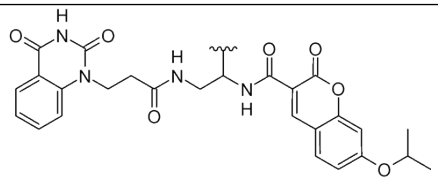	PARP2	Yes
A11/B255	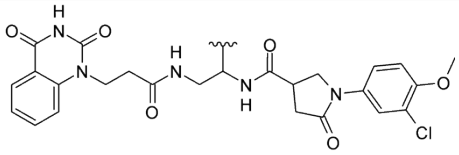	TNKS1/TNKS2/PARP2	Yes
A11/B330	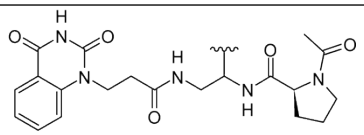	TNKS1/TNKS2/PARP2	No
A11/B77	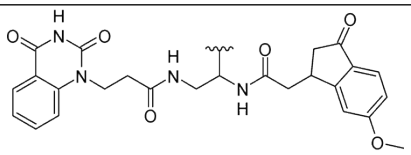	TNKS1/TNKS2/PARP2	Yes
A131/B199	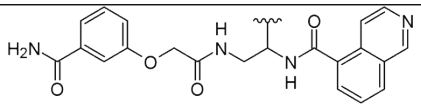	PARP2	Yes
A131/B355	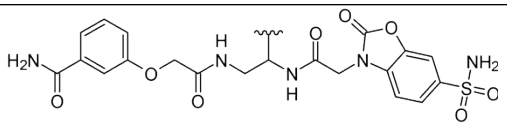	PARP2	Yes
A152/B346	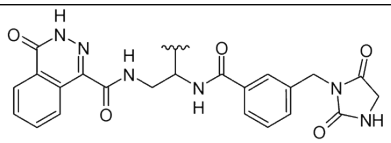	TNKS1	Yes
A153/B356	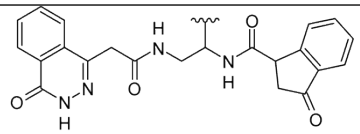	TNKS1	Yes
A153/B316	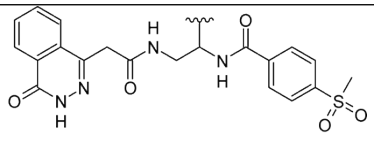	PARP2	Yes
A23/B184	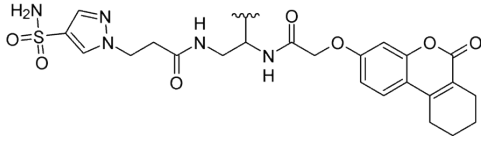	PARP1	Yes

A44/B190	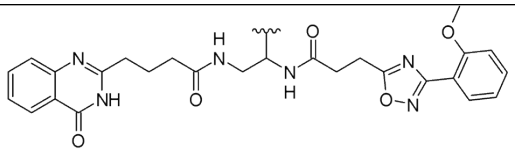	PARP1	Yes
A45/B145	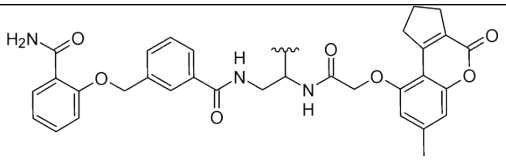	TNKS1	Yes
A45/B295	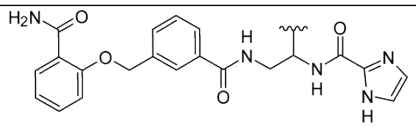	PARP1	Yes
A45/B299	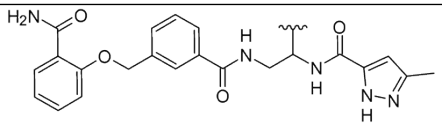	PARP2	Yes
A45/B304	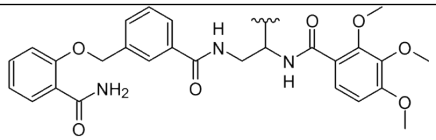	PARP2	Yes
A61/B101	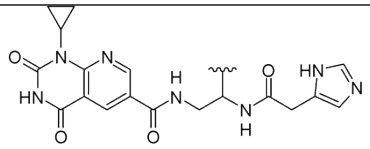	PARP2	No
A65/B101	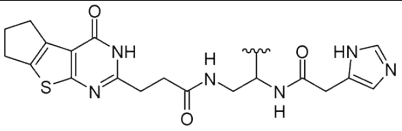	PARP1	Yes
A65/B101	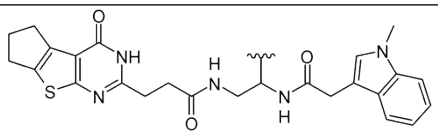	PARP1	Yes
A88/B354	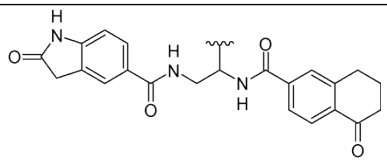	TNKS2	Yes
A96/B101	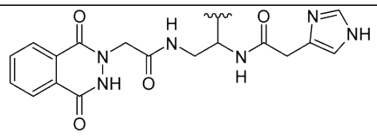	PARP1	Yes
A96/B122	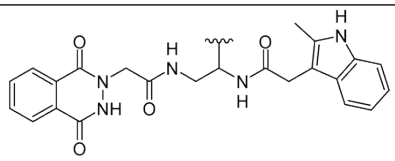	PARP2	Yes

A96/B213	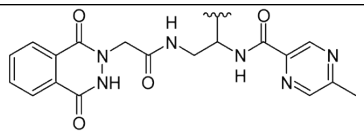	TNKS1	**Yes**
A96/B330	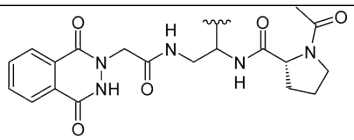	TNKS1/TNKS2	**Yes**

Supporting Table 3. Structures of tested molecules in Figure 3 and percent inhibition of PARP2 at different concentrations.

Hit	BB A	BB B	Category	% inhibition, PARP2			
				5nM	50nM	500nM	10^4nM
A108/B21	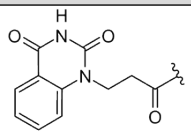	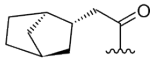	1	0	34	91	100
A108/B111	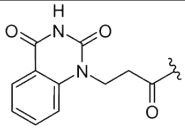	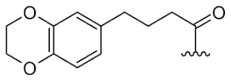	1	0	60	98	100
A108/B139	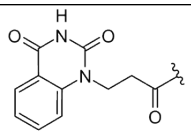	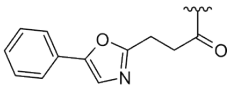	1	7	50	98	100
A108/B227	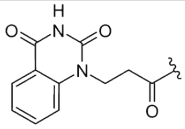	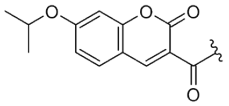	1	n.d.	5	80	100
A108/B193[a]	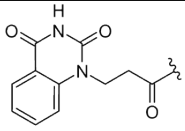	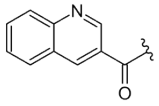	1	25	81	87	100
A45/B299	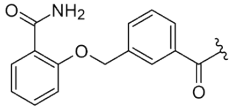	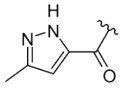	1	38	99	100	100
A45/B304	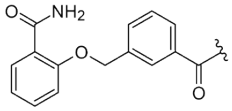	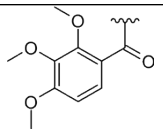	1	n.d.	36	93	100
A96/B122	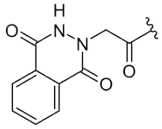	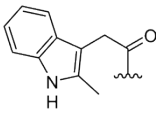	1	n.d.	18	79	100
A153/B316		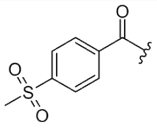	1	n.d.	13	58	100
A61/B101	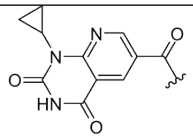	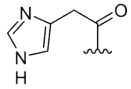	1	n.d.	n.d.	8	37
A131/B199	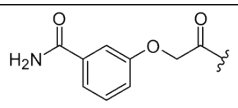	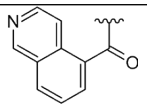	1	n.d.	n.d.	15	90

A131/B355		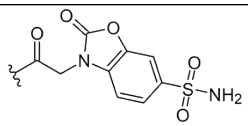	1	n.d.	n.d.	9	94
A108/B101			2	n.d.	0	64	100
A108/B182		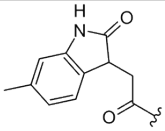	2	n.d.	9	88	100
A45/B145		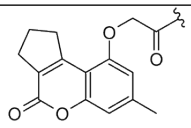	2	8	79	99	100
A45/B295		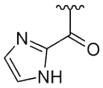	2	58	99	100	100
A96/B101	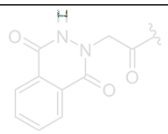		2	n.d.	n.d.	36	100
A96/B213		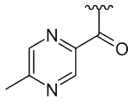	2	n.d.	0	52	100
A153/B356		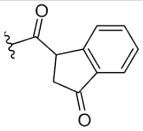	2	n.d.	28	89	100
A108/Ac			4	n.d.	12	62	100
A108/Bz		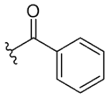	4	n.d.	25	95	100
A45/Ac			4	13	78	99	100
A96/Bz		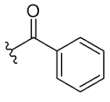	4	n.d.	0	46	100

A23/B184[b]	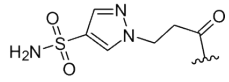	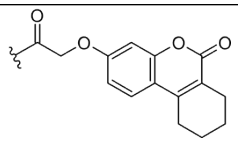	3	n.d.	n.d.	6	93
A44/B190[b]	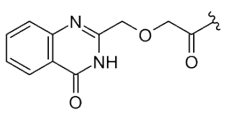	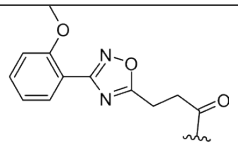	3	n.d.	n.d.	22	98
A65/B101[a]	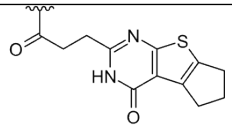		3	3	40	70	100
A152/B346	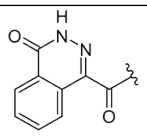	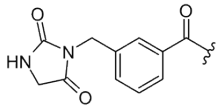	3	n.d.	3	51	100
A88/B354	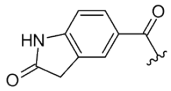	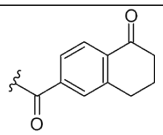	3	n.d.	n.d.	1	68
A7/B277	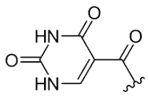	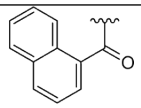	5	n.d.	n.d.	n.d.	54
A12/B286	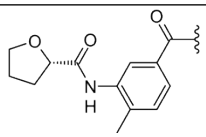	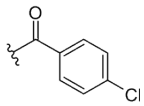	5	n.d.	n.d.	n.d.	16
A82/B354	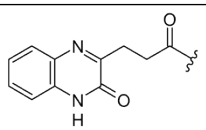	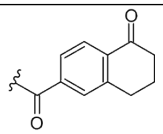	5	n.d.	n.d.	n.d.	0
A101/B322	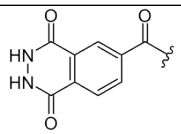	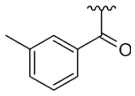	5	n.d.	n.d.	n.d.	0
A127/B178	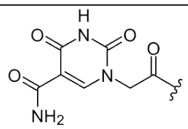	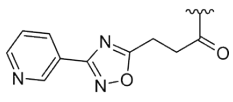	5	n.d.	n.d.	n.d.	16

Structures contain an ethylenediamine linker between the two carboxylic acid building blocks, except for structures labeled [a] that contain a methylcarboxamide derivative and [b] that contain a carboxamide derivative on this linker.

Supporting Table 4. Selectivity of selected compounds. Values in table correspond to percent inhibition of the indicated enzyme at the given concentration.

	PARP1				**PARP2**				**TNKS1**				**TNKS2**			
c[nM]	5	50	500	10^4	5	50	500	10^4	5	50	500	10^4	5	50	500	10^4
A45/B299	5	17	67	100	38	99	100	100	85	100	100	100	82	100	100	100
A108/B21	0	7	22	86	0	60	98	100	0	2	5	83	0	17	59	99
A108/B111	0	0	15	90	0	34	91	100	0	10	14	47	0	18	12	75

Supporting Table 5. Structures of hybrid molecules and percent inhibition of PARP2 at different concentrations.

Hit	BB A	BB B	Category	% inhibition, PARP2			
				5nM	50nM	500nM	10^4nM
A45/B21	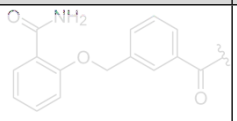		Potent_Low Selectivity	n.d.	69	n.d.	n.d.
A45/B111	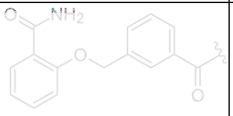		Potent_Low Selectivity	n.d.	78	n.d.	n.d.
A45/B111-A	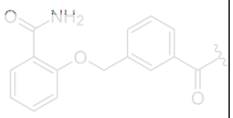	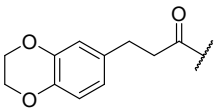	Potent_Low Selectivity	n.d.	85	n.d.	n.d.
A45/B111-B	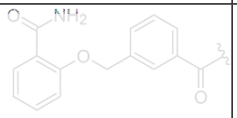	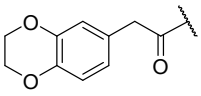	Potent_Low Selectivity	n.d.	69	n.d.	n.d.
A108/B21[a]			Selective_Modest Potency	13	46	97	n.d.

Structures contain an ethylenediamine linker between the two carboxylic acid building blocks, except for structures labeled [a] that contain a methylcarboxamide derivative and [b] that contain a carboxamide derivative on this linker.

PARP2

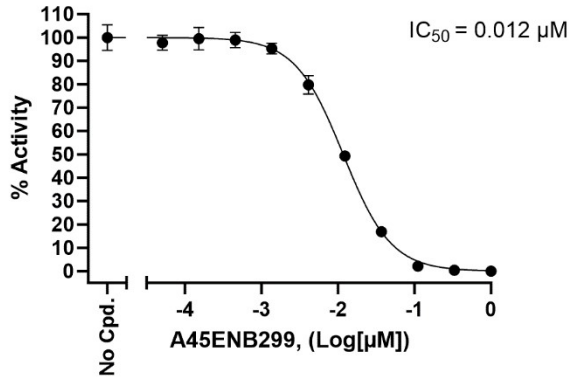

TNKS1

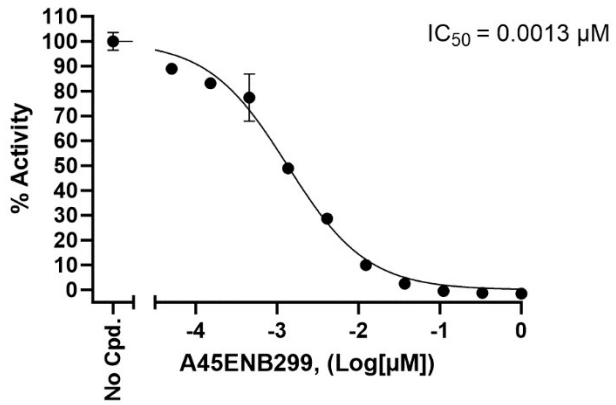

Supporting Figure 2. Dose-dependent inhibition of PARP2 and TNKS1 by A45-En-B299.

Supporting Table 6. Selectivity of selected PROTAC-like compounds. Values in table correspond to percent inhibition of the indicated enzyme at the given concentration.

Compound ID/structure		PARP1	PARP2		TNKS1	
		500 nM	10 nM	50 nM	10 nM	50 nM
A45DAPB145-						
-linker A3	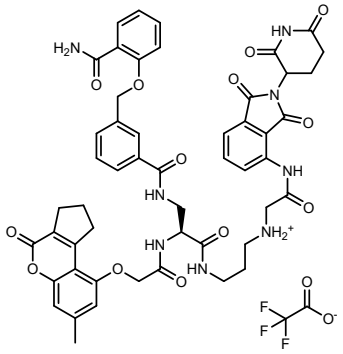	N.D.	N.D.	N.D.	N.D.	N.D.
-linker A4	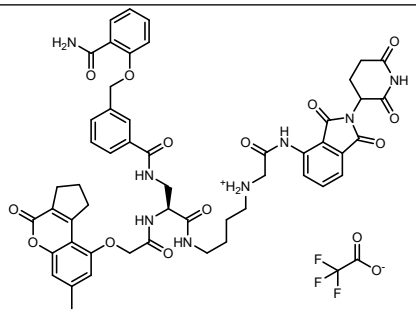	N.D.	N.D.	N.D.	N.D.	N.D.
-linker A5	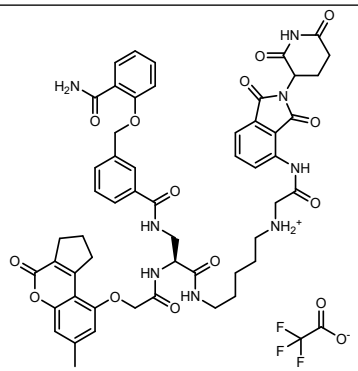	14	43	88	76	87
-linker A6	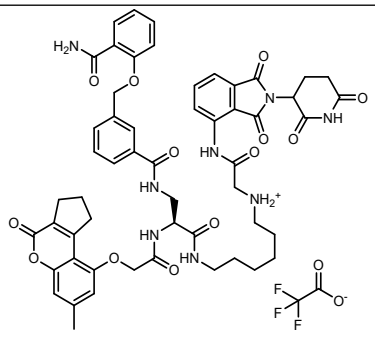	10	34	84	75	90

-linker A8	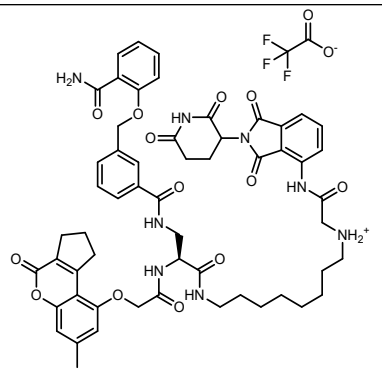	6	12	65	68	87
-linker B2,3	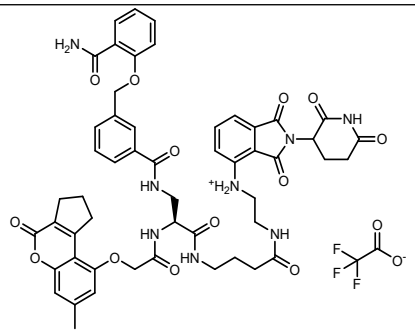	15	10	54	63	85
-linker B3,2	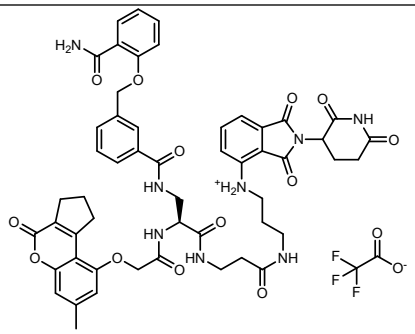	15	12	61	56	74
-linker B3,3	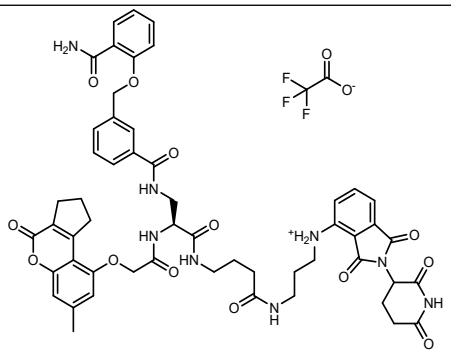	N.D.	N.D.	N.D.	N.D.	N.D.
A45DAPB299-		500 nM	10 nM	50 nM	10 nM	50 nM

-linker A3	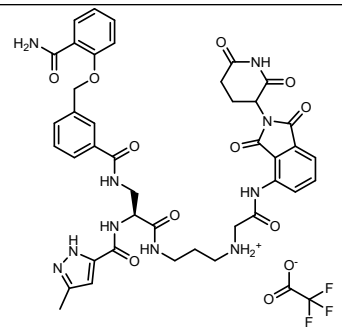	N.D.	N.D.	N.D.	N.D.	N.D.
-linker A4	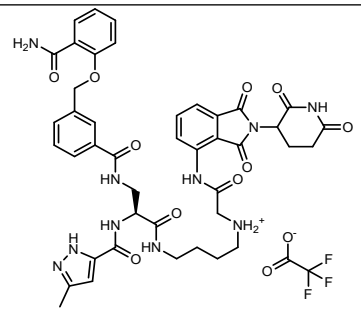	N.D.	N.D.	N.D.	N.D.	N.D.
-linker A5	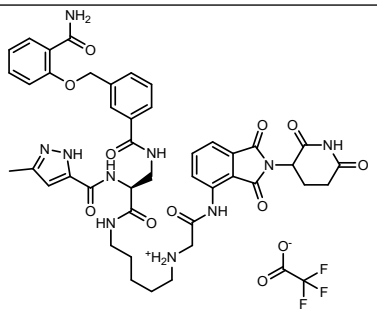	28	N.D.	53	N.D.	15
-linker A6	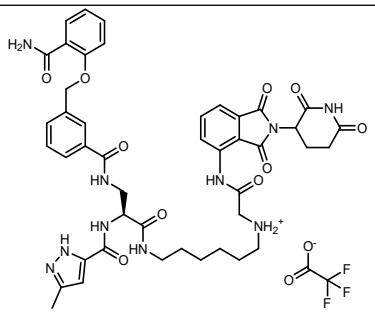	30	N.D.	74	N.D.	29
-linker A8	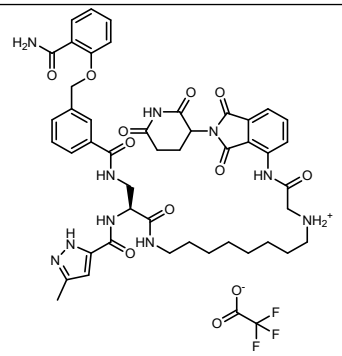	50	N.D.	79	N.D.	32

-linker B2,3	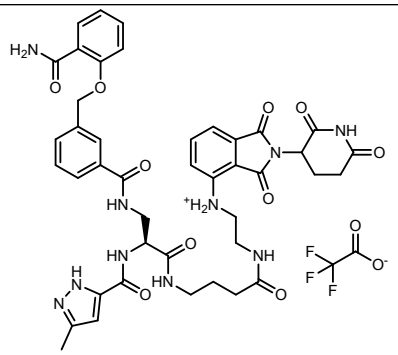	32	N.D.	52	N.D.	24
-linker B3,2	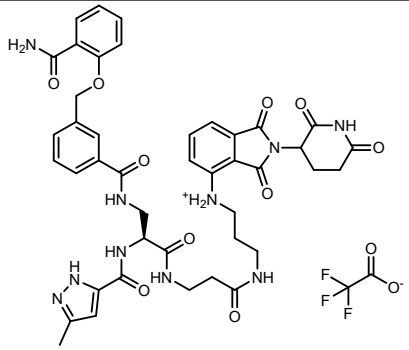	16	N.D.	66	N.D.	37

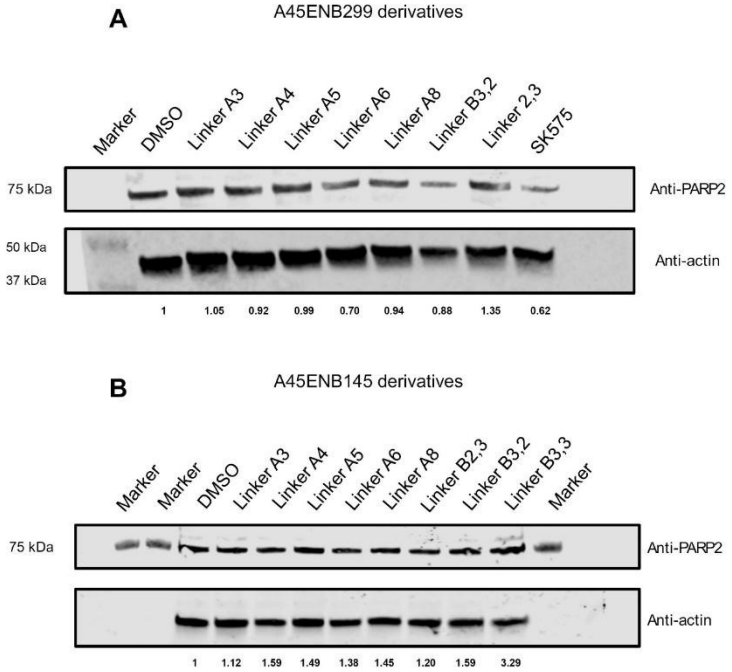

Supporting Figure 3. PARP2 degradation experiment. Numbers below the blots indicate densitometry calculations - values were corrected based on actin loading and normalized back to DMSO treatments (control). SK575- validated PARP1 PROTAC. Panel A – A45ENB299 derivatives, primary antibody: anti-PARP2 rabbit (ProteinTech); Panel B – A45ENB145 derivatives, primary antibody: anti-PARP2 mouse (Santa Cruz).

PARP2 degradation experiment

Cell culture

U2OS cells were cultured in Dulbecco's modified Eagle's media (DMEM, Gibco) supplemented with 10% fetal bovine serum (Gibco) and 1% penicillin/streptomycin (Gibco). For compound treatments, cells were seeded in 10-cm plates, and they were allowed to grow to about 80% confluence. Cells were treated with indicated compound treatments for 24 hours and control cells were treated with 0.1 % DMSO. After treatment period, cells were washed with cold PBS and then harvested in 1 mL of cold PBS using a cell scraper. Cells were pelleted at 300 x g for 10 minutes at 4^{o}C, and the resulting pellets were lysed using cold RIPA lysis buffer on ice for 10 minutes. The samples were then hard spun at 17,000 x g for 10 minutes and the clarified lysate was quenched with SDS loading buffer and boiled for 5 minutes.

Western blotting

The samples were analyzed on 4-12% Bis-Tris PAGE gel using 1x MES running buffer (Bio-Rad) at 170 V for about 40 minutes. Samples were then transferred to a PVDF membrane using semi-dry transfer at 20 V for 30 minutes in Towbin buffer. The membrane was then blocked with 3% dry milk in TBST buffer for 60 minutes. The Membrane was then incubated with primary antibodies (anti-actin and anti-PARP2) overnight at 4^{o}C at recommended dilutions (**Table 1**). Membranes were then washed 3x with TBST for 5 minutes and then incubated with secondary antibodies (1:10,000 for mouse secondary, 1:15,000 for rabbit secondary) for 60 minutes at room temperature. The membrane was washed 3x with TBST and 1x with milliQ water for 5 minutes. The blot was imaged using the Licor Odyssey system, and densitometry was performed using Licor Image Studio software.

Supporting Table 7. Antibodies used in the PARP2 degradation experiment.

Antibodies	Dilution	Manufacturer	Catalog No.
Mouse anti-Beta-actin	1:100	Cell Signaling Technologies	3700
Rabbit Anti-PARP2	1:1000	ProteinTech	55149-1-AP
Mouse Anti-PARP2	1:100	Santa Cruz Biotechnologies	sc-393310
IRDye 680CW goat anti-mouse	1:10000	LICOR	926-68070
IRDye 800 CW goat anti-rabbit	1:15000	LICOR	926-32211

Datasets:

Three datasets were used for the machine learning analysis of the DEL data:

- *DEL Dataset:* This dataset was generated from normalized sequence counts, averaged across two NADEL selections against PARP2. To avoid bias, values for A11 and A108, which represent the same building block, were averaged and designated as A108-compounds. Molecular structures were enumerated using the Enumerate Combinatorial Library function in DataWarrior and converted to SMILES format. These molecules included methylcarboxamide residues at the DNA-attachment linker position.
- *Experimental Dataset:* This dataset consists of 41 molecules with experimentally validated activity. Compounds were classified based on their percent inhibition of PARP2 at a concentration of 500 nM, with ≥50% inhibition labeled as "active" and <50% inhibition labeled as "inactive."
- *ChEMBL Dataset:* Active compounds were identified from the ChEMBL database using a Python code, targeting molecules that inhibit or bind to PARP2 (ChEMBL ID: CHEMBL5366) with an IC50 or Kd <500 nM. A total of 228 active molecules were identified. Additionally, 1000 randomly selected ChEMBL molecules were labeled as inactive. For molecules with several components (e.g. salts) the largest structure was selected as the molecule of interest.

Datasets are provided as supporting information for this manuscript as learning_data.csv (DEL dataset), PARP2_experimental_data.csv (experimental dataset), ChEMBL_-_Bioactives_-_200-500Da_no_salts_SMILES.csv (random inactives from ChEMBL database; 1,000 out of 10,000 compounds in file were randomly selected for the analysis; actives were extracted from ChEMBL using the ChEMBL ID CHEMBL5366 with a cutoff value of K_d or IC_{50} < 500 nM [see code on GitHub for details]).

Computational methods:

"The code, data, and examples used in this study are available at https://github.com/SnowyTheWestie/DEL_PARP_ML."

Leave-one-out-analysis: A leave-one-out-analysis was performed for every DEL member from the PARP2 selection that was classified as hit.

Logistic regression (LR): A random learn-test data split was applied to the DEL dataset with a 4:1 ratio using the SKLearn package. The learning data was then used to train a LR model using the corresponding function in the SKLearn package with an L2 penalty.

Undersampling: The majority class (non-hits) was undersampled by randomly removing members of the majority class until receiving the desired balance ration while retaining the members of the minority class (hits). Undersampling was performed using the *RandomUnderSampler* command from the Imbalance Learn Python package. Recall and F1-scores are the averages of five experiments with different balancing ratios and data splits; error bars are standard error of the measurements.

Oversampling: The minority class (hits) was oversampled by randomly amplyfying members of the minority class until receiving the desired balance ration while retaining the members of the majority class (non-hits). Oversampling was performed using the *RandomOverSampler* command from the Imbalance Learn Python package. Alternative the *SMOTEN* function, allowing the synthetic oversampling of the categorical features of

molecular fingerprints, from the Imbalance Learn Python package was used. Recall and F1-scores are the averages of five experiments with different balancing ratios and data splits; error bars are standard error of the measurements.

Cluster Analysis: PARP2 inhibitors from the ChEMBL database were analyzed by clustering. A similarity matrix was initially established based on the ECFP fingerprints using Jaccard distance. K-Means clustering was applied to the compounds with the number of clusters selected as 14. A principal component analysis was performed on the fingerprints for representation of the molecules and clusters in a 2-dimensional scatter plot. The PCA and K-Means functions of Scikit-Learn were used for the analysis.

Optimized hit classification threshold:

Exploration of ML algorithms: Different ML algorithms were explored to ensure that the obtained results were not a result of using logistic regression. Obtained values were averages of five separate experiments with distinct undersampling and data-split steps. The following functions and parameters were used:

- Random forest: *RandomForestClassifier* (Scikit-learn; n-estimators = 100)
- Support vector machine: *SVC* (Scikit-learn)
- Multilayer perceptron: *MLPClassifier* (Scikit-learn; hidden_layer_sizes: 100, 50)
- Naïve Bayers: *GaussianNB* (Scikit-learn)
- Elastic net: *LogisticRegression* (Scikit-learn; penalty='elasticnet', solver='saga', l1_ratio=0.5)
- Histogram gradient tree: *HistGradientBoostingClassifier*(Scikit-learn)

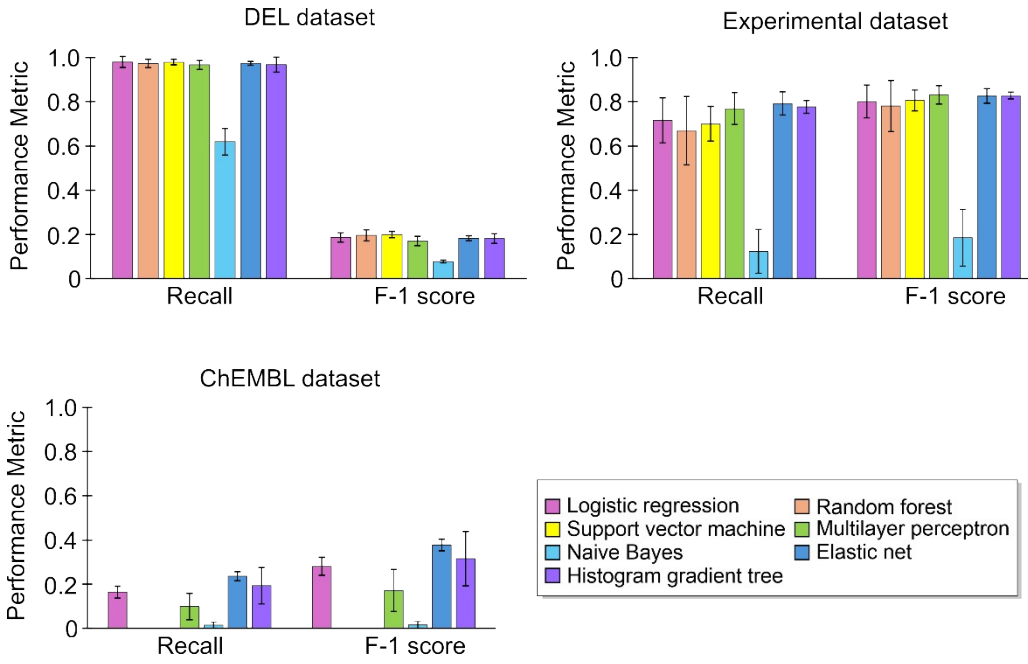

Supporting Figure 4. Comparison of the predictive performance of different ML models trained on the DECL data on the validation sets. Similar or worse recall values and F1-scores were observed across these models relative to LR. For ChEMBL compounds, LR and multi-layer perceptron showed comparable performance, while elastic net regularization, and histogram gradient tree performed slightly better. In contrast, random forest, support vector machines, and naïve Bayes failed to predict any active ChEMBL compounds. These findings

confirm that the observed effects stem from the structure of the DECL data rather than the choice of ML model.

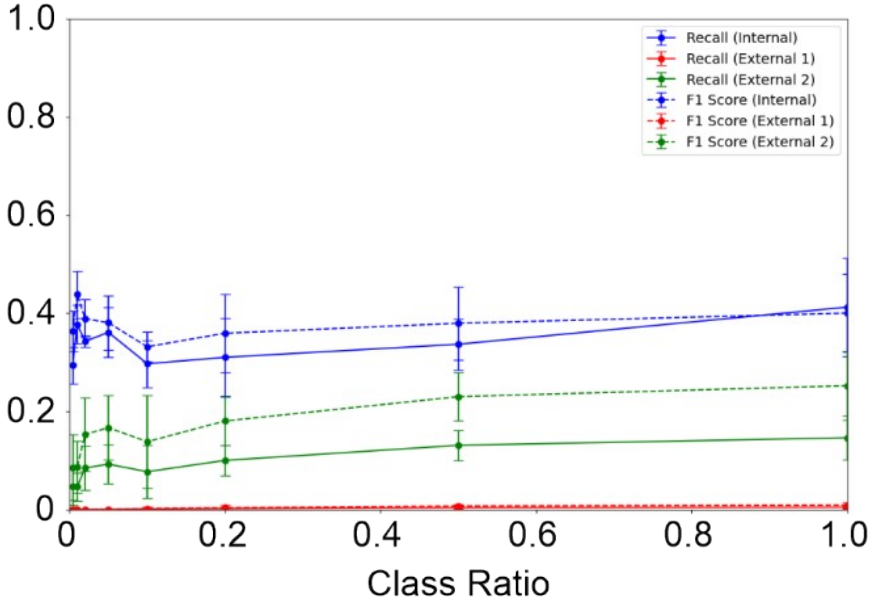

Supporting Figure 5. Effect of oversampling synthetic oversampling using the SMOTEN algorithm of the minority class in the learning set on recall (solid) and F1-score (dashed) of the internal validation set (blue), validation set of experimentally validated NADEL compounds (green), and ChEMBL validation set (red). Each datapoint is the average of five replicates of logistic regression analyses.

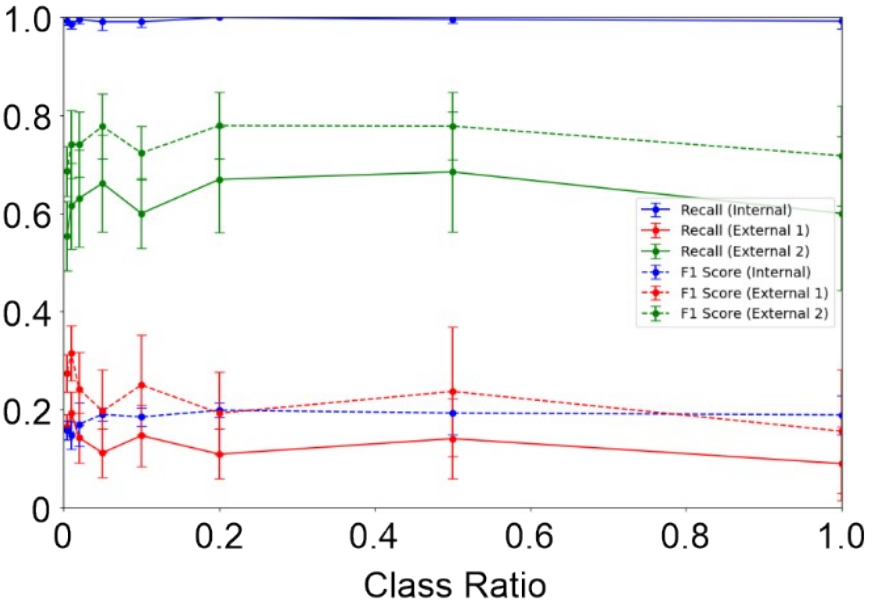

Supporting Figure 6. Effect of optimization of the threshold value based on receiver operating curves (see supporting figure S5) for the DEL dataset as well as random undersampling of the majority class in the learning set on recall (solid) and F1-score (dashed) of the internal validation set (blue), validation set of experimentally validated NADEL compounds (green), and ChEMBL validation set (red). Each datapoint is the average of five replicates of logistic regression analyses.

Class ratio	DEL dataset	Experimental dataset	ChEMBL dataset
Unbalanced	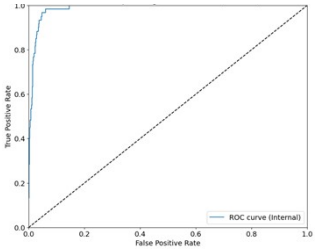	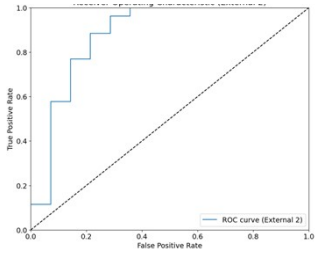	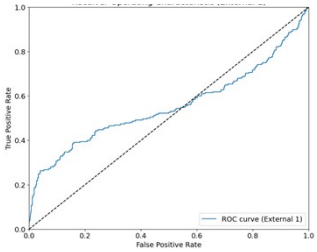
100	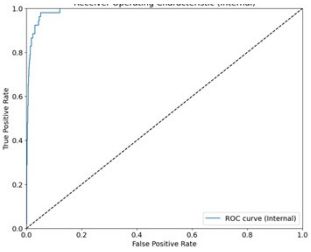	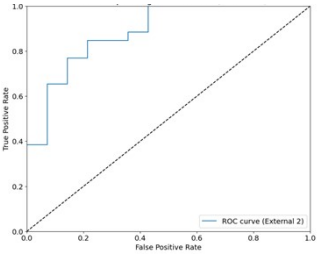	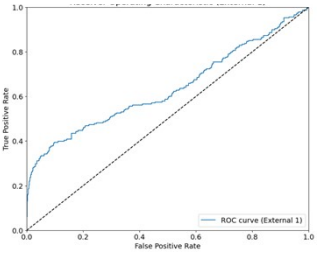
10	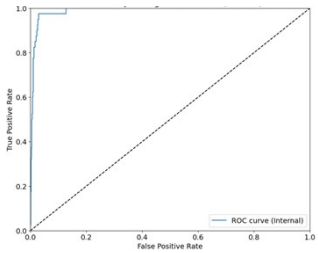	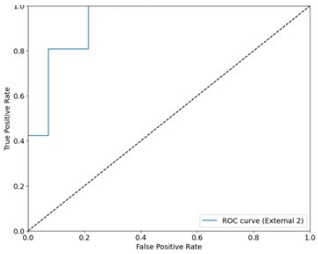	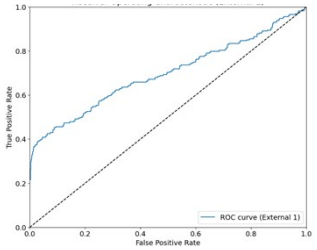
5	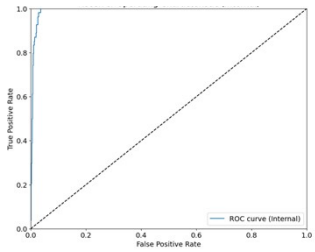	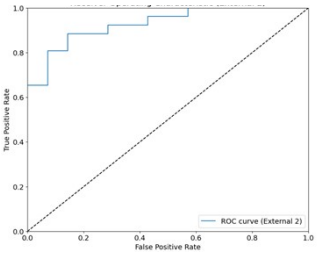	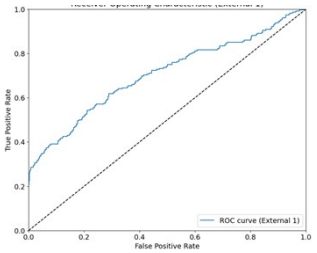
2	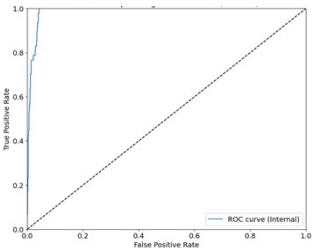	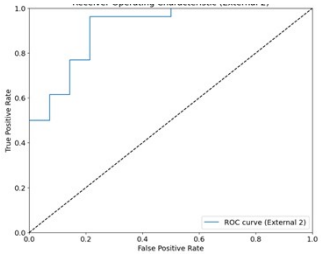	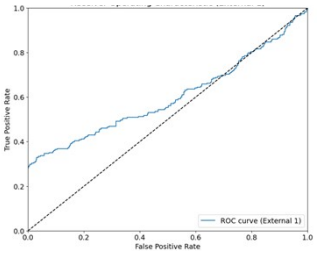
1	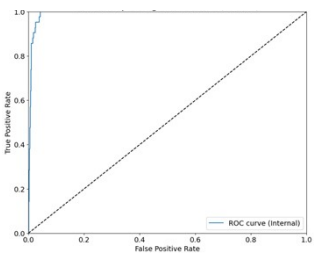	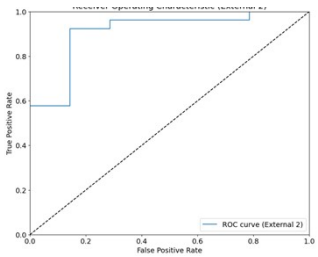	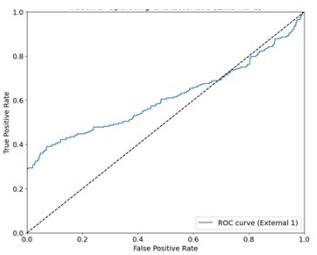

Supporting Figure 7. Representative receiver operator characteristic (ROC) curves for logistic regression models trained on the DEL data for the three validation datasets at different class balance rations obtained through random undersampling.

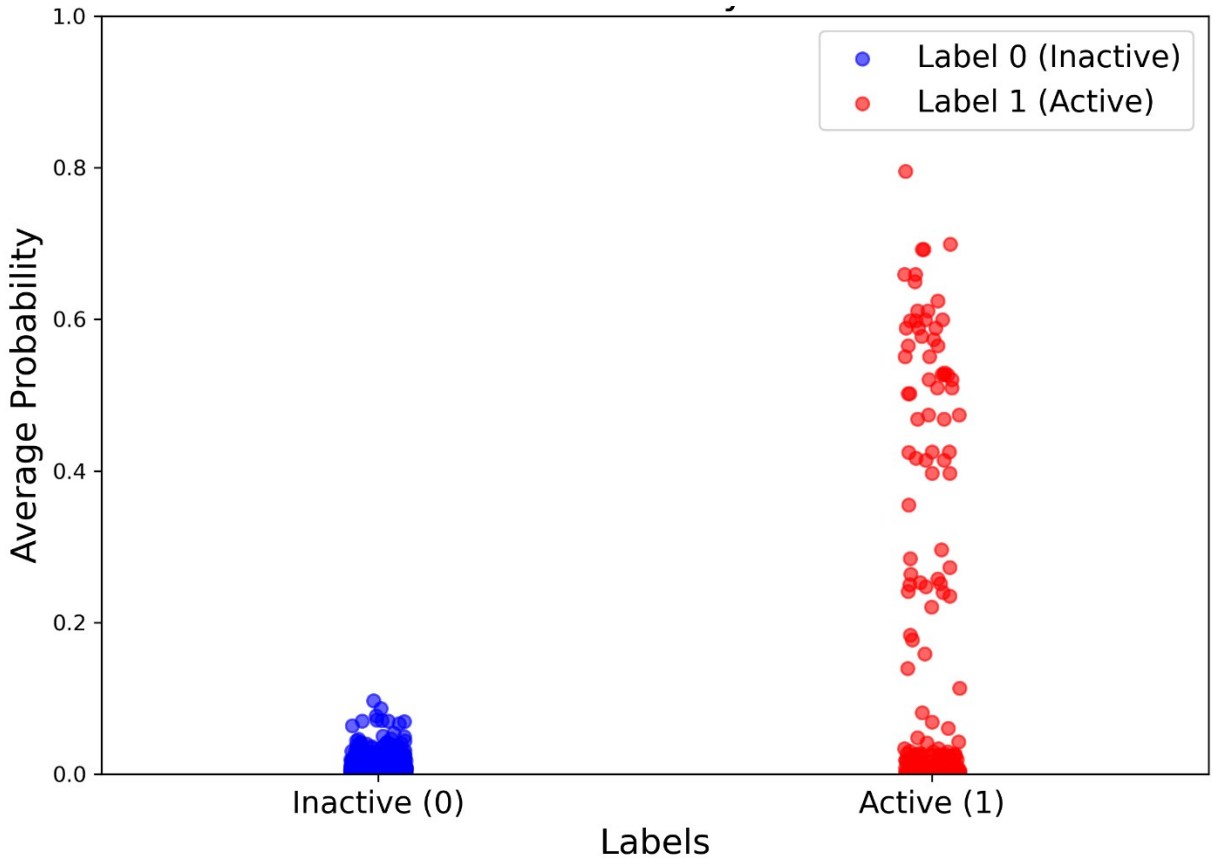

Supporting Figure 8. Averaged predicted probabilities from 10 logistic regression models trained on PARP2 NADEL data for ChEMBL compounds reported as active (IC50 or Kd < 500 nM; red) and random molecules (blue).

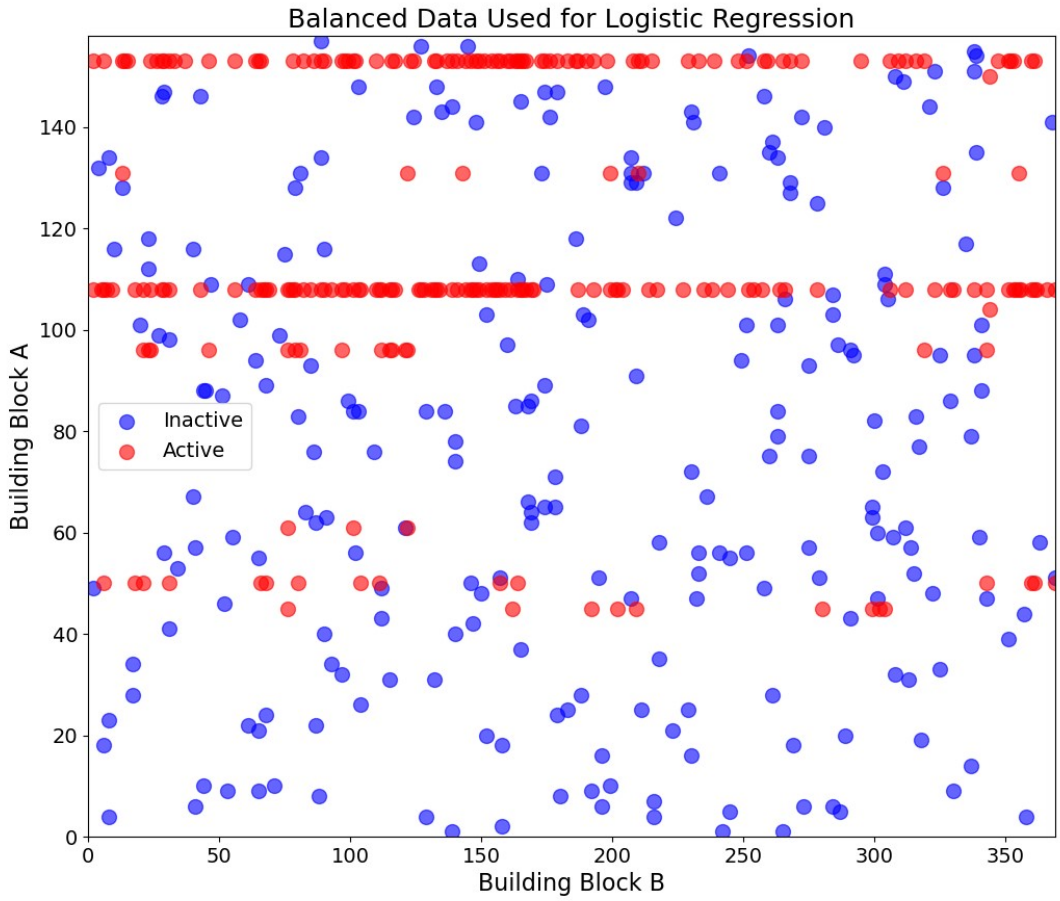

Supporting Figure 9. Representative example of balanced PARP2 data after undersampling. The majority of non-hits (blue, NSC < 10) were removed through random undersampling, while all hits (red, NSC ≥ 10) were retained. Due to the combinatorial nature of the DEL, most remaining molecules with specific building blocks belong to the minority class, leading the model to associate these building blocks with activity.

^{1}H and ^{13}C NMR spectra of the synthesized compounds

^{1}H NMR, 400 MHz, DMSO, compound (A96-En-Boc):

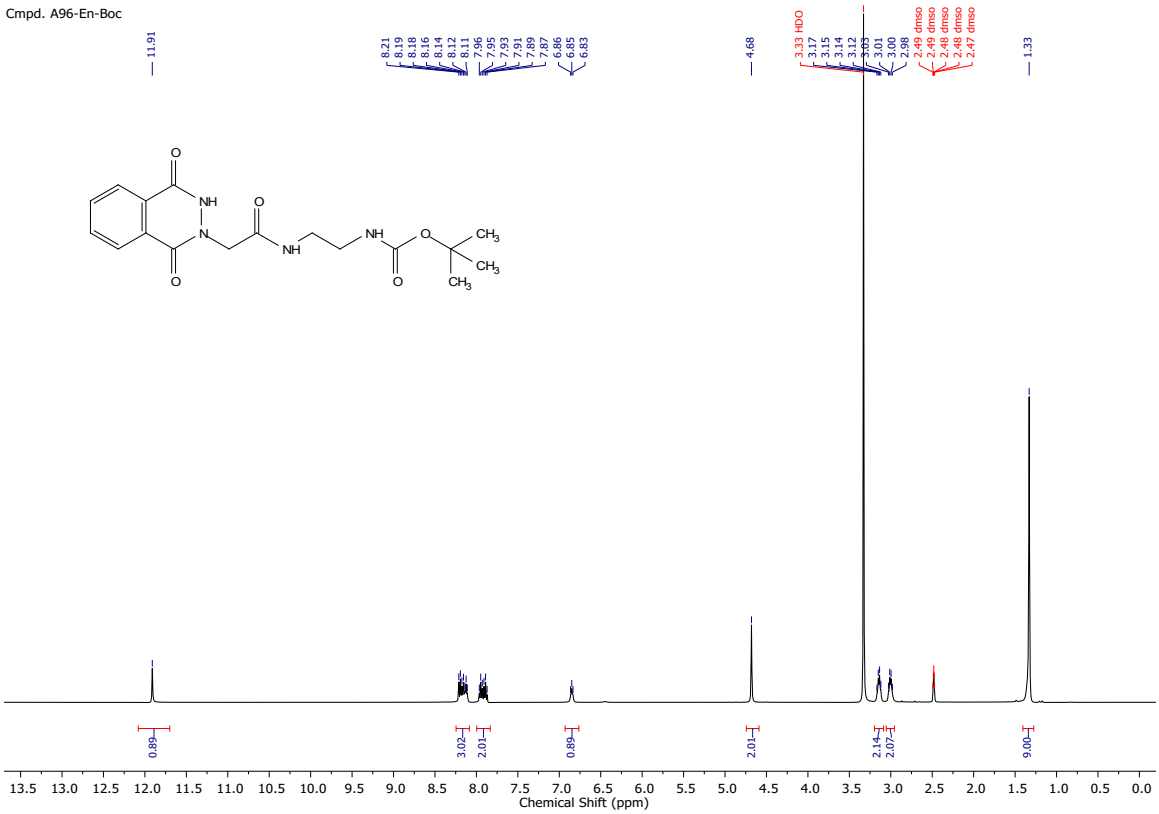

^{1}H NMR, 400 MHz, MeOD, compound (A96-En-NH_2TFA):

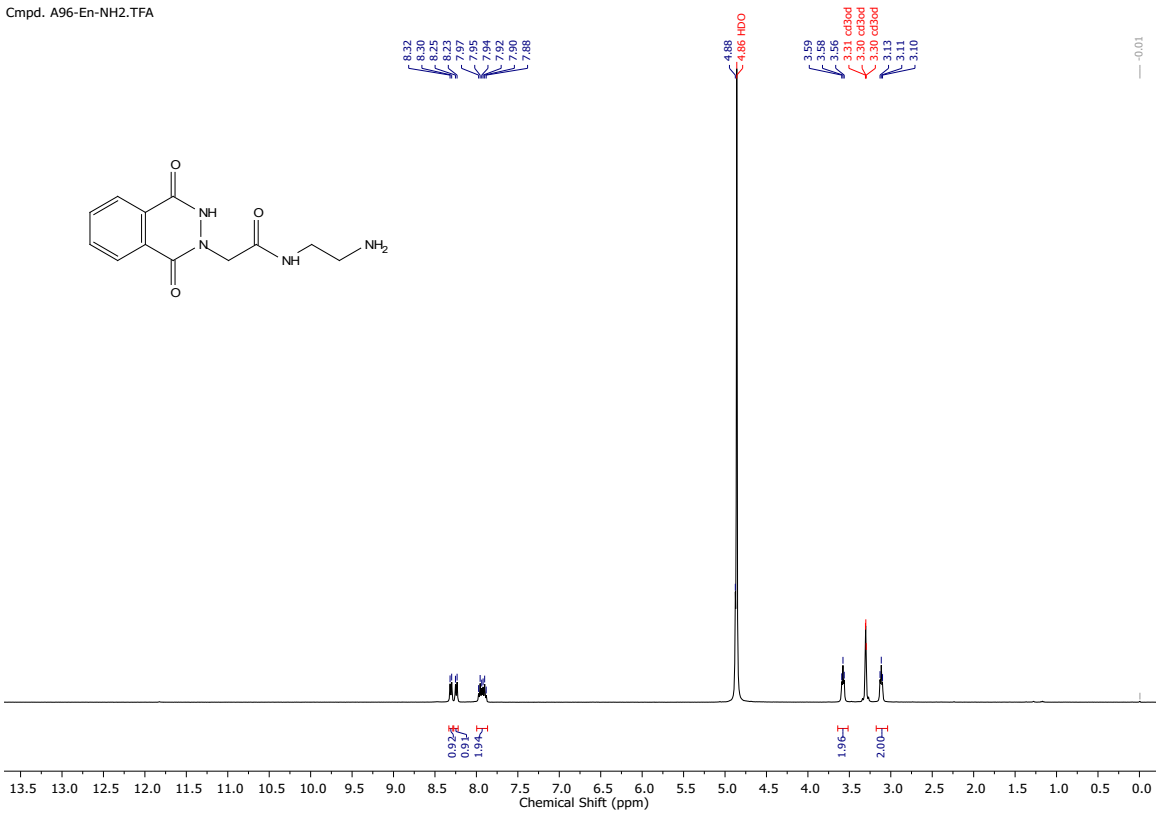

^{1}H NMR, 400 MHz, MeOD, compound (A96-En-B122):

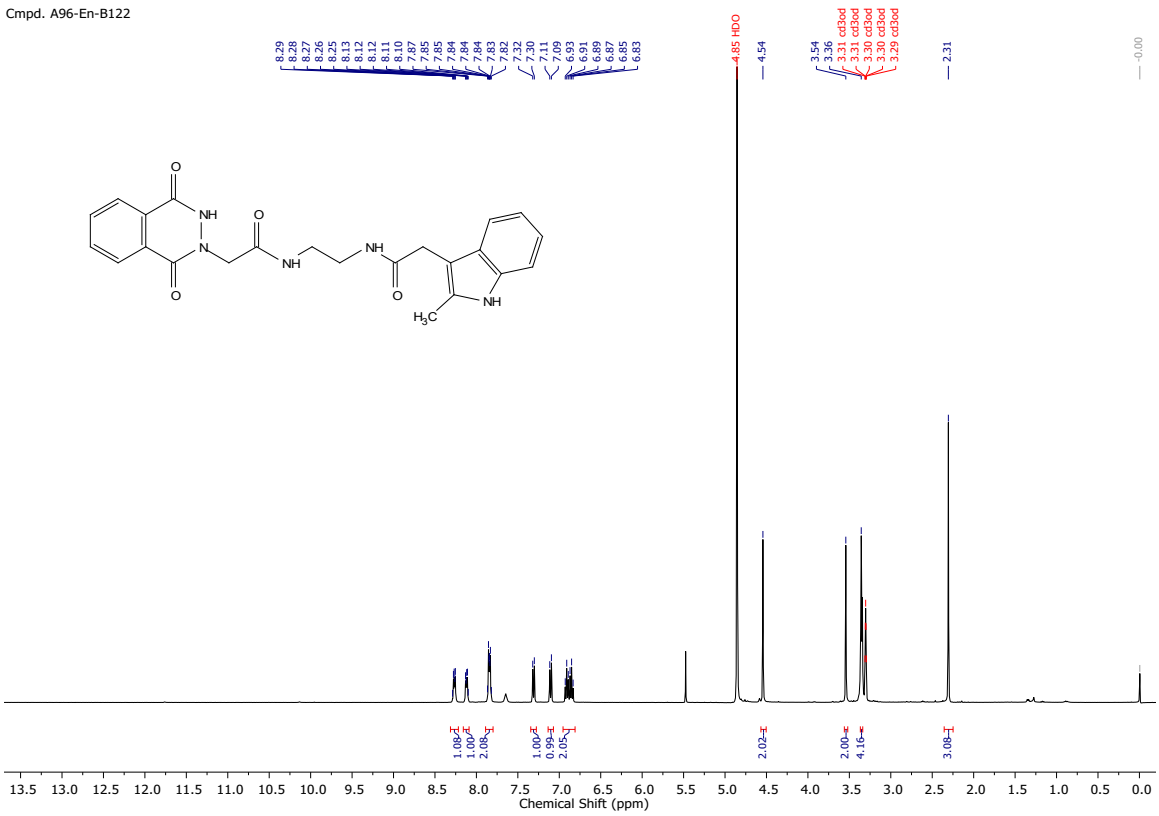

^{1}H NMR, 400 MHz, MeOD, compound (A96-En-B101):

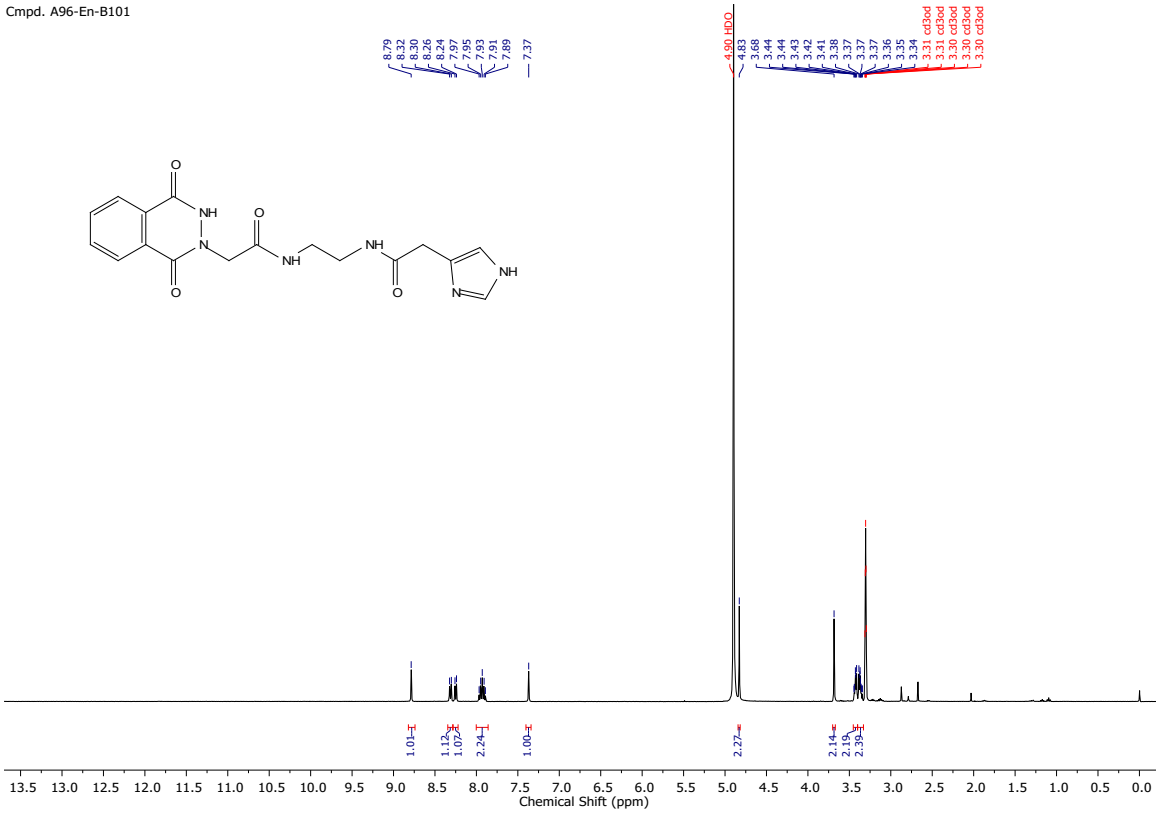

^{1}H NMR, 400 MHz, DMSO, compound (A96-En-Bz):

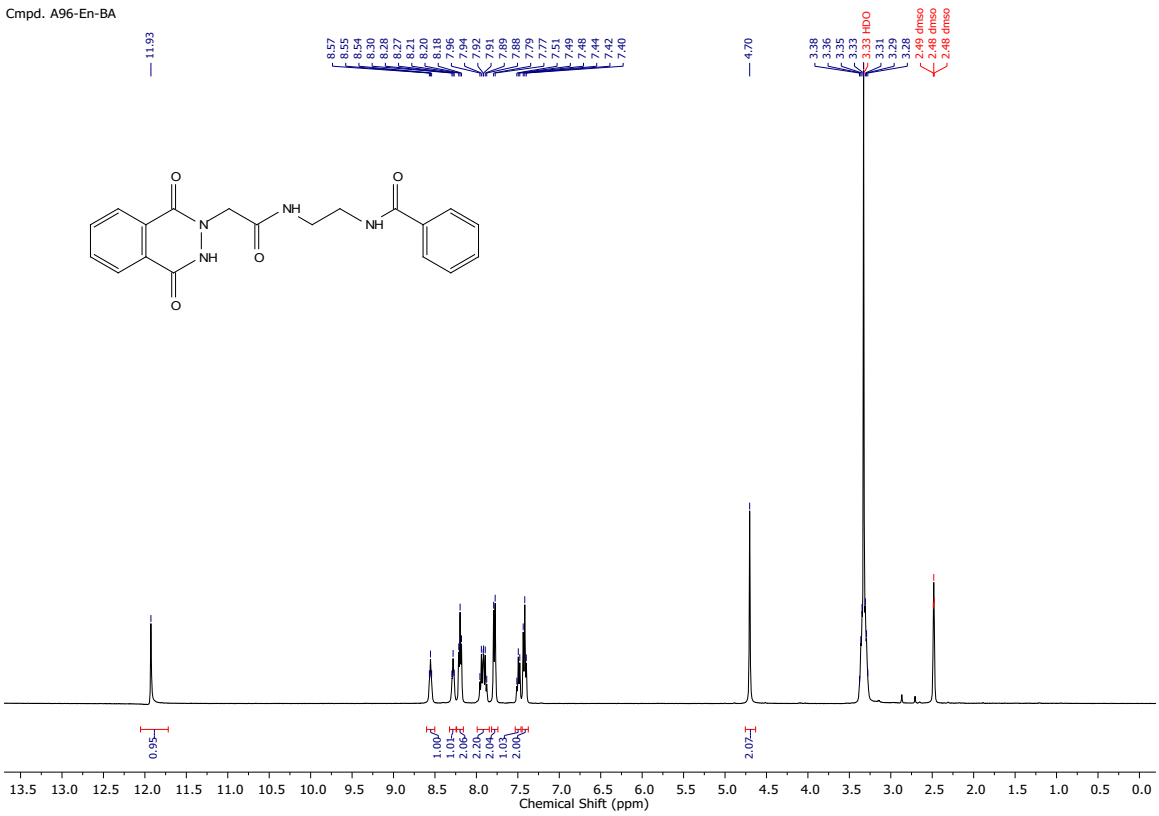

^{1}H NMR, 400 MHz, DMSO, compound (A45-En-Boc):

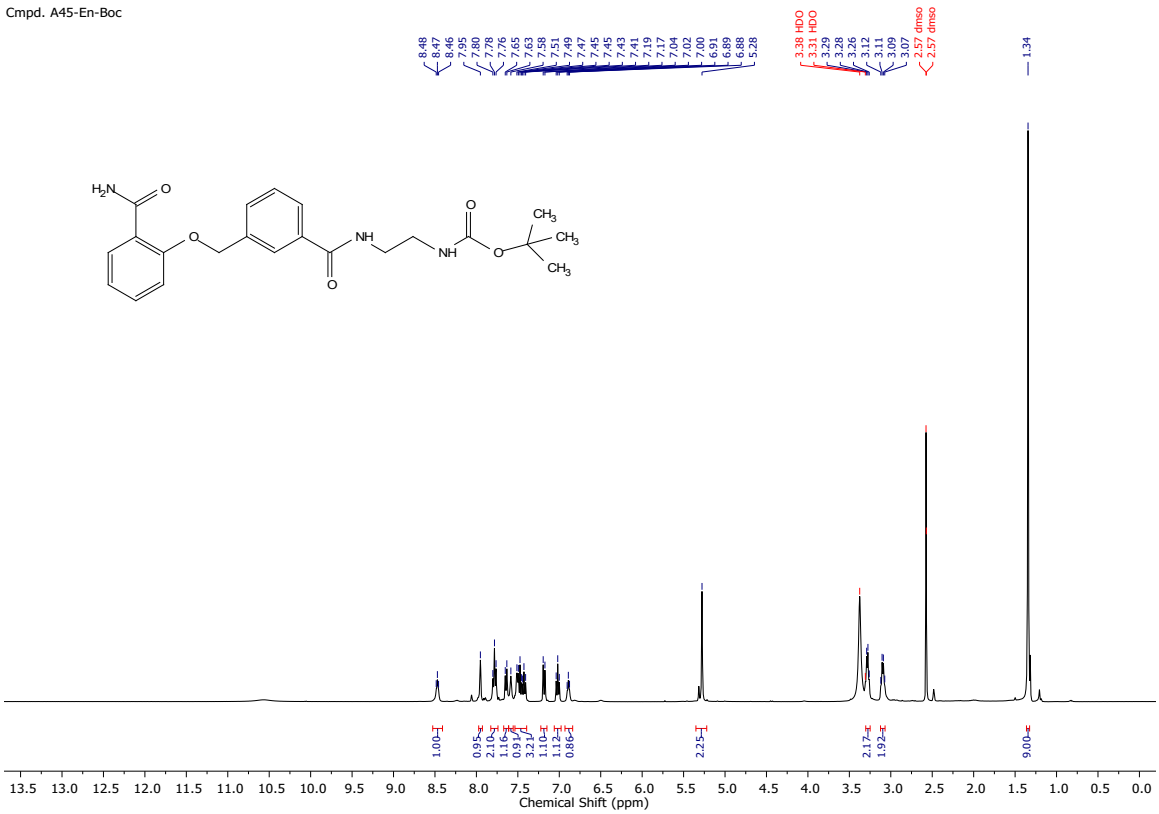

^{1}H NMR, 400 MHz, MeOD, compound (A45-En-NH$_2$TFA):

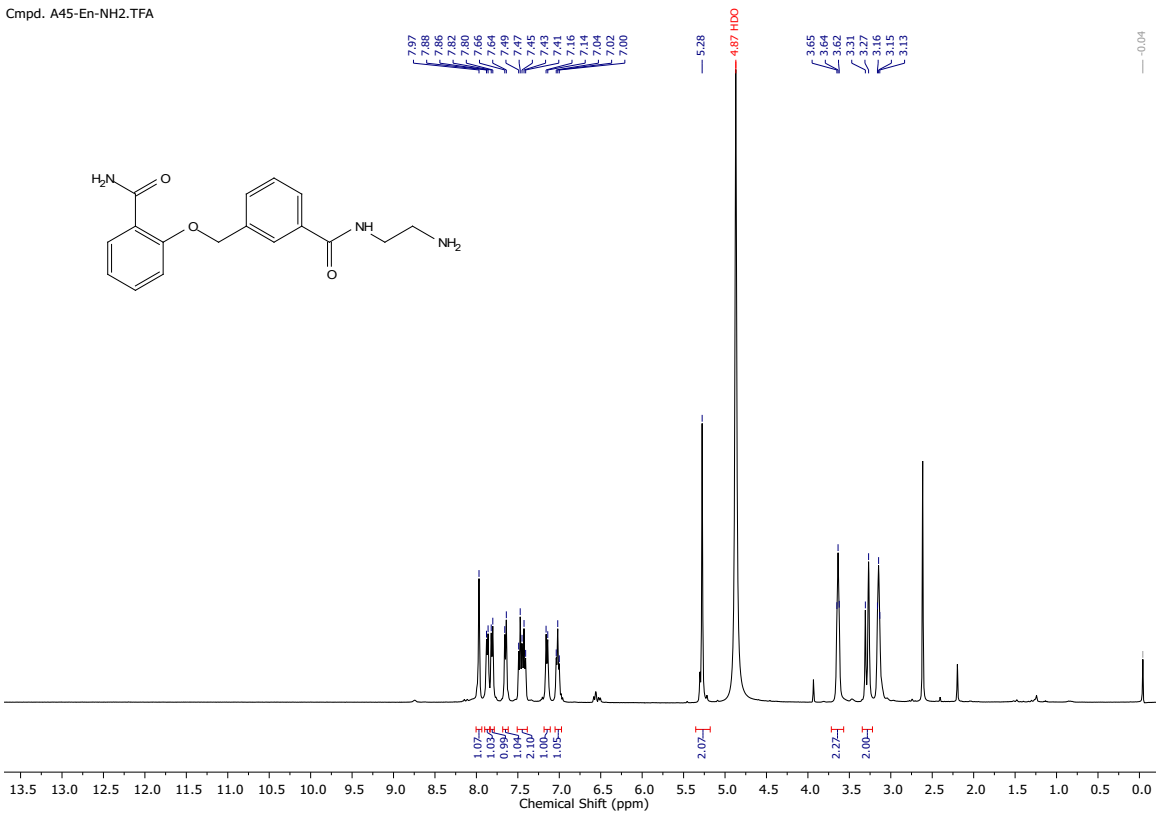

^{1}H NMR, 400 MHz, DMSO, compound (A45-En-B299):

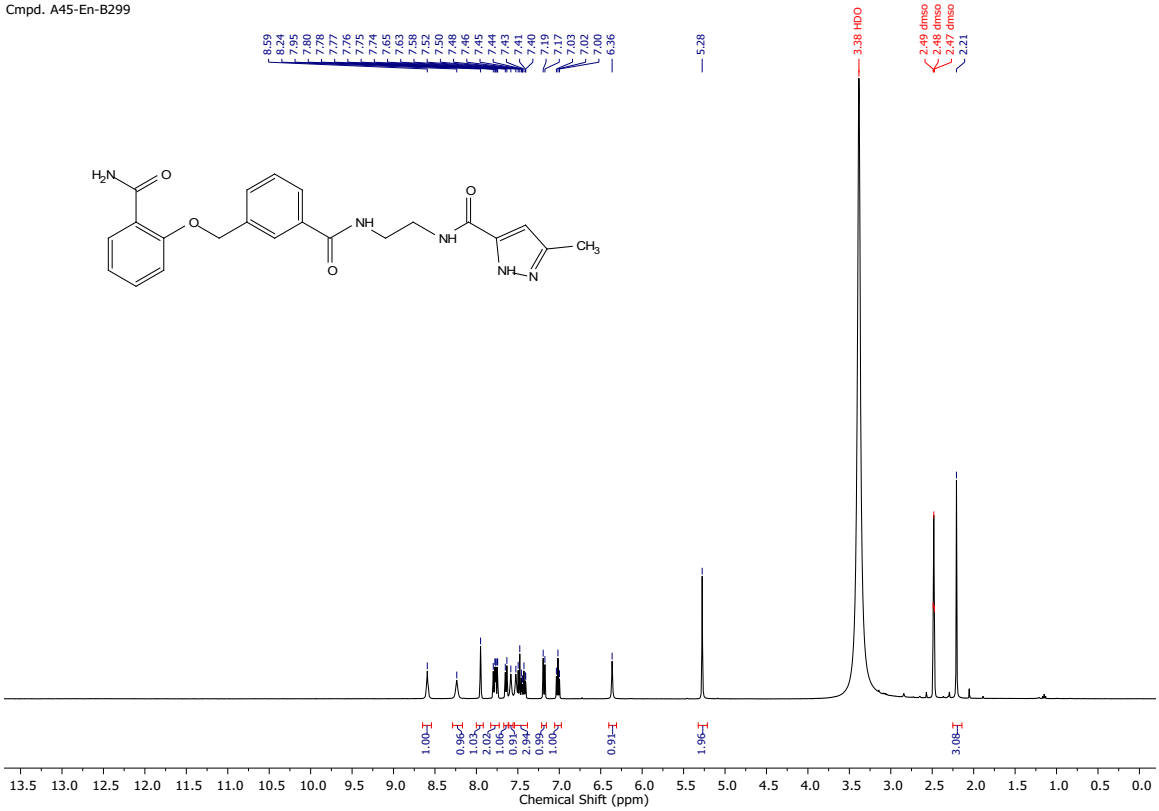

^{1}H NMR, 400 MHz, DMSO, compound (A45-En-B295):

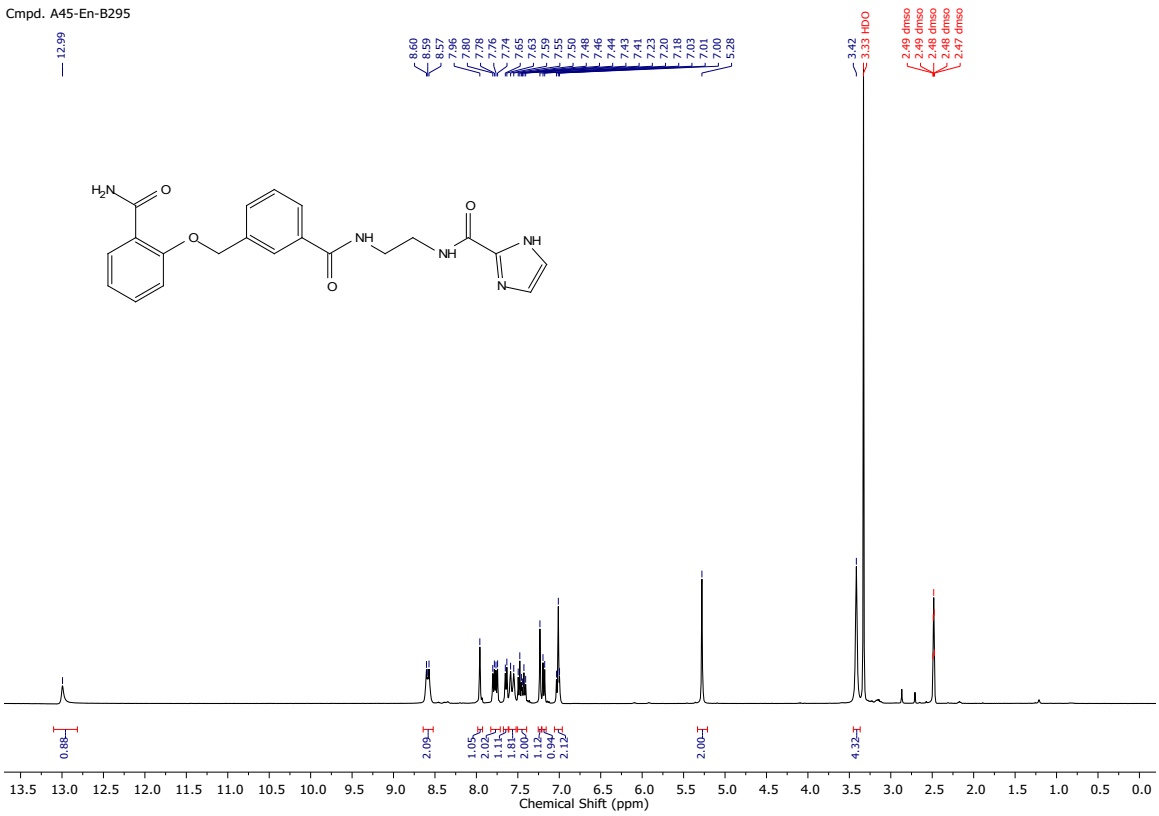

^{1}H NMR, 400 MHz, DMSO, compound (A45-En-Ac):

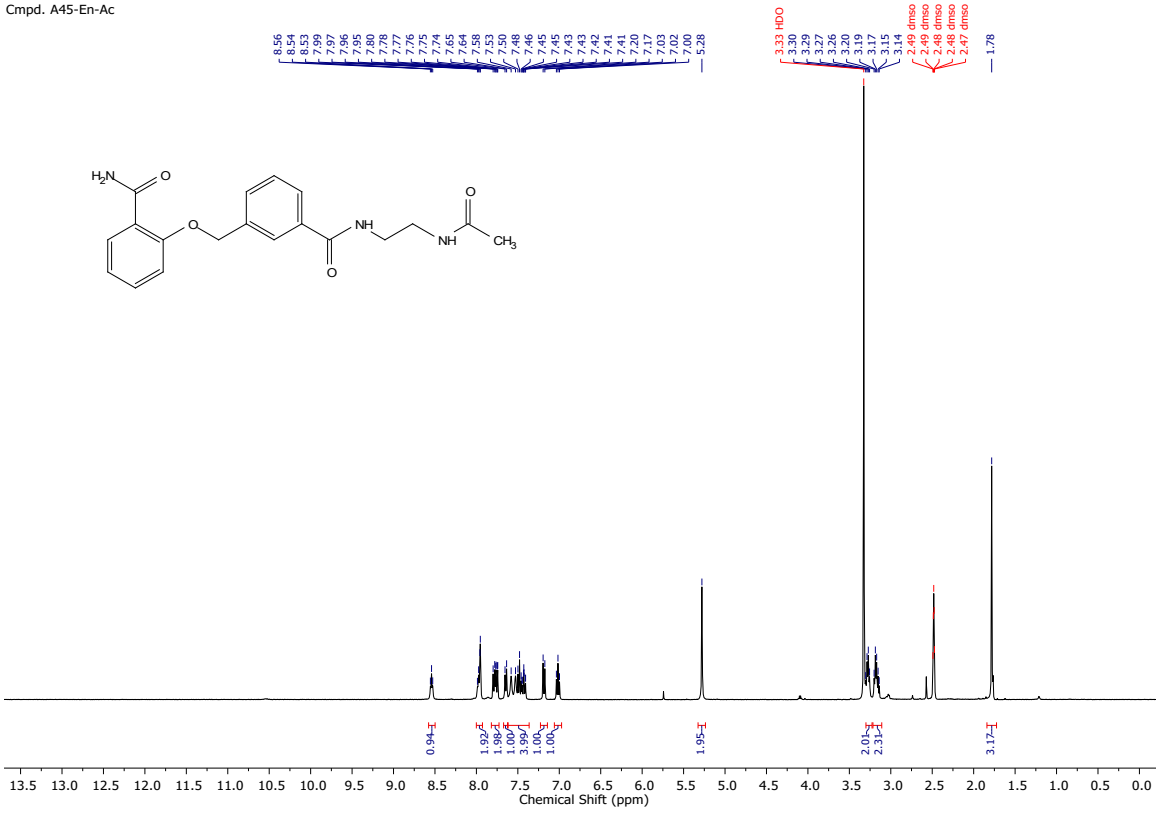

^{1}H NMR, 400 MHz, DMSO, compound (A45-En-B304):

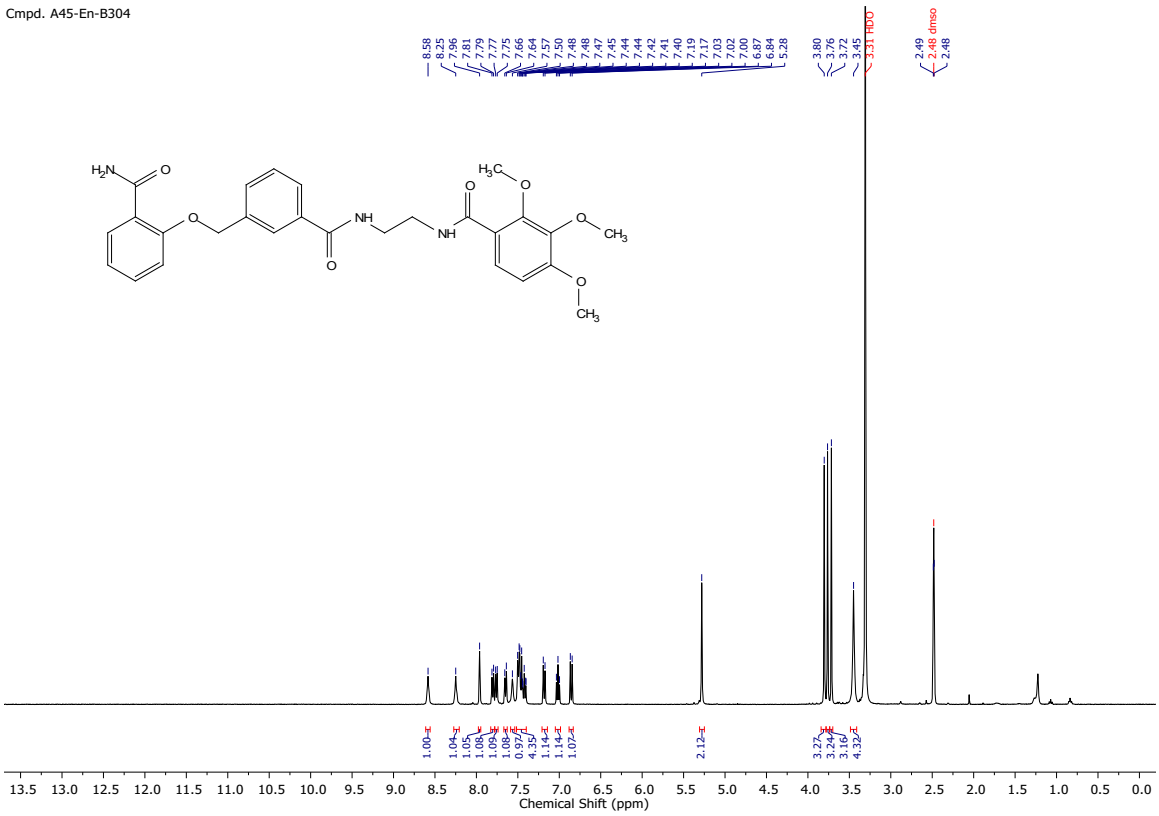

^{1}H NMR, 400 MHz, MeOD, compound (A45-En-B21):

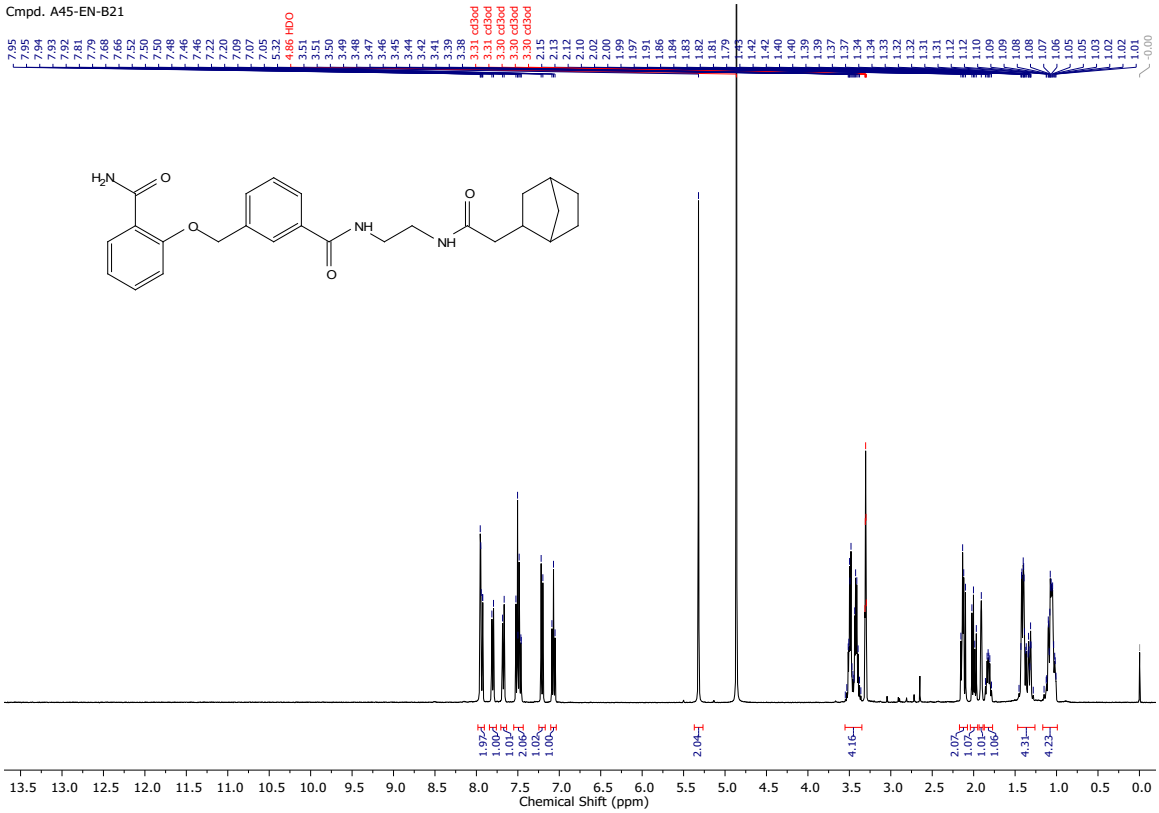

^{1}H NMR, 400 MHz, DMSO, compound (A45-En-B111):

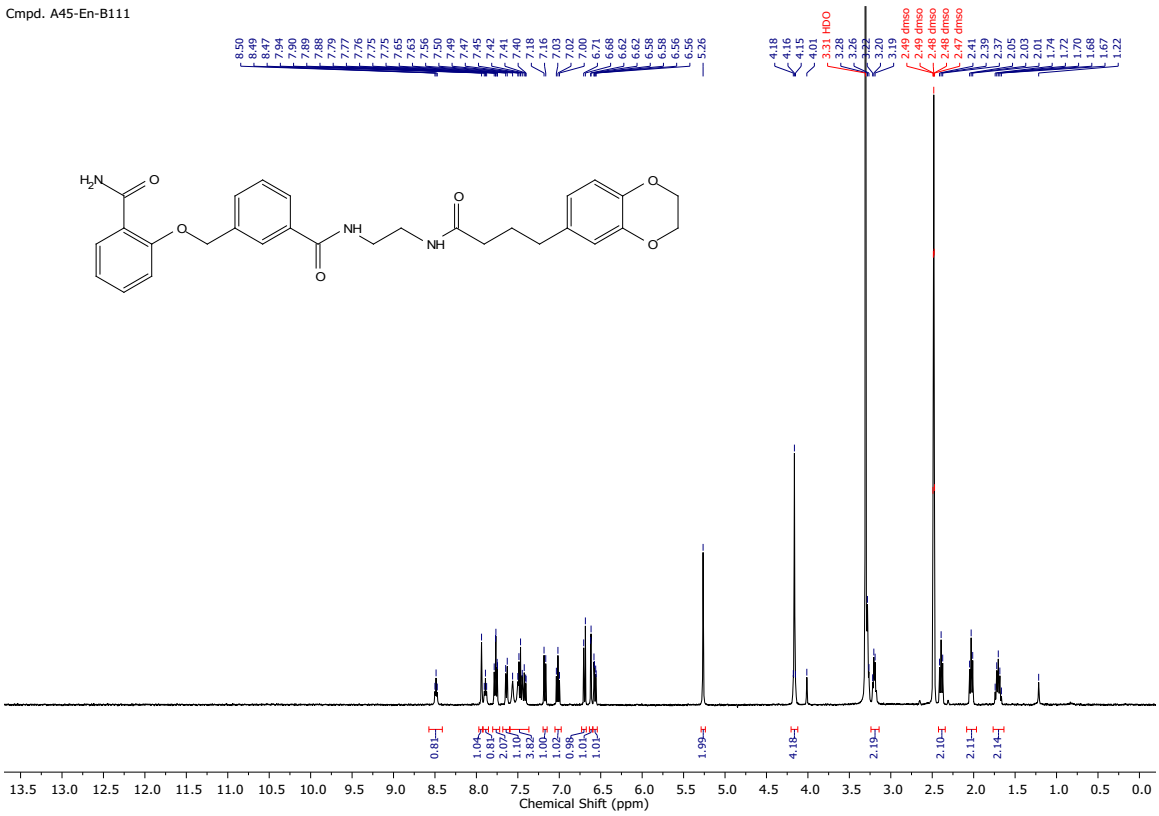

^{1}H NMR, 400 MHz, MeOD, compound (A45-En-B111-A):

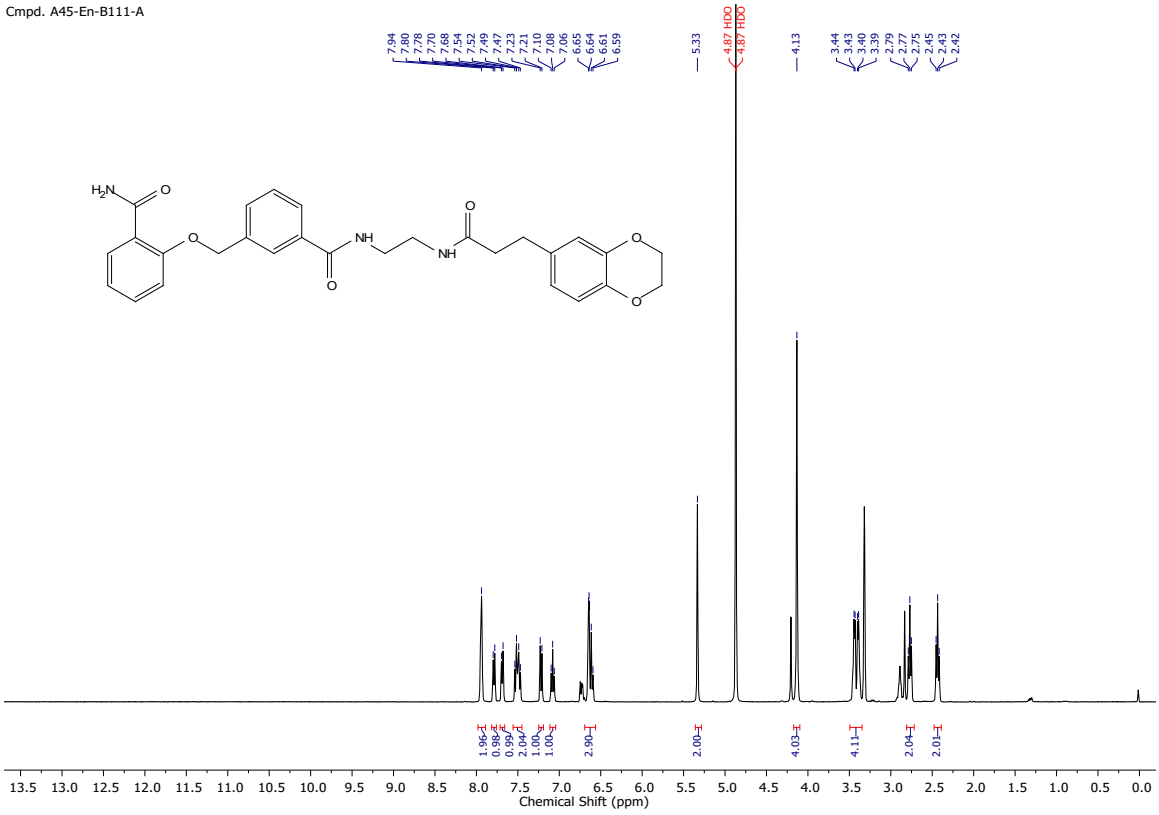

^{1}H NMR, 400 MHz, DMSO, compound (A45-En-B111-B):

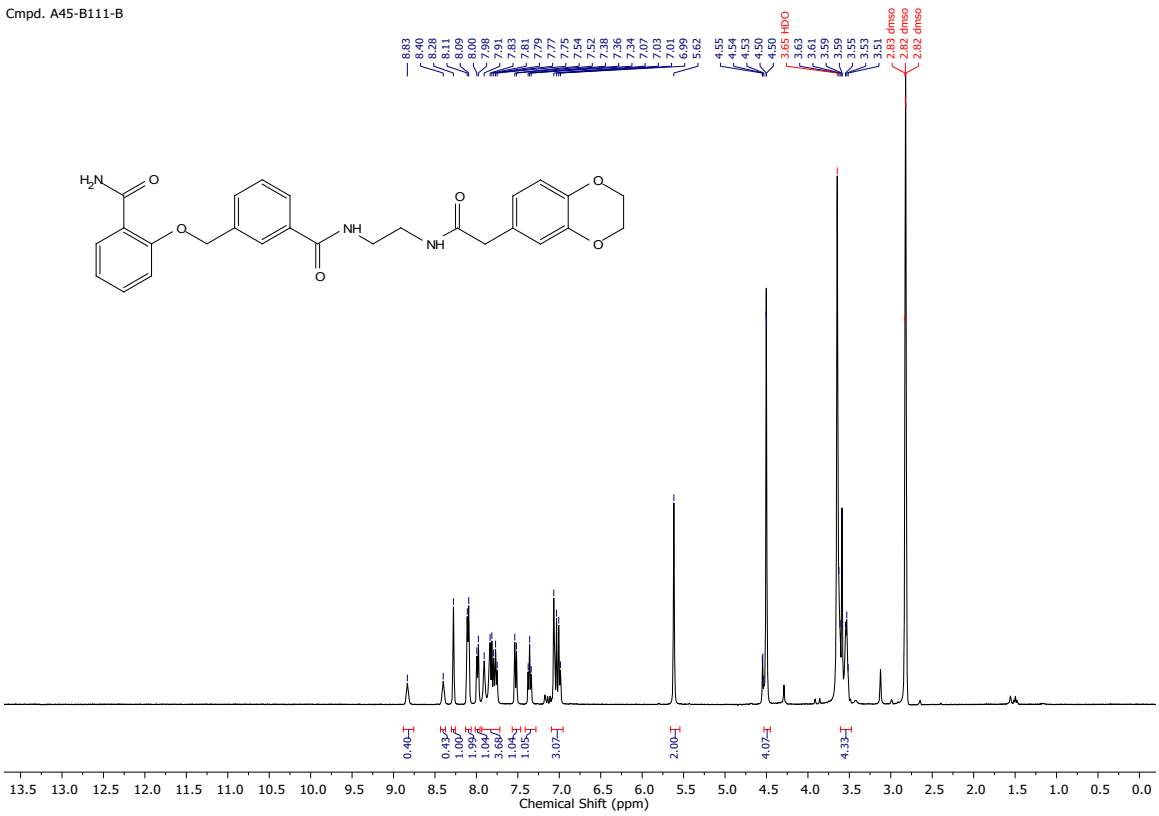

^{1}H NMR, 400 MHz, DMSO, compound (A11/A108-En-Boc):

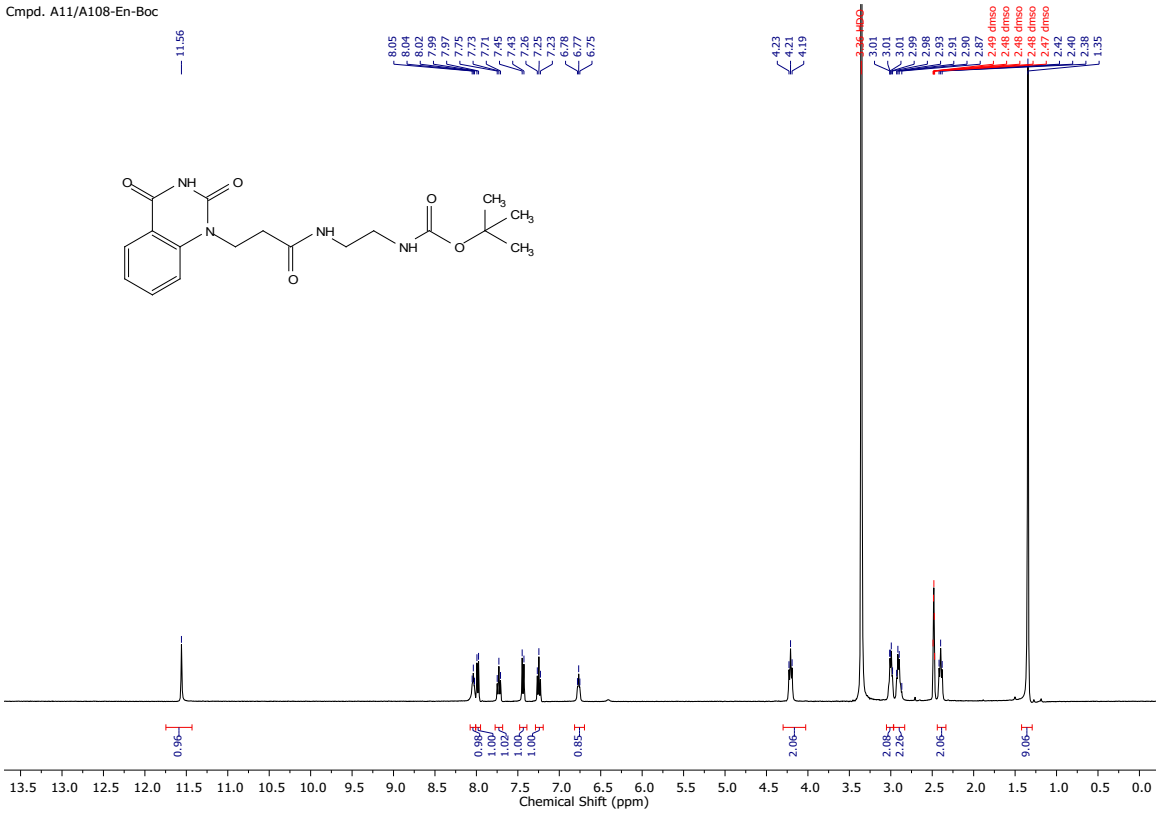

^{1}H NMR, 400 MHz, MeOD, compound (A11/A108-En-NH$_2$TFA):

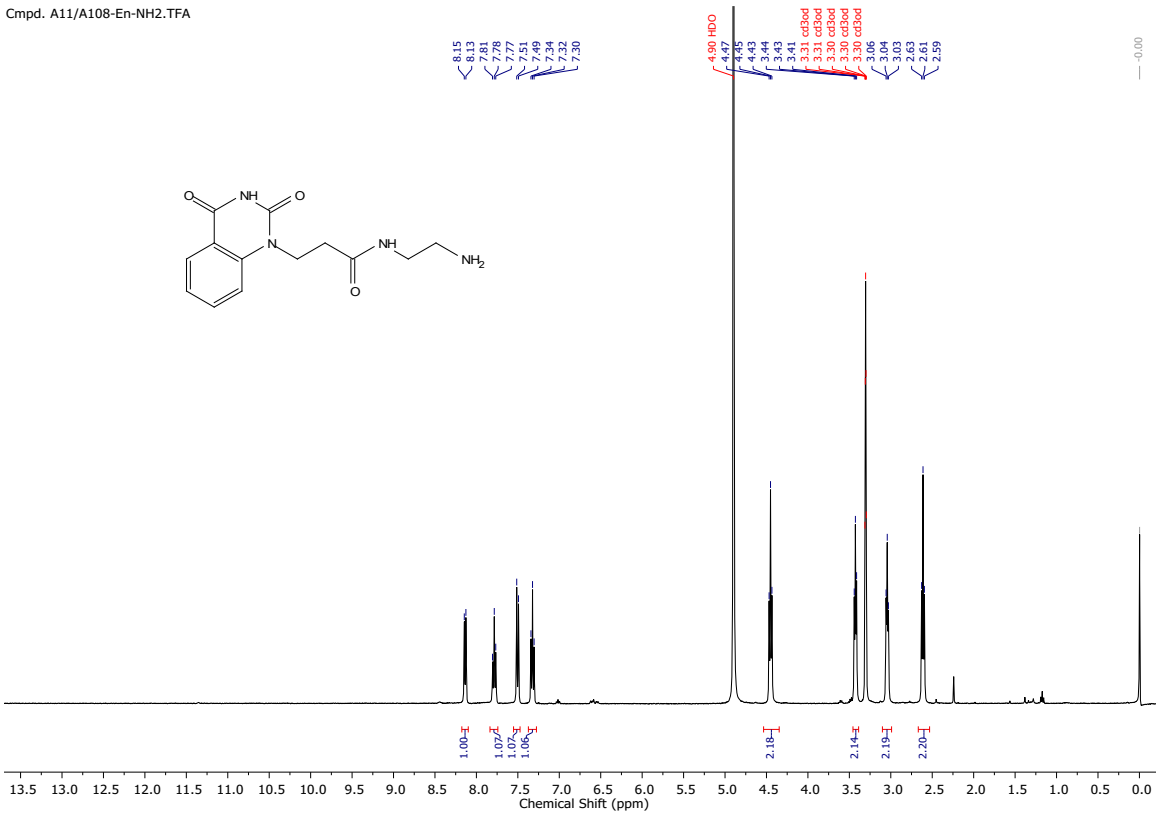

^{1}H NMR, 400 MHz, DMSO, compound (A11/A108-En-B111):

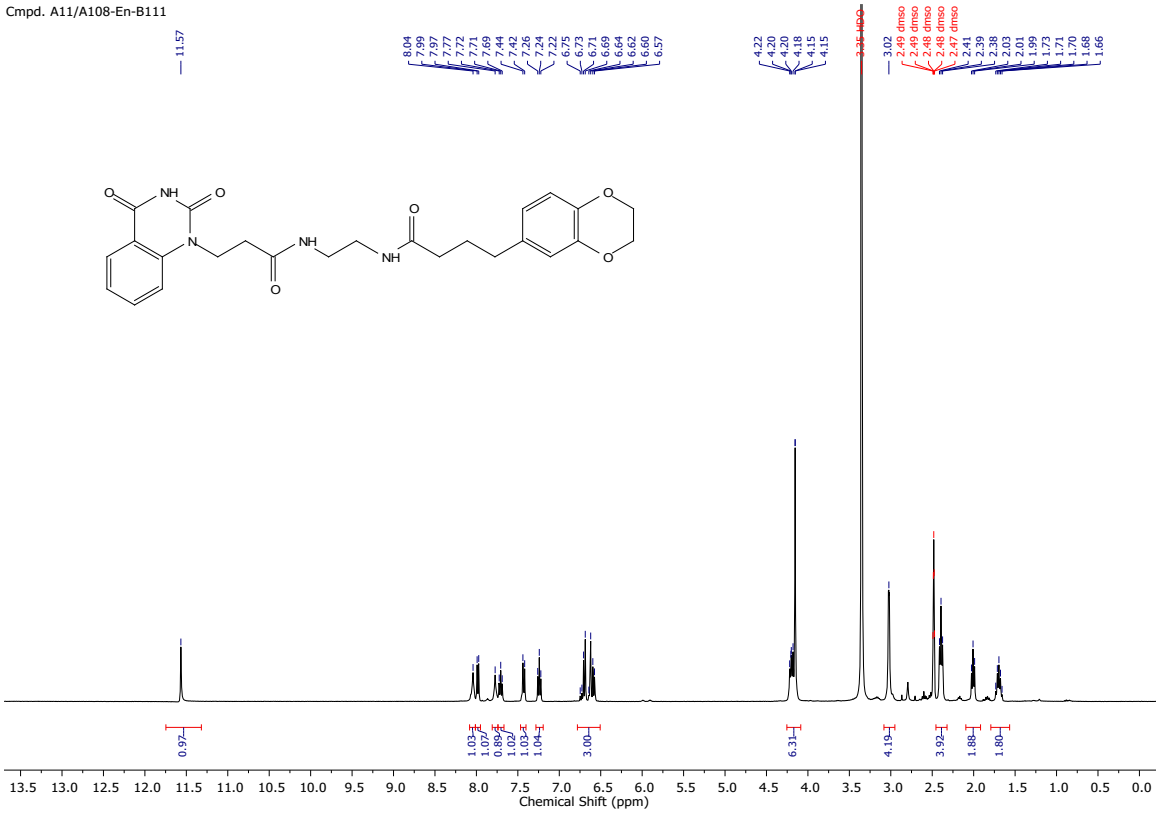

^{1}H NMR, 400 MHz, DMSO, compound (A11/A108-En-B21):

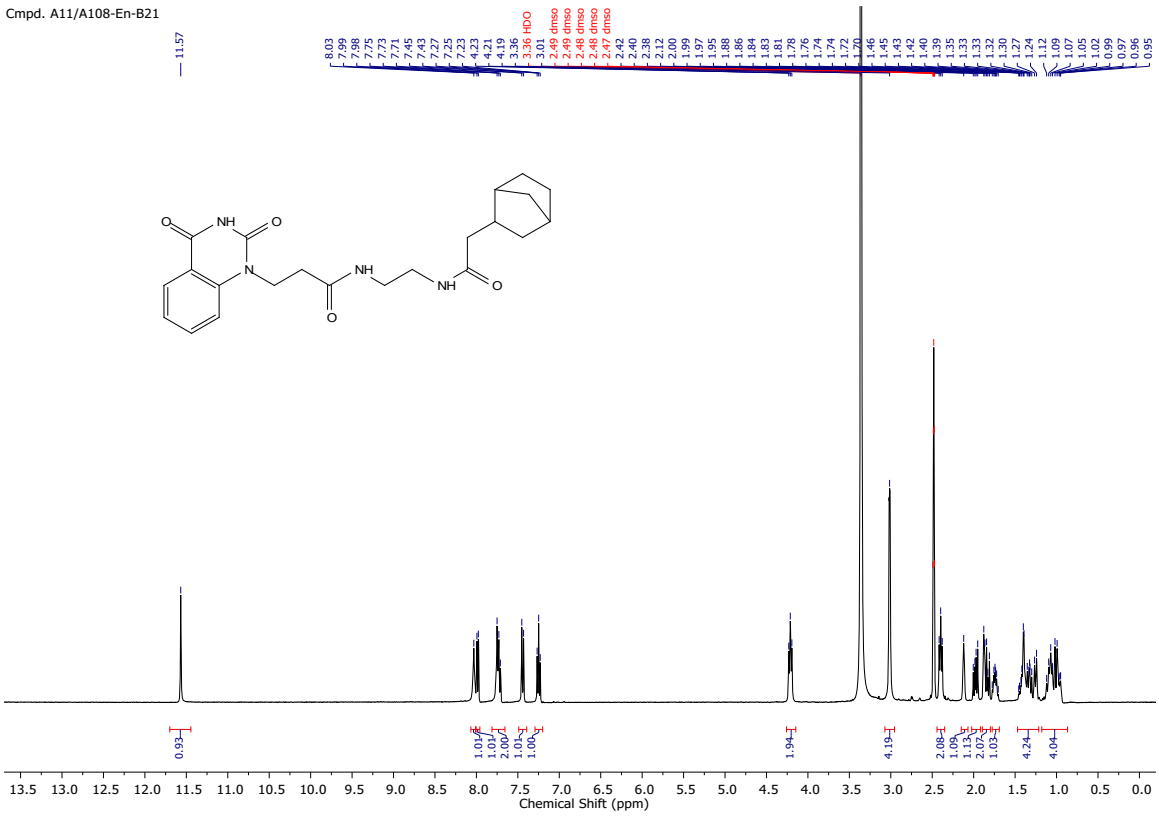

^{1}H NMR, 400 MHz, DMSO, compound (A11/A108-En-B227):

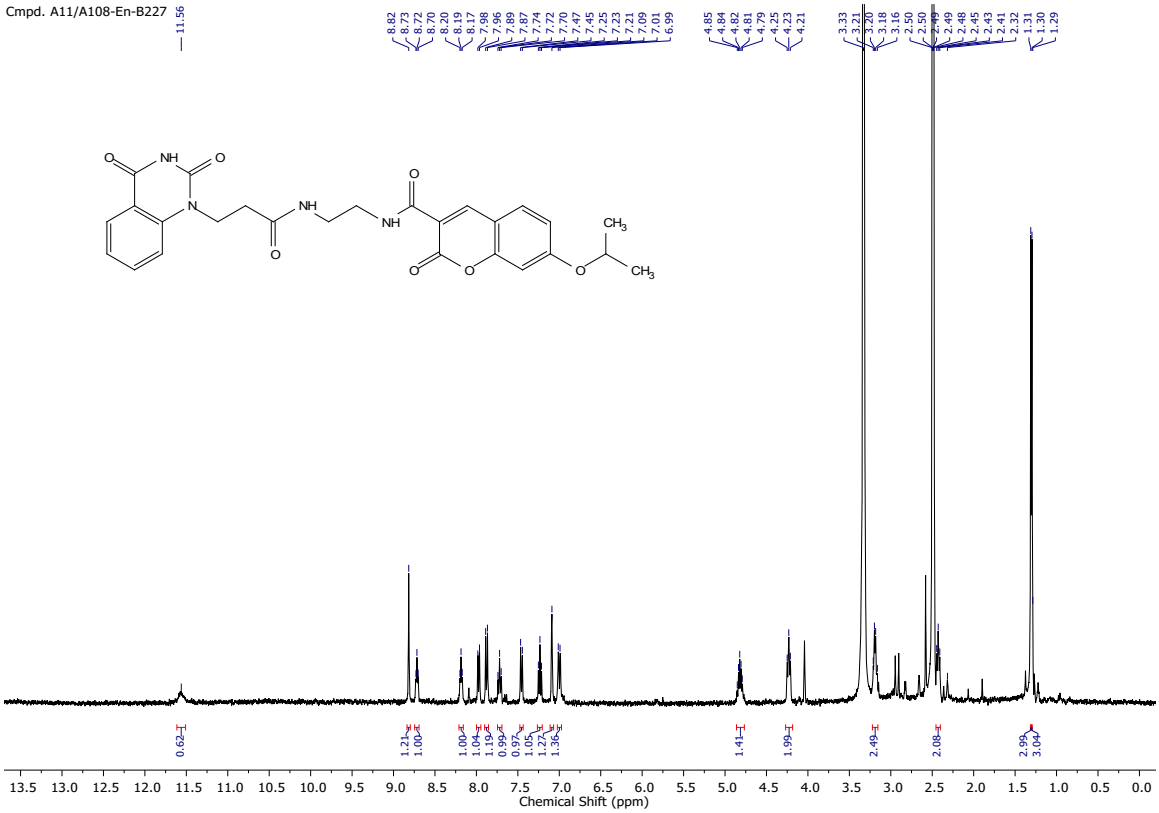

^{1}H NMR, 400 MHz, DMSO, compound (A11/A108-En-B139):

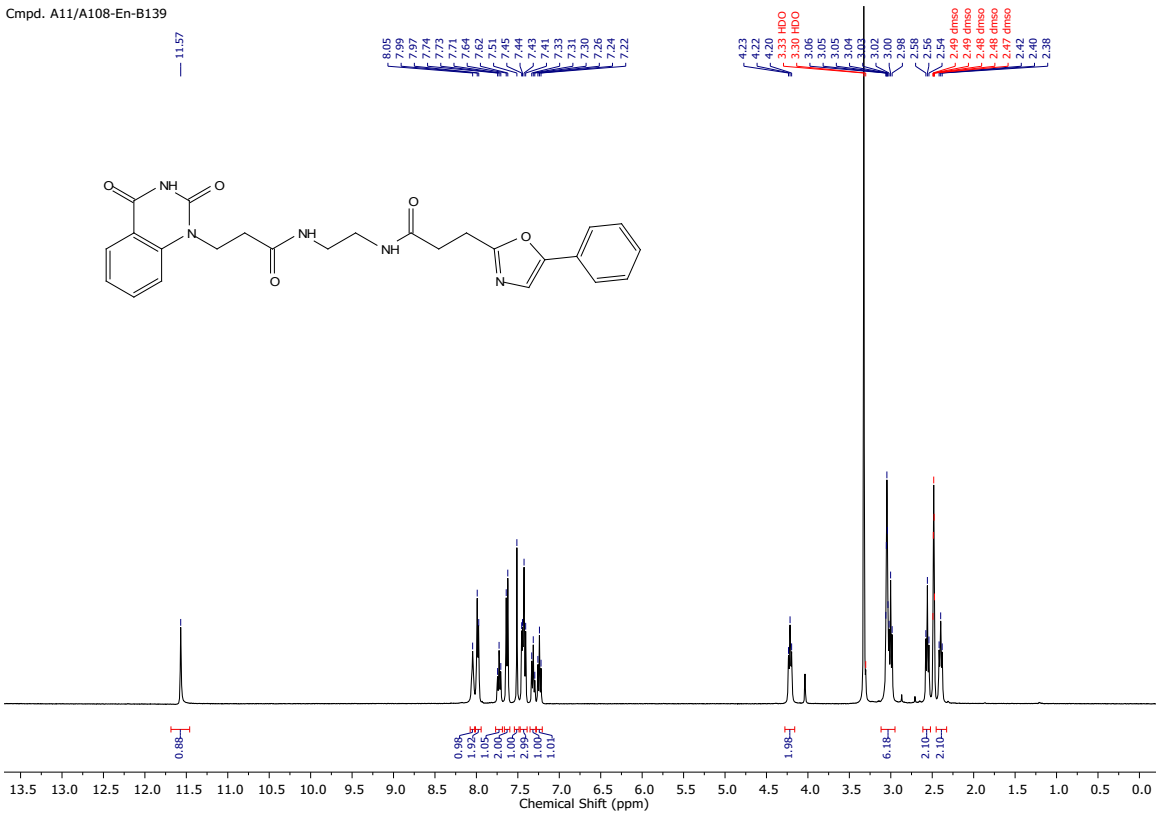

^{1}H NMR, 400 MHz, DMSO, compound (A11/A108-En-B101):

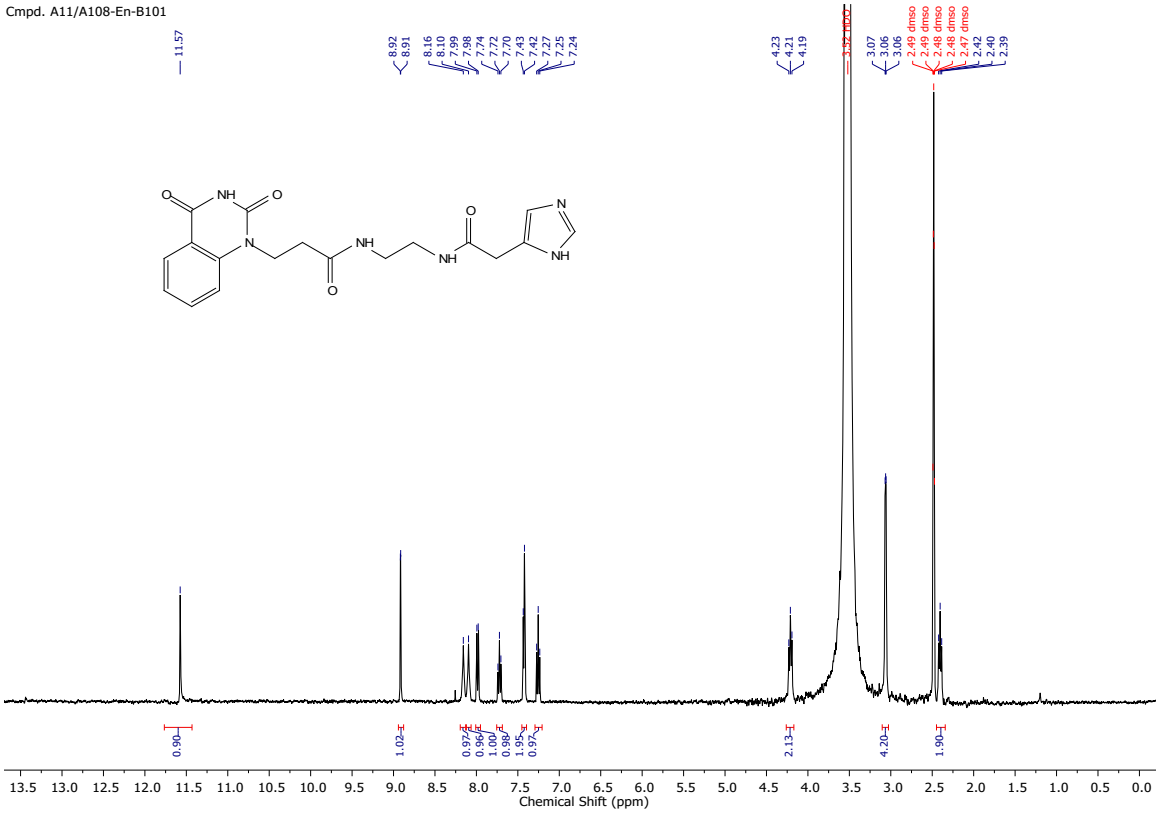

^{1}H NMR, 400 MHz, DMSO, compound (A11/A108-En-Bz):

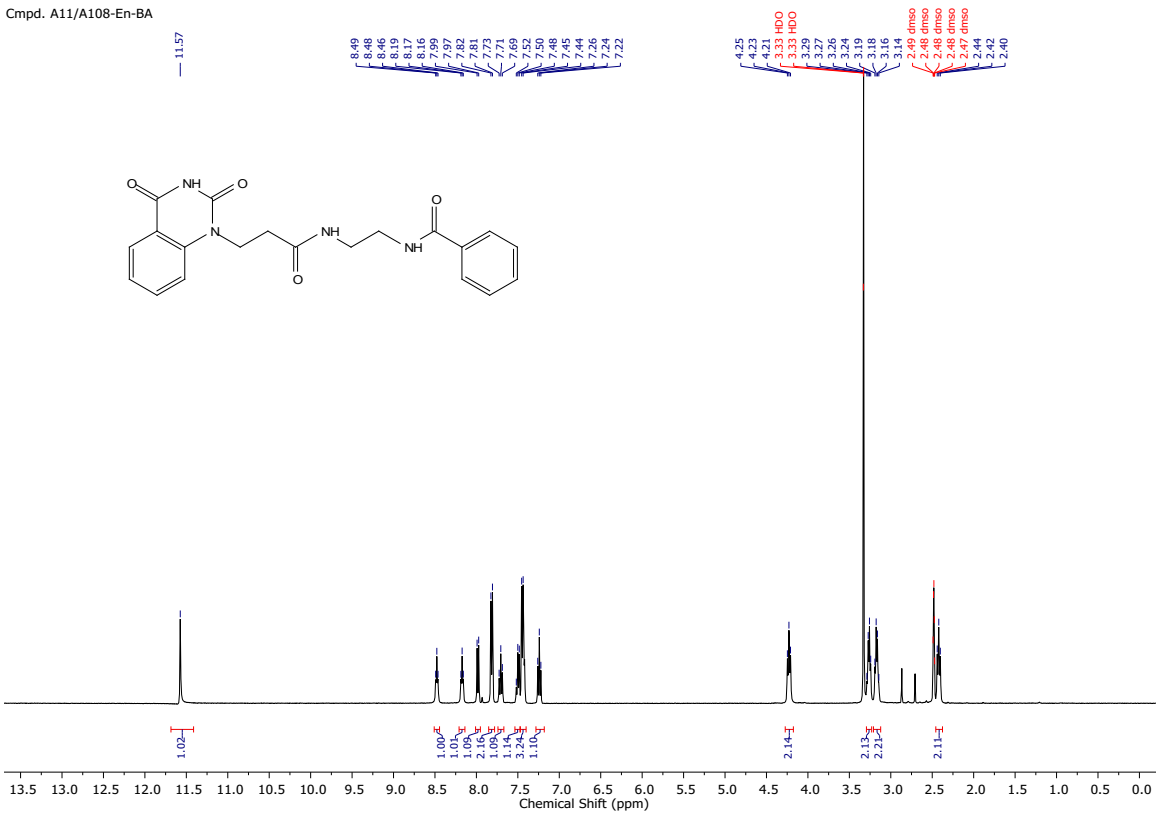

^{1}H NMR, 400 MHz, DMSO, compound (A11/A108-En-Ac):

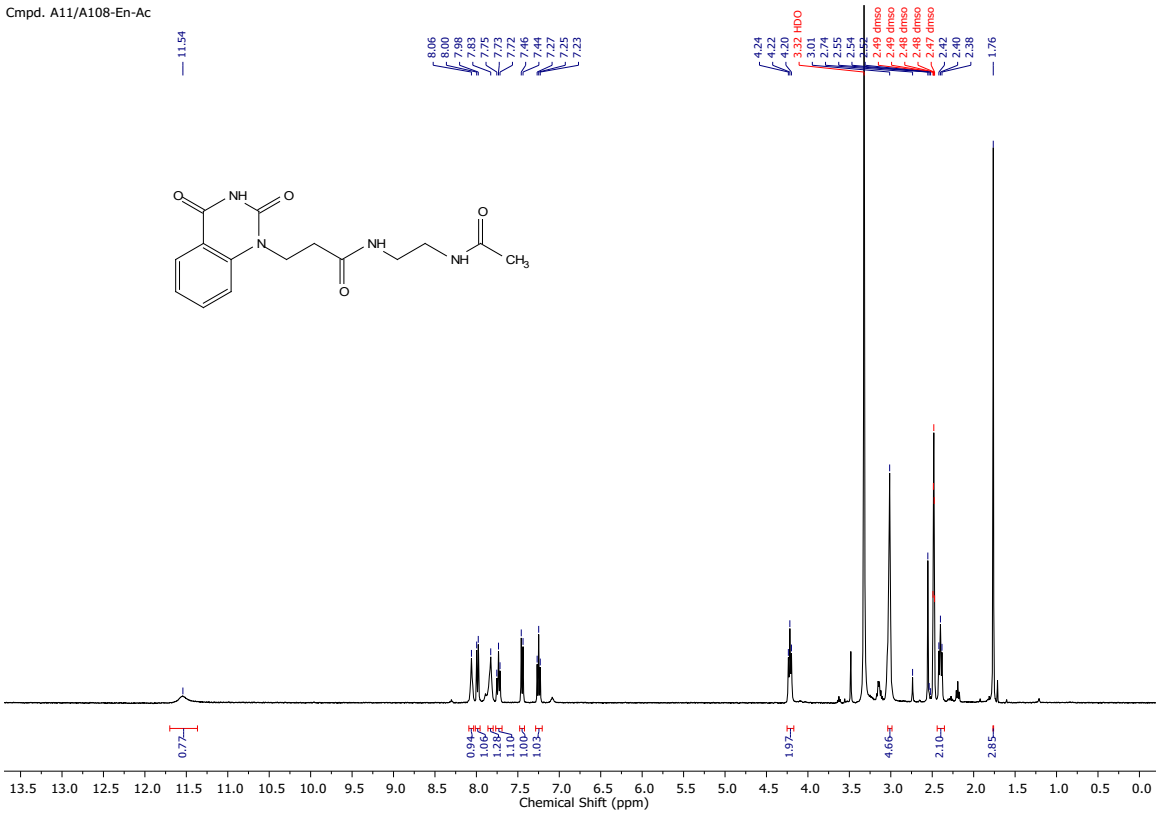

^{1}H NMR, 400 MHz, DMSO, compound (A44-En-B190):

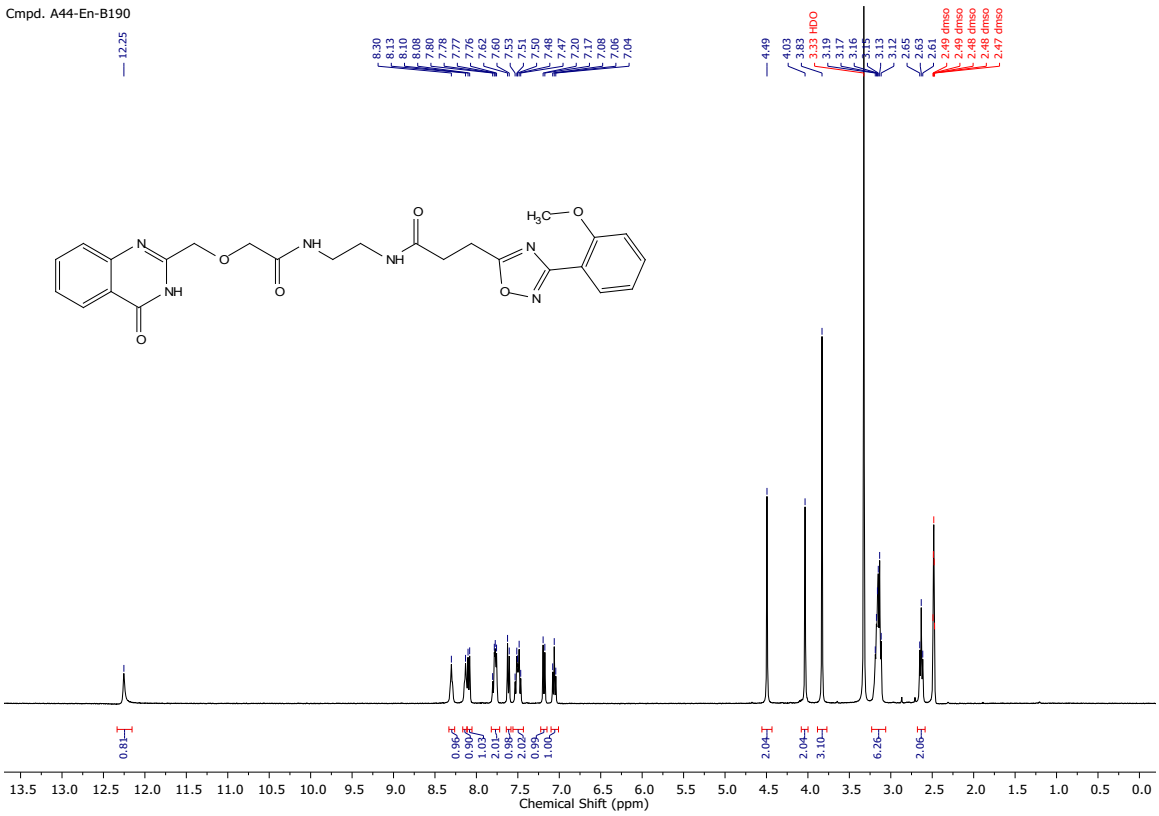

^{1}H NMR, 400 MHz, MeOD, compound (B316-En-Boc):

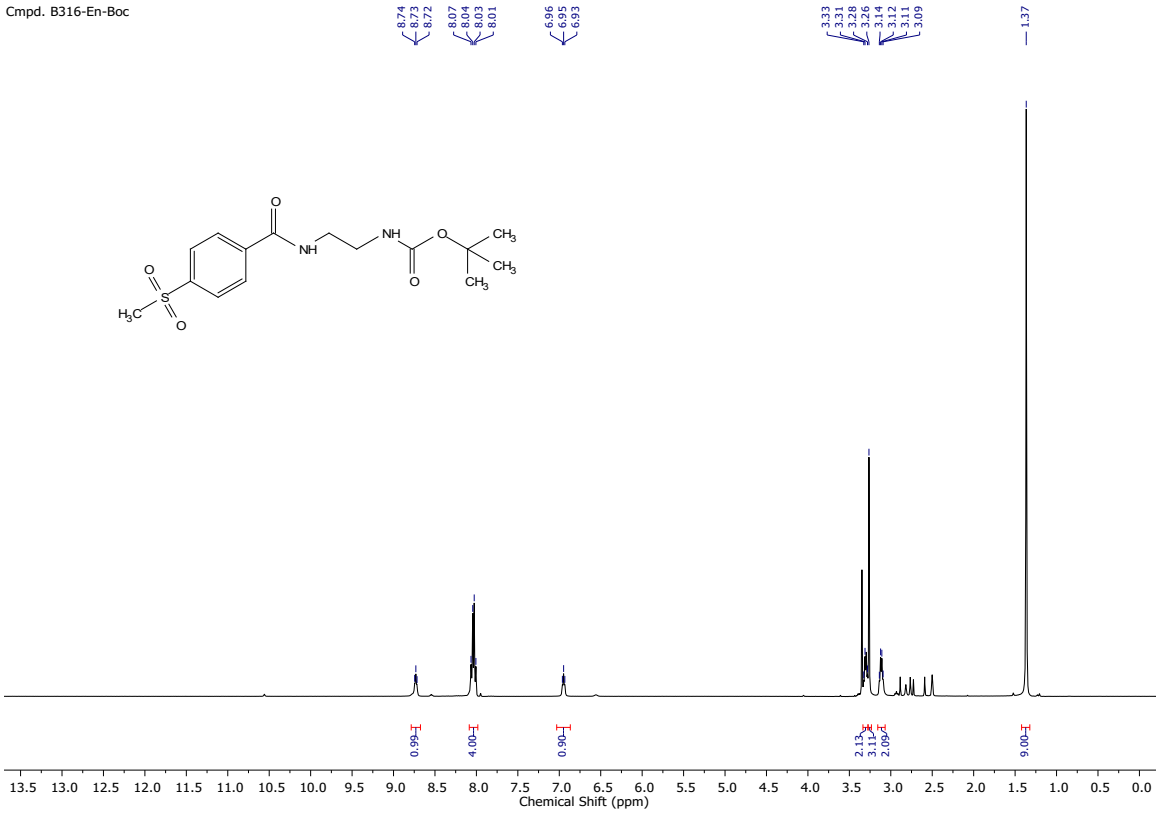

^{1}H NMR, 400 MHz, MeOD, compound (B316-En-NH_2TFA):

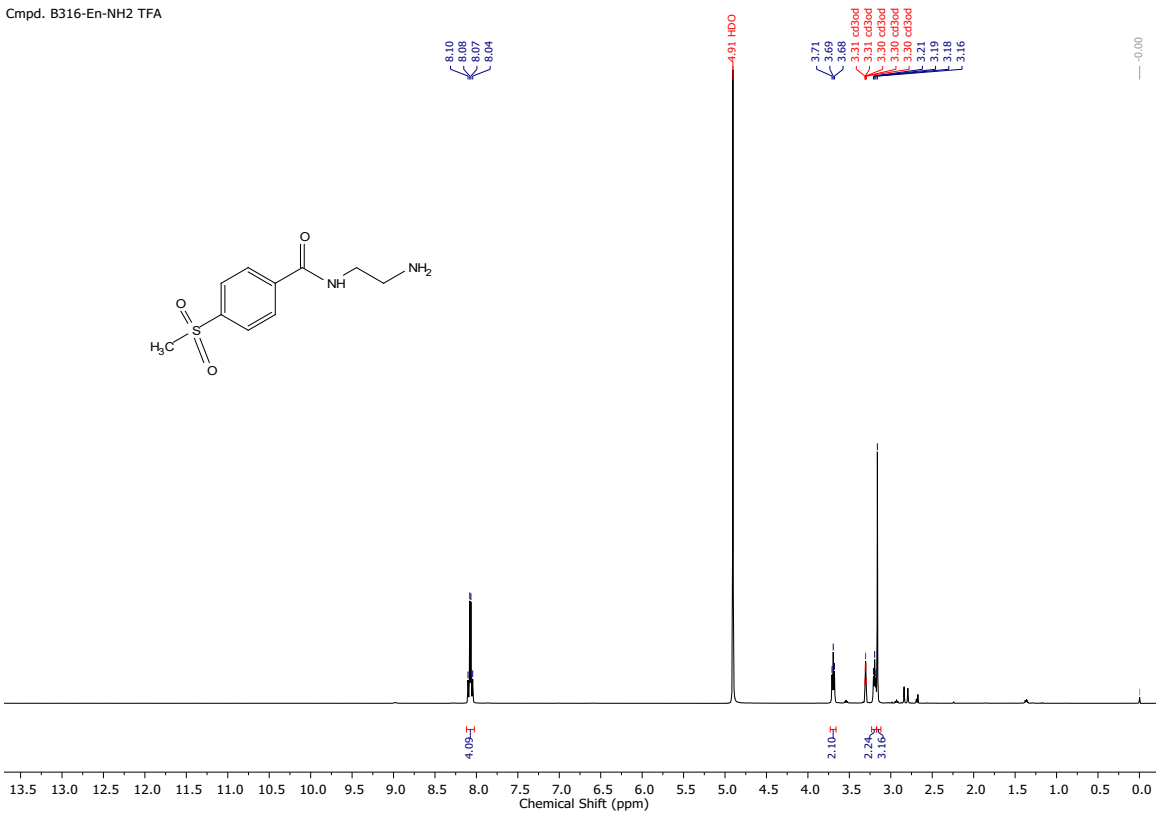

^{1}H NMR, 400 MHz, DMSO, compound (A153-En-B316):

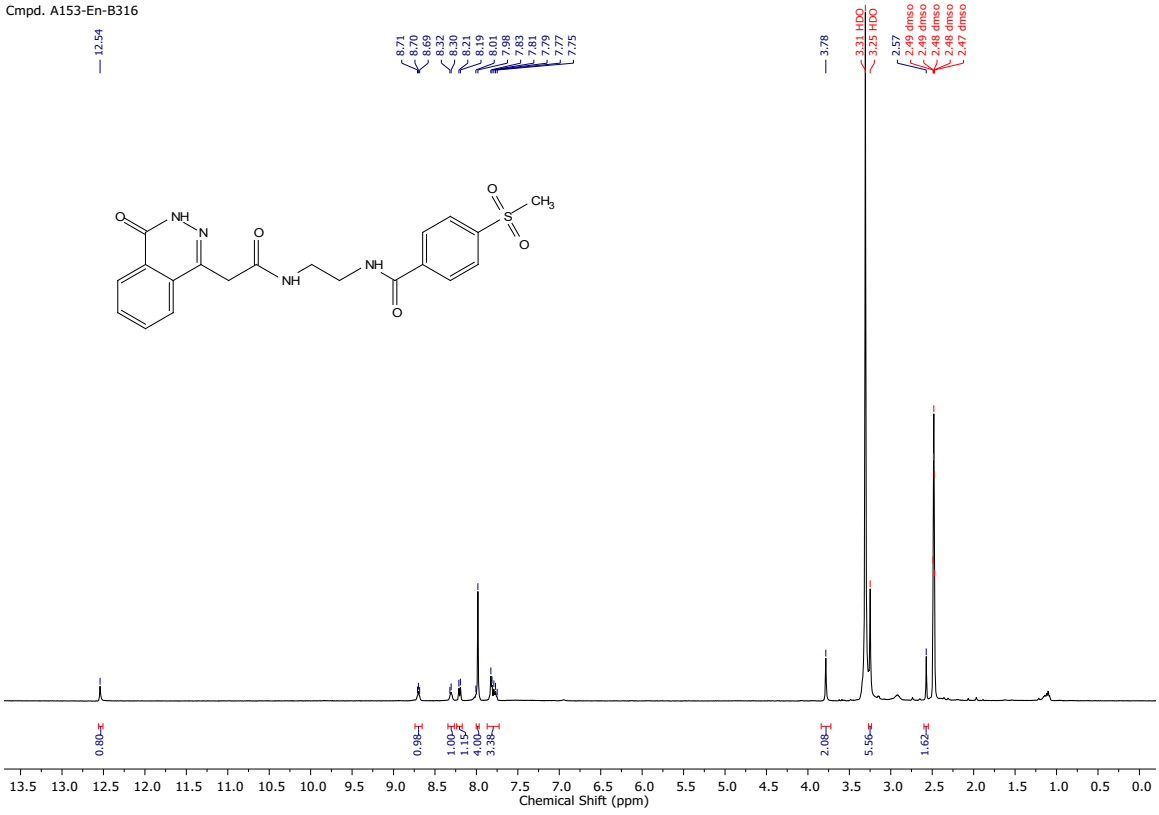

^{1}H NMR, 400 MHz, DMSO, compound (A153-En-B356):

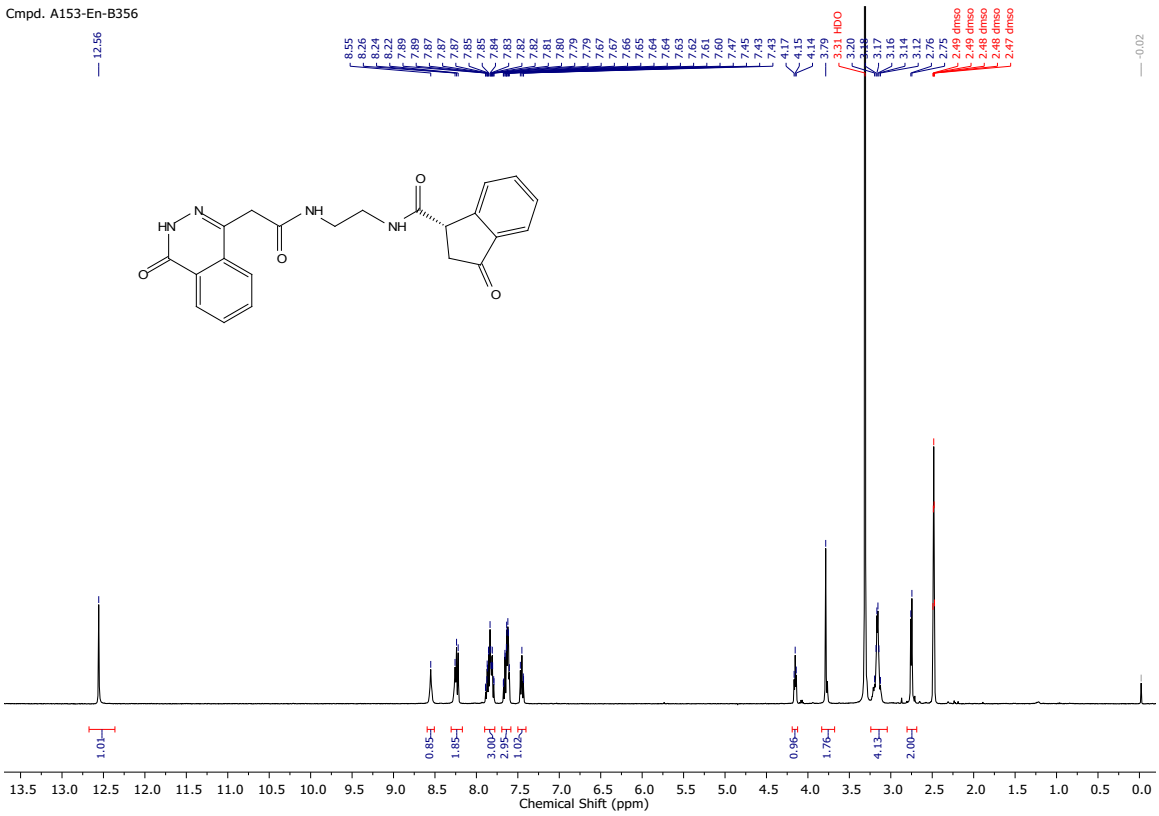

^{1}H NMR, 400 MHz, DMSO, compound (A131-En-Boc):

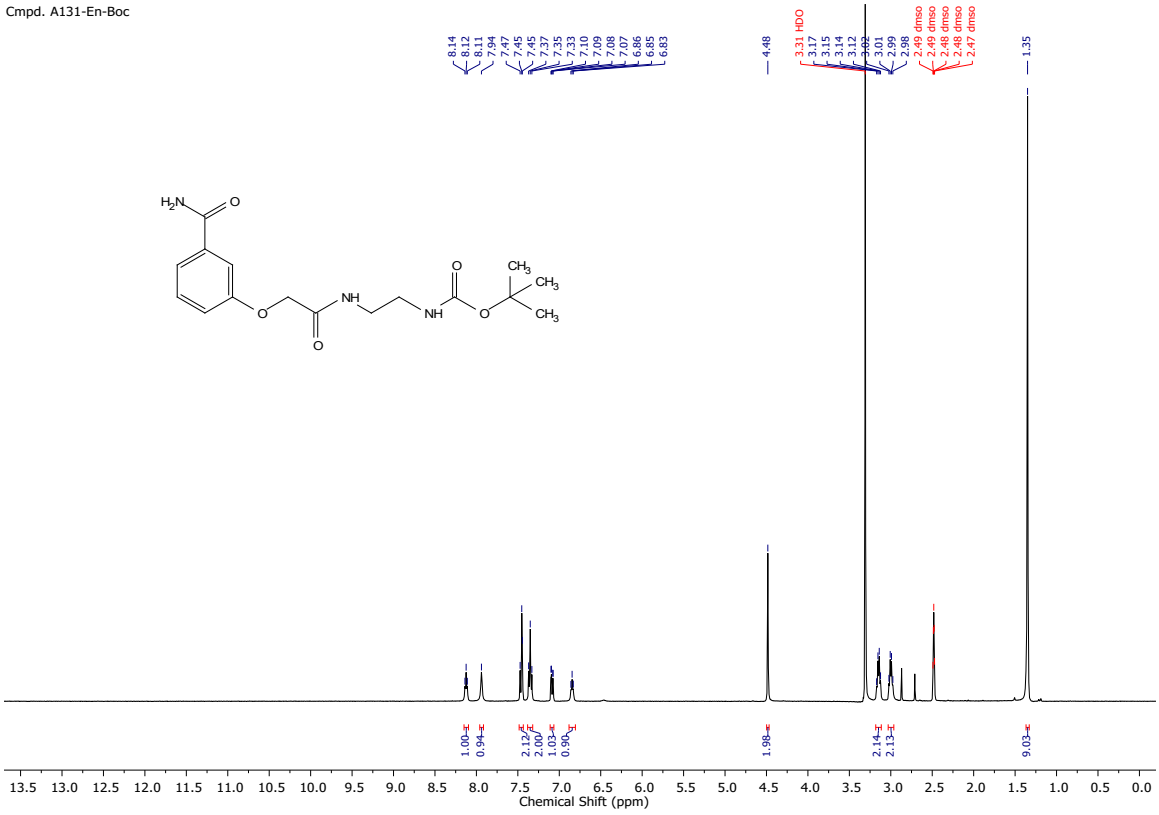

^{1}H NMR, 400 MHz, DMSO, compound (A131-En-NH_2TFA):

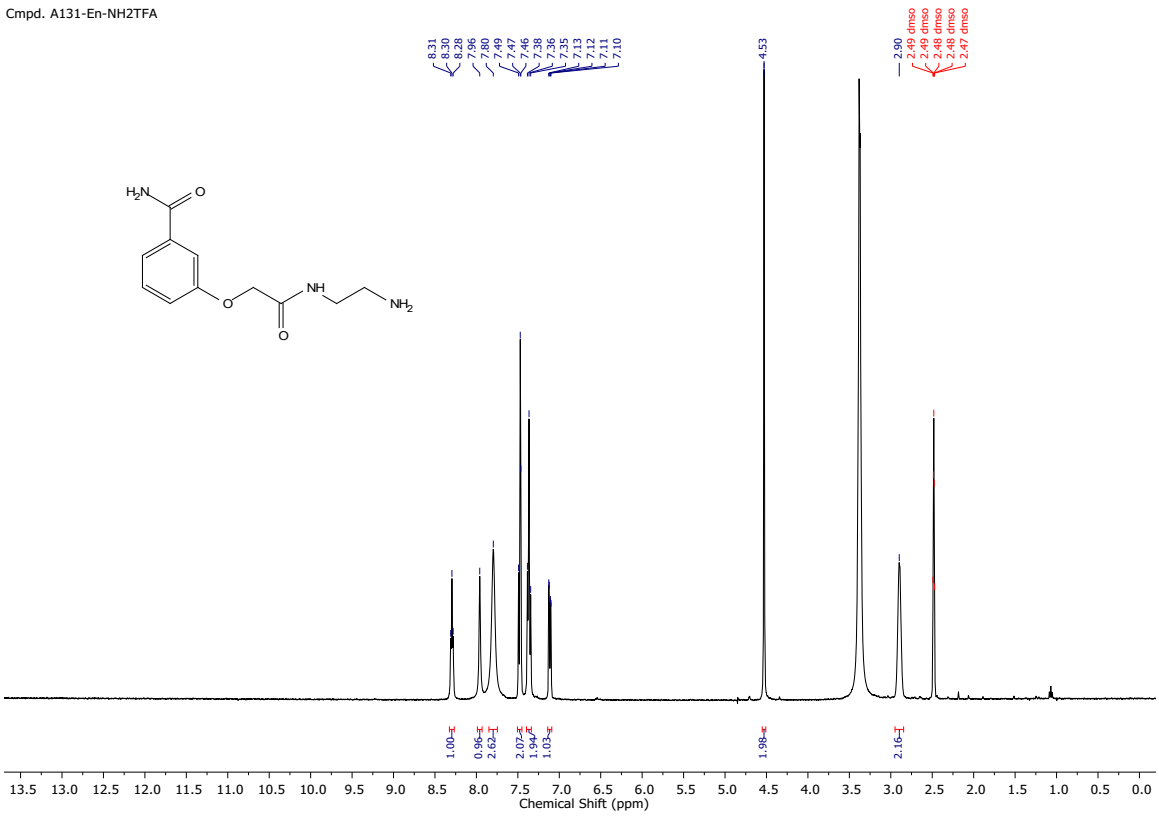

^{1}H NMR, 400 MHz, DMSO, compound (A131-En-B199):

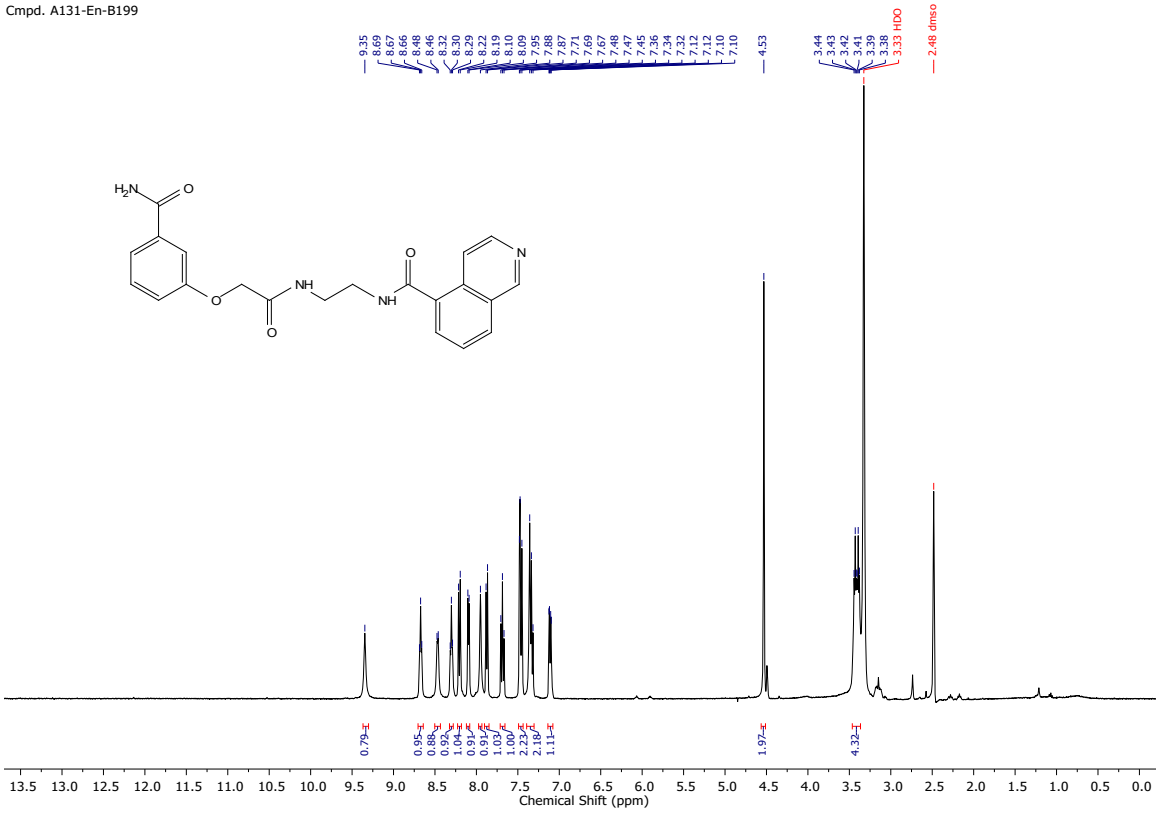

^{1}H NMR, 400 MHz, MeOD, compound (A131-En-B355):

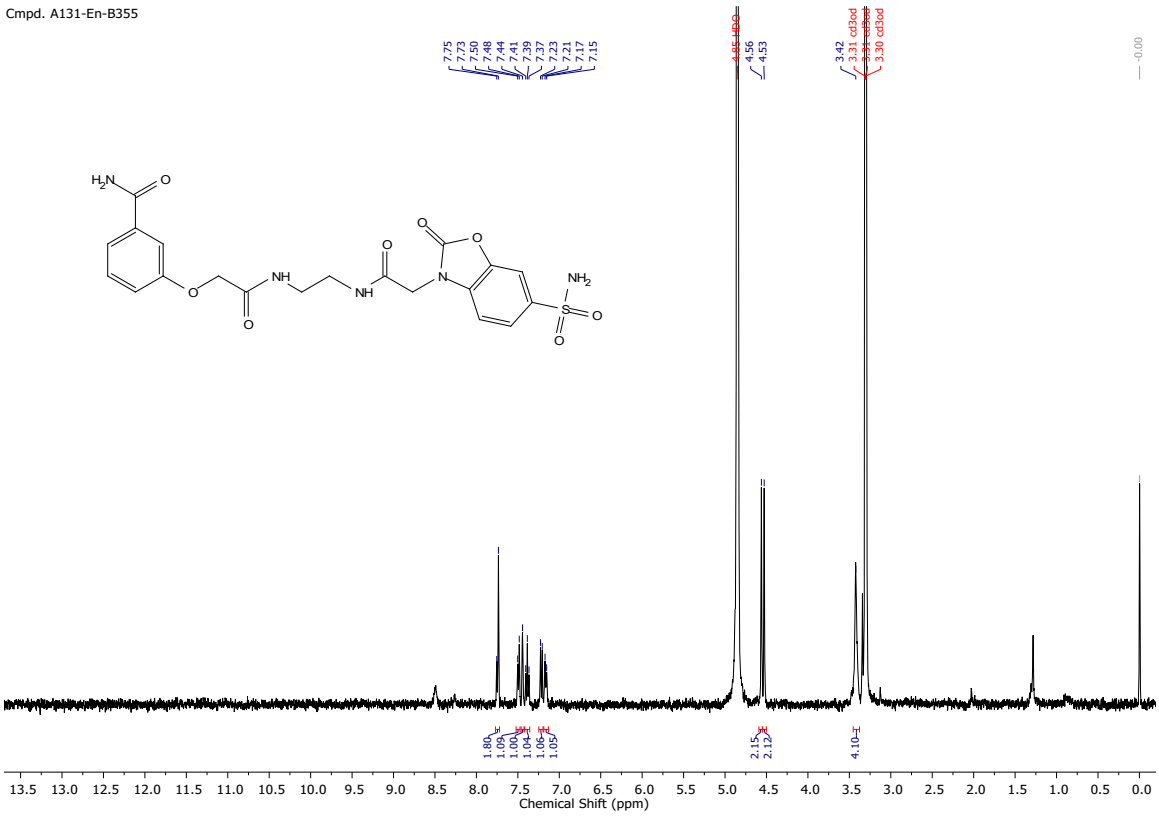

^{1}H NMR, 400 MHz, DMSO, compound (A88-En-Boc):

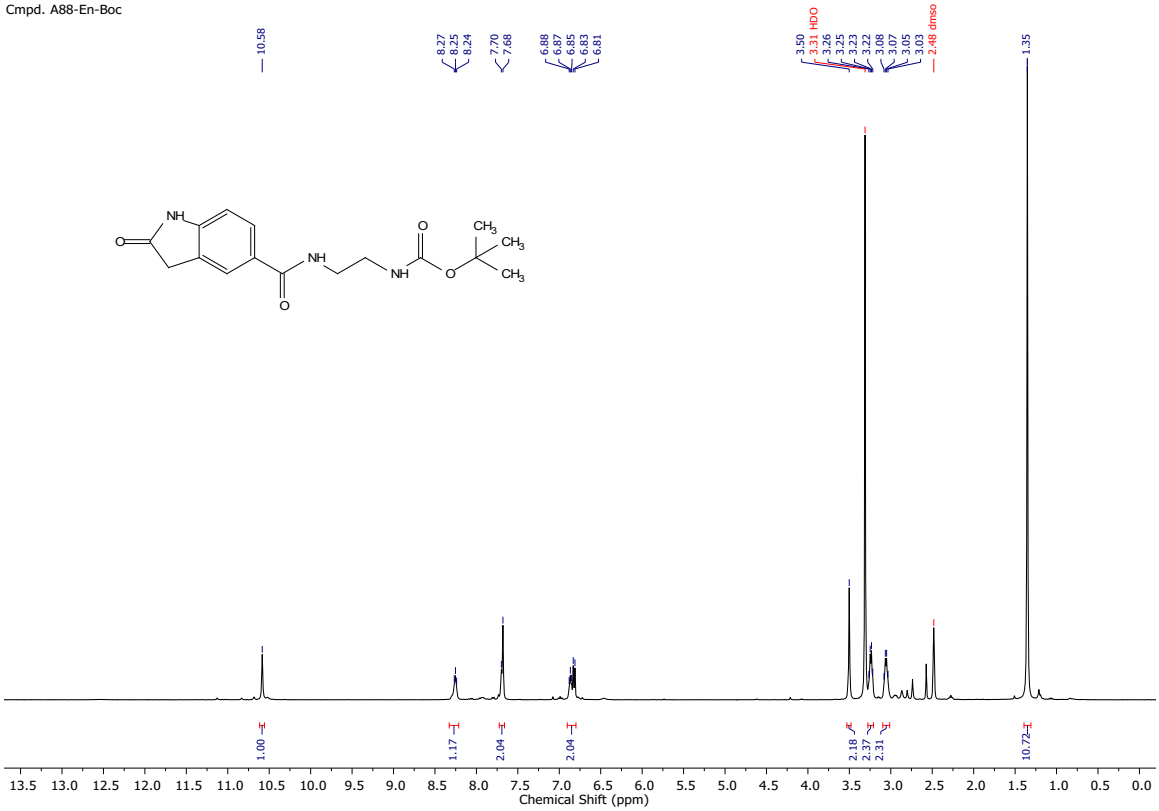

^{1}H NMR, 400 MHz, MeOD, compound (A88-En-NH$_2$TFA):

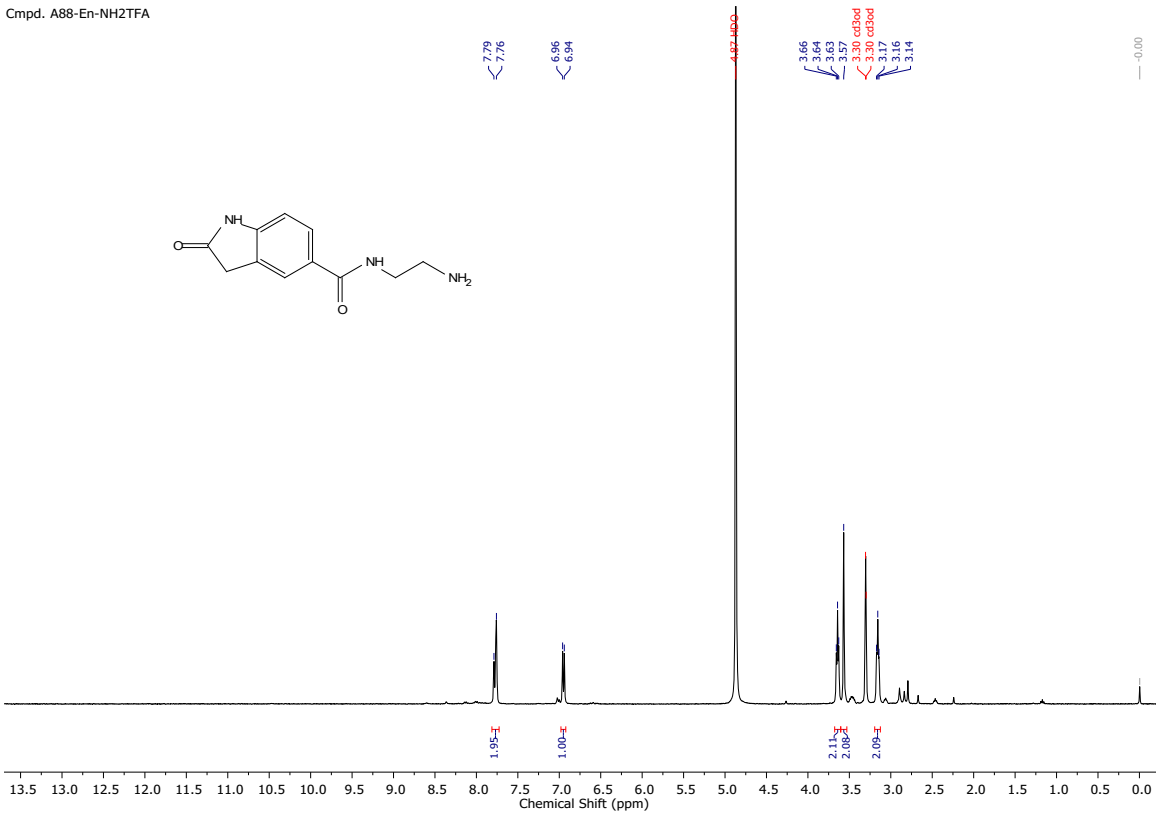

^{1}H NMR, 400 MHz, DMSO, compound (A88-En-B354):

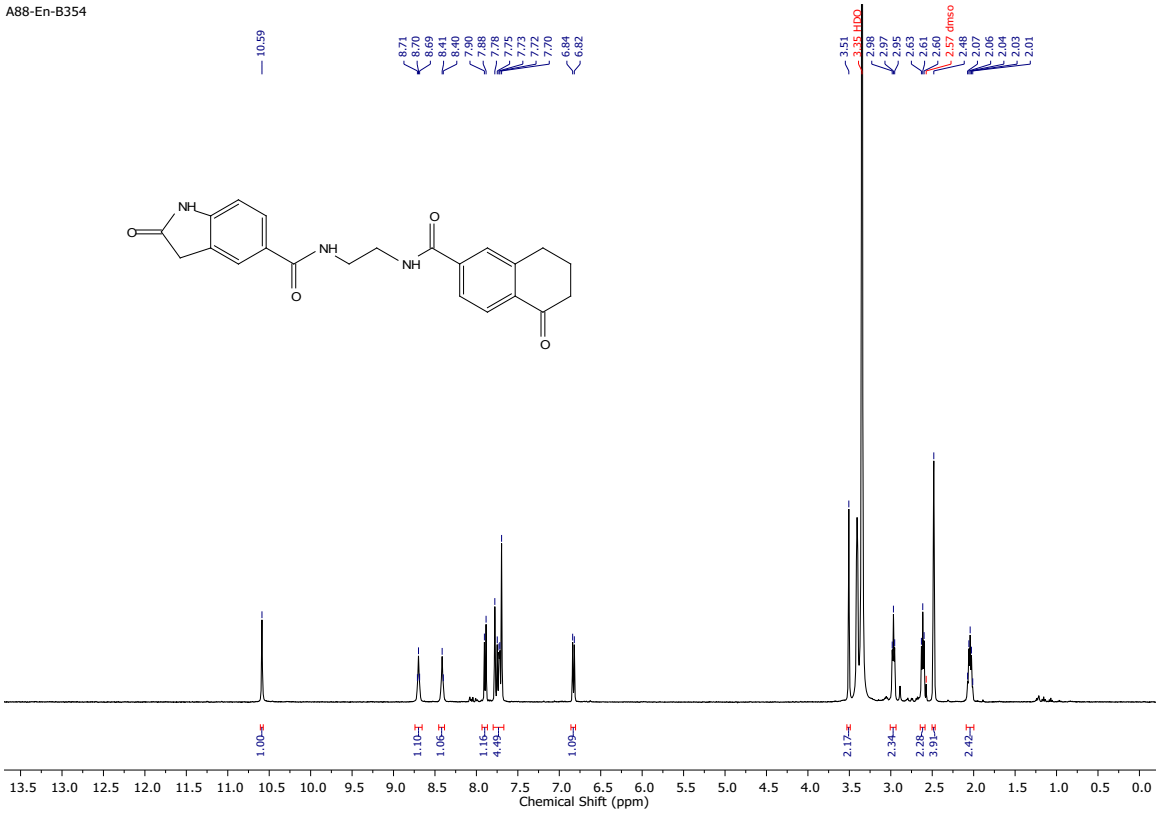

^{1}H NMR, 400 MHz, MeOD, compound (B101-En-Boc):

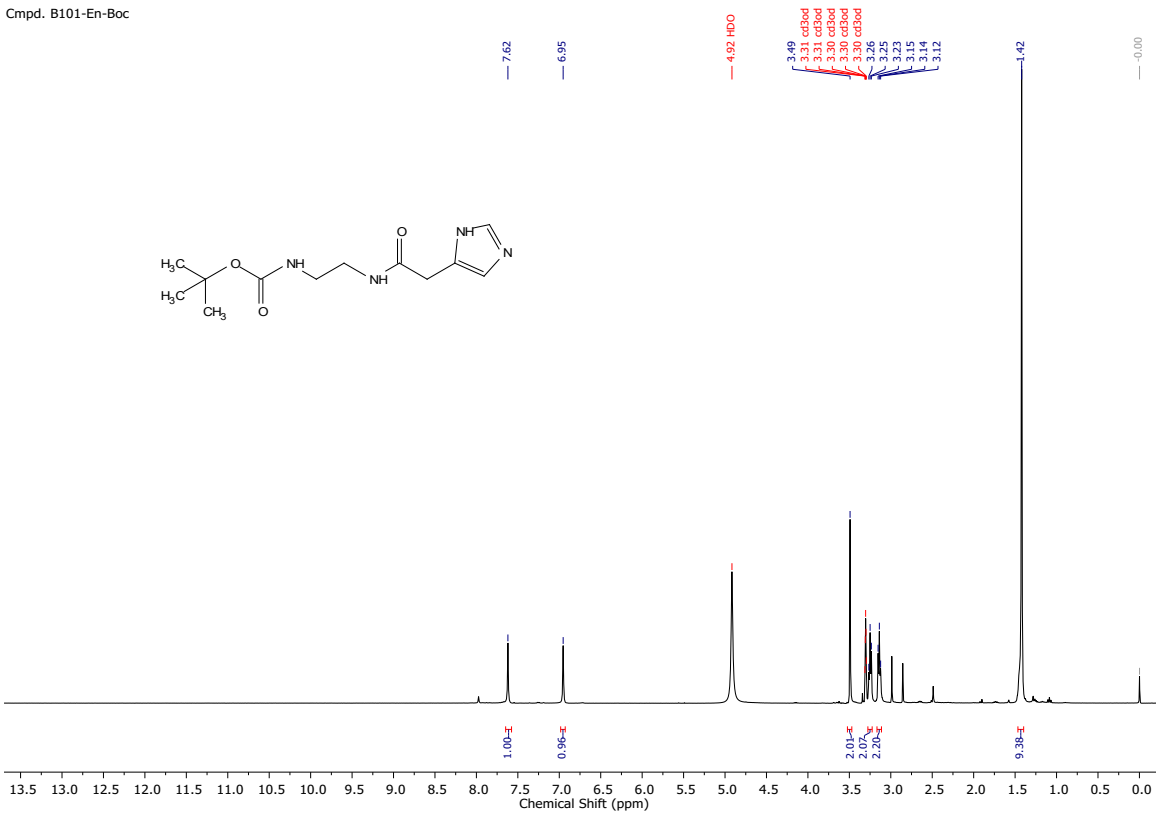

^{1}H NMR, 400 MHz, MeOD, compound (B101-En-NH$_2$TFA):

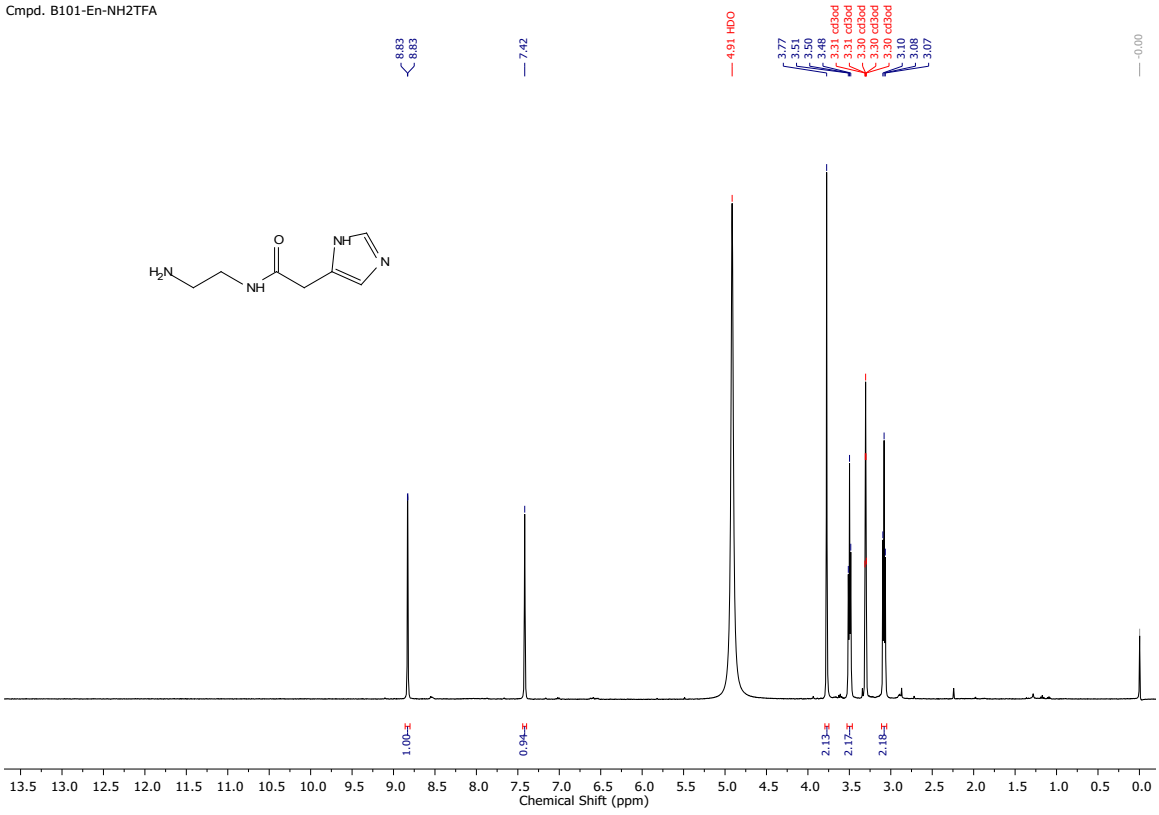

^{1}H NMR, 400 MHz, MeOD, compound (A61-En-B101):

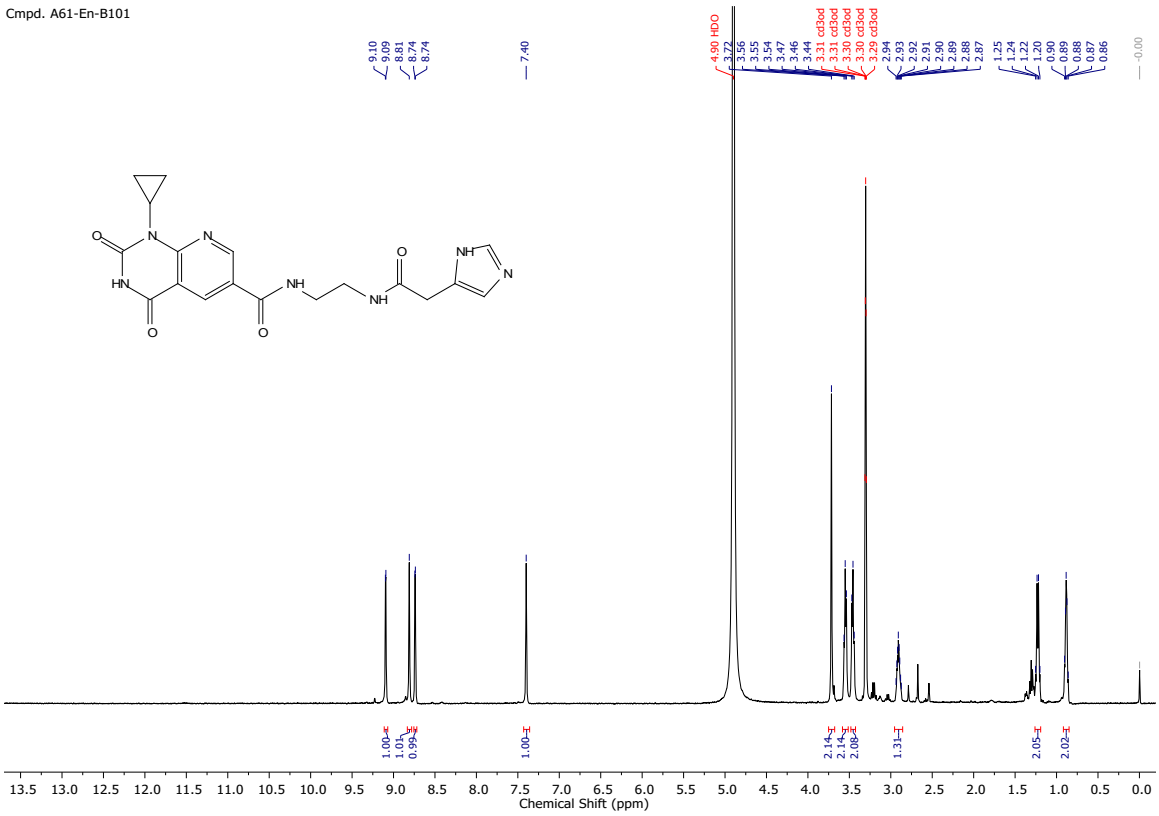

^{1}H NMR, 400 MHz, DMSO, compound (A12-En-B286):

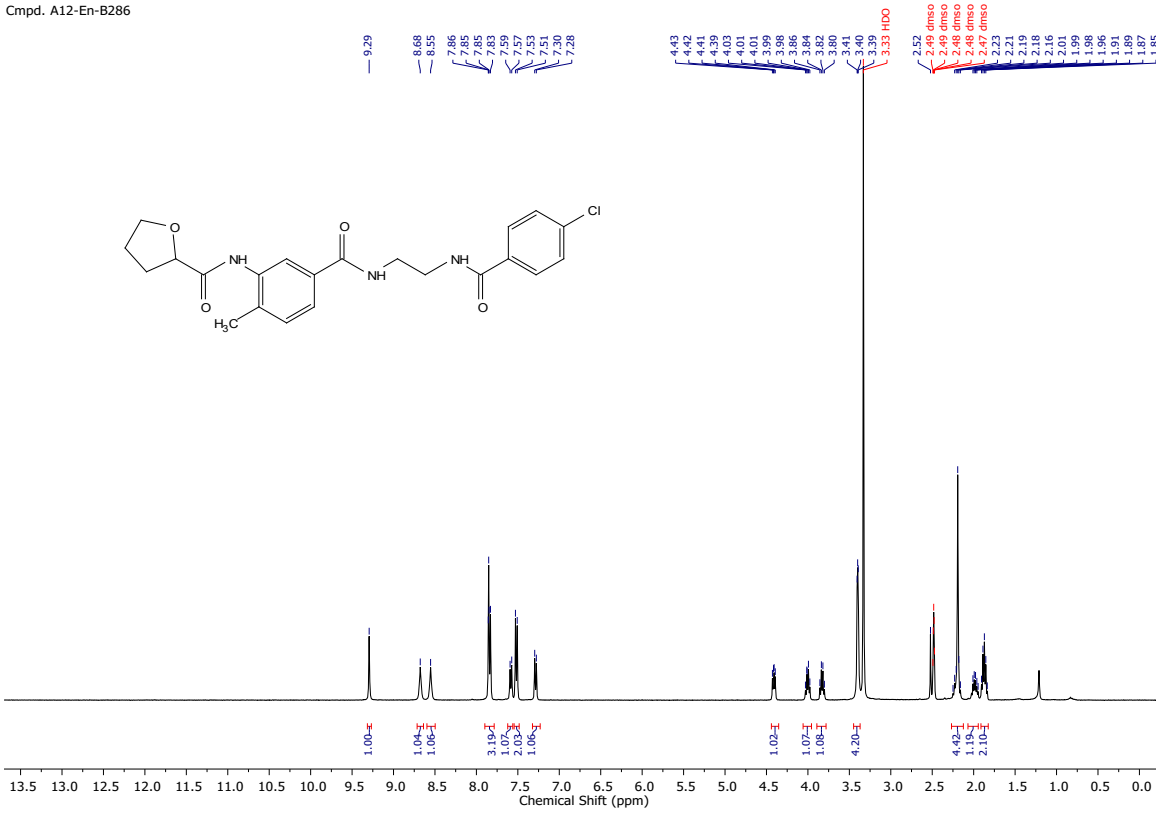

^{1}H NMR, 400 MHz, DMSO, compound (A7-En-B277):

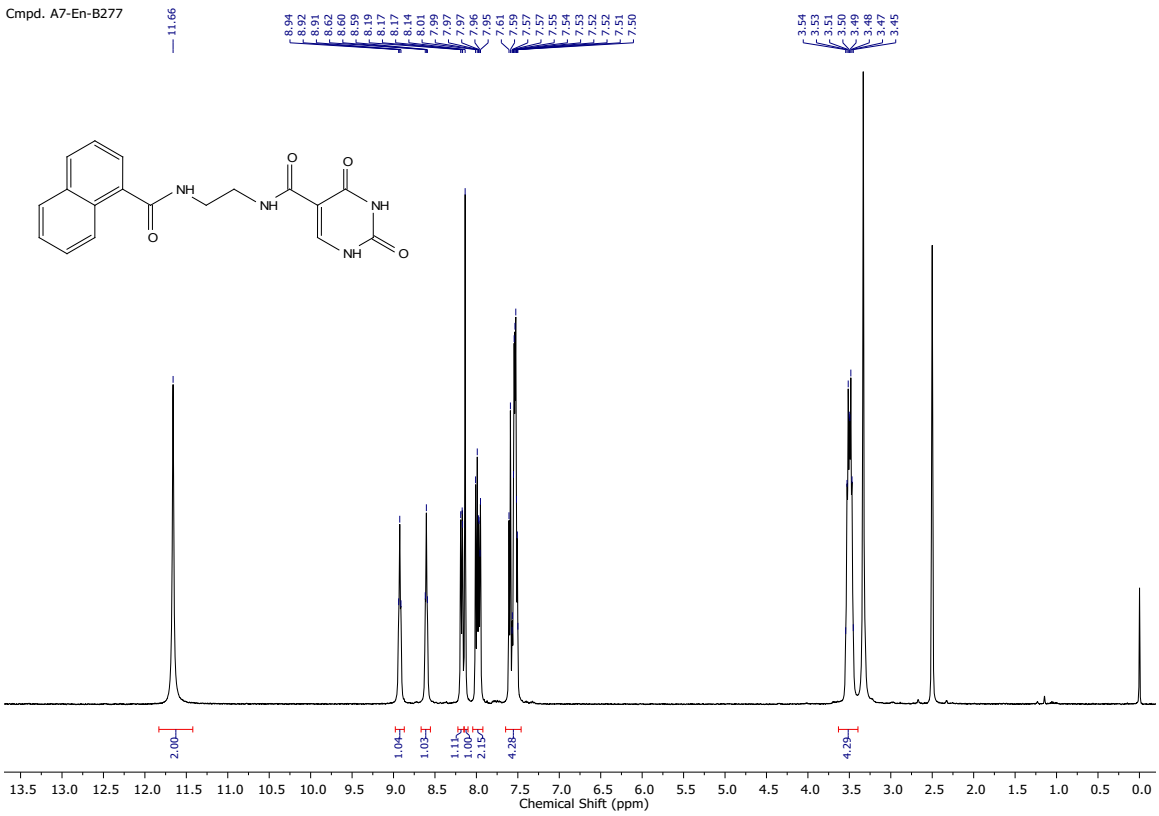

ESI+ MS, conjugate (TTT TTT-C12-A45-LINKER-B299):

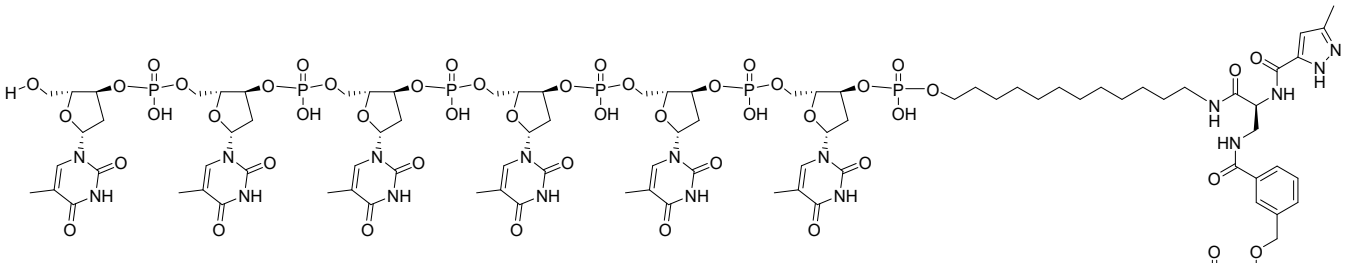

TTT TTT-C12-A45-LINKER-B299

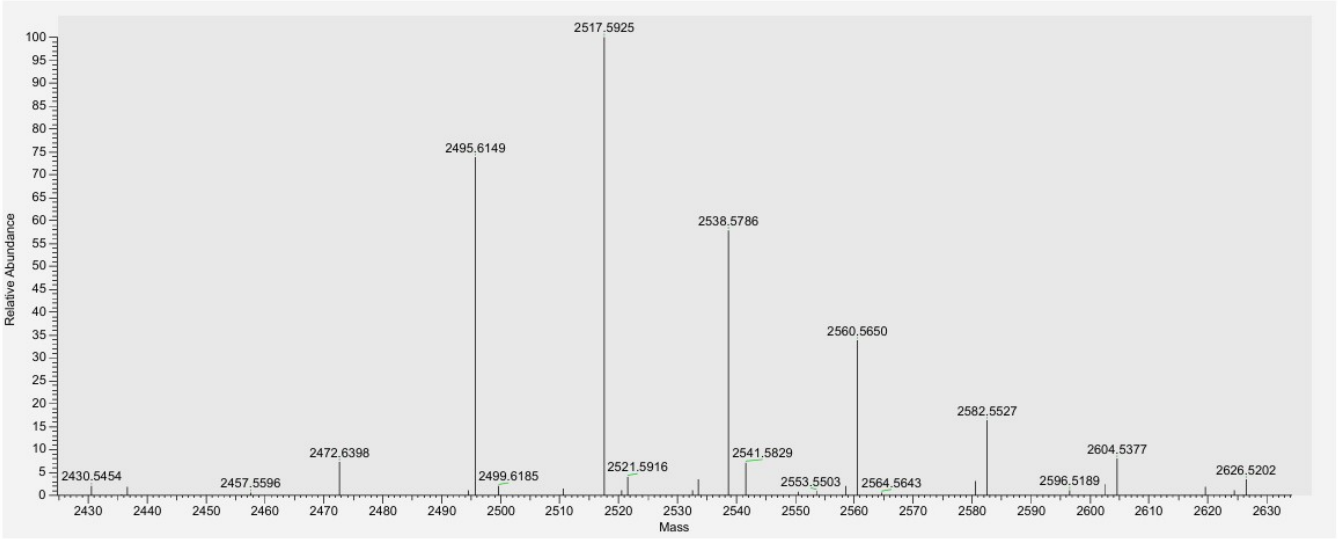

ESI+ MS, conjugate (TTT TTT-C12-A45-LINKER-B145):

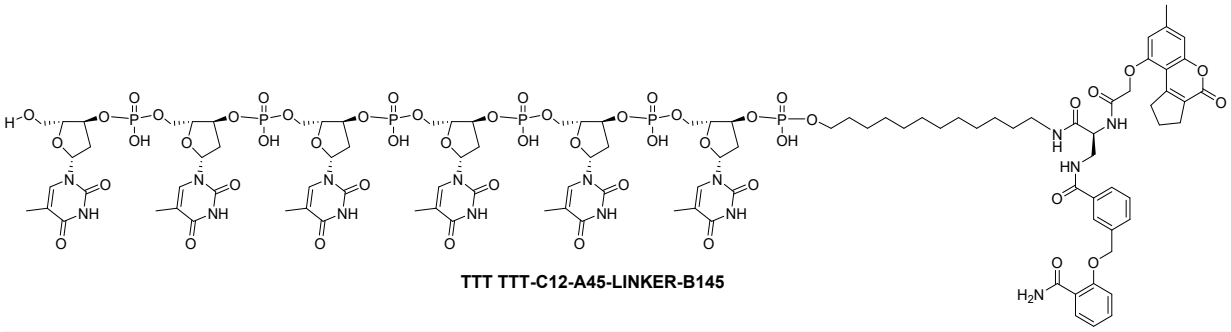

TTT TTT-C12-A45-LINKER-B145

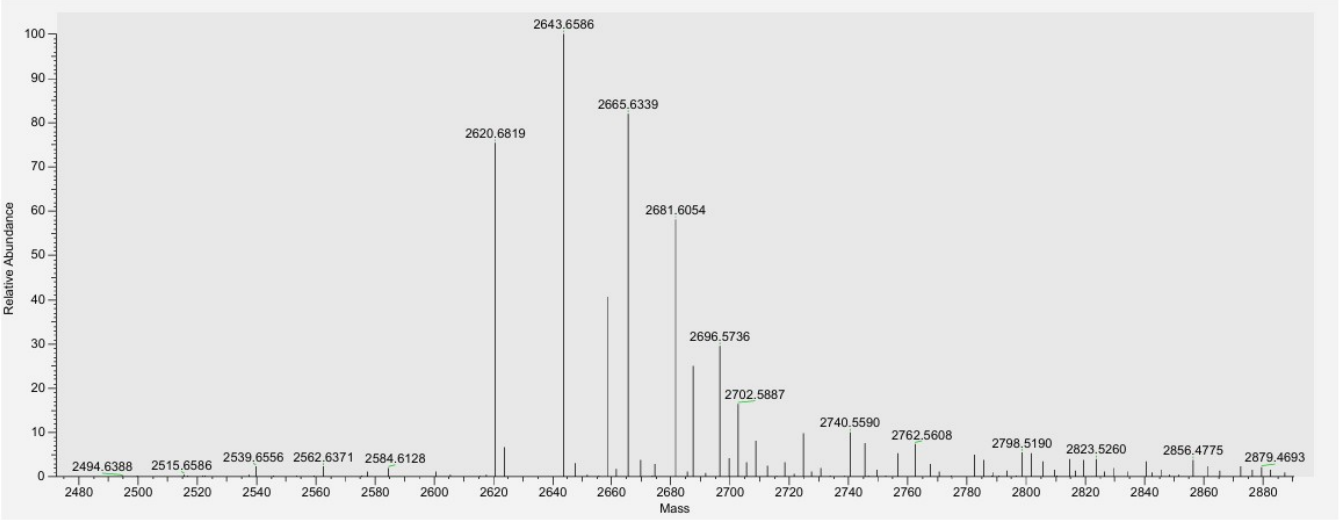

^{1}H NMR, 400 MHz, MeOD, compound (B299 DAP N-Boc Me ester):

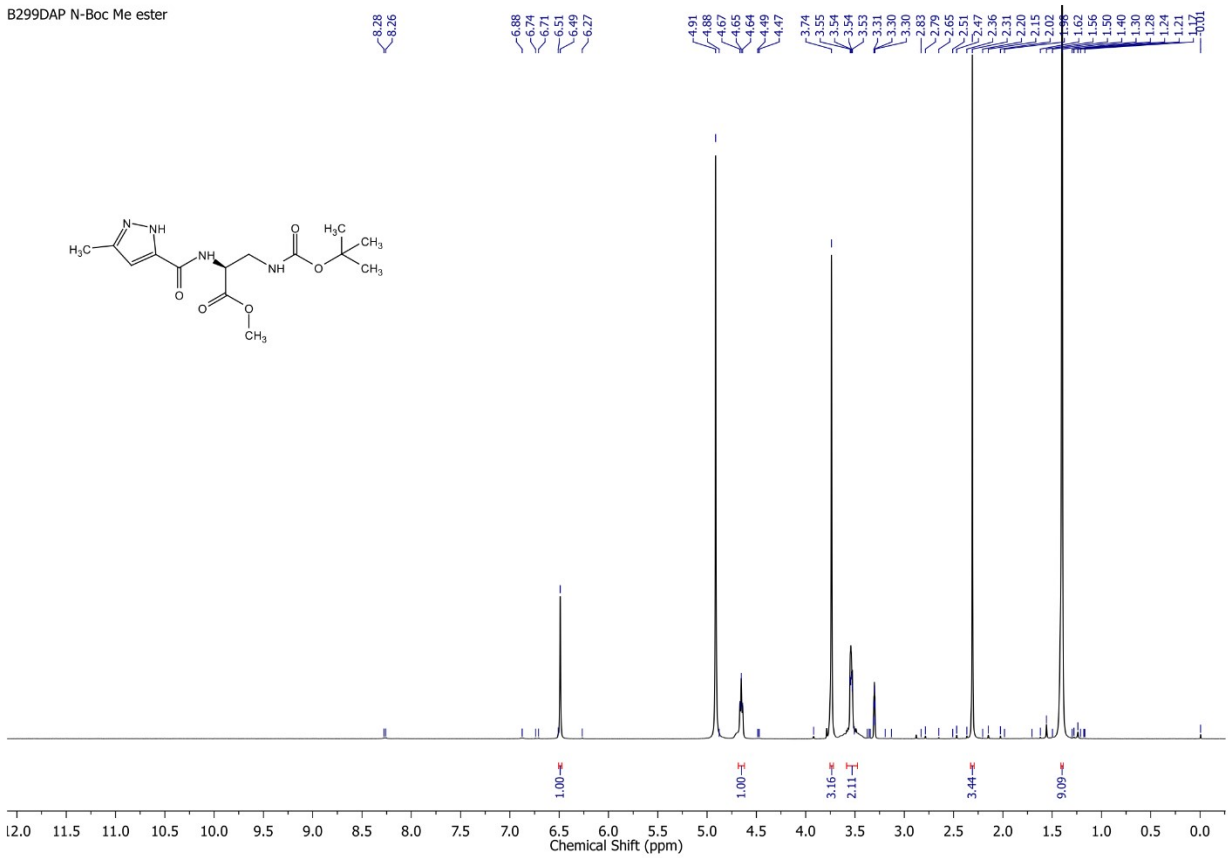

^{1}H NMR, 400 MHz, MeOD, compound (B299 DAP Me ester):

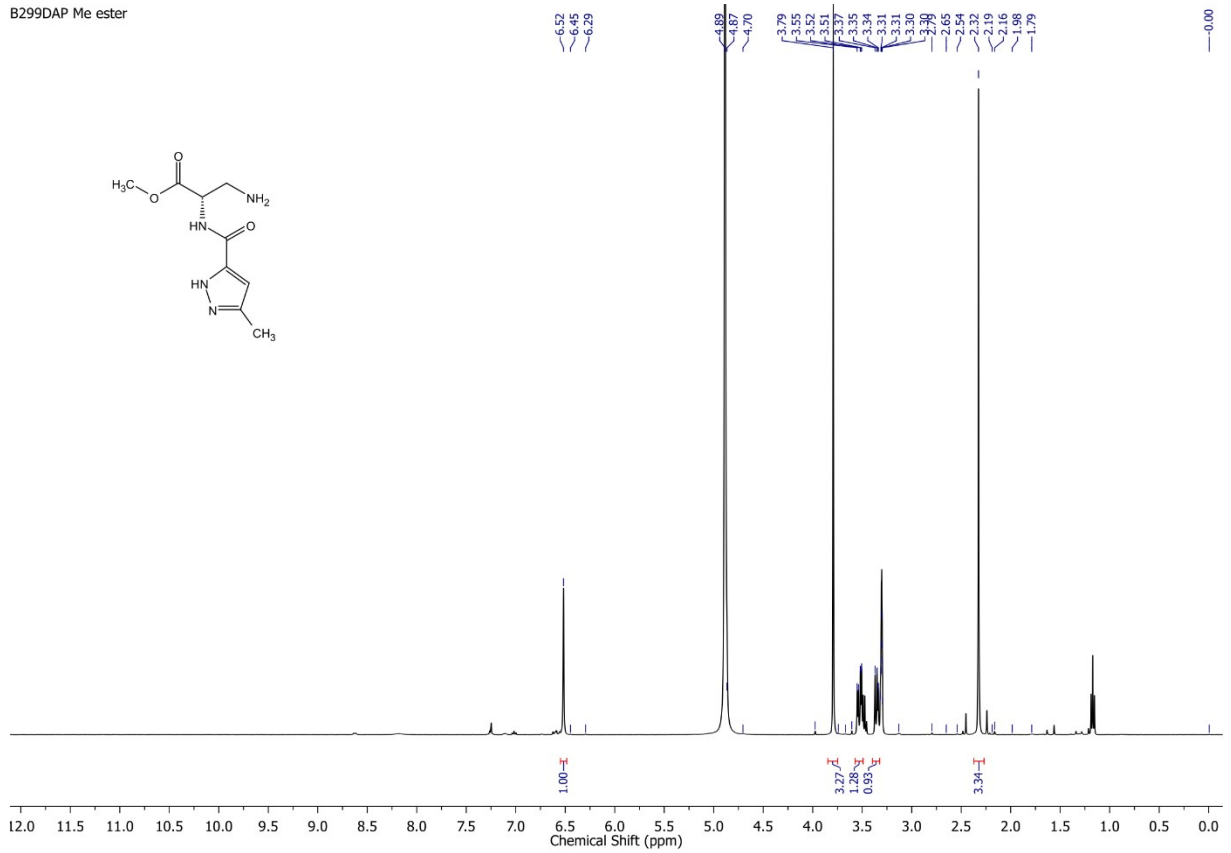

^{1}H NMR, 400 MHz, MeOD, compound (A45DAPB299 Me ester):

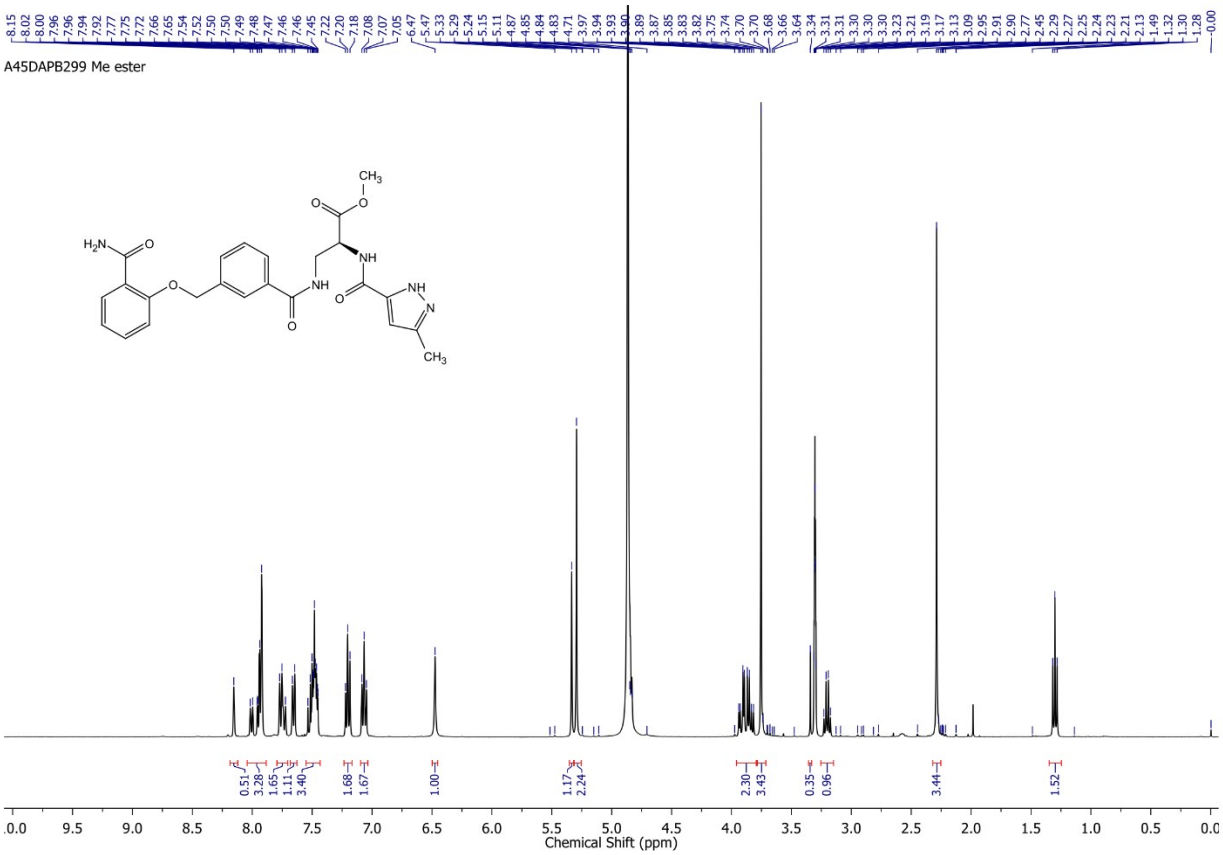

^{1}H NMR, 400 MHz, DMSO, compound (A45DAPB299):

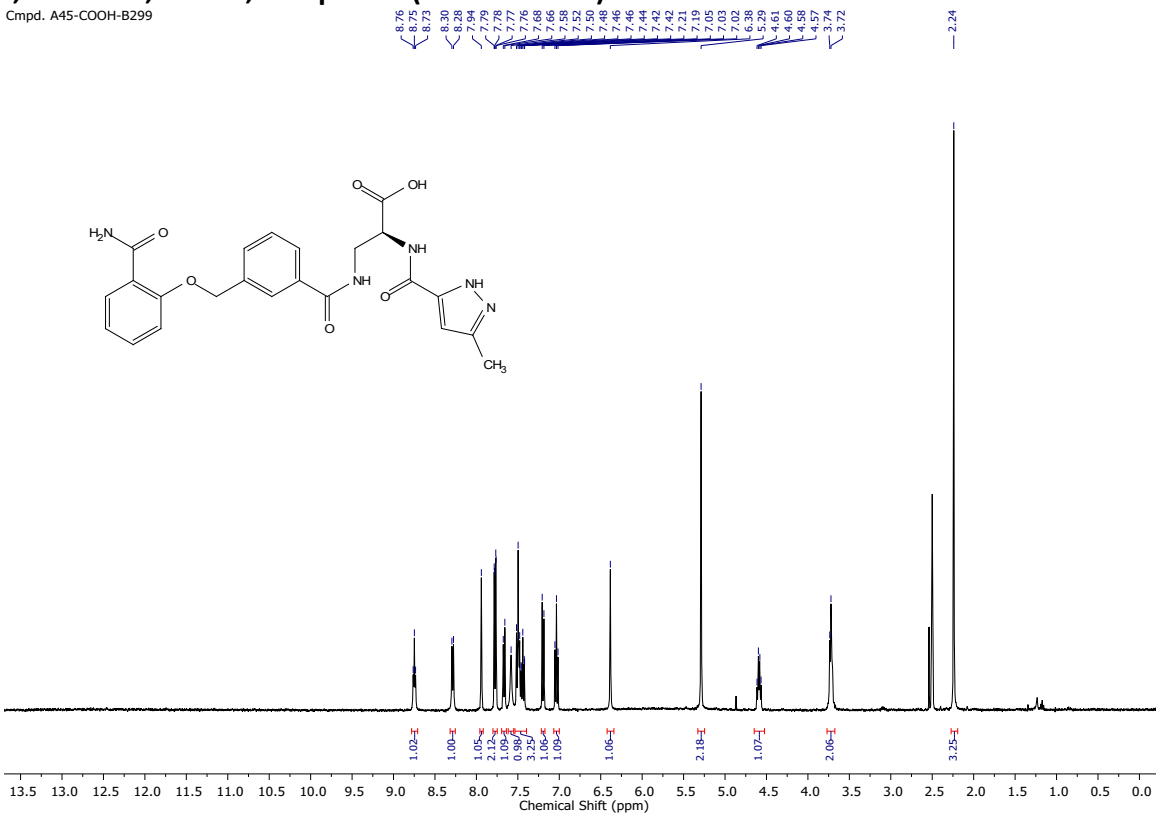

^{1}H NMR, 400 MHz, MeOD, compound (B145 DAP N-Boc Me ester):

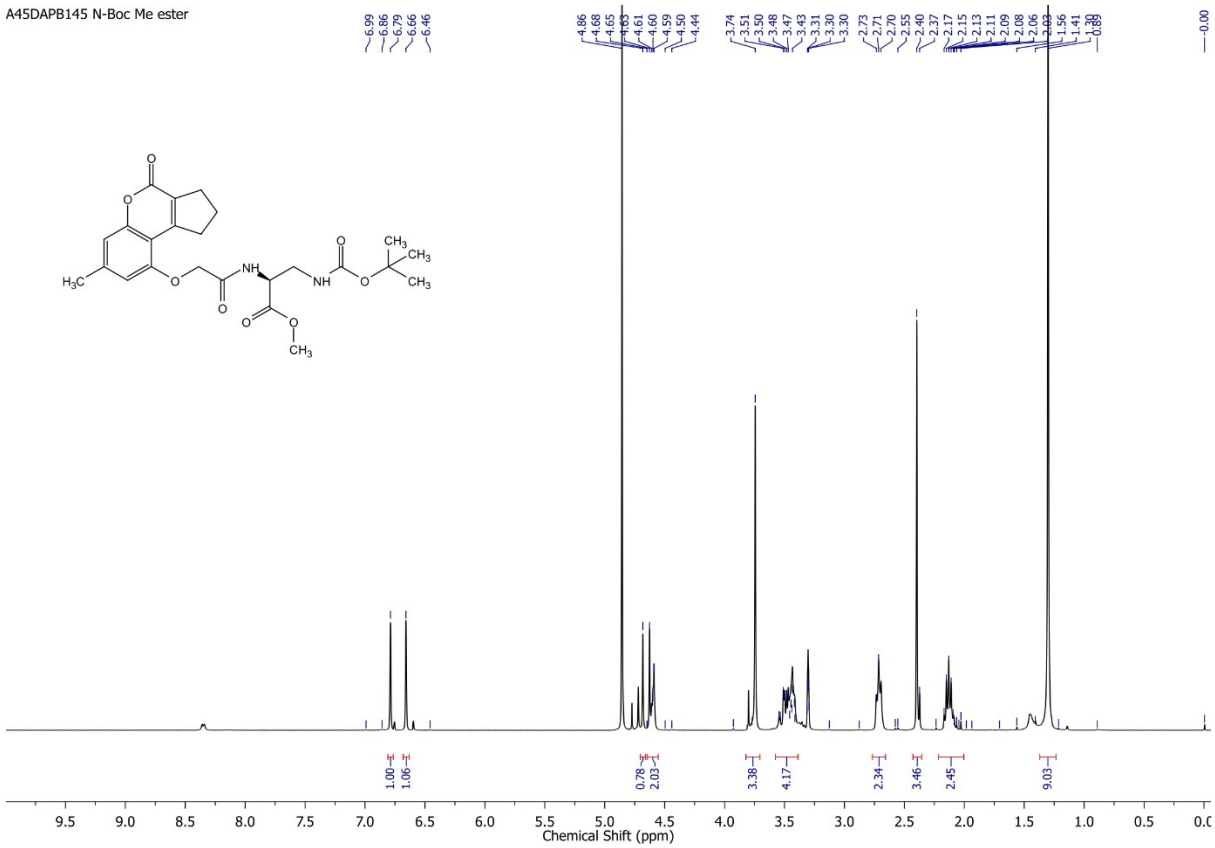

^{1}H NMR, 400 MHz, MeOD, compound (B145 DAP Me ester):

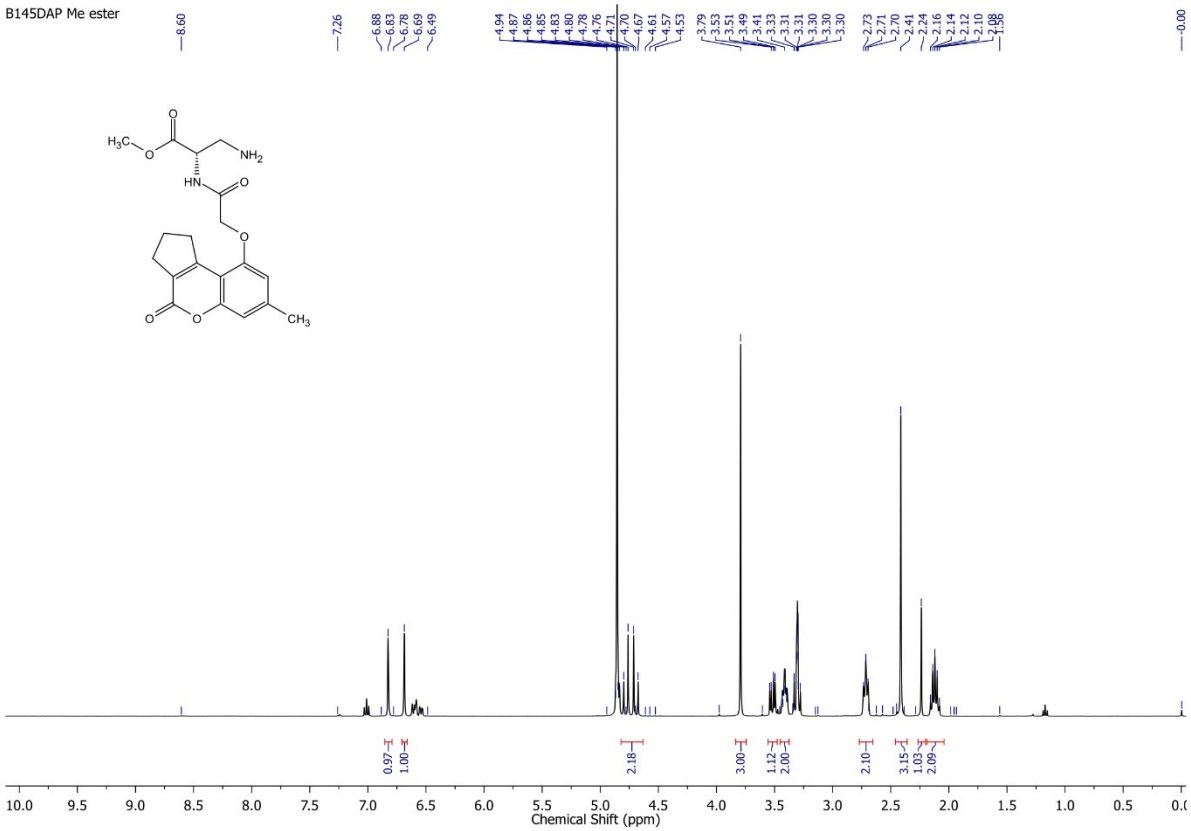

^{1}H NMR, 400 MHz, MeOD, compound (A45DAPB145 Me ester):

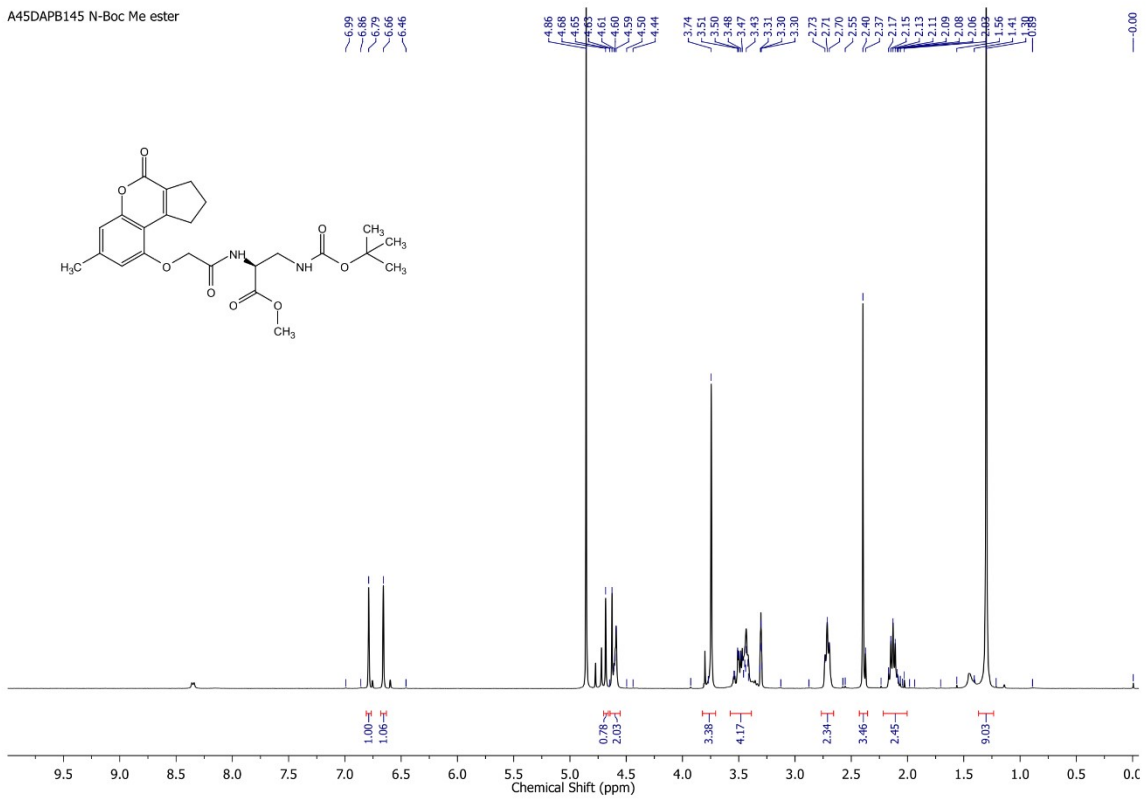

^{1}H NMR, 400 MHz, DMSO, compound (A45DAPB145):

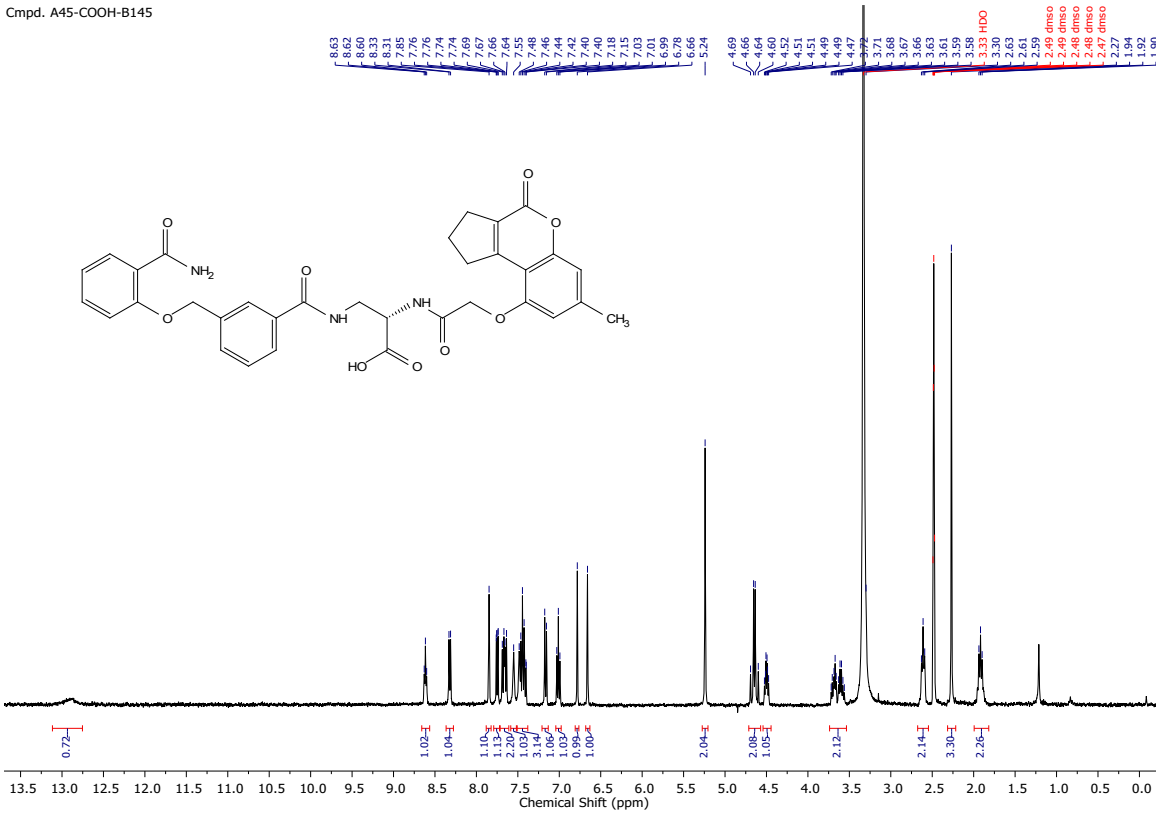

^{1}H NMR, 400 MHz, DMSO, compound (pomalidomide-chloroacetamide):

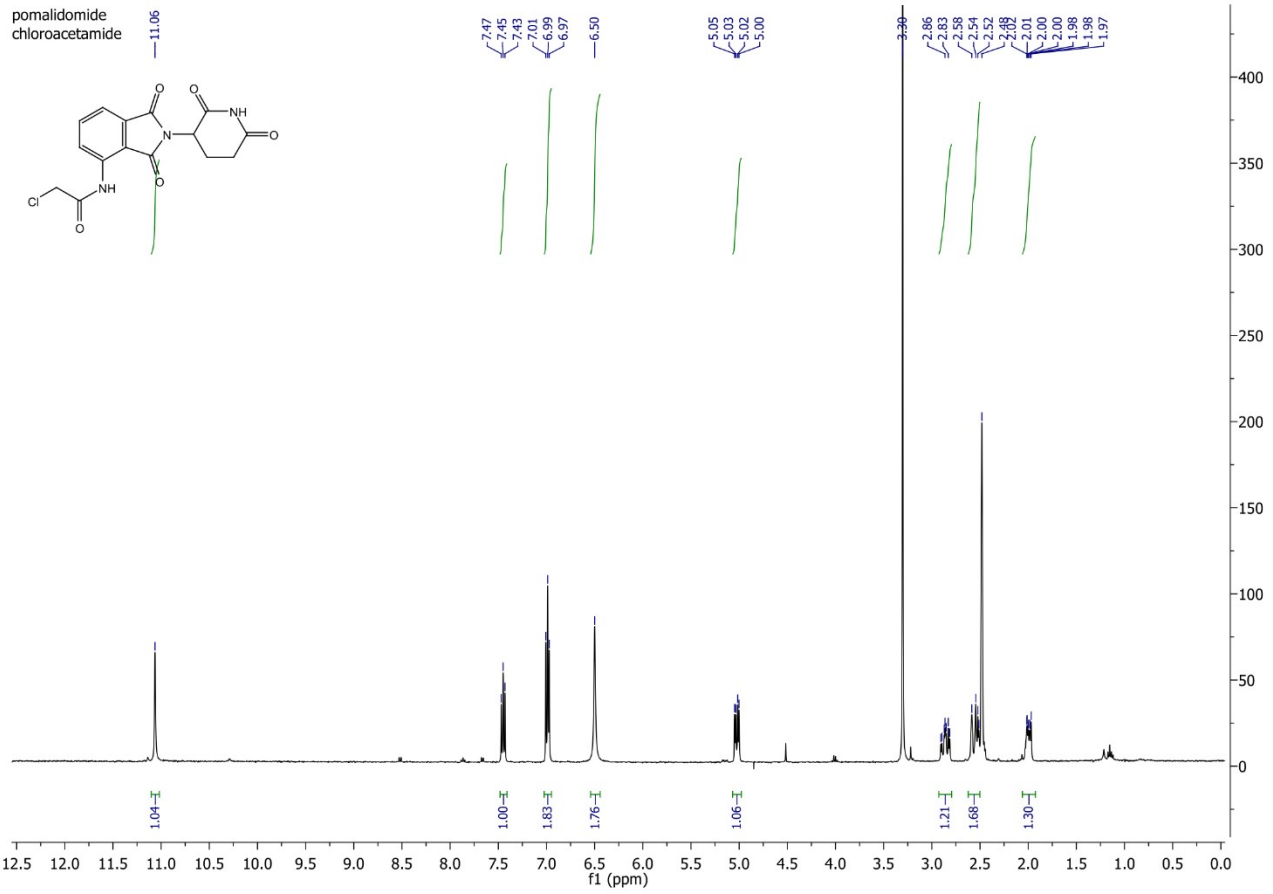

^{1}H NMR, 400 MHz, DMSO, compound (linker A3 TFA salt):

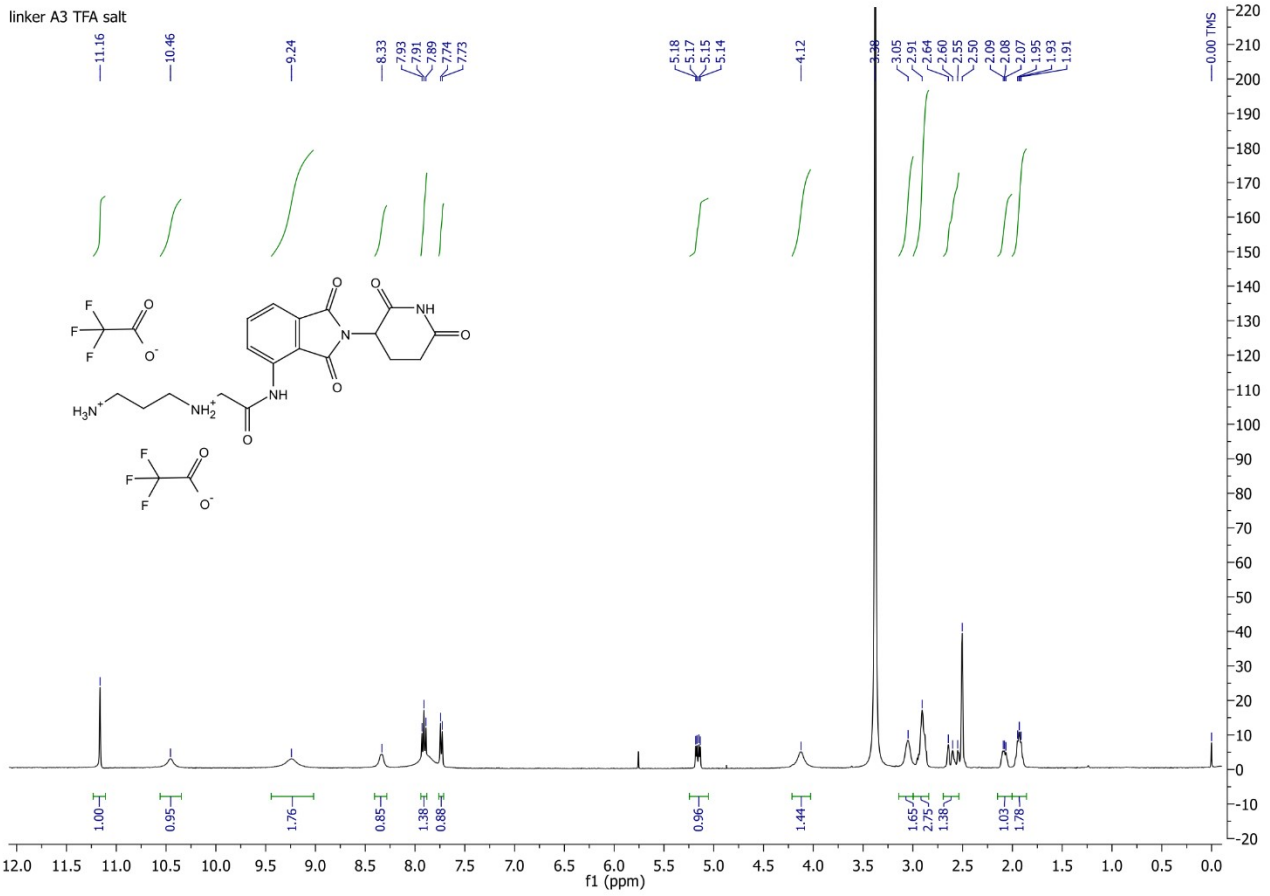

ESI+ MS, compound (linker A3 TFA salt):

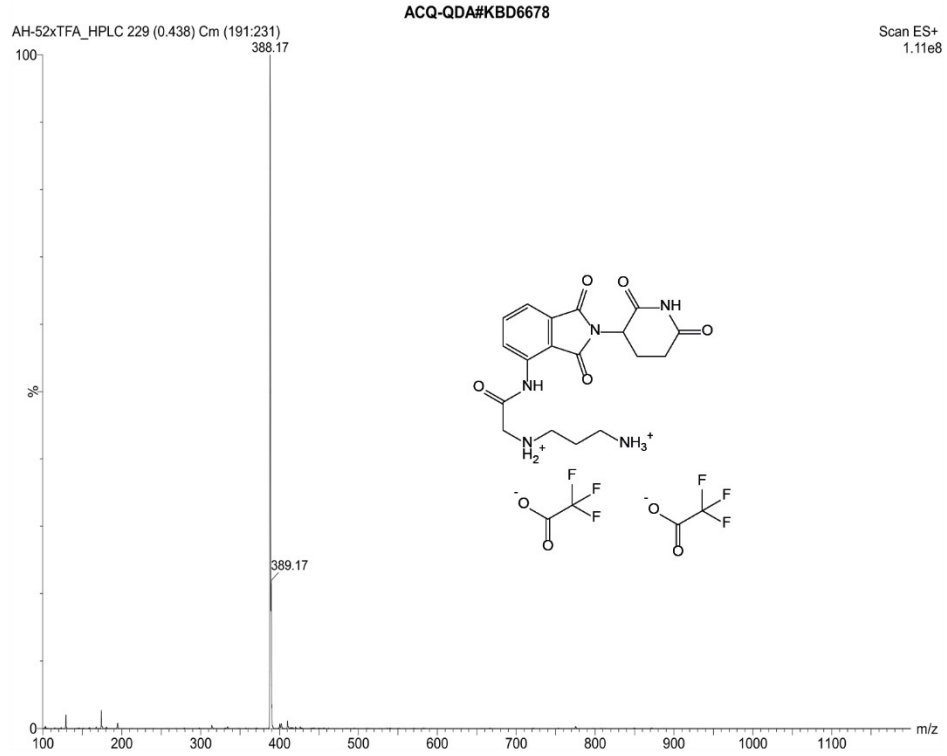

^{1}H NMR, 400 MHz, DMSO, compound (linker A4 TFA salt):

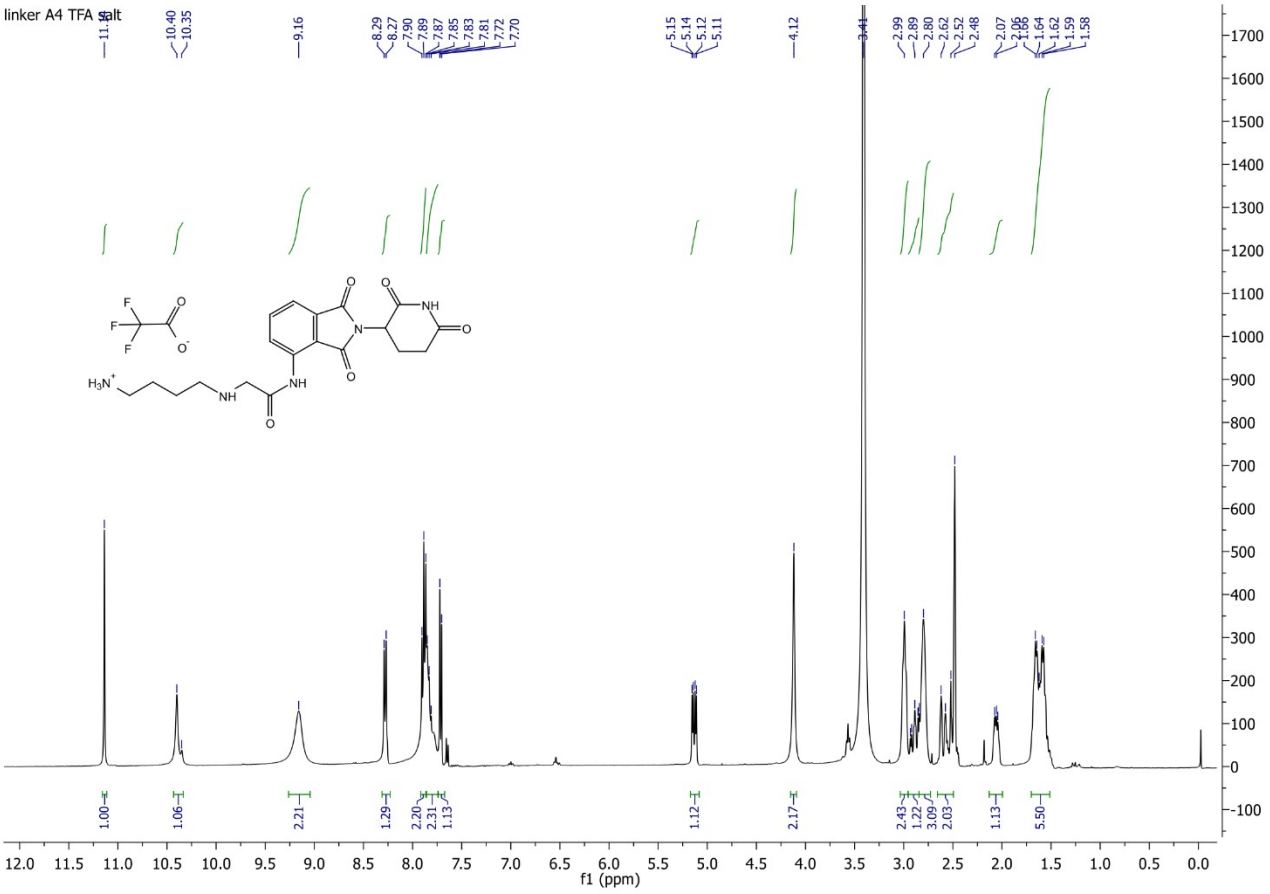

ESI+ MS, compound (linker A4 TFA salt):

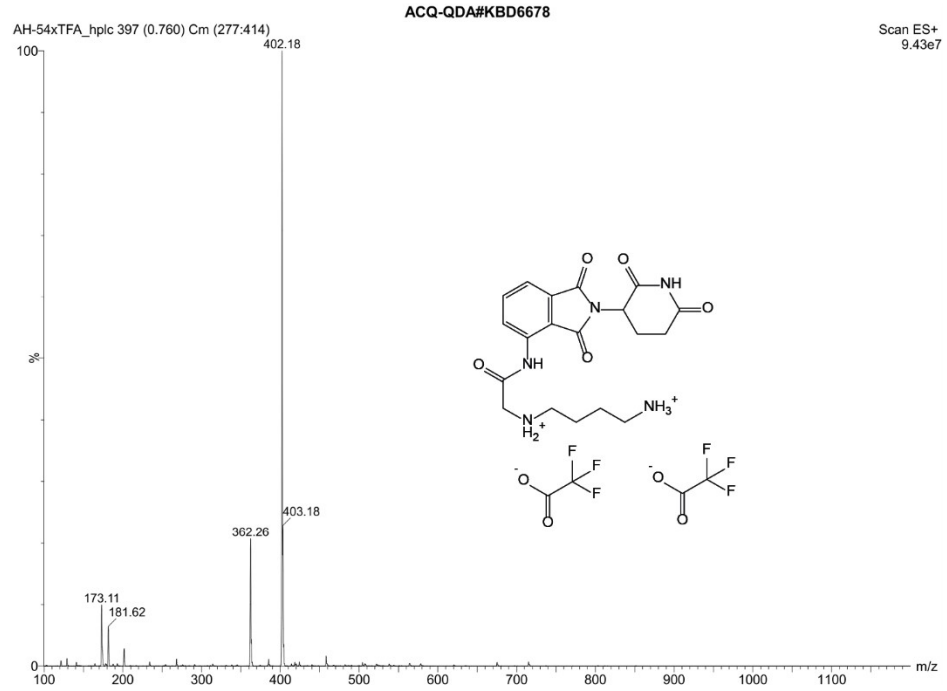

^{1}H NMR, 400 MHz, DMSO, compound (linker A5 TFA salt):

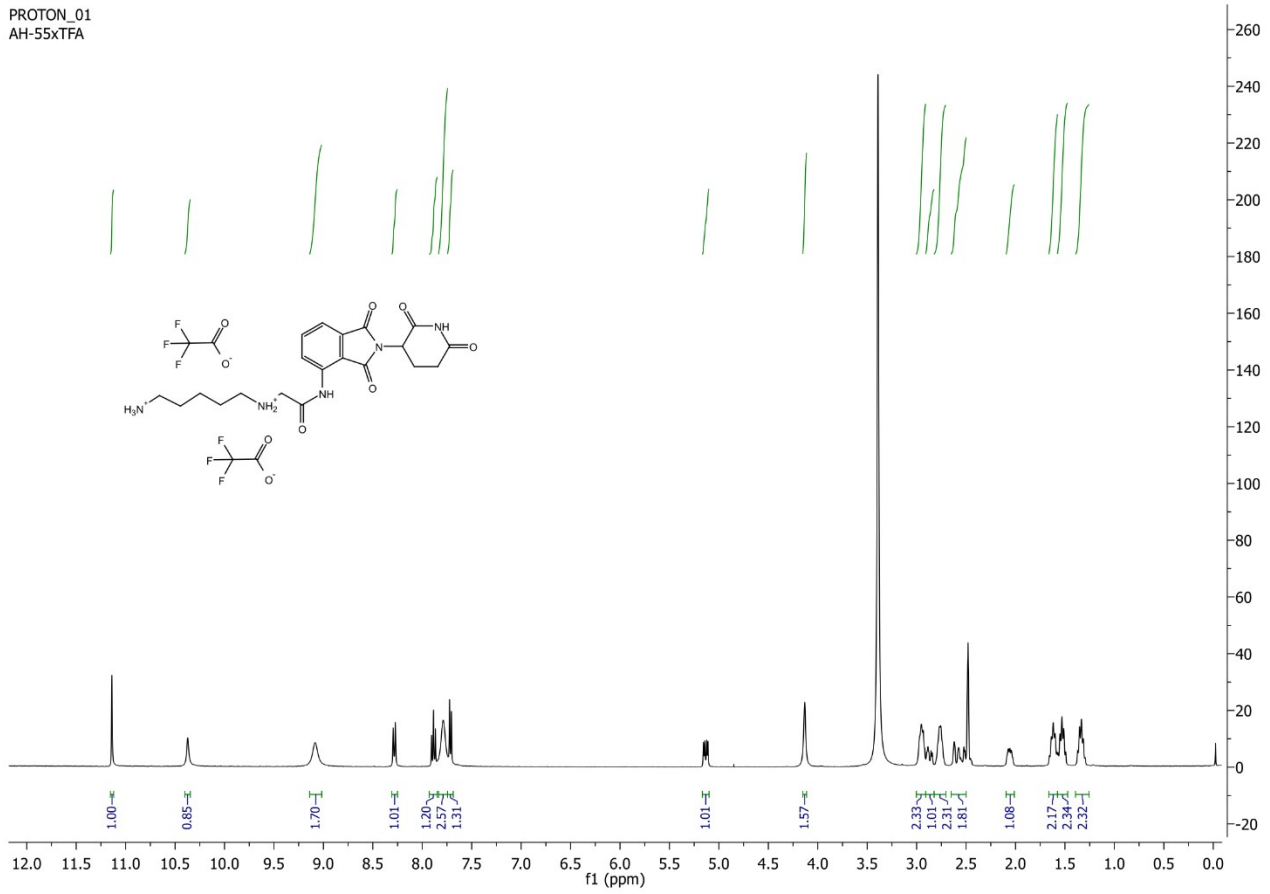

ESI+ MS, compound (linker A5 TFA salt):

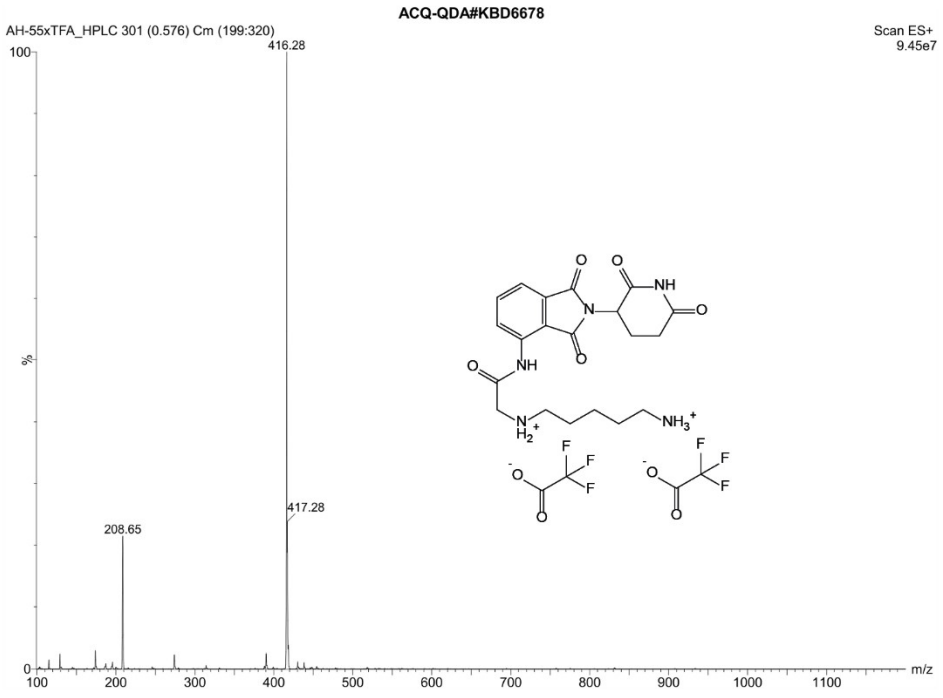

^{1}H NMR, 400 MHz, DMSO, compound (linker A6 TFA salt):

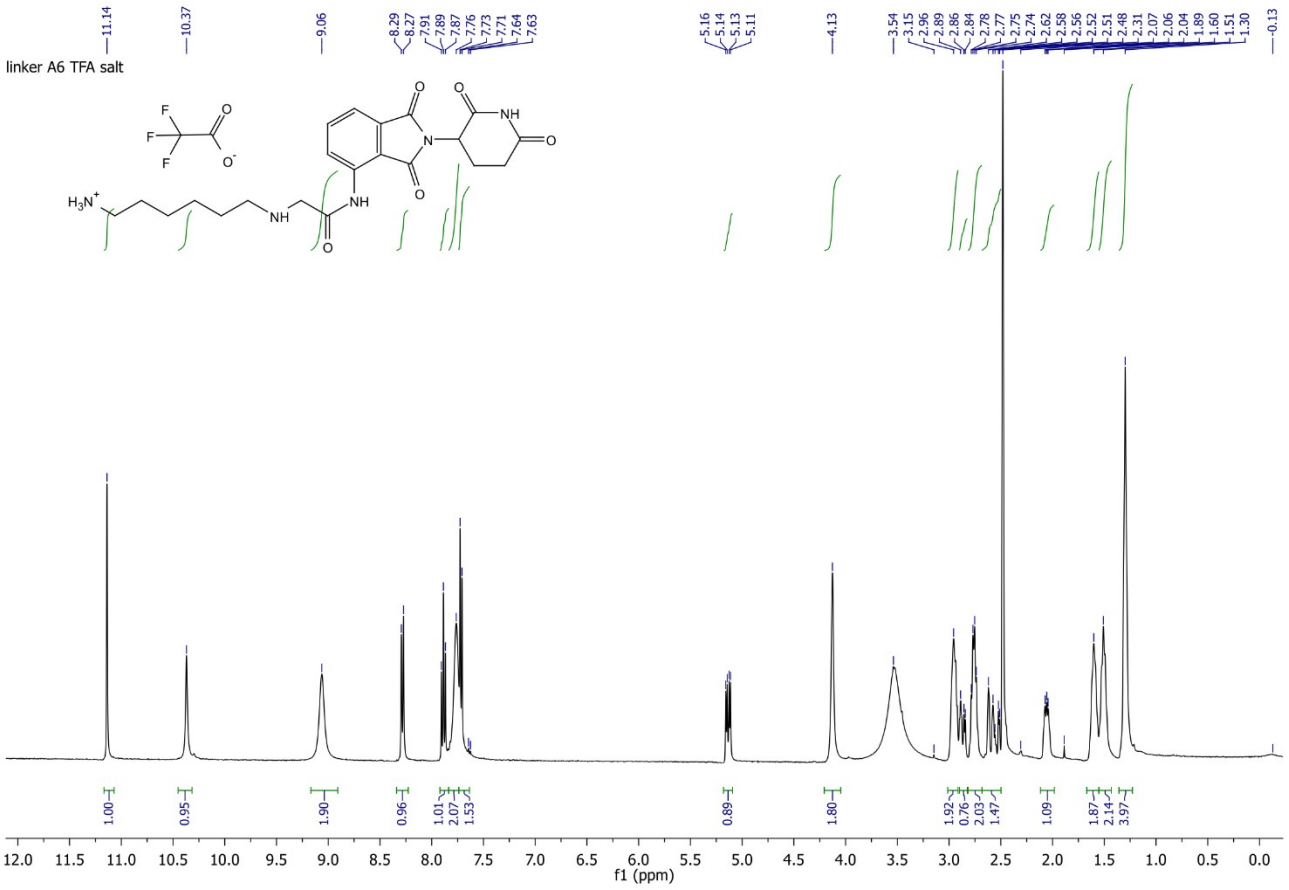

ESI+ MS, compound (linker A6 TFA salt):

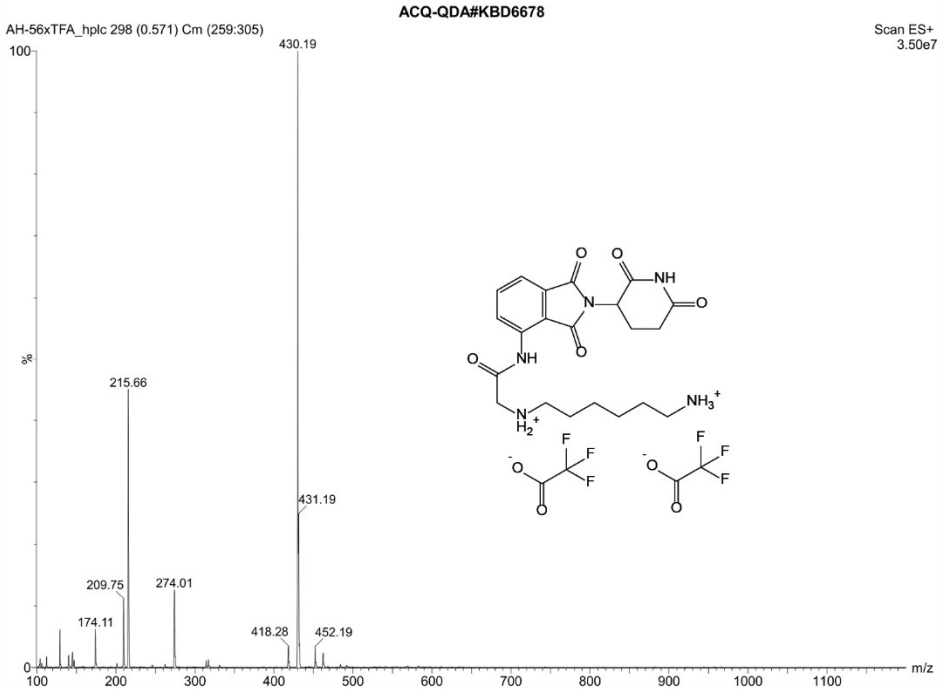

^{1}H NMR, 400 MHz, DMSO, compound (linker A8 TFA salt):

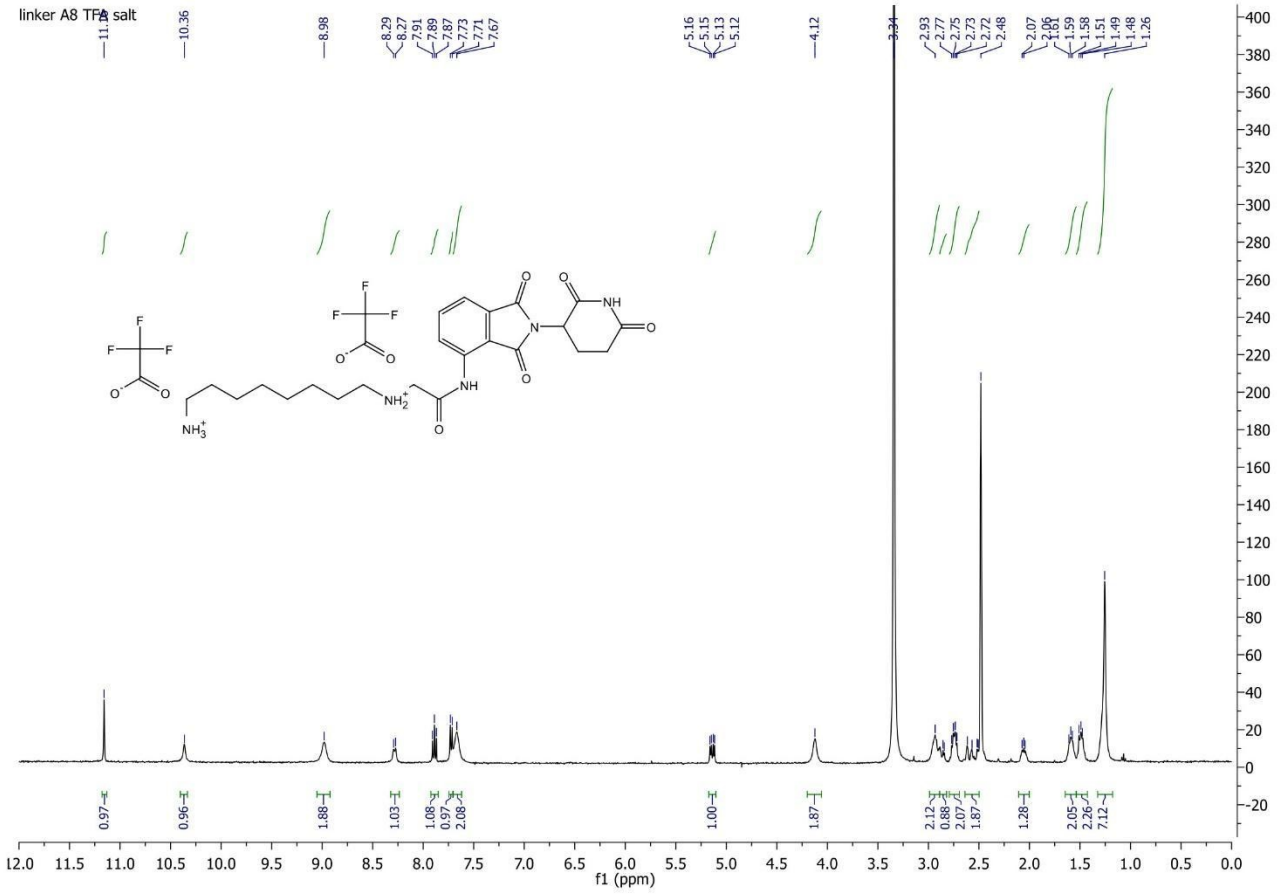

ESI+ MS, compound (linker A8 TFA salt):

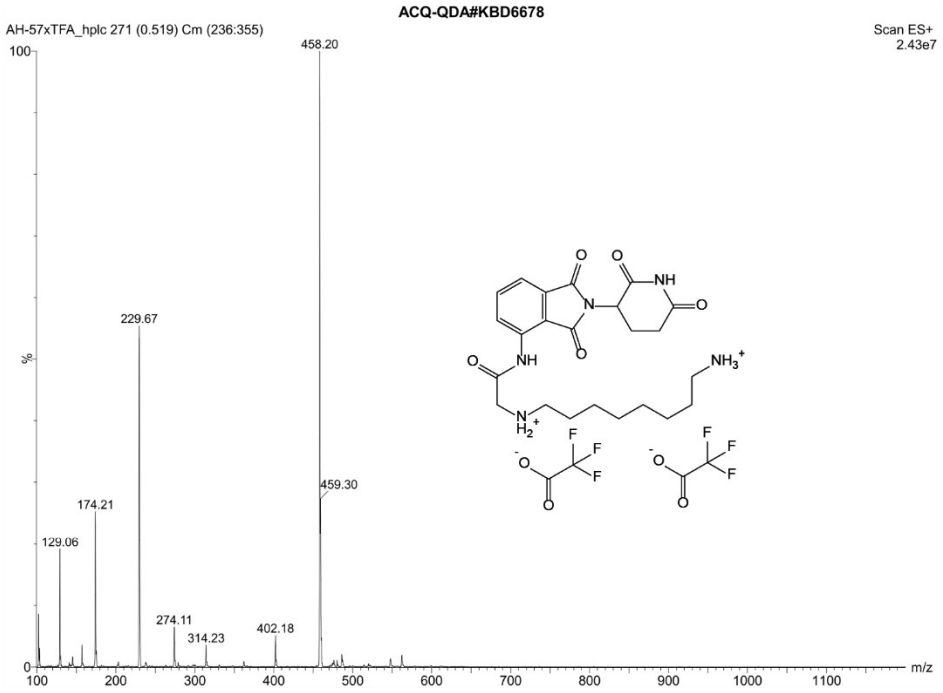

^{1}H NMR, 400 MHz, DMSO, compound (linker B2 intermediate TFA salt):

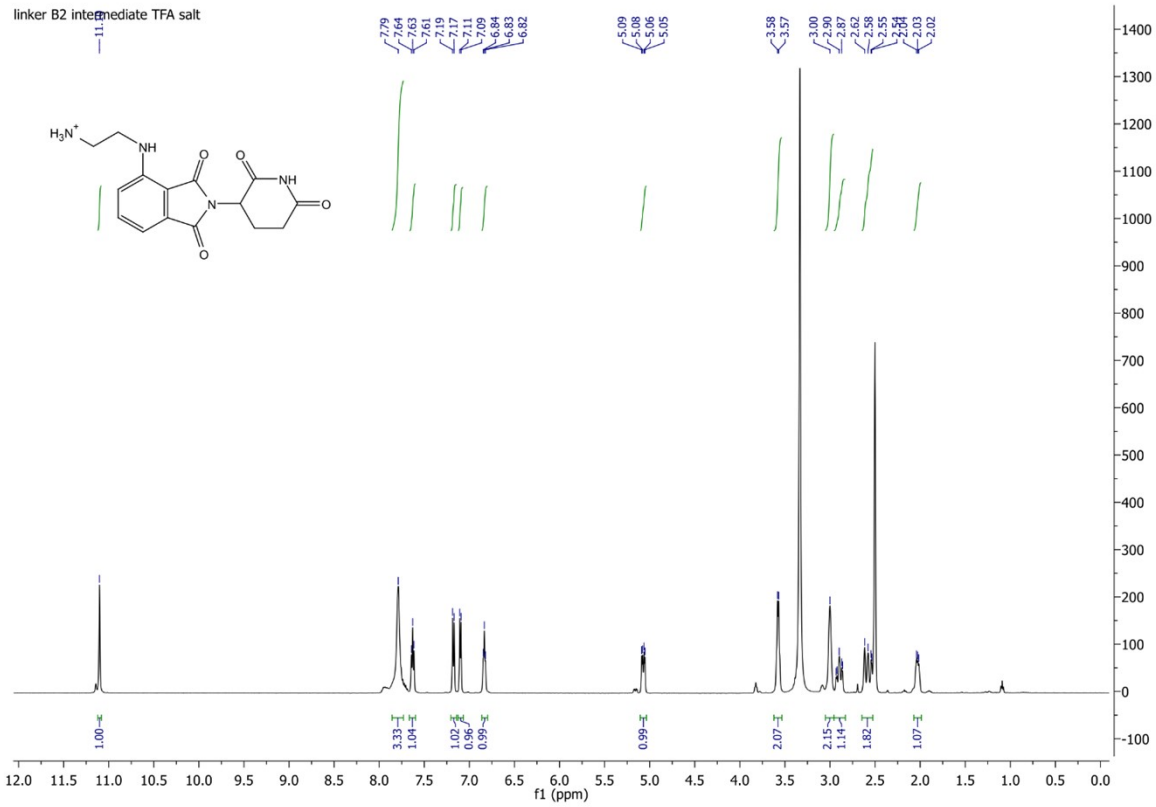

^{1}H NMR, 400 MHz, DMSO, compound (linker B2,3 N-Boc protected):

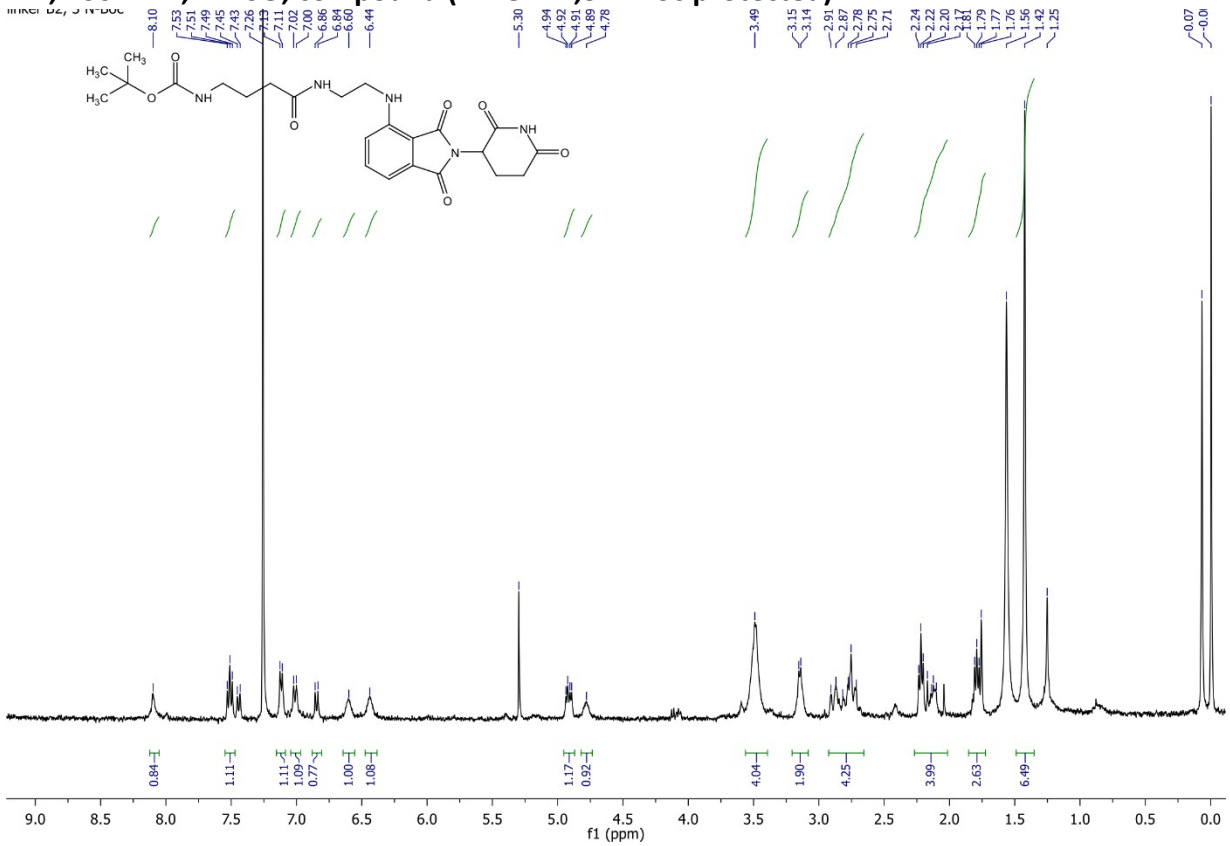

^{1}H NMR, 400 MHz, DMSO, compound (linker B2,3 TFA salt):

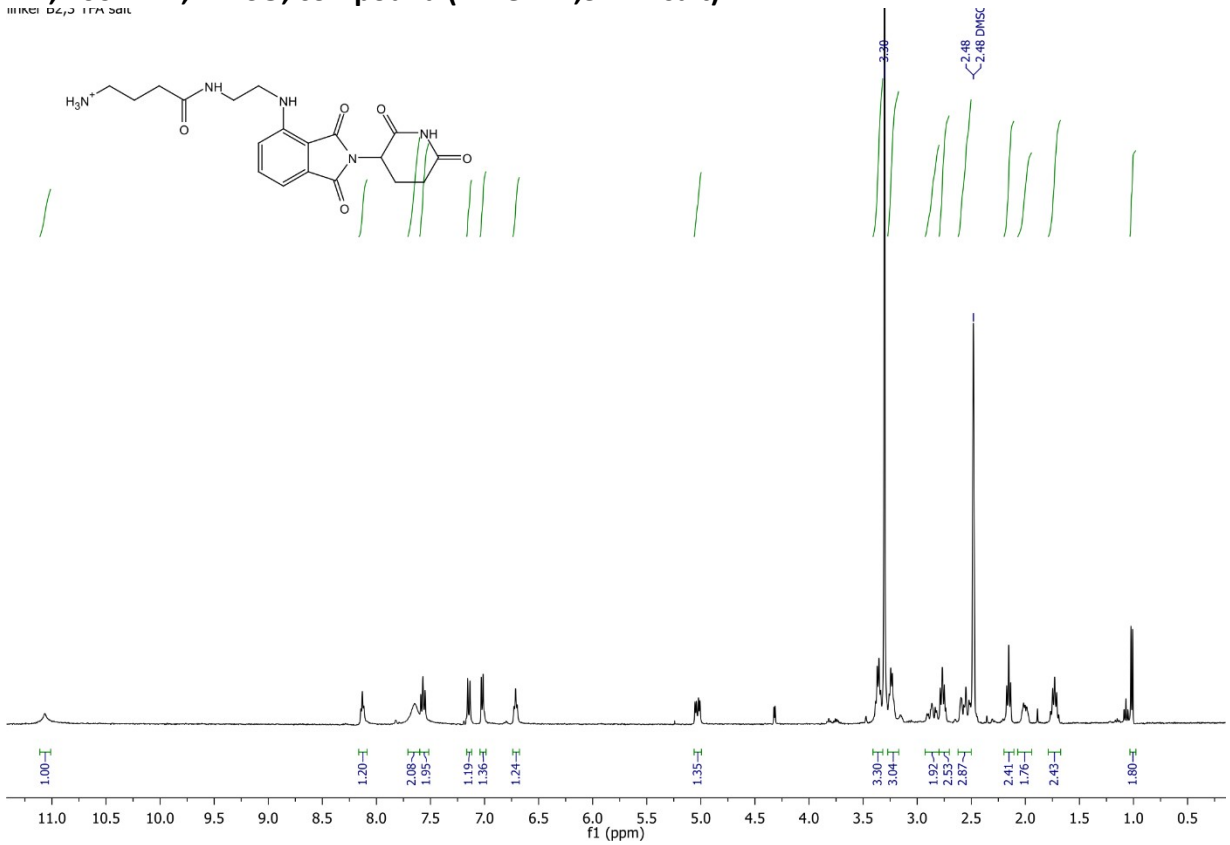

ESI+ MS, compound (linker B2,3 TFA salt):

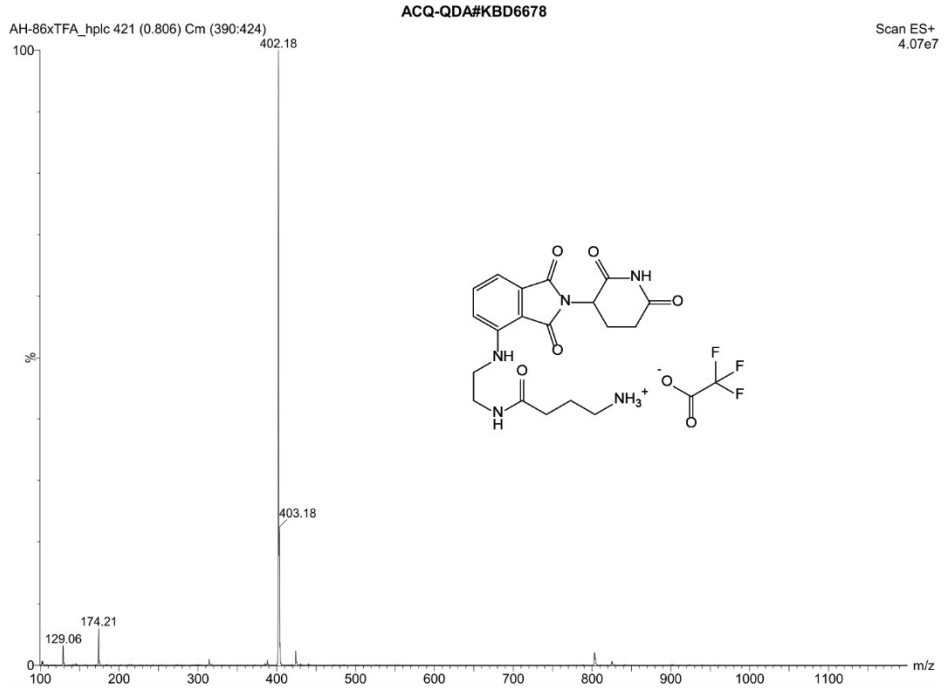

^{1}H NMR, 400 MHz, DMSO, compound (linker B3,2 N-Boc protected):

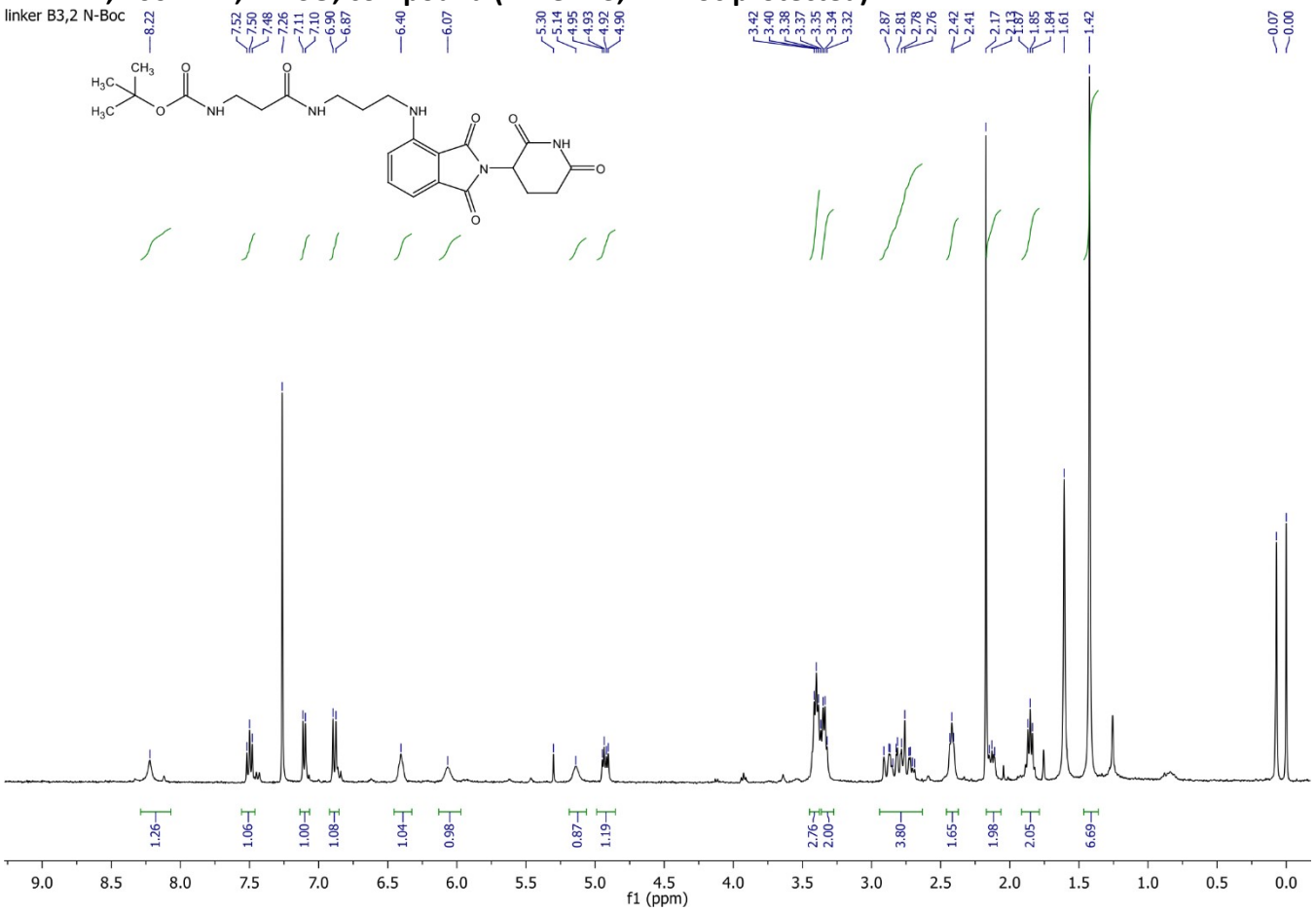

ESI$^+$ MS, compound (A45DAPB145-linker A3)

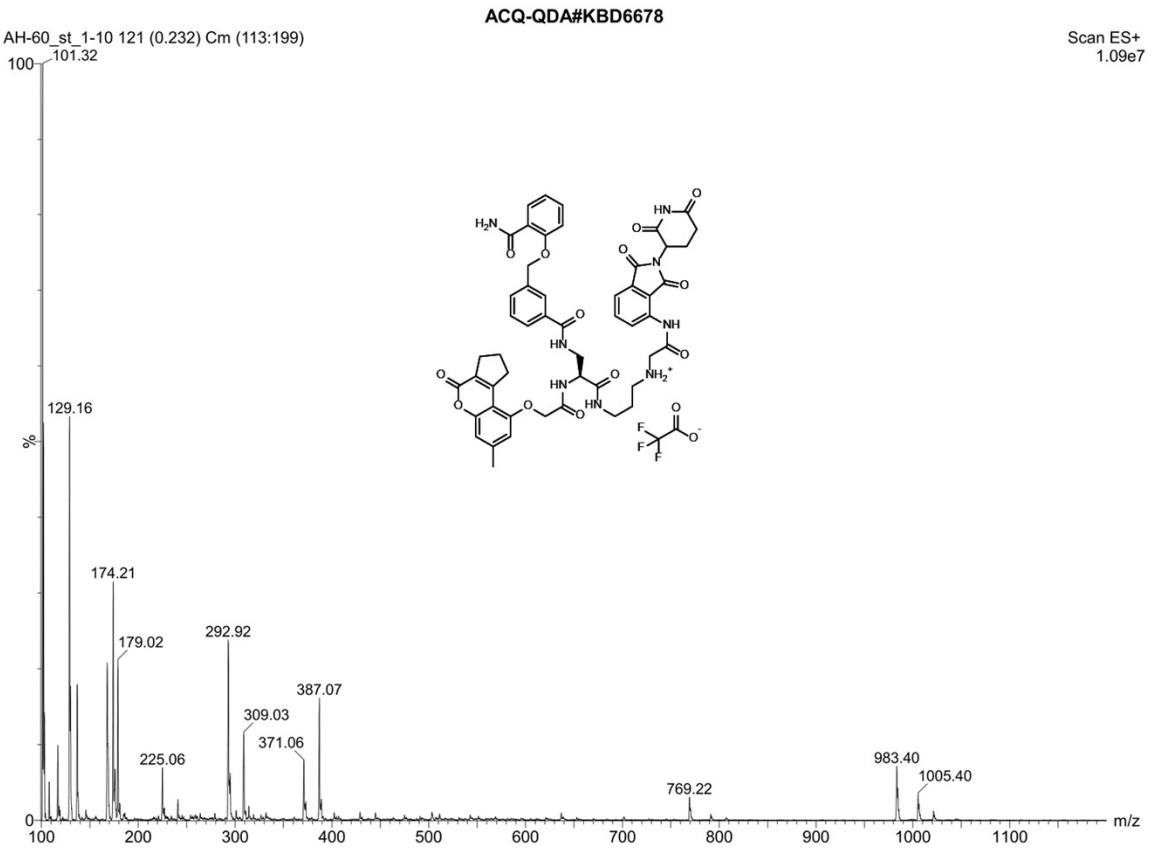

HPLC analysis of the A45DAPB145-linker A3 stock solution:

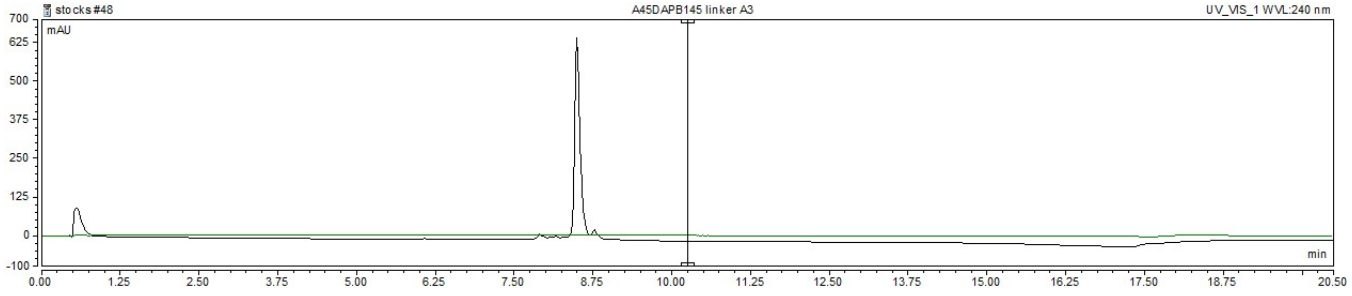

ESI$^+$ MS, compound (A45DAPB145-linker A4)

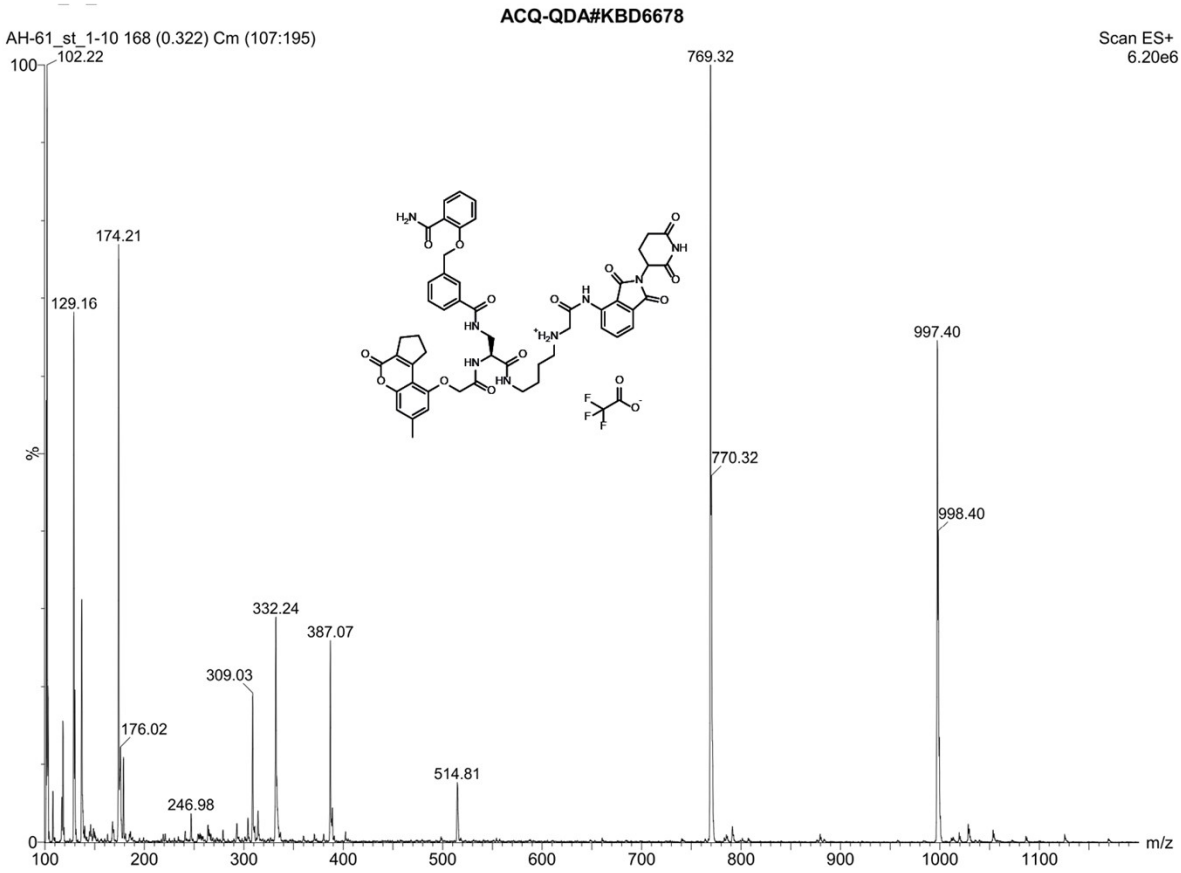

HPLC analysis of the A45DAPB145-linker A4 stock solution:

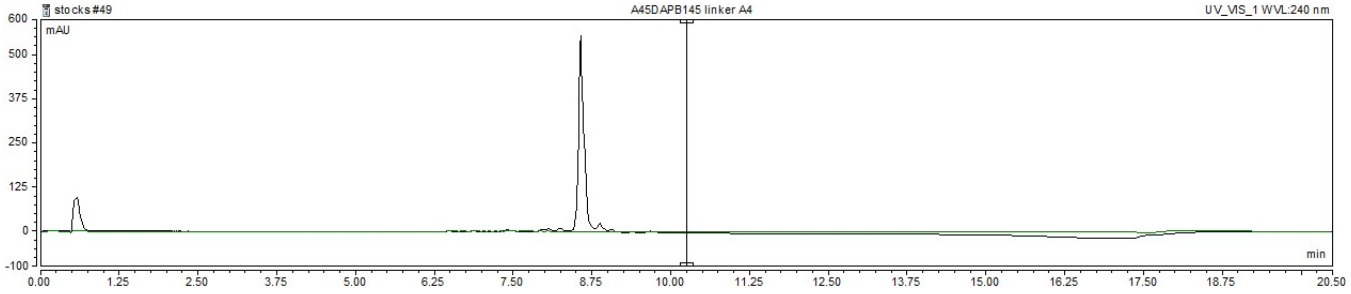

ESI$^+$ MS, compound A45DAPB145-linker A5)

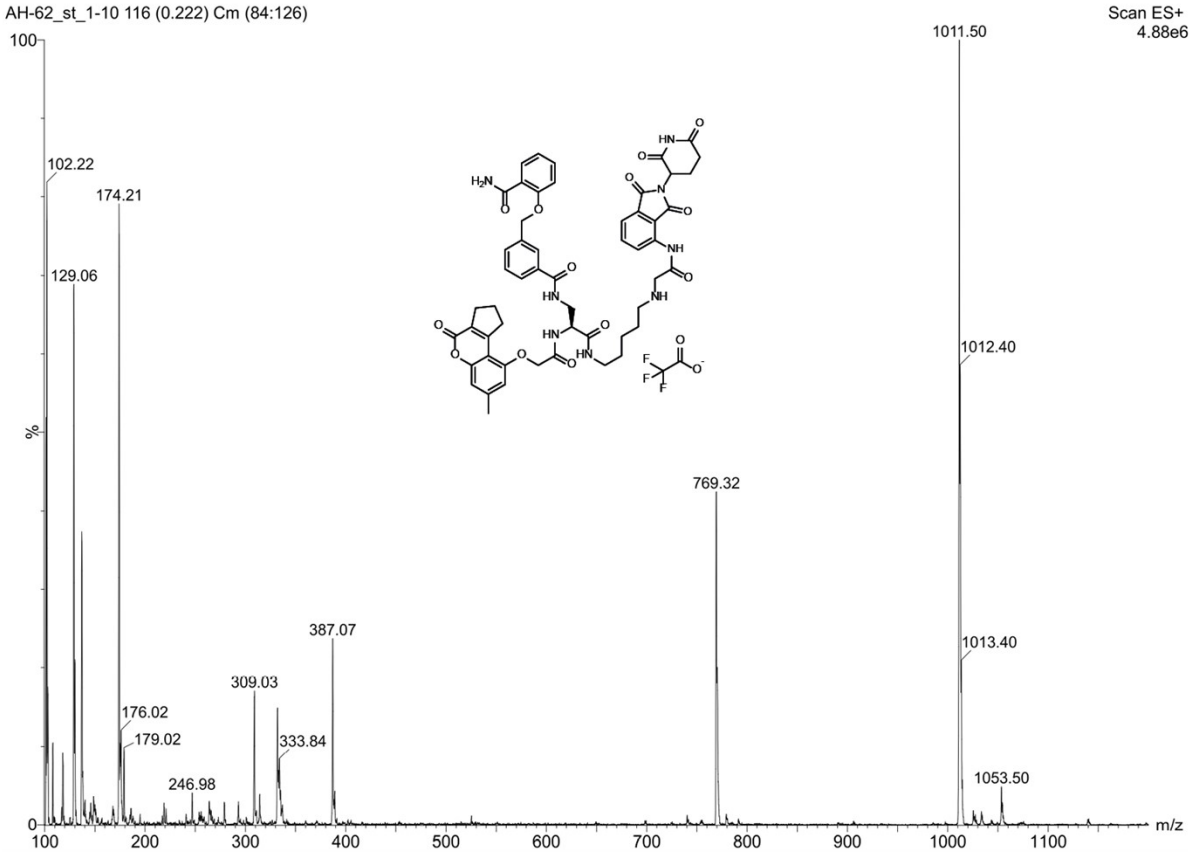

HPLC analysis of the A45DAPB145-linker A5 stock solution:

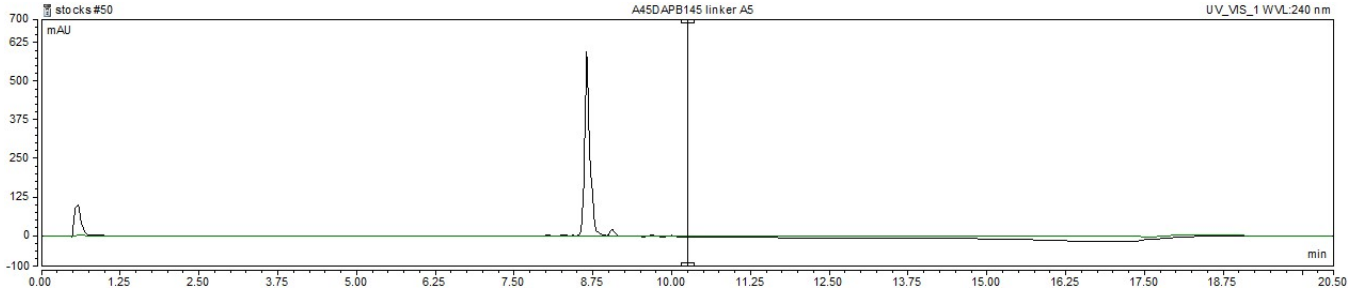

ESI$^+$ MS, compound (A45DAPB145-linker A6)

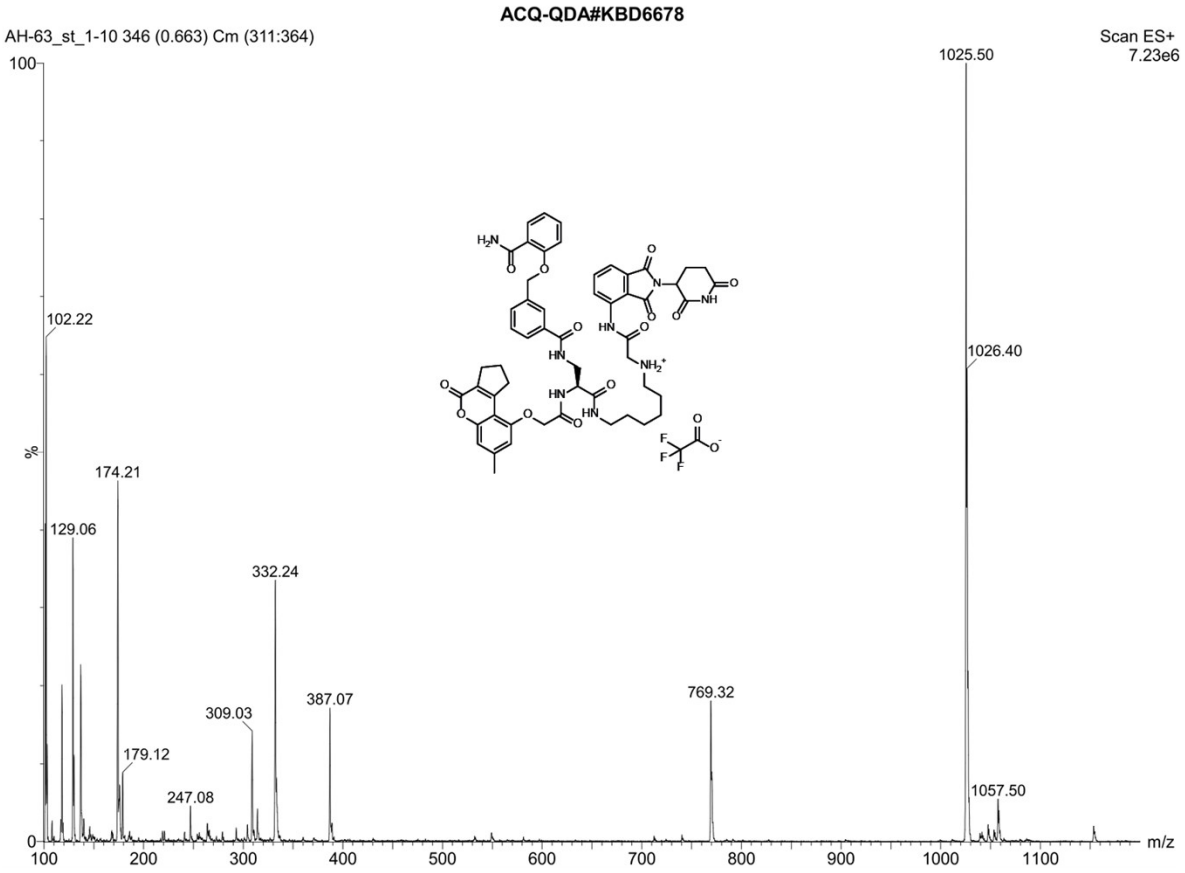

HPLC analysis of the A45DAPB145-linker A6 stock solution:

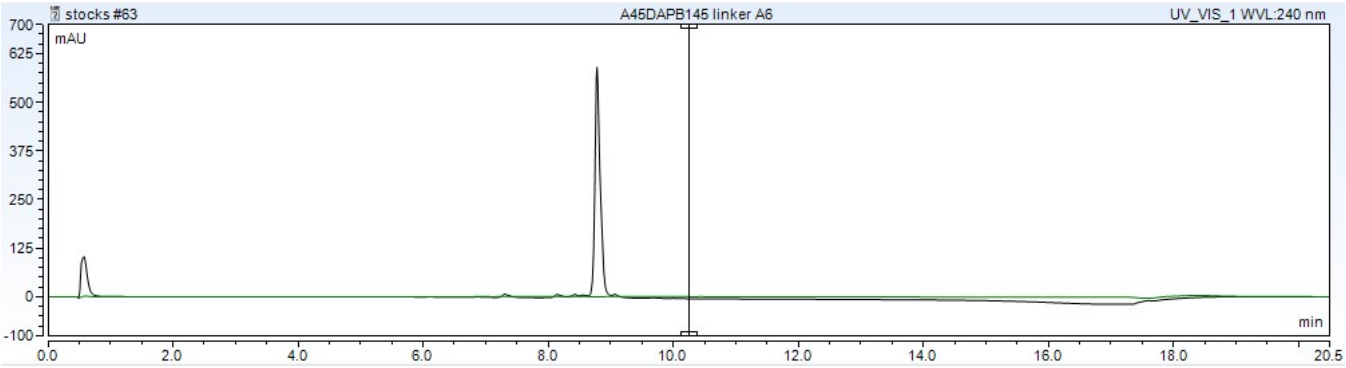

ESI$^+$ MS, compound (A45DAPB145-linker A8)

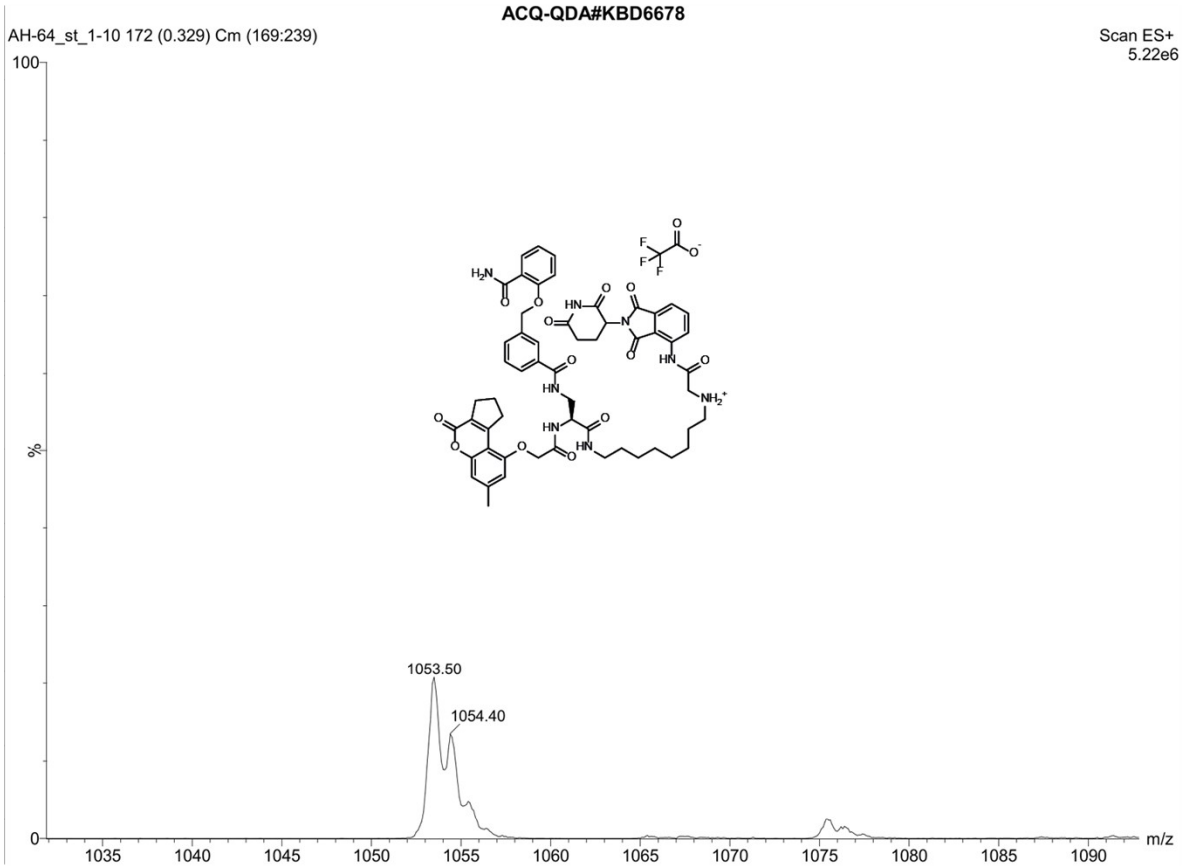

HPLC analysis of the A45DAPB145-linker A8 stock solution:

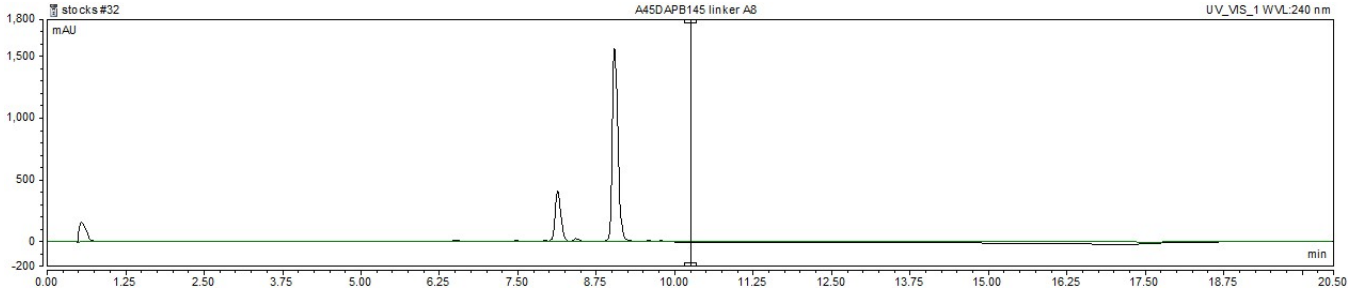

ESI$^+$ MS, compound (A45DAPB145-linker B2,3)

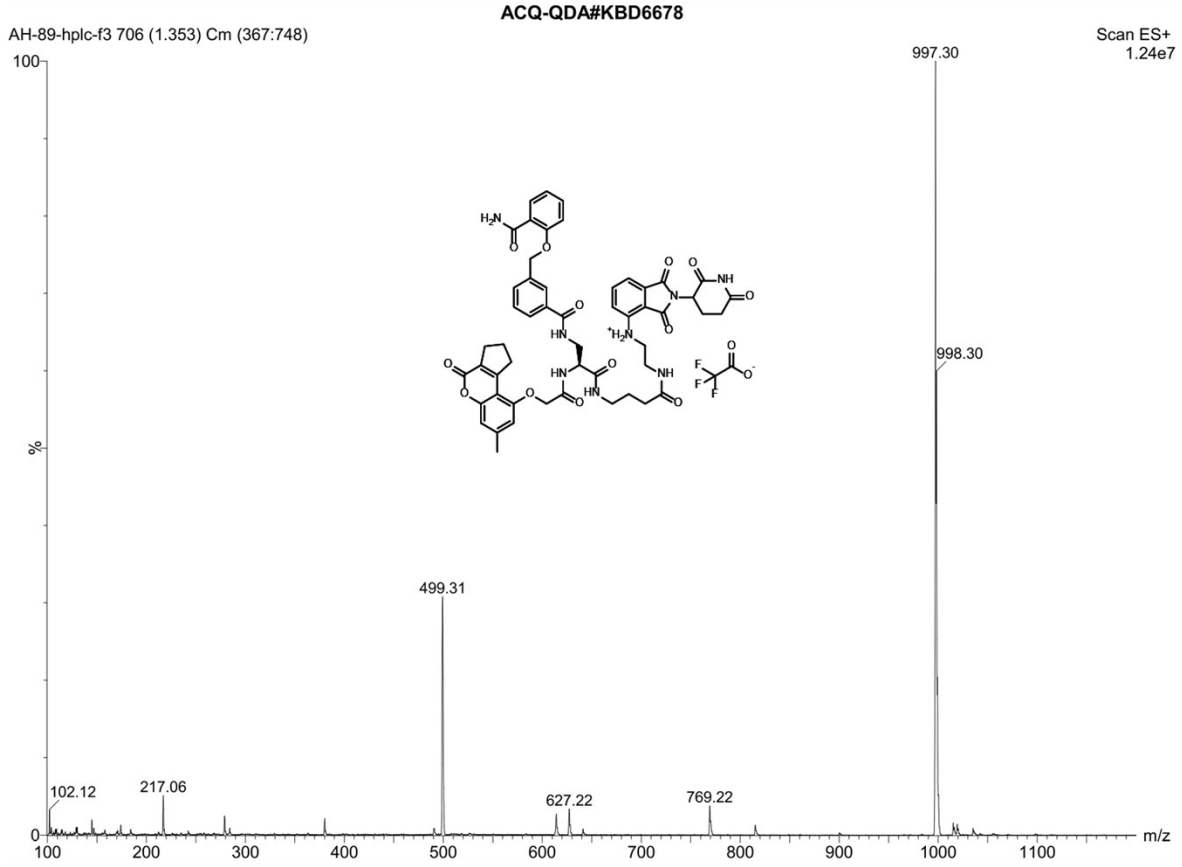

HPLC analysis of the A45DAPB145-linker B2,3 stock solution:

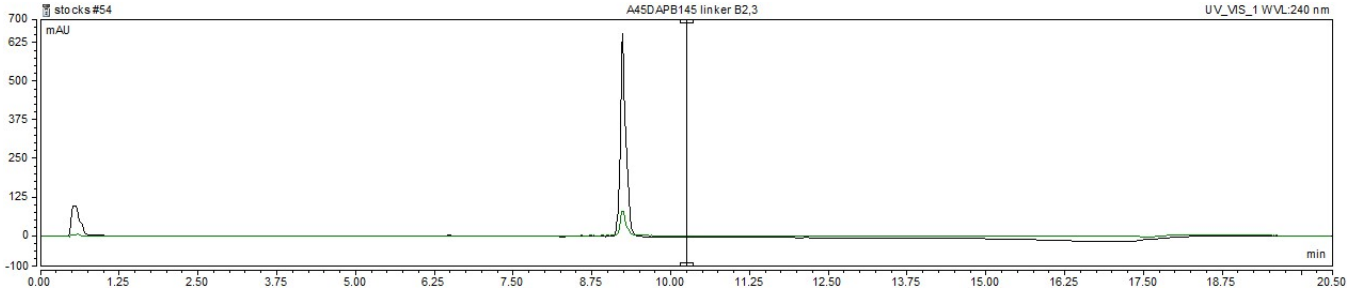

ESI$^+$ MS, compound (A45DAPB145-linker B3,2)

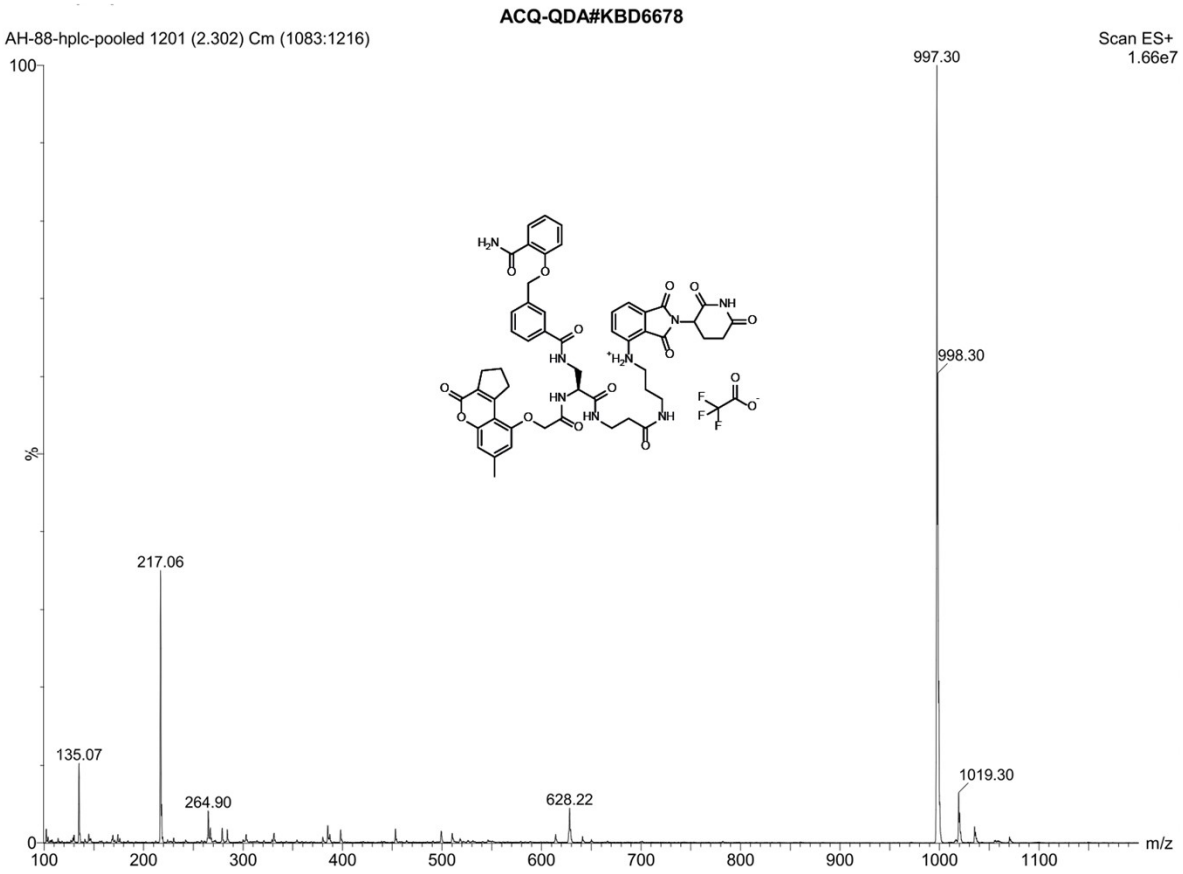

HPLC analysis of the A45DAPB145-linker B3,2 stock solution:

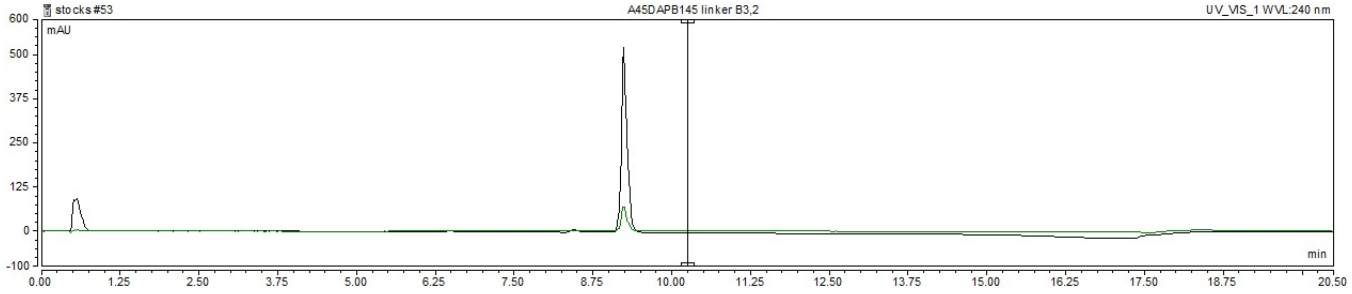

HPLC analysis of the A45DAPB145-linker B3,3 stock solution:

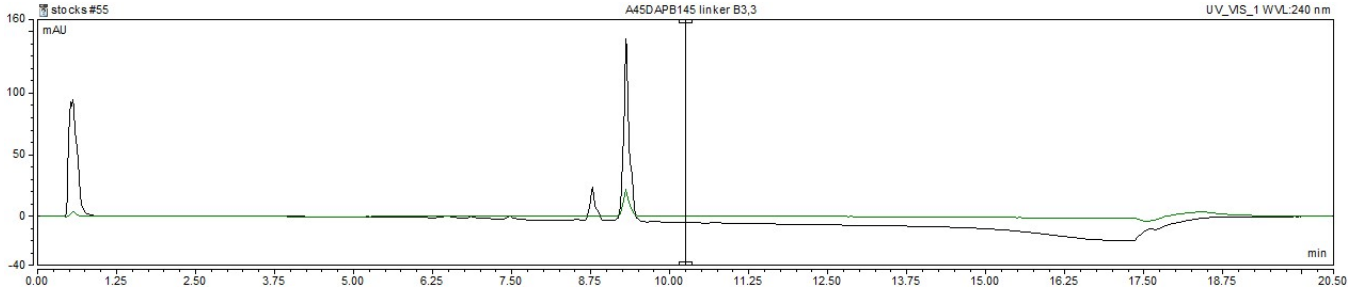

ESI$^+$ MS, compound (A45DAPB299-linker A3)

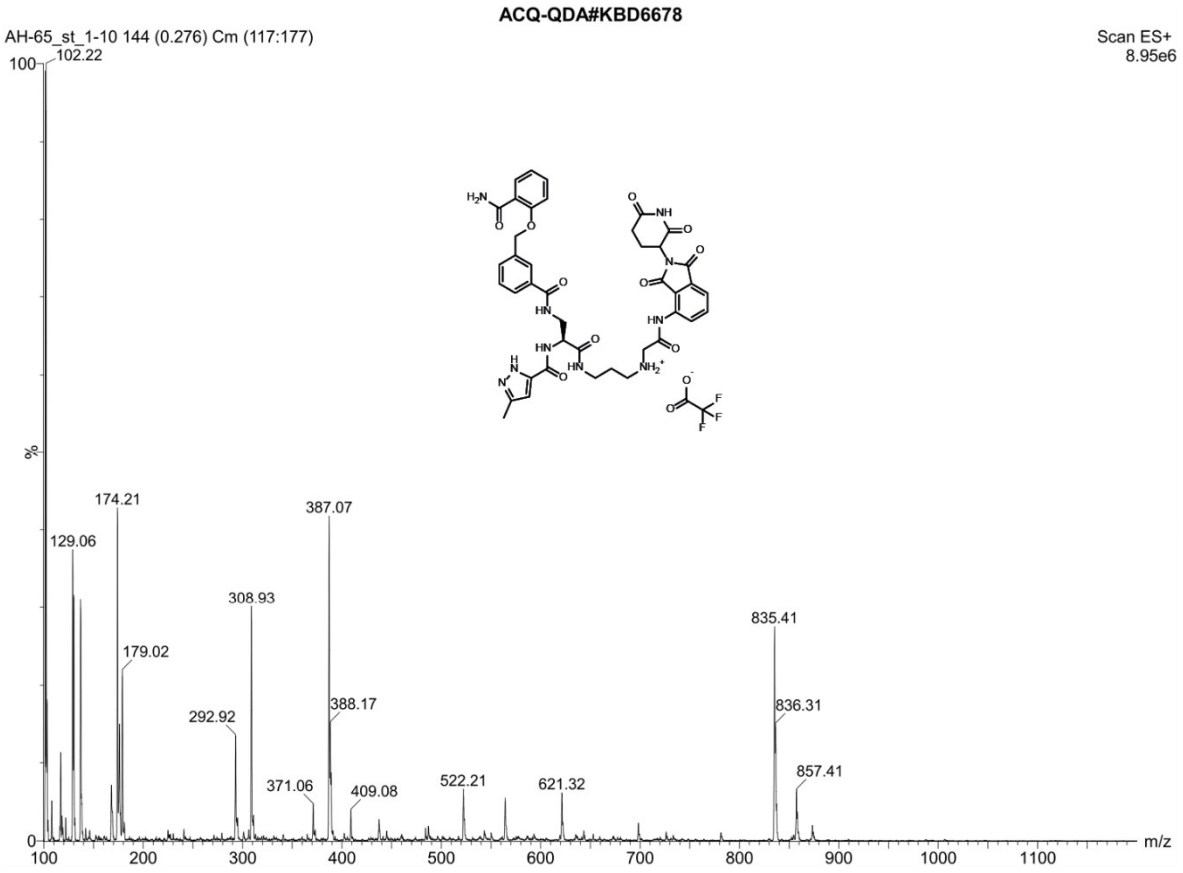

HPLC analysis of the A45DAPB299-linker A3 stock solution:

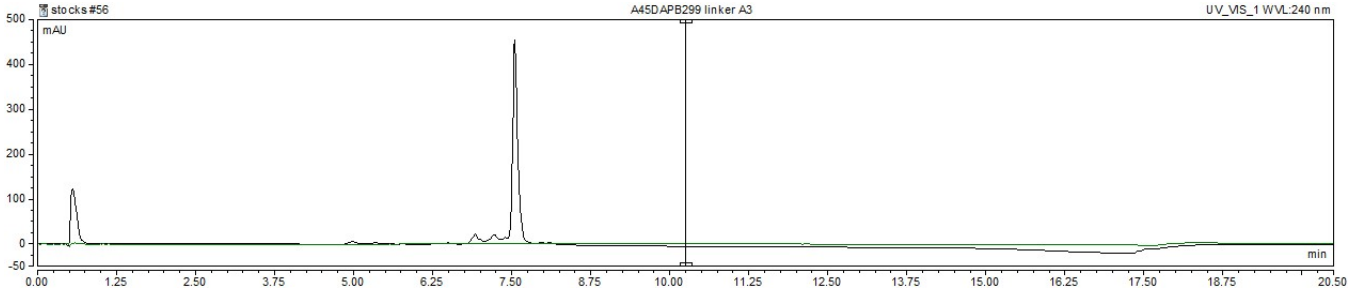

ESI$^+$ MS, compound (A45DAPB299-linker A4)

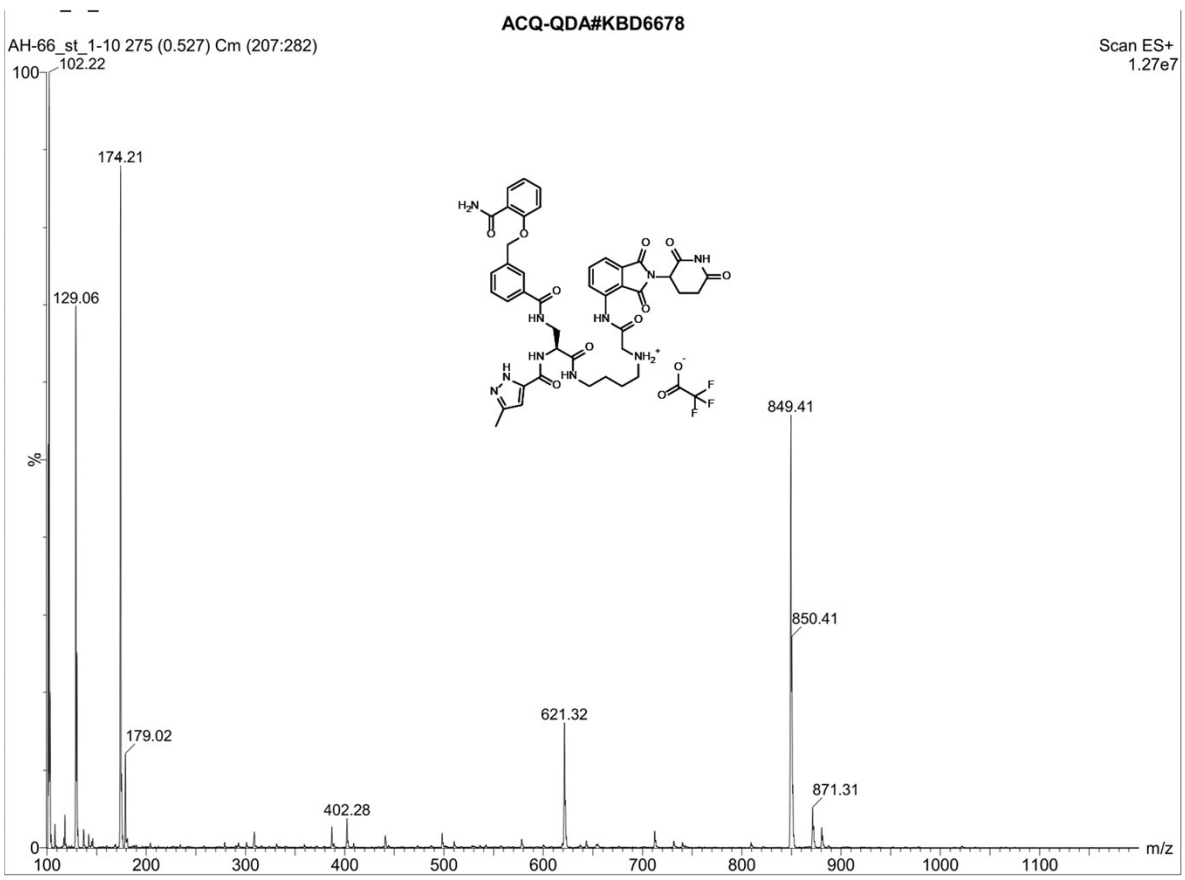

HPLC analysis of the A45DAPB299-linker A4 stock solution:

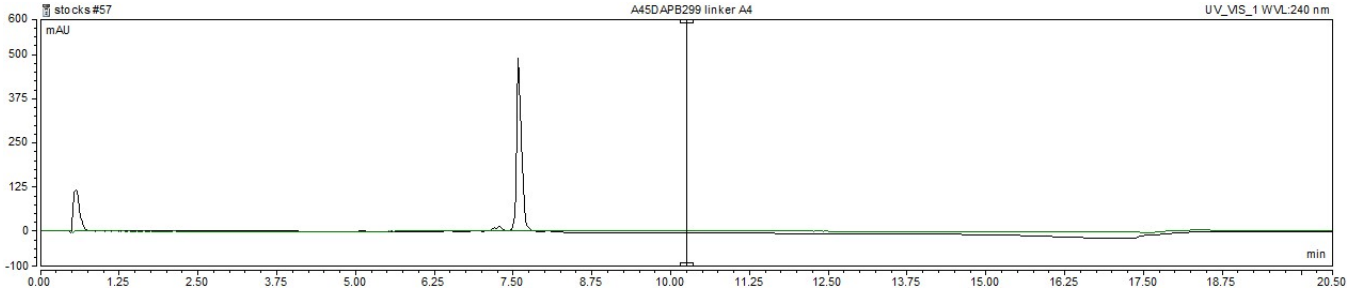

ESI^{+} MS, compound (A45DAPB299-linker A5)

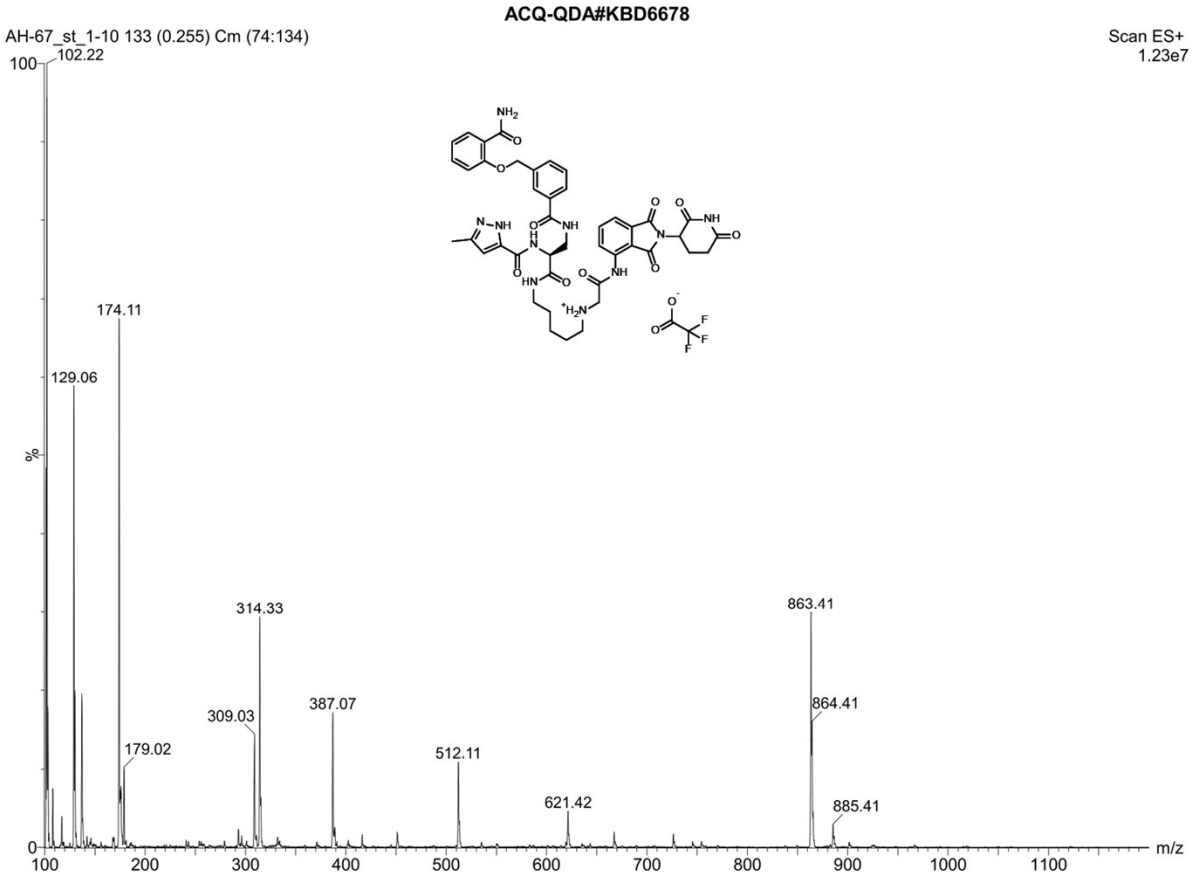

HPLC analysis of the A45DAPB299-linker A5 stock solution:

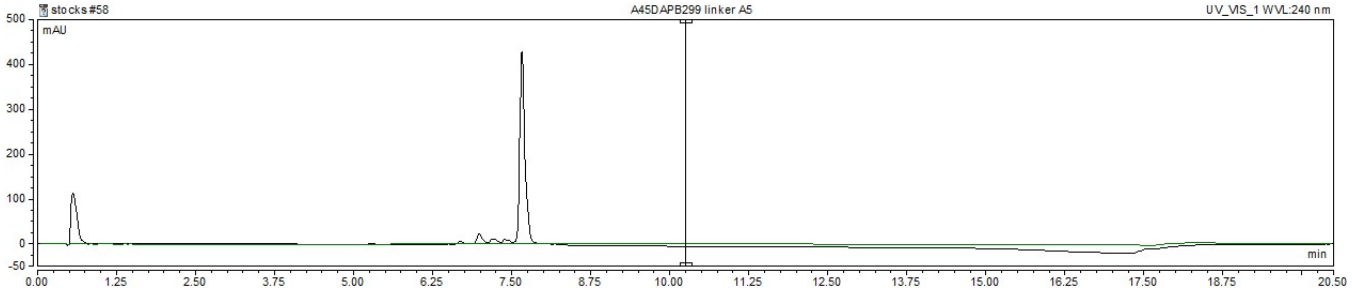

ESI$^+$ MS, compound (A45DAPB299-linker A6)

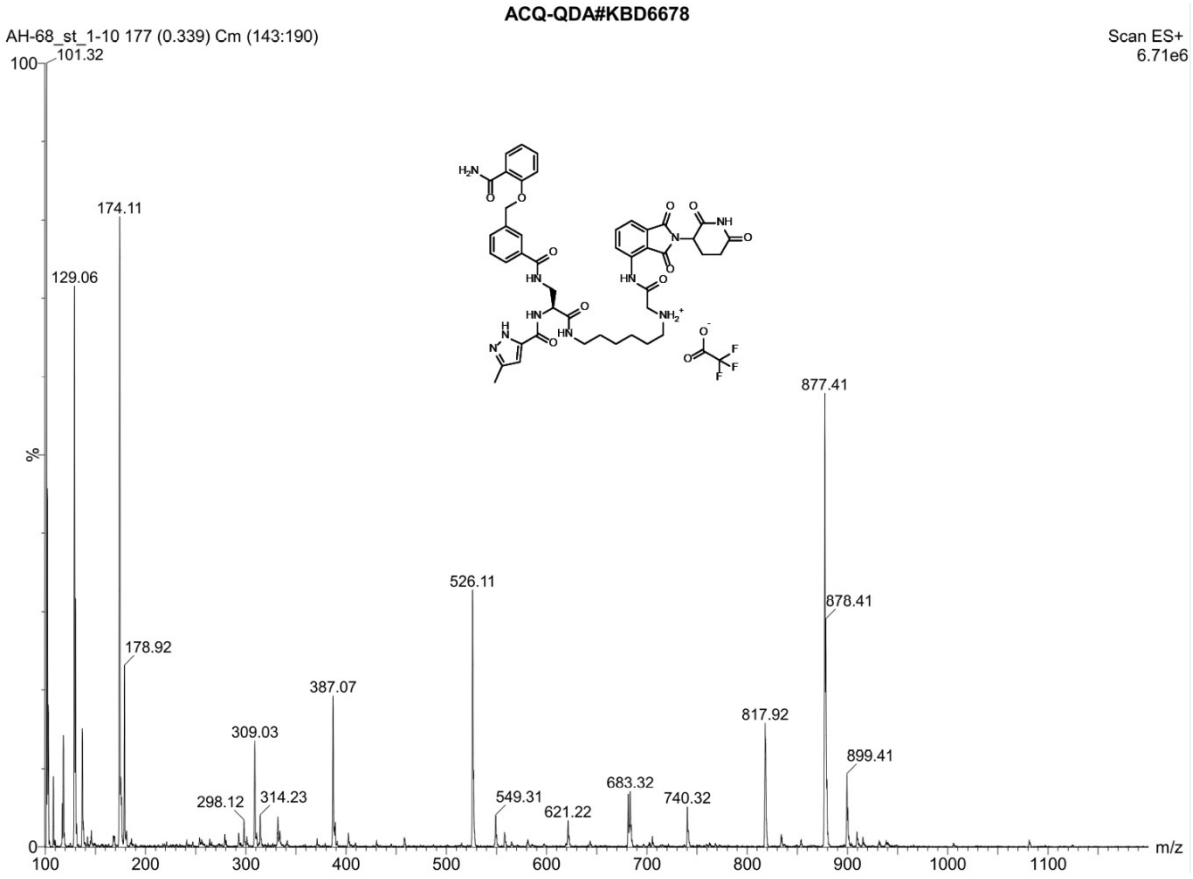

HPLC analysis of the A45DAPB299-linker A6 stock solution:

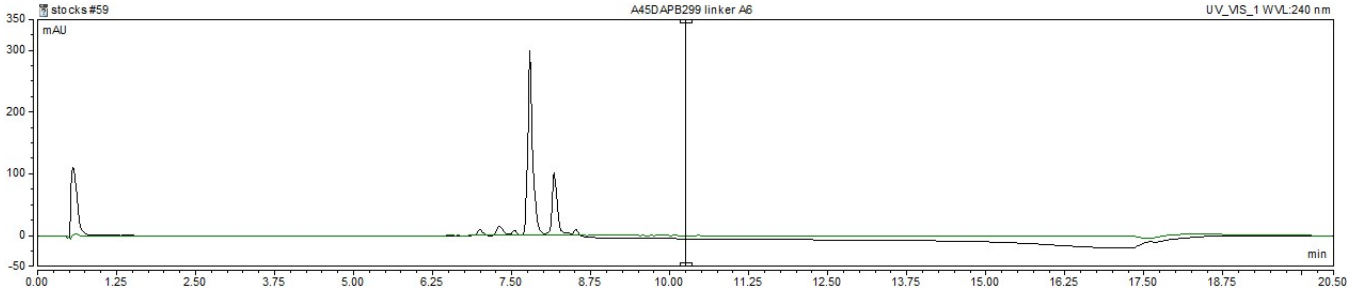

ESI$^+$ MS, compound (A45DAPB299-linker A8)

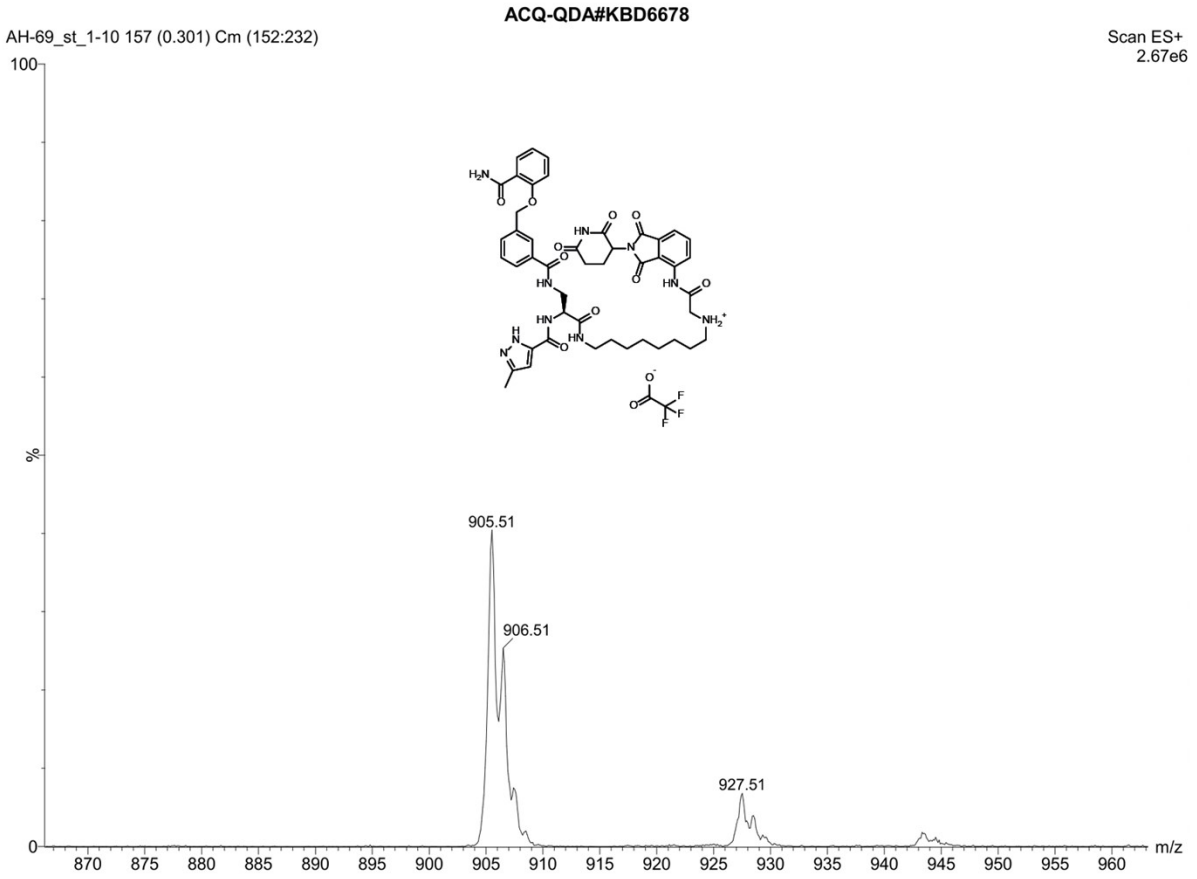

HPLC analysis of the A45DAPB299-linker A8 stock solution:

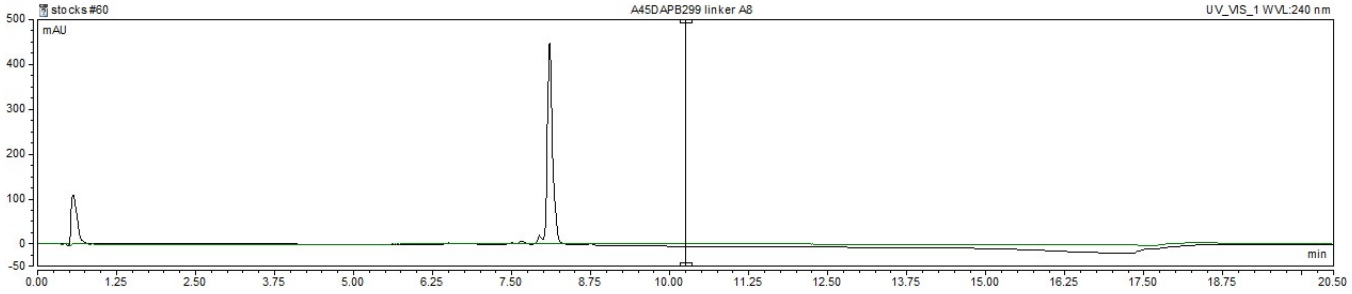

ESI$^+$ MS, compound (A45DAPB299-linker B2,3)

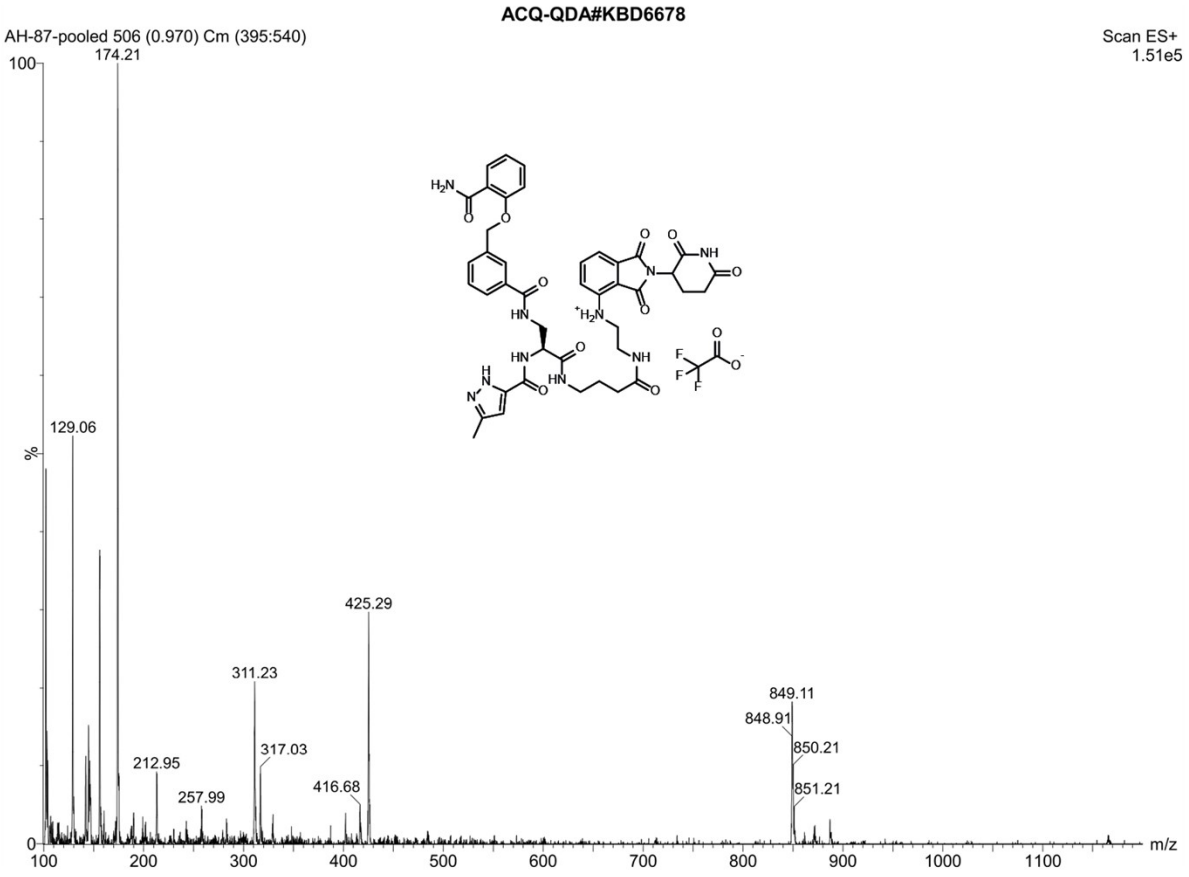

HPLC analysis of the A45DAPB299-linker B2,3 stock solution:

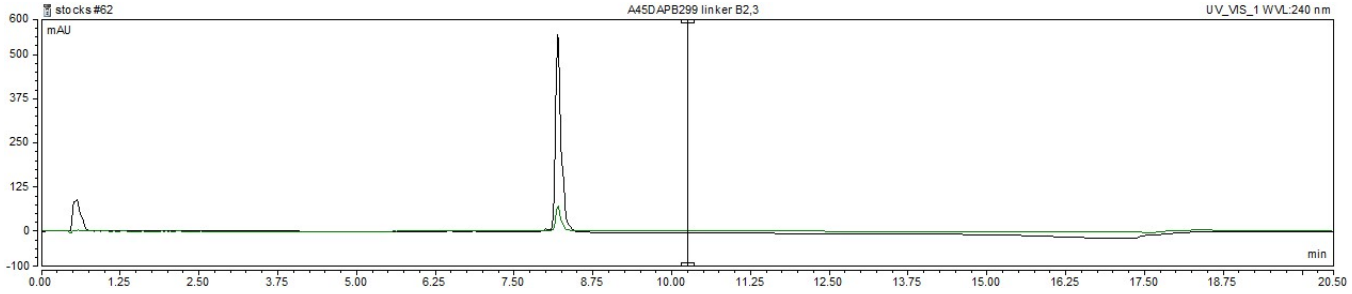

HPLC analysis of the A45DAPB299-linker B3,2 stock solution:

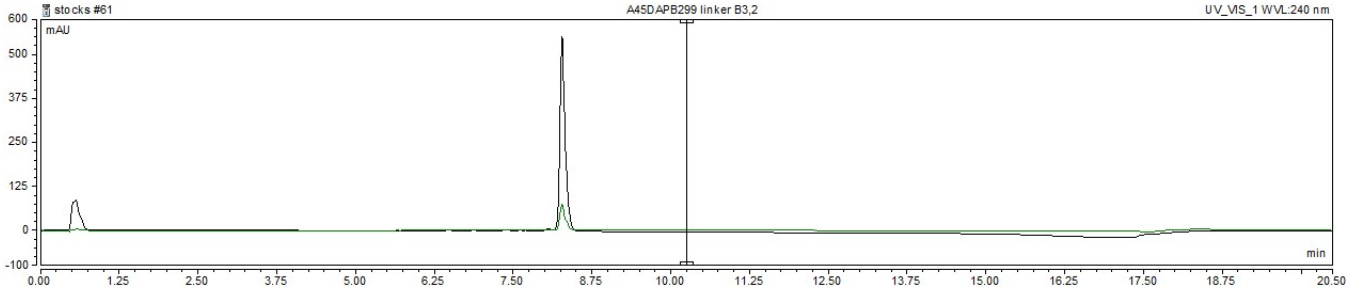

References:

(1) Montoya, A. L.; Glavatskikh, M.; Halverson, B. J.; Yuen, L. H.; Schüler, H.; Kireev, D.; Franzini, R. M. Combining pharmacophore models derived from DNA-encoded chemical libraries with structure-based exploration to predict Tankyrase 1 inhibitors. *Eur J Med Chem* **2023**, *246*, 114980. DOI: 10.1016/j.ejmech.2022.114980.

(2) Yuen, L. H.; Dana, S.; Liu, Y.; Bloom, S. I.; Thorsell, A. G.; Neri, D.; Donato, A. J.; Kireev, D.; Schuler, H.; Franzini, R. M. A Focused DNA-Encoded Chemical Library for the Discovery of Inhibitors of NAD(+)-Dependent Enzymes. *J Am Chem Soc* **2019**, *141* (13), 5169-5181. DOI: 10.1021/jacs.8b08039.

(3) Franzini, R. M.; Ekblad, T.; Zhong, N.; Wichert, M.; Decurtins, W.; Nauer, A.; Zimmermann, M.; Samain, F.; Scheuermann, J.; Brown, P. J.; et al. Identification of structure-activity relationships from screening a structurally compact DNA-encoded chemical library. *Angew Chem Int Ed Engl* **2015**, *54* (13), 3927-3931. DOI: 10.1002/anie.201410736.

(4) Decurtins, W.; Wichert, M.; Franzini, R. M.; Buller, F.; Stravs, M. A.; Zhang, Y.; Neri, D.; Scheuermann, J. Automated screening for small organic ligands using DNA-encoded chemical libraries. *Nat Protoc* **2016**, *11* (4), 764-780. DOI: 10.1038/nprot.2016.039.